UNIVERSITY of BRADFORD Library

University of Bradford eThesis

This thesis is hosted in Bradford Scholars – The University of Bradford Open Access repository. Visit the repository for full metadata or to contact the repository team

© University of Bradford. This work is licenced for reuse under a Creative Commons Licence.

Pharmacological evaluation of novel polysialyltransferase inhibitors as anti-metastatic agents and development of analytical methods for assessment of polysialylation inhibition

In vitro assessment of the effects of novel polysialyltransferase inhibitors on tumour cell function and development of quantitative HPLC-based methods for evaluation of novel polysialyltransferase inhibitors

Sara Mahmoud Youssef Ibrahim ELKASHEF

Submitted for the degree of Doctor of Philosophy

Institute of Cancer Therapeutics

University of Bradford

2016

Abstract

Sara Mahmoud Youssef Ibrahim Elkashef

Title: Pharmacological evaluation of novel polysialyltransferase inhibitors as anti-metastatic agents and development of analytical methods for assessment of polysialylation inhibition

Subtitle: In vitro assessment of the effects of novel polysialyltransferase inhibitors on tumour cell function and development of quantitative HPLC-based methods for evaluation of novel polysialyltransferase inhibitors

Keywords: Cancer, Metastasis, Polysialic acid, Polysialyltransferase, Migration

Polysialic acid (polySia) is a carbohydrate polymer highly expressed during embryonic development but rarely expressed during postnatal development. Two polysialyltransferase (polyST) enzymes are responsible for the synthesis of polySia: ST8SiaII and ST8SiaIV. During oncogenesis polySia is re-expressed and it modulates cell-cell and cell-matrix adhesion, migration, invasion and metastasis. PolySia expression is strongly associated with poor clinical prognosis and correlates with aggressive and invasive disease in neuroblastoma and many other tumours. PolyST inhibition thus presents a novel, selective and largely unexplored therapeutic opportunity to reduce tumour dissemination.

Progress towards development of polyST inhibitors has been limited by lack of an efficient technique for quantitative assessment of enzyme activity. We have validated a highly sensitive cell-based and cell-free high throughput HPLC-based inhibition assays. Using isogenic cell lines (C6-STX: polySia+/ST8SiaII+ and C6-WT: polySia-/ST8SiaII-) and naturally polySia expressing human neuroblastoma cells (SH-SY5Y), a set of ST8SiaII inhibitors designed and synthesised in house were evaluated for their ability to reduce polySia expression and to modulate cell migration in vitro. We have identified CMP-sialic acid precursors, including ICT-3176, which

reduced polySia expression and tumour cell migration by up to 70%. These effects were only found in cell lines expressing ST8SiaII and polySia.

Furthermore, we have investigated the possible additive anti-migratory effect of combining polyST inhibition with the inhibition of certain signalling pathways that have been previously suggested to be modulated by polySia expression. Out of these combinations it was found that combining ST8SiaII and C-MET/ALK inhibition had a synergistic effect on inhibiting cancer cell migration. Additionally, the effect of polySia expression on cancer cell behaviour under hypoxic conditions was examined, where it was found that polySia expression enhanced cell migration and survival and inhibits cell adhesion.

In summary, polyST inhibitors which dramatically decrease cell migration *in vitro* through modulation of polySia assembly were identified, using optimised cell-free and cell-based assays. Initial investigations into the role of polySia in hypoxia were also accomplished. This work paves the way for development of a novel therapeutic for the treatment of neuroblastoma.

Acknowledgement

While my name may be alone on the front cover of this thesis, I am by no means its sole contributor. Rather, there are a number of people behind this piece of work who deserve to be both acknowledged and thanked here.

Above all, I would like to thank my wonderful parents Prof. Mahmoud Elkashef and Dr. Hoda Saeed who had always believed in me and supported me. My hard-working parents have sacrificed their lives for my siblings and myself and provided unconditional love and care. I would like to thank them for all the times they had comforted me when I was sad or stressed, taken care of me when I was unwell and celebrated with me every successful moment since I was a kid. I would certainly say that I would have never reached any of this without them. They had always been and will always be my inspiration and my role models.

My deep gratitude goes to my supervisors Dr. Robert Falconer and Prof. Paul Loadman. I consider Dr. Falconer as not only an excellent supervisor but also as a mentor who had constantly motivated and supported me, he has always been understanding, kind and responsible and he is one of the main people in my life who have greatly influenced my scientific personality. I would also like to thank Prof. Loadman who was one of the main reasons why I decided to pursue my PhD in the Institute of cancer therapeutics after I saw how much a brilliant supervisor he is when I had my MSc degree under his supervision in 2011. I genuinely could not have imagined having better supervisors for my PhD study. Each of you have given of your time, energy and expertise and I am richer for it.

My sincere thanks also go to Dr. Simon Allison, for his guidance and insightful comments during my work on flow cytometry technique, Dr. Virginie Viprey for her help on the migration assay technique and Dr. Goreti Riberio Morais for all her help and support with the chemistry of the inhibitors described in this thesis.

I thank my fellow lab mates: Rene Ankrah, Hamza Abumansour, Haneen Basheer and Sadr Ul-shaheed for their support throughout my lab work and their joyful conversations that made the lab work time much more pleasurable.

I will forever be thankful to, Professor Mohammed Eltanani for being helpful and providing advice and support many times during my PhD. His scientific inputs, personal helps and friendly nature has always made me feel great.

My appreciation goes to my closest friends and roommate, Lina Elsalem, who was always a great support in all my struggles and frustrations. Thank you for listening, offering me advice, and supporting me through this entire process and most importantly, preparing delicious Jordanian food.

To my loving siblings Shaymaa, Heba and Amr, and my adorable nephews Shady, Badr and Mahmoud thank you for your thoughts, well-wishes/prayers, phone calls, e-mails, texts, visits, advice, and being there whenever I needed you.

Last but not least I would like to thank, soon to be, Dr. Mohammed Elkashef, my best friend, my colleague, my soulmate and my brother. I would like to thank him for his unremitting encouragement. Put simply, I have never met anyone who believes in me more. Thank you for making me more than I am. Thank you, for motivating me to keep reaching for excellence. Thank you for everything that you are.

I dedicate this thesis to

my parents and my beloved sisters and brothers

for their constant support and unconditional love.

I love you all dearly.

Table of contents

Table of figures

List of tables

List of abbreviations

A

AJ: Adherens junction

ATP: Adenosine triphosphate

ALK: Anaplastic lymphoma kinase

AMP: Adenosine monophosphate

B

BDNF: Brain-derived neurotrophic factor

C

CAMK Iiα: Calmodulin-dependent protein kinase IIα

COG: Children's Oncology Group

CIL: Contact inhibition of locomotion

CMP: Cytidine monophosphate

CMP-Neu5Ac: CMP-N-acetylneuraminic acid

C6-STX/C6-WT: Glioma isogenic system

$CaCl_2$: Calcium chloride

$CoCl_2$: Cobalt chloride

C-MET: Hepatocyte growth factor receptor

D

DP: Degree of polymerisation

DP1: A monomer of α2,8-linked Sia (DP = 1)

DP3: A trimer of α2,8-linked Sia (DP = 2)

DP4: A tetramer of α2,8-linked Sia (DP = 3)

DMSO: Dimethyl sulfoxide

DLD-1: Colorectal carcinoma cell line

DMEM: Dulbecco's Modified Eagle Medium

DMB: 1,2-diamino-4,5-methylenedioxybenzene

DAPI: 4′,6-diamidino-2-phenylindole

E

Endo-N: Endoneuroaminidase-NE

EMT: Epithelial mesenchymal transition

ECM: Extracellular matrix

EGFR: Epidermal growth factor receptor

F

FBS: Fetal bovine serum

FD: Fluorescence detector

FGF-2: Fibroblast growth factor-2

FGFR: Fibroblast growth factor receptor

FAK: Focal adhesion kinase

FYN: Tyr-protein kinase FYN

FDA: Food and Drug Administration

G

GFP: Green fluorescent protein

GPI: Glycosylphosphatidyl-inositol

GAP43: Growth associated protein 43

GDNF: Glial cell line-derived neurotrophic factor

GT3: Trisialyl lactoside

GT3–FCHASE: 6-(fluorescein-5-carboxamido) hexanoicacid N-hydroxysuccimidylester

H

HIF: Hypoxia-inducible transcription factors

HRE: Hypoxia-responsive element

HGF/SF Hepatocyte growth factor/scatter factor

HPLC: High performance liquid chromatography

I

Ig-CAM: Immunoglobulin cell adhesion molecule family

IC_{50}: The concentration needed to inhibit a biological or biochemical function by half

IC_{20}: The concentration needed to inhibit a biological or biochemical function by 20%

K

kDa: Kilodalton

Km: The Michaelis constant

M

MS: Mass spectrometry

Mwt: Molecular weight

MRM: Multiple reaction monitoring

MAb 735: Anti polySia antibody

MAPK: Mitogen-activated protein/extracellular signal-related kinase

MEM: Minimum essential medium

MMOAs: Molecular mechanisms of action

µM: Micromolar

$MgCl_2$: Magnesium chloride

MTT: 3-(4, 5-Dimethylthiazol-2-yl)-2, 5-diphenyltetrazolium bromide

ManPent: N-pentanoylmannosamine (ICT-3141)

ManProp: N-propanoylmannosamine (ICT-3128)

N

NT4: Neurotrophic factor 4

NIH-3T3: Mouse embryonic fibroblast cells

NeuAc: N-acetylneuraminic acid

N-cadherin: Neural cadherin

NCAM, CD56: Neural cell adhesion molecule

NRS-PBS: Normal mouse serum prepared in PBS

nM: Nanomolar

nm: Nanometer

ND: Not determined

O

OSA: Oligosialic acid

OSC-19: Head and Neck cell line

P

PH: Logarithmic measure of hydrogen ion concentration

PolySia: Polysialic acid

PVDF: Polyvinylidene difluoride

PBS: Phosphate-buffered saline

PolyST: Polysialyltransferase

P value: Calculated probability

PKB/ AKT: Protein kinase B

PS: Phosphatidylserine

PKCβII: Protein kinase CβII

PO2: Oxygen pressure

PDGF: Platelet-derived growth factor

PI: Propidium iodide

PKCβII: Spectrin-GAP43-protein kinase CβII

P53: Tumour suppressor p53

PAPS: 3'-phosphoadenosine-5'-phosphosulfate

R

RPTPα: Receptor type Tyr-protein phosphatase-α

RNL-1: Anti NCAM antibody

RP: Reversed phase

RdRp: RNA-dependent RNA polymerase

RPM: Round per minute

RTK: Receptor tyrosine kinase

S

SAR: Structure activity relationship

SPIs: Signalling pathway inhibitors

SiaProp: N-propanoyl sialic acid

SH-SY5Y: Neuroblastoma cell line

T

TJs: Tight junctions

TFA: Trifluoroacetic acid

TRK: Tropomycin receptor kinase

TKIs: Tyrosine kinase inhibitors

U

UPLC: Ultra-high performance liquid chromatography

V

VEGF: Vascular endothelial growth factor

VHL: Tumour suppressor gene VHL

Chapter 1. General introduction

1.1. Cancer

Due to its widespread occurrence and high mortality rates, cancer has become a disease of huge concern and fear among the public. Despite the significant improvement in cancer diagnostic and treatment options, the mortality rate for all cancers combined is still high (Figure 1.1)[1-4]. Cancer represents a condition in which out of control cell growth occurs. This situation is caused by both external factors (radiation, tobacco smoking and chemicals) and/or internal factors (impaired immunity or inherited mutations). In general, cancers arise from the accumulation of genetic and epigenetic changes and abnormalities in cancer-associated signalling pathways, causing the acquisition of cancer-related phenotypes to create what is called ''tumour microenvironment'' which promotes tumour carcinogenesis [5].

Figure 1.1 World-wide cancer statistics (A) and cancer statistics of the UK (B) (Source: CRUK).

Six hallmarks of cancer have been identified as essential for carcinogenesis [6]. During the multistep process of human tumour pathogenesis, cells should acquire these hallmark capabilities to be able to grow, proliferate, invade other tissues and evade immune destruction. Sustaining growth signalling could be considered as the most fundamental trait of cancer cells, which

enables them to sustain a chronic proliferation even when they are not receiving messages to grow [6]. To achieve that, cancer cells either produce growth factor ligands themselves to which they can respond, or send stimulatory signals to normal cells within the supporting tumour-associated stroma to stimulate these cells to supply cancer cells with various growth factors. Evasion of apoptosis is another hallmark of cancer: in normal cells, apoptosis is triggered in response to different physiological stresses in order to maintain tissue homeostasis. However, apoptosis is attenuated in tumours via different strategies most commonly by the loss of tumour protein p53 (TP53) tumour suppressor function or by increasing the expression of anti-apoptotic regulators. In order to address the need for nutrients and oxygen supply and evacuation of metabolic waste and carbon dioxide, cancer cells generate a tumour-associated neovasculature in a process known as angiogenesis, i.e. the ability to grow new blood vessels [6,7]. During tumour progression, an “angiogenic switch” is relatively permanently activated in order to maintain the formation of new blood vessels to supply tumour cells with their needs [8]. Unlimited replicative potential is acquired by the cancer cells in order to generate macroscopic tumours, which means that, in contrast to normal cells, tumour cells keep replicating no matter how many times they have already done so, which is linked to the ability of tumour cells to maintain telomeric DNA at lengths sufficient to avoid triggering senescence or apoptosis. Finally, for a tumour cell to be malignant it should acquire the ability to metastasise and invade surrounding tissues. Metastatic dissemination is the last step in tumour progression, and is considered as the main difference between the benign and malignant tumours (Figure 1.2) [6].

Besides these six established hallmarks, two emerging hallmarks of cancer has also been reported which are: reprogramming of cellular energy metabolism in order to support continuous cell growth and proliferation, replacing oxidative phosphorylation which is the metabolic program that operates in most normal tissues. And second involves active evasion of immune system attacks [6].

The acquisition of different cancer hallmarks is made possible by two enabling characteristics: the development of genomic instability in cancer cells, which generates random genetic changes that control hallmark capabilities. And second modulation of the inflammatory state of premalignant lesions that is driven by cells of the immune system, some of which serve to promote tumour progression through various means [6].

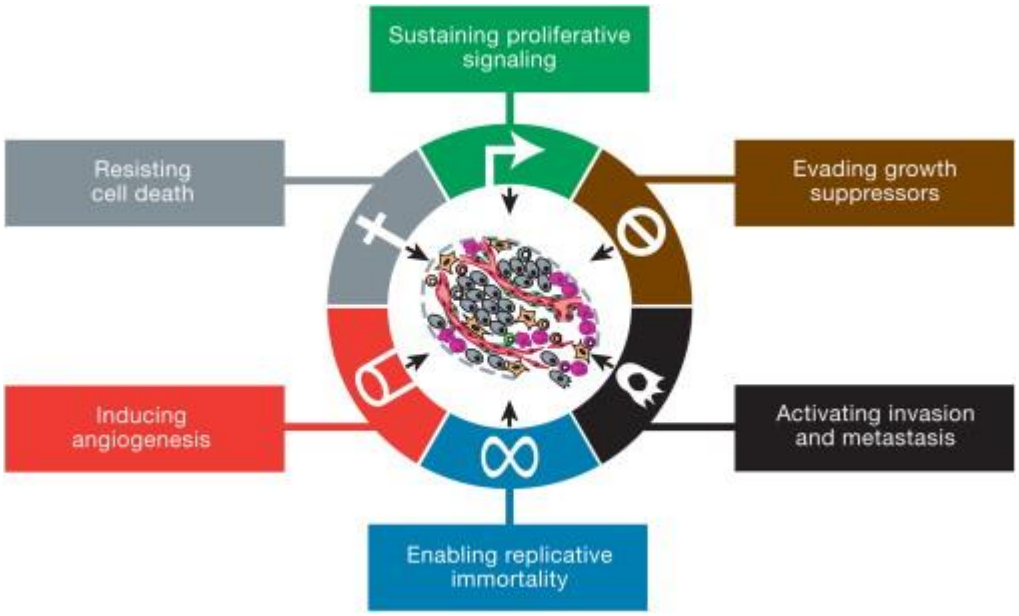

Figure 1.2 The 'Hallmarks of Cancer' as proposed by Hanahan and Weinberg. An illustration of the six hallmarks acquired by the cancer cells during tumour pathogenesis [6].

Although many studies have been performed in this field, the current success of cancer prevention, diagnosis and treatment is relatively low [2]. The events leading to cancer are not fully understood and as such, there is an enormous need for further studies and for novel ideas and theories to improve cancer treatment and diagnostic options.

1.2. Metastasis

Cancer is specifically characterised by the ability of tumour cells to metastasise from the primary tumour to other organs [9]. Metastasis resistant to therapy is the major cause of mortality from cancer [10]. It could be considered as one of the greatest challenges to the oncologist, due to its

unpredictable onset and its great impact on the prognosis of the disease; one localised tumour can often be easily removed by surgery, but for hundreds of metastases this is impossible. The majority of cancer cases may have no or few symptoms related to their metastasis and consequently, many patients show metastasis by the time of diagnosis and metastasis prevention may not be relevant. However, the development of anti-metastatic drugs could help in stopping further metastases in patients who are diagnosed in early stages, minimise invasion locally within the affected organ, reduce the transfer to further metastatic phenotype in addition to simply being used as prophylactic treatment for cancer patients at high risk for development of metastasis [9].

Furthermore, in recent studies metastasis-to-metastasis spread was found to be common; metastasis can occur in the form of spread between distant sites, rather than simply as separate waves of invasion directly from the primary tumour. This mechanism occurs either through *de novo* monoclonal seeding of daughter metastases or through the transfer of multiple tumour clones between metastatic sites [11]. In a study by Matthew K. *et al*., it was found that, in prostate cancer patients, a distant bone metastasis caused a local recurrence. It was observed that cross-metastatic site seeding is combined with dynamic remoulding of subclonal mixtures in response to therapy causing subsequent emergence of therapy-resistant disease [12]. The development of potent anti-metastatic drugs would thus help to prevent cross-metastasis and consequently improve the prognosis of the disease.

The most common sites of cancer metastasis are the lungs, bones and liver. However, most cancers have the ability to spread to many other parts of the body. Cancerous cells invade important organs and cause mortality by different mechanisms. Physical obstruction and malfunction of vital organs are some of the most common causes of mortality by cancer metastasis due to the serious problems they might cause, such as respiratory failure, hepatic failure and cardiovascular insufficiency [13]. Other impairments that could be induced by the spread of tumour cells throughout the body are the competition between cancer and normal cells for nutrients and oxygen as well as secondary infection due to immunodeficiency [14].

The preference of cancer cells to spread to certain metastatic locations is justified in different ways such as the ‘’seed and soil‘’ hypothesis by Stephen Paget in 1889, which proposed that metastasis depends on cross-talk between selected cancer cells (the 'seeds') and specific organ microenvironments (the 'soil') [15], and the James Ewing theory which assumes that metastatic dissemination occurs by a matter of anatomy; the directionality of blood flow, where organs in close proximity ‘*en route*’ are likely to be main site of metastasis for a particular primary tumour. However, some types of metastasis cannot be explained by this hypothesis, for example a particular kidney cancer may always metastasise towards the thyroid which cannot be explained easily by anatomy [9]. This field has developed over the past century passing by different breakthroughs. The conclusion of these studies so far suggests that the interactions of tumour cells with homeostatic factors that promote tumour cell growth, survival, angiogenesis, invasion and metastasis are the major regulators for metastatic potential and that the outcome of metastasis process depends on both intrinsic factors of the tumour cells and the response of the host tissue [15]. Further studies are needed to reveal the factors that contribute to the success of the metastatic process since at the cellular level only 1 in 10,000 metastasising cells can potentially grow into a new metastatic deposit [9]. Understanding the pathogenesis of metastasis at the systemic, cellular and molecular levels are therefore important goals of cancer research.

1.2.1. Incidence of metastasis and associated risk factors

Primary tumours can be classified into those with “good” or “poor” prognoses based on their metastatic potential. All cancers have the potential to spread, whether metastases develop or not depends on many factors. For example, a subset of breast tumours can be identified as being predisposed to metastasis, even when no clinical evidence for metastatic spread is apparent at the time of tumour resection [16]. According to their abnormality under a microscope, cancer cells are classified into different grades. Tumour grades are used as an indicator to how quickly the tumour is likely to grow and

spread. Pathologists commonly describe tumour grade by four degrees of severity: Grades 1, 2, 3, and 4 (which is a general grading system while individual tumour types have their own grading system), When cancer cells resemble normal cells, it is graded as grade 1. Tumours of this type tend to grow and multiply relatively slowly, and are generally considered to exhibit non-aggressive behaviour. On the other hand, Grade 3 or Grade 4 tumour cells do not bear any resemblance to normal cells of the same type, and their spread is expected to be faster than tumours with a lower grade (Table 1.1) [17].

Table 1.1 Guidelines for grading tumours. Illustration of the general tumour grading system and description of each grade, reflecting the appearance of tumour cells under a microscope [17].

Grade	Meaning
GX	Grade cannot be assessed (Undetermined grade)
G1	Well-differentiated (Low grade)
G2	Moderately differentiated (Intermediate grade)
G3	Poorly differentiated (High grade)
G4	Undifferentiated (High grade)

Other factors that contribute to tumour metastatic potential are the length of time the cancer has been present; the risk of metastasis increases the longer a tumour is in the body. The genetic makeup also affects the tumour metastatic potential; molecular analyses of cancer cells in various stages of progression have revealed that alterations in tumour suppressor genes and oncogenes accumulate during tumour progression and correlate with the clinical aggressiveness of cancer. As a result, it is possible to predict metastasis in certain types of cancer by detecting certain genetic alterations. A number of genes have been found to control the induction or suppression of metastasis in experimental models [18,19]. It was discovered that genetic alterations are generally associated with the initiation of cell transformation in

normal cells, which leads to the loss of intercellular and/or extracellular matrix mediated cell-cell adhesion. These transformations in the genetic material allow tumour cells to undergo rapid multiplication and to generate more modifications in adhesion and motility-related molecules which permits their escape from the original site and consequently allow them to acquire invasive characteristics [20].

1.2.2. Mechanisms of metastasis

The multistep process of invasion and metastasis has been structured as a sequence of distinct phases, often termed the invasion-metastasis cascade. This cascade starts with the outgrowth of a metastatic lesion, which requires the development of a vascular network to supply tumour cells with nutrients for an expanding tumour mass initially supplied by simple diffusion. This necessitates the synthesis and secretion of angiogenic factors in order to establish a capillary network from the surrounding host tissue [21]. Afterwards, the tumour cells invade the surrounding tissues and penetrate thin-walled venules, such as lymphatic channels, which offer very little resistance to penetration by tumour cells and provide the most common route for tumour cell entry into the circulation, where most of the tumour cells are destroyed by the host's immune response. Afterwards, the surviving single tumour cells or tumour aggregates detach from the blood vessels and become trapped in the capillary beds of distant organs by adhering either to capillary endothelial cells or to sub-endothelial basement membrane that might be exposed, where they extravasate and proliferate within the organ parenchyma to form micrometastases. Once they do, the cells can again invade the host stroma, penetrate blood vessels, and enter the circulation to produce secondary metastases (Figure 1.3)[15]. Generally, these steps are essential, and the same, for all tumours to metastasise and the metastatic process will not succeed if any one step fails [21,22].

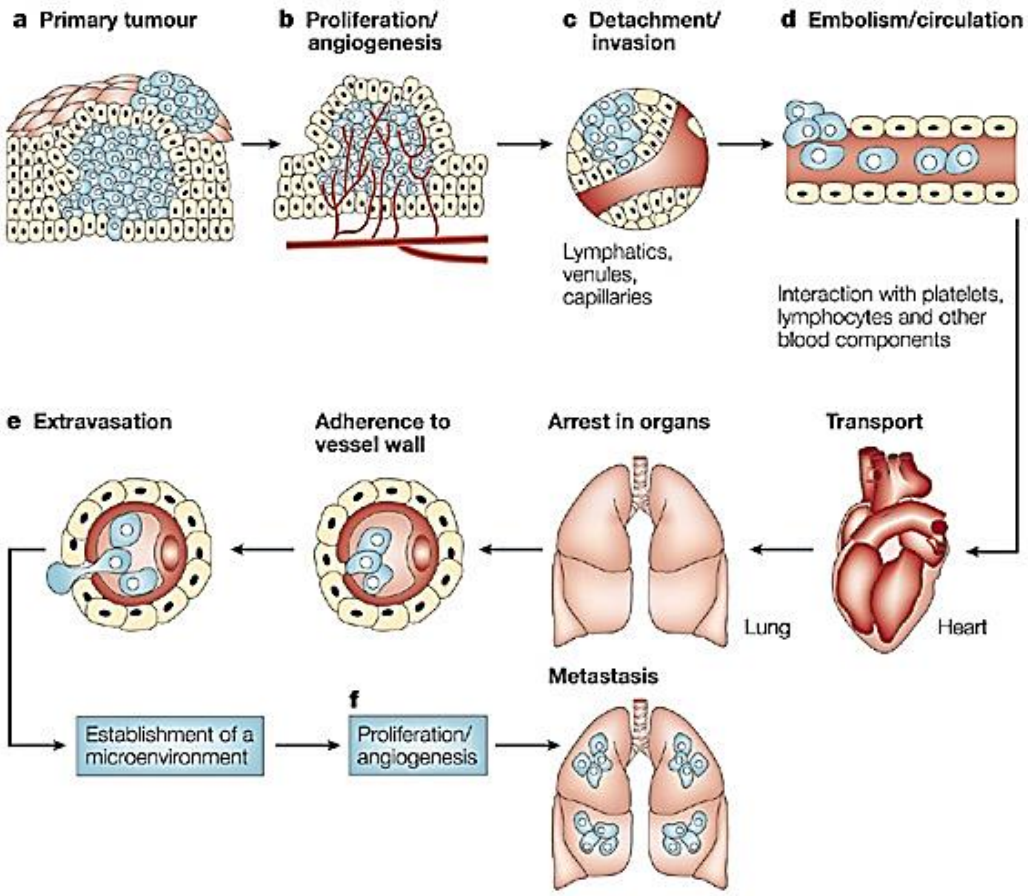

Figure 1.3 Main steps in the metastatic process [23].

Activation of epithelial to mesenchymal transition (EMT) is thought to be an event in malignant cancer that is responsible for promoting tumour metastasis and invasiveness. EMT is a biological process that allows a polarised epithelial cell, which normally interacts with basement membrane via its basal surface, to undergo multiple biochemical changes that enable it to assume a mesenchymal cell phenotype, which includes enhanced migratory capacity, invasiveness, elevated resistance to apoptosis, and greatly increased production of extracellular matrix (ECM) components (Figure 1.4) [23,24].

Epithelial cells form polarised sheets or layers of cells that are connected laterally via several types of cellular junctions, including adherens junctions, desmosomes, and tight junctions. In contrast, mesenchymal cells embed themselves inside the ECM and rarely establish tight contact with neighbouring cells [24].

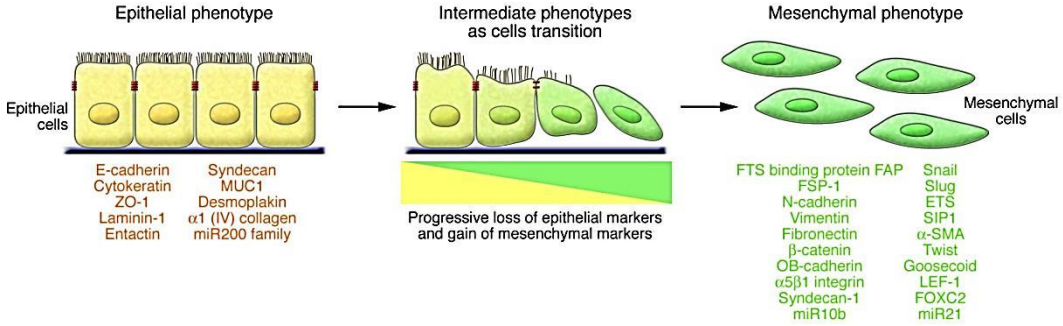

Figure 1.4 Schematic representation of EMT in metastatic cancer [24].

Many of the hallmark EMT effector molecules are subcellular structure proteins that demarcate the epithelial or mesenchymal identity of a cell. During EMT, key molecular components of these structures are subjected to various levels of regulation. For example, the genes encoding various epithelial junction proteins, such as E-cadherin, α-catenin, and γ-catenin, are down-regulated at the mRNA and protein levels. Among them, E-cadherin is regarded as a gatekeeper of the epithelial state in various epithelial cell types. During EMT, cells must switch from expressing epithelial cadherin (E-cadherin) to expressing neural cadherin (N-cadherin) for contact inhibition of locomotion (CIL) to occur; the process by which a cell changes its direction of migration upon collision with another cell [23,25].

Activation of EMT is considered essential to allow carcinoma cells to lose cell–cell junctions and dissociate from each other for single-cell migration and invasion [24].

Since colonisation demands tumour cells to restart proliferation upon extravasation into a foreign microenvironment, reversion of EMT (MET) occurs to provide such growth advantage [23].

It is known that the potential of tumour cells to metastasise depends on their pre-programmed metastatic capacity (poor prognosis signature) and epigenetic factors provided by the adjacent tumour microenvironment to promote invasion and metastases [22]. Metastasis-competent cells must perform a variety of tasks, which are likely to be regulated by transient or permanent changes in DNA, RNA or proteins. The best characterised alteration involved in the metastatic process is the alteration in the cell-cell

and cell-matrix interactions which is controlled by a number of adhesion molecules such as integrins, fibronectin, immunoglobulin-cell adhesion molecules and cadherins [5].

Adhesion molecules play a pivotal role in the development and progression of cancer. Alteration of the function of these molecules in neoplastic cells results in the loss of intercellular adhesion, desquamation of tumour cells from the underlying lamina propria, allowing tumour cells to escape from their site of origin, degrade the extracellular matrix, acquire a more motile and invasive phenotype, and finally, invade and metastasise. Besides participating in tumour invasiveness and metastasis, adhesion molecules significantly contribute to a variety of functions including signal transduction, cell growth, differentiation, site-specific gene expression, morphogenesis, immunologic function, cell motility, wound healing, and inflammation [26].

Adhesion between vertebrate cells is generally mediated by three types of adhesion junctions: adherens junctions (AJs), tight junctions (TJs), and desmosomes [27]. Together they constitute the intercellular junctional complex, which has an important role in defining the physiological function of a cell. Cadherins are the principal components of AJs and desmosomes, which cluster at sites of cell–cell contact in most solid tissues. The cadherin superfamily consists of classical cadherins, which are the main mediators of calcium dependent cell–cell adhesion, and non-classical cadherins, which include desmosomal cadherins and the recently discovered large subfamily of protocadherins [27,28].

1.3. Neural cell-adhesion molecule (NCAM)

One of the best-studied members of the immunoglobulin cell adhesion molecule (Ig-CAM) family, which are crucial components of cadherin-based adherens junctions, is the neural cell adhesion molecule (NCAM, CD56). NCAM was the first cell adhesion molecule to be characterised and has been studied extensively. It is encoded by a single gene, located on chromosome 11 in humans and on chromosome 9 in mice [28,29].

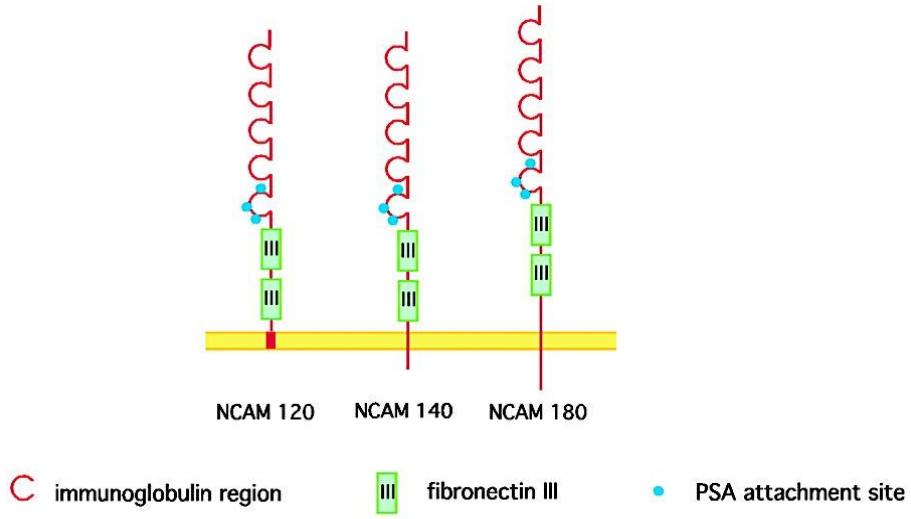

Figure 1.5 Structure of the different membrane-bound forms of the neural cell adhesion molecule (NCAM). The extracellular part of all NCAM isoforms consists of 5 immunoglobulin-like and 2 fibronectin type III-like domains. The 120-kDa NCAM isoform is linked to the membrane through a phospholipid anchor. The 140-kDa NCAM and 180-kDa NCAM isoforms, in contrast, are anchored to the cell membrane and have specific intracellular domains, through which they can interact with the cytoskeleton or components of the postsynaptic density. Blue dots demarcate the attachment sites for polySia polymers on NCAM [33].

1.3.1. NCAM structure

NCAM is a cell surface glycoprotein normally distributed along intracellular boundaries, without being associated with specific adhesive structures such as adherens junctions or tight junctions. NCAM consists of five immunoglobulin domains (Ig 1-5) and two fibronectin type III repeats (F3) (Figure 1.5) [30]. Analyses of NCAM by electron microscopy have revealed a bent rod-like structure located after Ig5. The angle of the bend at the hinge-region between N-terminal (approx. 18 nm) and C-terminal (approx. 10 nm) parts varies considerably (50–140°) with an average value of 98°, which provides sufficient internal flexibility for NCAM to fit within the cell-cell distance [30,31].

Several NCAM isoforms exist, which are either linked to the plasma membrane by a glycosylphosphatidyl-inositol (GPI) anchor (NCAM120) or have *trans*-membrane and cytoplasmic domains (NCAM140 and NCAM180, the numbers refer to their relative molecular weights) (Figure 1.5). In addition to the three main isoforms, the molecule also exists in a secreted form

(soluble NCAM), produced by the expression of the so called SEC-exon that contains a stop codon, giving rise to a truncated form of the extracellular part of NCAM with a molecular weight of around 115 kDa [32]. This high structural diversity of NCAM is due to alternative splicing and dynamically regulated post-translational modifications. During development, NCAM140 and NCAM180 are transiently expressed in the nervous system as well as in several other tissues [33]. Expression of these isoforms, also called "embryonic" isoforms, plays a pivotal role in developmental events such as neuronal cell migration, differentiation and proliferation. In the adult, however, NCAM120 is the major isoform to be expressed in the nervous system, in skeletal muscle cells as well as some neuroendocrine tissues [30].

1.3.2. NCAM function

NCAM is abundantly expressed on developing myotubes and motor axons, and after synapse formation becomes confined to the neuromuscular junctions (NMJ), where it is expressed both presynaptically and postsynaptically as well as on Schwann cells. Although NCAM can act as a homophilic adhesion molecule, the defects in synaptic maturation that we observed are more consistent with a role for presynaptic NCAM in helping to target and organize other presynaptic molecules via intracellular signalling cascades or direct protein–protein interactions [34].

1.3.2.1. NCAM role in cell-cell adhesion and neuronal survival

The major function of NCAM is to promote cell-cell adhesion and as a result, to create and maintain tissue integrity [33]. NCAM mediates calcium independent cell-cell adhesion by means of homophilic *trans*-interactions. An anti-parallel interaction takes place between the Ig1-Ig3, Ig2-Ig2, and the Ig2-Ig3 contacts [30], with an NCAM on one cell binding to the NCAM on an adjacent cell. The combination of these *trans*-interactions, at cell-cell contact with *cis*-homophilic binding, the parallel interaction of the NCAM molecules mediated by the Ig1-Ig2 contact, reflects an interaction between NCAM

molecules present on the same cell surface and results in the formation of zipper like structures (Figure 1.6) [35]. This property is particularly important during development when single cells needs to bind to each other to form tissue integrity. Besides that, this property is also important in modulating tissue permeability rather than establishing cell polarity; tight junctions mostly act to control paracellular permeability in epithelial and endothelial cells, and to establish a boundary that restricts lipid and protein diffusion between the apical and basolateral membrane domains of these cells, thus establishing cell polarity. The adhesive properties of adherens junctions are also important for creating a boundary at the cell membrane that limits the free movement of membrane proteins and promotes the establishment of cell polarity. Notably, adherens junctions frequently act in concert with tight junctions to control cell permeability and cell polarity [28].

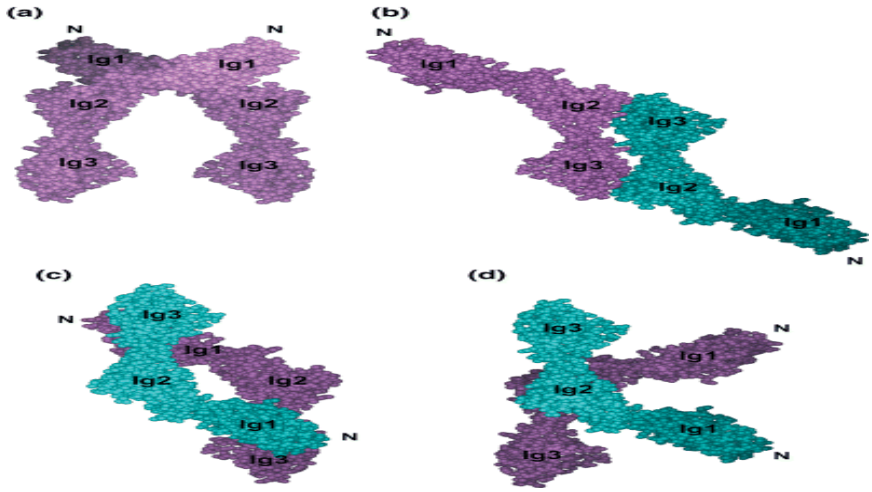

Figure 1.6 NCAM-NCAM interactions. Parallel and anti-parallel interactions identified in the crystal structure of the first three N-terminal Ig modules of NCAM. The parallel interaction mediated by the first and second Ig modules is shown in (a), whereas the anti-parallel interactions are shown in (b), (c) and (d). In (b), the interaction is mediated by the second and third Ig modules, in (c), by the first and third Ig modules, and in (d), by two second Ig modules from two different NCAM molecules. In all cases the modules are observed from the same viewpoint [31,35].

The joined forces of the first three Ig modules represent the strength of NCAM-mediated adhesion; the Ig1 and Ig2 modules of NCAM mediate both *cis* and *trans* interactions, while Ig3 is involved only in *trans* interactions. Although *cis* interactions between the Ig1-Ig2 modules do not mediate cell-cell interactions themselves, some studies suggest they have a role in the

stability of the *trans* interactions. In other words, the formation of *cis* dimers may be a prerequisite for the establishment of *trans* interactions [35].

Besides having a role in maintaining tissue integrity, NCAM-NCAM interactions mediate neural development through the activation of calmodulin-dependent protein kinase IIα (CAMK IIα) which activates receptor type Tyr-protein phosphatase-α (RPTP α) that promotes the activation of Tyr-protein kinase FYN (FYN) resulting in the stimulation of focal adhesion kinase and neurite outgrowth and neuronal survival. NCAM interactions also stimulate the recruitment of growth associated protein 43 (GAP43) resulting in the formation of spectrin-GAP43-protein kinase CβII (PKCβII) signalling complex that promotes cytoskeletal remodelling and neurite outgrowth [35,36].

1.4. Polysialylation of NCAM

The most prominent post-translational modification of NCAM is polysialic acid (polySia), a homopolymer of α-2,8-linked sialic acid residues which is added to specific N-glycan attachment sites in the fifth immunoglobulin like domain of NCAM (Figure 1.5, 1.7). PolySia is abundantly expressed throughout embryonic development and down-regulated during maturation and differentiation. In the adult brain, polySia-NCAM is only expressed in areas that retain a high degree of plasticity such as the hippocampus and the olfactory bulb, albeit its expression is relatively lower than that expressed during embryogenesis. PolySia-NCAM also regulates synaptic plasticity, including such processes as learning and memory consolidation [37-39].

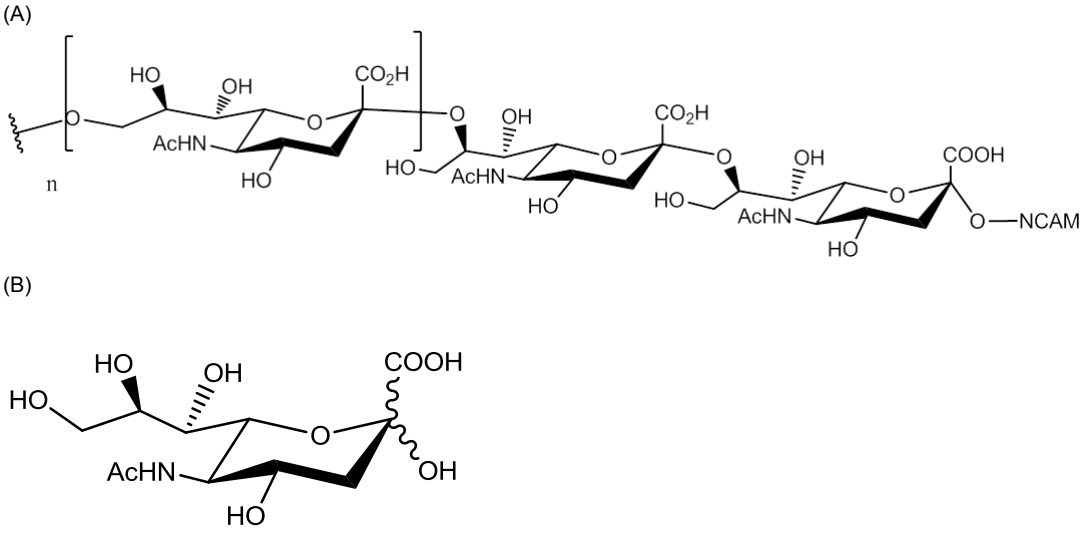

Figure 1.7 Chemical structure of polySia (A) and sialic acid monomer (B)[38].

1.4.1. N-linked polysialylation biochemistry

The assembly of an oligosaccharide on an isoprenoid lipid (dolichol) from nucleotide activated monosaccharides on the cytoplasmic side of the membrane by a set of specific glycosyltransferases and the subsequent translocation of the lipid-linked oligosaccharide is a unifying scheme in all systems [40].

For polySia synthesis, the oligosaccharide is further extended by lumen-oriented polysialyltransferases, which use dolichylphosphate-bound monosaccharides as substrates [41].

1.4.2. Polysialyltrasferase enzymes

Polysialylation of NCAM is catalysed by polysialyltransferase enzymes (PolySTs). PolySTs transfer Neu5Ac monomer units from the activated sugar donor CMP-Neu5Ac to the non-reducing end of the growing polySia polymer [42].

In mammals the polySia chain is synthesised by two Golgi-resident enzymes, ST8SiaII (STX) and ST8SiaIV (PST), which have a strong specificity for their protein targets. These enzymes are found in the carbohydrate-active

enzymes database (CAZy) family GT-29, along with all other mammalian sialyltransferases [32,42].

There are more than 20 different sialyltransferases involved in the biosynthesis of sialylated glycoproteins and glycolipids. To date only 15 different human sialyltransferase cDNAs have been cloned and characterised. Each of the sialyltransferase genes is differentially expressed in a tissue-, cell type-, and stage-specific manner to regulate the sialylation pattern of cells. These enzymes differ in their substrate specificity, tissue distribution and various biochemical parameters [43].

ST8SiaII and ST8SiaIV belong to the family of six genes encoding alpha 2,8-sialyltransferases (Table 1.2). ST8SiaII has been described at first as the initiating enzyme that transfers the first sialic acid residue to the 8-hydroxyl of Neu5Ac residue α2,3-linked to the terminal position of N-linked glycans, mainly found attached to the neural cell adhesion molecule (NCAM). Both ST8SiaII and ST8SiaIV catalyse the transfer of sialic acid through α-2,8-linkages onto sialic acid residues and co-operatively elongate the polySia chain using CMP-Sia as a donor substrate [43].

The protein structures of ST8SiaII and ST8SiaIV each consist of a short cytoplasmic region connected to a transmembrane (TM) region that is joined to an intra-luminal region. The intra-luminal region consists of a stem region and a catalytic domain, and sialyl motifs L (Large), S (Small), III, and VS (Very Short), which are a common feature of all α-2,3-, α-2,6-, and α-2,8-sialyltransferases. Sialyl motif L is positioned in the centre of the enzyme and is characterized by a 55-amino-acid region that serves as a donor substrate (CMP-Sia) binding site. Sialyl motif S is located at the C-terminal region of the enzyme and consists of 28 amino acid residues that are involved in the binding of both donor and acceptor substrates. Sialyl motif VS is also located in the C-terminal region and is reported to be involved in catalytic activity. Key histidine (H) and glutamic acid (E) residues in this motif are highly conserved between the sialyltransferases. Motif III (YHYYD) is located between sialyl motif S and VS and is also involved in the catalytic activity of

both ST8SiaII and ST8SiaIV [44]. In addition, a novel polybasic polysialyltransferase domain (PSTD; 32 amino acids) identified next to the motif S in both polysialyltransferases, which is only observed in the two polySTs and not in other sialyltransferases, was demonstrated to be involved in polysialylation activity. More recently, a second conserved polybasic motif, named polybasic region (PBR), was identified close to sialyl motif L in ST8SiaII and ST8SiaIV. The PBR consists of 35 amino acids, of which seven are the basic amino acids arginine (R) and lysine (K), and is involved in NCAM-specific polysialylation, highlighting a crucial role in acceptor-substrate recognition. These basic amino acids are considered to be important for IgV specific polysialylation of NCAM through binding via acidic patch of first FNIII domain (Figure 1.8) [44,45].

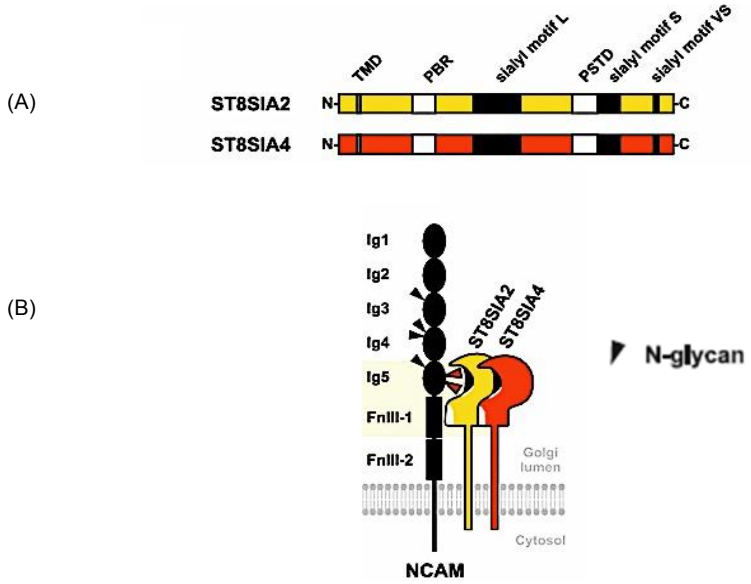

Figure 1.8 Schematic representation of ST8SiaII and ST8SiaIV enzymes (A).Both polySTs consist of a short N-terminal cytosolic part, a transmembrane domain (TMD), a stem region and a C-terminal catalytic domain. The large (L), short (S) and very short (VS) sialyl motifs conserved in all mammalian sialyltransferases are depicted as black boxes. The two polyST specific domains, termed polybasic region (PBR) and polyST specific domain (PSTD), are shown as white boxes. B) Domain structure and molecular requirements for polysialylation of NCAM [46].

Table 1.2 Summary of the human alpha-2,8-sialyltransferases.

Sialyltransferases	Structures formed	Reference
ST8Sia I	Neu5Acα2-8 Neu5Acα2-3Galβ1-4Glc-Cer	[47]
ST8Sia II	Neu5Acα2-8 Neu5Acα2-3Galβ1-4GlcNAc	[48]
ST8Sia III	Neu5Acα2-8 Neu5Acα2-3Galβ1-4GlcNAc	[49]
ST8Sia IV	Neu5Acα2-8 $(Neu5Ac\alpha2\text{-}8)_nNeu5Ac\alpha2$-3Galβ1-R	[50]
ST8Sia V	Gangliosides G_{D1c}, G_{T1a}, G_{Q1b}, G_{T3}.	[51]
ST8Sia VI	$Neu5Ac\alpha2\text{-}(NeuAc\alpha2,3)_6$-Gal	[52]

1.4.2.1. Distinct Functions of ST8SiaII and ST8SiaIV

The dynamic regulation of polysialylation during development is mainly accomplished by the up- and down-regulation of the polySTs. As shown in rodents, ST8SiaII is mainly involved in polySia biosynthesis during brain development, whereas ST8SiaIV seems to be the major polyST of the adult brain where it persists. Studies to define distinct roles for each enzyme have been performed *in vitro* using soluble forms of ST8SiaII and ST8SiaIV and *in vivo* using knock-out mouse models [46,53].

Single knock-out mouse models lacking either ST8SiaII or ST8SiaIV allowed for a detailed analysis of the *in vivo* polysialylation capacity of the remaining polyST. At postnatal day one, a time point of maximal polySia expression, loss of ST8SiaIV is completely compensated by the remaining activity of ST8SiaII. Conversely, the absence of ST8SiaII causes a 40 % reduction of polySia. Moreover, the range of different lengths of the polySia chains produced by either enzyme was similar [46].

In total, studies showed a reduced polysialylation efficiency of ST8SiaIV in comparison to ST8SiaII *in vivo*, which might result from a less efficient recognition of and/or binding to NCAM by ST8SiaIV. This is consistent with the fact that ST8SiaII is the prevailing enzyme in the developing brain where utmost synthesis of polySia chains is required, whereas ST8SiaIV constitutes the dominant enzyme in adulthood, in which the expression of polySia NCAM is considerably reduced and restricted to distinct areas of the brain [54].

The human ST8SiaII gene is located on chromosome 15 and the corresponding enzyme consists of six exons. Although the promoter region of the ST8SiaII gene has not been well examined in vitro, the schizophrenia-associated haplotype block of ST8SiaII appears to localize in several putative consensus motifs and transcriptional factor binding sites, including those for CCAAT, MZF1, CREB, GATA, TATA, and SP1. In the mouse genome, ST8SiaII expression is driven by SP1-binding motifs present in a TATA-less GC-rich domain and by the cAMP-CREB cascade. It is also reported that ST8SiaII is under the control of Pax3, a member of a paired homeobox family of evolutionary conserved transcription factors that are important for brain development [55].

1.4.3. Effect of polysialylation on NCAM-mediated cell adhesion

The large size and negative charge of the polySia carbohydrate physically inhibits NCAM-NCAM homophilic binding and thus attenuates cell–cell adhesion [56]. In other words, in the developing nervous system, polySia-NCAM has been shown to promote plasticity of cell-cell interactions during cell migration and neurite outgrowth, changing NCAM function from a pro-adhesive to a pro-migratory molecule, facilitating axon path-finding and plastic changes in the embryonic and adult nervous system, and its expression under different pathological conditions implies a role in neural regeneration and repair.

1.4.4. Effect of polysialylation on NCAM-dependent signalling implicated in the regulation of tumour cell proliferation, survival and differentiation

Recent studies have revealed that the expression of polySia affects NCAM-dependent signalling involved in the regulation of tumour cell proliferation, survival and differentiation. This function of polySia appears clearly different from its role as a positive regulator of chain migration and axon fasciculation and from the anti-adhesive properties of polySia [37].

A study by Seidenfaden *et al*., showed that in both rhabdomyosarcoma and neuroblastoma tumours, NCAM polysialylation results in a significant increase in proliferative response, determined by metabolic assays, to different growth factors such as brain-derived neurotrophic factor (BDNF) nerve growth factor and fibroblast growth factor-2 (FGF-2). Degradation of polySia using endoneuramindase-N (an enzyme that selectively cleaves polySia from NCAM) led to inhibition of cell growth, while growth of the NCAM- and polySia-negative neuroblastoma cell lines was unaffected.

Polysialylation of NCAM induces inhibition of mitogen-activated protein/extracellular signal-related kinase (MAPK) dependent survival and differentiation in neuroblastoma cell lines; activation of MAPK after polySia removal exerts a survival promoting, anti-apoptotic effect [37], which is consistent with the results of another study reported by K. Eggers. *et al* [57].

Polysialylation of NCAM was also found to exert an inhibitory effect on neurite outgrowth and significantly decreased the number of neurite bearing cells [57], which may have implications for cancer cells.

In conclusion, studies suggest that polySia acts as a negative regulator of heterophilic NCAM signals at sites of cell-cell contact, which after down regulation of polySia trigger the cell to cease proliferation and to differentiate. The dynamic regulation of polySia therefore provides the control over an instructive signal for tumour cell growth [37,57].

1.4.5. Effects of polySia on cellular interactions

PolySia serves as a potent negative regulator of cell interactions via its unusual biophysical properties. The role of polySia as a control element of specific NCAM interactions has been uncovered from *in vitro* studies [58]. As mentioned earlier, loss of polySia in neuroblastoma cells initiates NCAM trans-interactions at cell–cell contact sites, leading to reduced proliferation in favour of neuronal differentiation via activation of the MAPK pathway. Interestingly, in myoblasts and muscle-derived tumour cell lines a similar approach induced differentiation into a muscle-specific phenotype, indicating a general differentiation-promoting activity initiated by polySia-deprived NCAM. Another interesting outcome of the cellular studies was the heterophilic nature of the polySia-sensitive NCAM signals [58,59].

Different possible modes are implicated in the action of polySia. PolySia might mask NCAM and consequently, removal of polySia or lack of polysialylation induces specific *trans* homophilic or heterophilic NCAM interactions. This may involve *cis*-dimerisation of non-polysialylated NCAM. PolySia might also behave as a negative regulator of cell surface apposition by attenuation of adhesive *trans*-interactions of NCAM and other molecules, e.g. cadherins. PolySia also could function as a scavenger molecule, facilitating interactions of soluble factors with cell surface receptors such as BDNF, as mentioned earlier (Section 1.4.3.). Alternatively, polySia could be permissive by modulating inhibitory *cis* NCAM-interactions. (see Figure 1.9) [58].

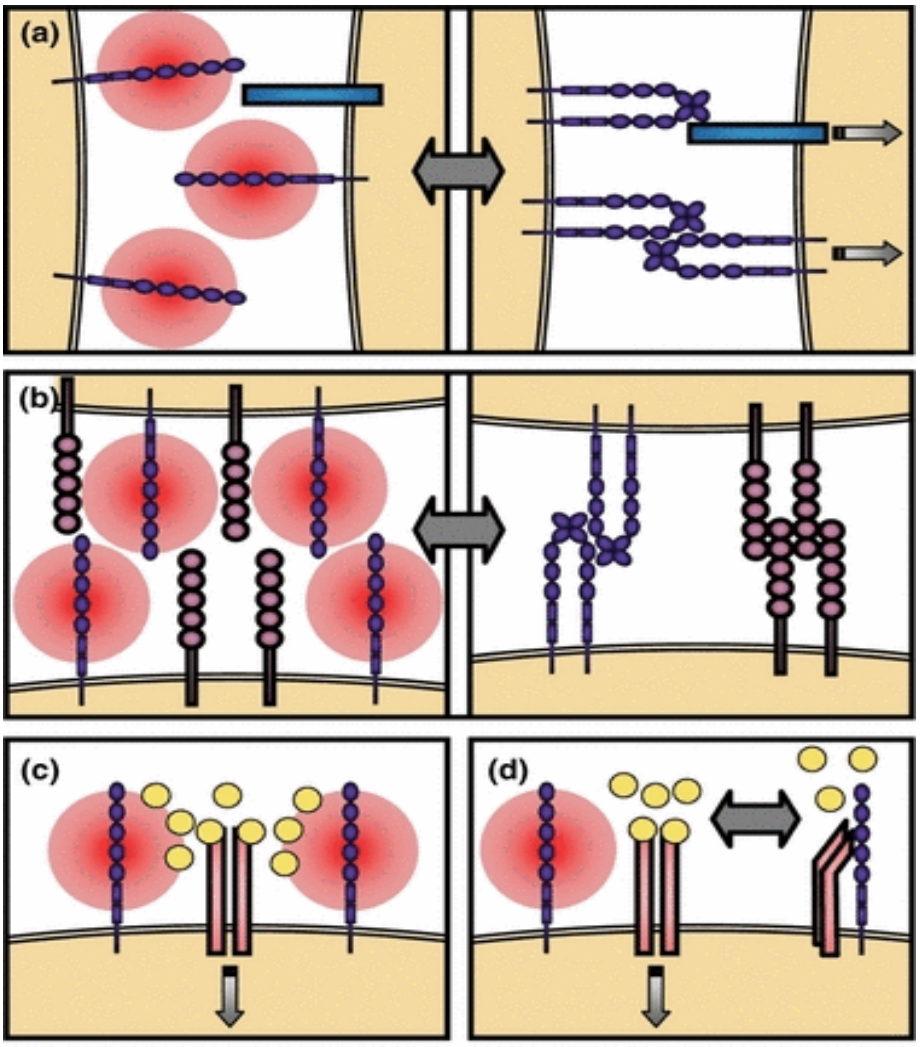

Figure 1.9 Possible modes of polySia action. (a) PolySia masks NCAM. (b) PolySia as a negative regulator of cell surface apposition. (c) PolySia as a scavenger molecule facilitating interactions of soluble factors with cell surface receptors (d) polySia could be permissive by modulating inhibitory cis NCAM-interactions [58].

1.4.6. Effect of polySia expression on cancer prognosis

As an onco-developmental antigen, polySia is re-expressed during progression of a number of malignant human tumours, including small cell lung carcinoma, Wilms' tumour, neuroblastoma, breast cancer and rhabdomyosarcoma (Table 1.3). In these tumours, polysialylation of NCAM correlates with increased metastatic potential, tumour progression and poor prognosis (Figure 1.10-1.11) [37,60]. The mechanism by which polySia-NCAM promotes metastasis in tumour tissues is analogous to its mechanism during cell migration and neurite outgrowth.

Besides increasing inter-membrane repulsion due to the negative charge of the polySia chains, it also modulates the NCAM-NCAM interactions as well as NCAM interactions with other molecules that promote tumour metastasis, which will be discussed later (Chapter 4).

Table 1.3 Expression of polySia-NCAM in selected types of cancer and its effect on cancer metastasis and prognosis.

Type of cancer	Expression
Neuroblastoma	• Majority of neuroblastoma samples express the neural cell adhesion molecule (NCAM) [61]. • Studies achieved by Glüer S. et al., showed that the expression of polySia-NCAM correlates with the histological differentiation, stage, other tumour markers and course of disease [32,62]. • PolySia-NCAM expression correlates with the malignancy of neuroblastoma cells and their tendency to metastasise. PolySia-NCAM serum concentrations also correlate to the amount of polySia-NCAM positive tumour cells [63,64]. • Another study performed by Irene Y. et al., showed that ST8SiaII marker status (positive versus negative) was strongly associated with both progression-free and overall survival [65](Figure 1.11B).
Glioblastoma (GBM)	• PolySia-NCAM is an adverse prognosis factor in glioblastoma [66]. • Analysis of 56 GBM biopsies in a study performed by Amoureux M. et al., showed that PolySia-NCAM was expressed by approximately two thirds of the GBM biopsies at variable levels. • PolySia-NCAM content was found to be an adverse prognosis factor for both overall survival (OS) and disease free survival (DFS) [67](Figure 1.10).
Breast Cancer	• Studies suggest that the pathophysiology of breast cancer involves the aberrant regulation of polySia expression [60,68]. • In study done by Wang X. et al., polySia expression was significantly higher in malignant breast cancer cells (where it appeared to facilitate cell migration and motility) than in non-malignant cells. Enhanced polySia expression levels were also observed during epithelial-mesenchymal transition (EMT) [60].
Pituitary tumours	• In pituitary tumours in humans, expression of polySia-NCAM is strongly related to tumour invasion and confirms the clinical diagnosis of aggressiveness [69]. • Study accomplished by Wierinckx A. et al., showed that NCAM was expressed in the healthy anterior pituitary and in all pituitary tumours. In contrast, polySia-NCAM was not found in the healthy pituitary gland, but was expressed in 46.3% of typical pituitary tumours and in 85% of the tumours selected as highly aggressive [70]. • Another study carried out by Trouillas J. et al., showed that, in four lineages of rat pituitary transplantable tumours, the highest polySia-NCAM expression was seen in tumours that grew beneath the skin, invaded the kidney, and metastasized[69]

Type of cancer	Expression
Wilm's tumour	• PolySia represents an onco-developmental antigen in human kidney [71]. • A study performed by Sylvia G. et al., showed that polySia-NCAM serum concentration was elevated in children with Wilm's tumour [72]. • Study performed by Jurgen R. et al showed that polySia-NCAM is re-expressed in the malignant Wilms tumour [73].
Small cell lung cancer (SCLC)	• Expression of polySia-NCAM was found in SCLC, which was characterised by high metastatic potential and rapid cell proliferation [74]. • In a study carried out by Lantuejoul S et al., immunostaining of NCAM and polySia-NCAM were compared in 120 neuroendocrine (NE) lung tumours, including 17 typical carcinoids, 3 atypical carcinoids, 30 large cell NE carcinomas and 70 small cell lung carcinomas, as compared with 25 adenocarcinomas and 25 squamous cell carcinomas [75]. PolySia-NCAM expression was significantl in high-grade tumours, with 24 of 30 positive cases in large cell NE carcinomas and 65 of 70 positive cases in small cell lung carcinoma, the expression of polySia-NCAM was found to be correlated with low overall survival [75,76]. In one particular study, SCLC cells expressing different amounts of polySia were isolated from the NCI-H69 cell line by clonal dilution of cells. After subcutaneous inoculation of these tumour cells, tumour cells expressing polySia produced more intracutaneous metastasis than tumour cells poorly expressing polySia, although a comparable amount of NCAM was expressed in these variants [35].
Rhabdomyos-arcoma (RMS)	• PolySia-NCAM expression is high in serum of patients with advanced stages of rhabdomyosarcoma (RMS)[77] • Results of study carried out by Laurent D. et al., showed that enzymatic removal of polySia on i.p. RMS primary tumours decreased the formation of metastases when compared to untreated animals [78]. • Study by Glüer S. et al., showed that in seven children with RMS, only patients with extensive disease showed high expression of polySia-NCAM [72].

(A)

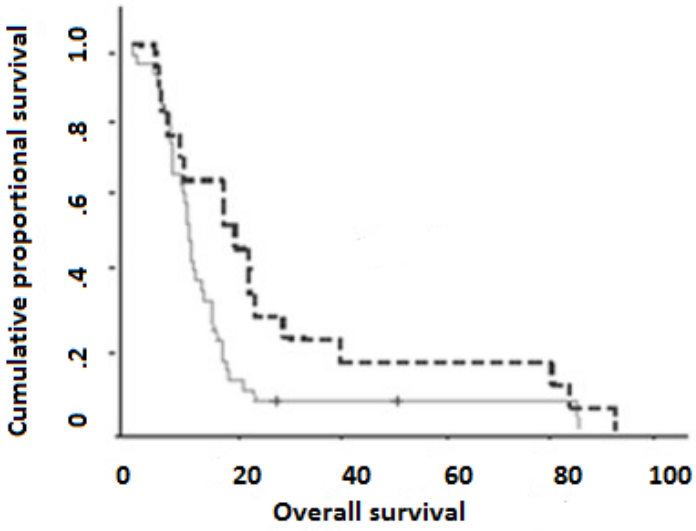

(B)

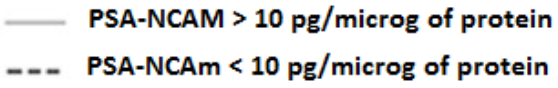

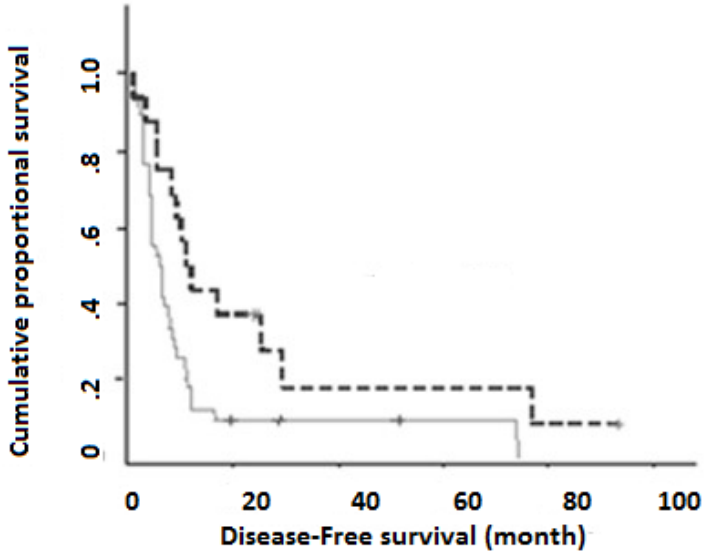

Figure 1.10 PolySia-NCAM expression in glioblastoma patients correlated to A) overall survival and B) disease-free survival. PSA in these figures refers to polySia [67].

(A)

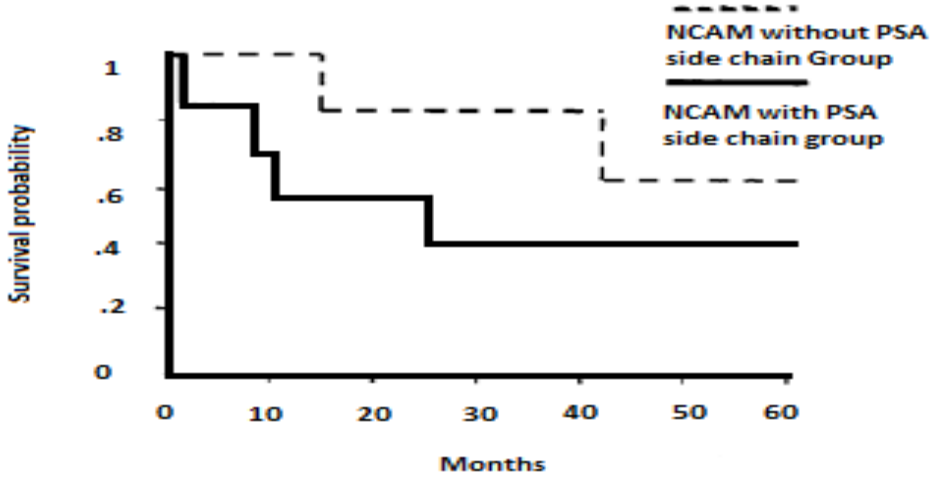

(B)

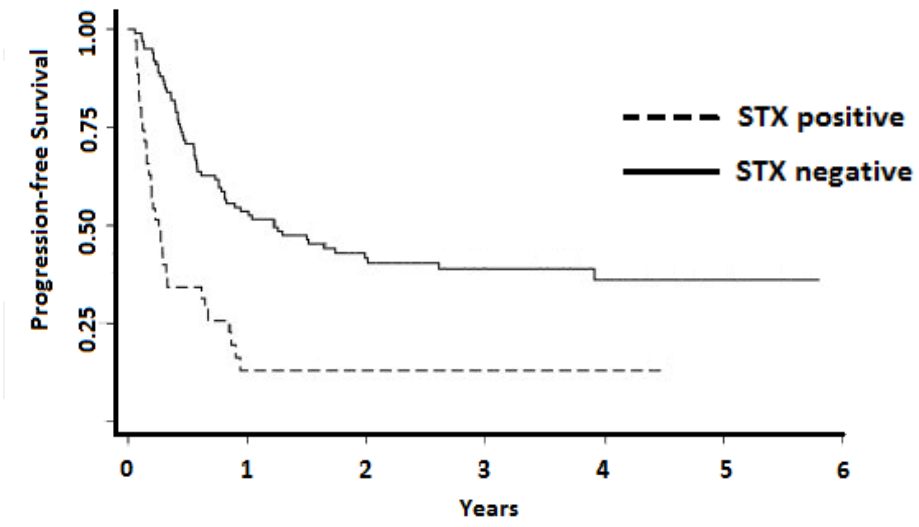

Figure 1.11 Kaplan-Meier curves of NCAM with/without polySia in SCLC patients (A). The probability of survival of patients with samples expressing NCAM without polySia is significantly higher than that of those expressing polySia, (B) Progression-free survival with respect to ST8SiaII status among neuroblastoma patients [76,79]

PolySia-NCAM is expressed by approximately two thirds of the glioblastoma patients at variable levels and was found to be an adverse prognosis factor for both overall survival and disease free survival (Figure 1.10)[67]. The same effect on prognosis was also reported in both SCLC and neuroblastoma patients. In a study on SCLC patients, 88% of the patients were positive for NCAM. Among the NCAM positive patients 60% were positive for polySia. The probability of survival of the NCAM subgroup without polySia was significantly higher than that of the NCAM with polySia expression.

Studying ST8SiaII expression in 39 NB tumours and 8 cell lines showed that ST8SiaII expression was high among NB tumours of all stages, as well as neuroblastoma cell lines of different phenotypes.

1.5. The role of polySia expression in neuroblastoma

Neuroblastoma is the most common extracranial solid tumour of infancy. It is an embryonal malignancy of the sympathetic nervous system arising from neuroblasts (pluripotent sympathetic cells) [80]. The clinical presentation varies depending on the location, size and functional characteristics. They are aggressive tumours that frequently metastasise.

Overall prognosis for children with neuroblastoma is mixed. Five-year survival in children diagnosed between 2000-2007 was 91% in infants, 59% in children aged 1-4 years, 52% in children 5-9 years, and 56% in patients aged 10-14 years. Teenagers and adults with neuroblastoma have significantly worse outcome than younger children. Survival drops steeply after the first year from diagnosis, so there is a large gap between 1-year and 3-year survival [81,82].

Neuroblastoma prognosis significantly depends on the stage of the disease and Children's Oncology Group (COG) risk groups (Table 1.4). Children in the low-risk group typically have a 5-year survival rate that is higher than 95%, while in children in the intermediate-risk group, the 5-year survival rate is around 90% to 95%. High-risk group patients, however, have a 5-year survival rate of less than 50% [83,84]. There is thus a desperate need for new

therapies to save the lives of children with these high-risk cancers. For these reasons, and due to the body of research associating neuroblastoma with polySia, neuroblastoma is a key tumour of interest at the Institute of Cancer Therapeutics. Human neuroblastoma cell line SH-SY5Y was used as a model for the experiments carried out in the studies described in this thesis.

Table 1.4 Staging system and children's oncology group (COG) risk groups of neuroblastoma [83].

<table>
<tr><td rowspan="5">Low risk</td><td colspan="2">Stage</td><td>Cancer distribution</td></tr>
<tr><td colspan="2">1</td><td>Cancer is still in the area where it started;</td></tr>
<tr><td rowspan="2">2</td><td>A</td><td>The cancer is still in the area where it started and on one side of the body, but not all of the visible tumour could be removed by surgery.</td></tr>
<tr><td>B</td><td>The cancer is on one side of the body and may or may not have been removed completely by surgery.</td></tr>
<tr><td colspan="2">3</td><td>The cancer has not spread to distant parts of the body, but cannot be removed completely by surgery or is still in the area where it started and is on one side of the body; It has spread to lymph nodes that are relatively nearby but on the other side of the body. Or the cancer is in the middle of the body and is growing toward both sides.</td></tr>
<tr><td rowspan="3">Intermediate risk</td><td rowspan="2">4</td><td>4</td><td>The cancer has spread to distant sites such as distant lymph nodes, bone, liver, skin, bone marrow, or other organs.</td></tr>
<tr><td>4S</td><td>The child is younger than 1 year old. The cancer is on one side of the body.</td></tr>
<tr><td>High risk</td><td colspan="3">Any child who is Stage 2A or 2B, older than age 1, whose cancer has extra copies of the MYCN gene
Any child who is Stage 3, younger than age 1, whose cancer has extra copies of the MYCN gene
Any child who is Stage 3, older than age 1, whose cancer has extra copies of the MYCN gene
Any child who is Stage 3, older than 18 months of age, whose cancer has unfavorable histology
Any child who is Stage 4, whose cancer has extra copies of the MYCN gene regardless of age
Any child who is Stage 4 and older than 18 months
Any child who is Stage 4 and between 12 and 18 months old whose cancer has extra copies of the MYCN gene, unfavorable histology, and/or normal DNA ploidy (a DNA index of 1)
Any child who is Stage 4S (younger than age 1), whose cancer has extra copies of the MYCN gene.</td></tr>
</table>

1.5.1. Epidemiology and Current neuroblastoma therapy in the clinic

Neuroblastoma is a complex disease with many contradictions and challenges [85]. Surgery alone is used to manage low-stage (stages I and II) neuroblastoma, but multiple-agent chemotherapy is the conventional therapy for patients in the more advanced stages of disease. Interestingly, infants with disseminated neuroblastoma have favourable outcomes with combined chemotherapy and surgery. In contrast, children older than 1 year with high-stage neuroblastoma have very poor survival rates despite intensive multimodal therapy [85].

1.5.1.1. Epidemiology of neuroblastoma

Neuroblastoma is a malignancy of the cells of the neural crest. The neural crest forms in the third to fourth week of embryonal development and some of these cells differentiate and migrate to create the sympathetic nervous system. Tumours may arise anywhere along the sympathetic nervous system, but are found most frequently in the adrenal glands (approximately 40% of tumours) or elsewhere in the abdomen, chest, or pelvis [86,87].

Neuroblastoma is the most common tumour in children less than 1 year of age. It is the third most common childhood cancer, after leukaemia and brain tumours, and is the most common solid extracranial tumour in children. Neuroblastoma accounts for approximately 15 percent of all paediatric cancer fatalities [86]. Many factors, such as age at diagnosis and stage of disease, in addition to the molecular, cellular and genetic features of the tumour, determine whether it will spontaneously regress or metastasize and become refractory to therapy [87].

It has been suggested that the incidence of neuroblastoma has increased in recent years. It is of interest to determine whether this is in part the result of increased surveillance and screening or is rather due to increases or changes in potential risk factor distributions. Little is known about the causes of neuroblastoma, and currently no recommendations exist for disease prevention [86].

1.5.1.2. Current neuroblastoma therapy in the clinic

Current trends in chemotherapy for the management of high-risk neuroblastoma include dose-intensive chemotherapy followed by resection of the primary tumour, myeloablative therapy using escalating chemotherapeutic combinations (possibly followed by autologous bone marrow infusion), and biological response modifiers that cause tumour differentiation and a reduction in tumour involvement of the bone marrow. The common chemotherapeutic agents include cisplatin, doxorubicin, cyclophosphamide and the epipodophyllotoxins (teniposide and etoposide). Radiotherapy is also used. Following treatment, patients receive 'minimal residual disease therapy', which currently consists of 13-*cis*-retinoic acid (which is thought to cause differentiation of neuroblastoma cells) and anti-GD2 immunotherapy (Unituxin). Unituxin was recently approved by the FDA and EMA specifically for neuroblastoma (in combination with GM-CSF, Interleukin-2) and is a rare example of a cancer agent that was trialled in children first (i.e. before adults) [88-90].

Despite achievements in neuroblastoma treatment field, there are still a lot of challenges. High-risk neuroblastoma continues to prove resistant to therapy: the overall survival in this disease while improved remains below 50 percent (Figure 1.12) [91,92].

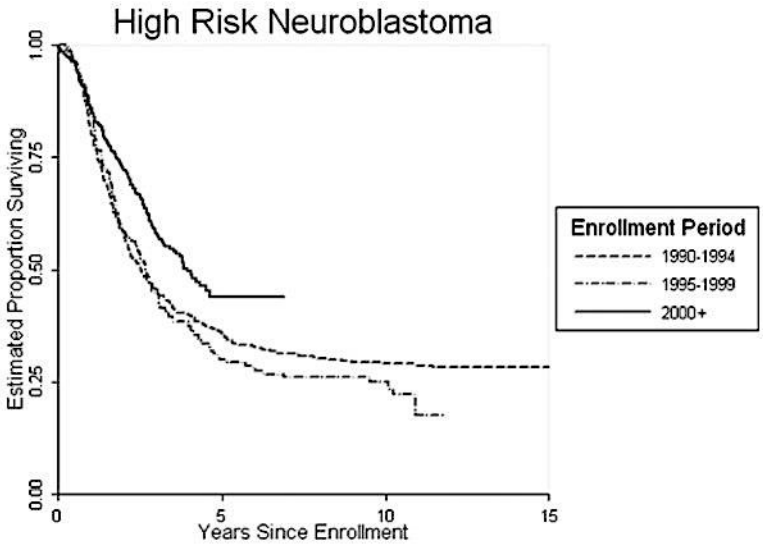

Figure 1.12 The children's oncology group treatment trials in high risk Neuroblastoma [91].

1.5.2. Glycobiology of neuroblastoma

There is evidence that changes in glycolipids and protein glycosylation pathways are associated with neuroblastoma biological behaviour [32]. Several tumour-associated carbohydrate antigens have been shown to be involved with tumour proliferation, invasion, angiogenesis, metastasis and immunity, such as the ganglioside GD2. This glycosphingolipid is highly expressed in neuroblastoma [93] and is the target for the aforementioned Unituxin, a monoclonal antibody. GD2 is a key example that supports targeting polySia in neuroblastoma.

PolySia interferes with cellular adhesion, and correlates with neuroblastoma progression and poor prognosis, as well as the expression of ST8SiaII [32,94]. High polySia-NCAM levels have been correlated with malignant potential and poor prognosis of neuroblastoma [32].

PolySia has a direct impact on neuroblastoma tumour-cell growth. The presence of polySia-NCAM has been shown to increase proliferative cell activity *in vitro* [95]. PolySia plays an important role as regulator of neuroblastoma cell migration. It was demonstrated that the migratory effect is NCAM-dependent, but independent of FGF receptor activity [57]. Removal of polySia from the cell-surface led to reduced proliferation and metastasis [95].

1.6. Validation of polysialyltransferases as anti-cancer drug targets

Several studies have been performed in order to validate polysialylation of NCAM or rather the enzymes responsible for this process as a potential target for cancer treatment. Those studies focused on determining the effect of inhibition of NCAM polysialylation on cancer growth, survival and metastasis. Studying the effect of inhibition of the NCAM polysialylation process was achieved using various techniques such as the use of endoneuroaminidase-NE (Endo-N), an enzyme which recognises and cleaves internal α-2,8-sialic acid bonds to digest polySia, siRNA knockdown of polysialyltransferase enzymes or by *in vivo* studies employing tumour cells with differential expression of polySia. These studies showed that removal of polySia from the cell surface led to the induction of NCAM signals, reduced proliferation, growth inhibition and increased cell-cell interaction of tumour cells [37,77,96].

1.6.1. Endoneuroaminidase–NE treatment

1.6.1.1. Effect of polySia removal on tumour cell growth and proliferation.

Using Endo-N to specifically degrade polySia *in vitro* and to remove it from the cell surface, neuroblastoma (SH-SY5Y, Kelly, and LAN-5) and rhabdomyosarcoma (TE671) cells (all NCAM- and polySia-positive) showed a similar reduction in cell growth, while this was not observed using an NCAM- and polySia-negative neuroblastoma cell line (LS). Heat-inactivated Endo-NE, colominic acid or N-acetylneuraminic acid were used as control and led to no effect on cell growth. The reduction of tumour cell growth was confirmed by counting the cells in some of the experiments. The absence of apoptosis after Endo-NE treatment was confirmed by a cell-death ELISA, and the analysis of BrdU incorporation revealed that the Endo-NE-induced reduction of cell growth was associated with a significant decline in proliferation. Thus, the observed growth inhibition was due to reduced rates of proliferation [37].

1.6.1.2. Effect of polySia removal on NCAM-mediated cell-cell contact in tumour cells

The cell surface distribution of polySia and NCAM was studied by Seidenfaden R., et al. using immunogold detection with energy-filtering transmission electron microscopy; polySia appears in clusters on SH-SY5Y cells and is predominantly localised at sites of tight cell-cell contacts. PolySia digestion by Endo-NE did not change NCAM-immunoreactivity at contact sites. However, a two day-incubation with Endo-NE led to an increase in NCAM-positive contact zones. It was found also that even if seeded as single cell suspension at low densities, the tumour cells used in this study never grew without any contacts between each other, which suggests that polySia expression correlates with decreased cancer cell-cell adhesion [37,97].

1.6.2. SiRNA knockdown of NCAM and/or ST8SiaII/IV

In agreement with the results obtained with Endo-NE treatment, siRNA knockdown of NCAM and/or ST8SiaII/IV, in a study performed by Schreiber et al., showed significant increase in the aggregation capacity of NCAM, polySia and ST8SiaII/IV positive pancreatic PANC-1 and AsPC-1 cells in the case of polysialyltransferase knockdown. Addition of a neutralizing E-cadherin antibody to the siRNA-treated AsPC-1 cells completely abolished the increase in aggregation and thus confirmed that the improved aggregation was mediated by polySia-NCAM interaction with E-cadherin. The ability of PANC-1 cells to migrate was also examined after siRNA treatment. It was found that inhibition of ST8Sia-II/IV expression significantly reduced the enhanced cell migration [96].

Instead of using SiRNA knockdown, ldlD-14 (Chinese hamster ovary) cells were utilised in a study by Feng Guan et al. The ldlD-14 cell line is a useful model for studying polySia role in NCAM function. The UDP-Gal 4-epimerase deficiency characteristic of ldlD-14 cells results in low internal pools of UDP-Gal when cells are grown in the absence of Gal. Addition of Gal on N-glycan termini is the essential step for polySia synthesis on NCAM. In this situation, incomplete N-glycan on ldlD-14 cells lacked the factors of Gal for the

attachment of polySia. Using transfected ldlD/N140 cells, restoring normal cell phenotype was achieved by addition of Gal. Results showed that NCAM bearing polySia was associated with enhanced cell proliferation and migration, suggesting that polySia overexpression promotes metastasis [98].

1.6.3. In vivo experiments (Correlation of polySia-NCAM expression with tumour metastatic potential)

Several studies have been performed in order to examine the effect of NCAM polysialylation on tumour metastatic potential. It was found that tumours bearing polySia are highly metastatic and that polySia-NCAM expression correlates with metastatic occurrence. In a study by Daniel et al., a relationship between polySia expression and the metastatic process was established by manipulating polySia expression in a novel animal metastatic model in nude mice by using TE671 cells which strongly express polySia-NCAM. Endo-N was verified to be non-toxic *in vivo* where no histological changes were observed after intra-peritoneal administration of 350 Endo-N units. It was found that lung and liver metastases as well as peritoneal carcinosis were formed after TE671 cells were injected intravenously, intramuscularly and intraperitoneously. Cleavage of polySia on NCAM by Endo-N treatment decreased the number of lung or liver metastases [78].

In another study by Suzuki M. et al. polySia-expressing C6-ST8SiaIV/II glioma cells were inoculated into the caudate putamen of the mice brain. Significantly more tumour invasion was observed, in particular to the corpus callosum, as compared to mock-transfected cells. On the other hand, C6 cells negative for polySia barely showed invasion to the corpus callosum under the same conditions [66]. These results were further confirmed in most recent studies were polysialyltransferase deficient mice ST8siaII/IV$^{-/-}$ mice lacking polySia expression demonstrated decreased tumour growth and metastasis [38]. These studies provide direct evidence that polySia contributes towards tumour metastatic potential.

The polysialylation of NCAM was found to reduce the adhesiveness of tumour cells. In a study by Valentiner U. et al., lung metastases were

examined for both polySia-NCAM negative (Kelly and SK-N-SH) and positive (LAN-1 and LAN-5) tumours. It was found that neuroblastoma cells expressing polySia-NCAM disseminate as single cells in the parenchyma of the lung, whereas cells of tumours without or with weak polySia-NCAM expression leave the primary tumour and adhere as cell clusters to the vascular vessel but do not transmigrate or do so very slowly, respectively [77].

These results, as a whole, indicate that, polysialylation of NCAM in different tumour types favours tumour metastasis and invasion and subsequently recurrence of the disease. Taken together, this validates the polysialyltransferase enzymes as anticancer drug targets.

1.7. Polysialyltransferase inhibitors

The significant effect of polySia on tumour prognosis and pathogenesis suggests a case for drugs that are designed to inhibit the polysialylation of NCAM. Moreover, the design of a selective inhibitor of ST8SiaII will help to elucidate the differences between the two enzymes, ST8SiaII and ST8SiaIV through the determination of the effect of selective inhibition of each enzyme on the chain length of the synthesised polySia chains and the percentage of the reduction of total polySia and consequently give an understanding on which enzyme is more important for polySia synthesis in tumour tissues.

Although these two enzyme products are very similar in terms of substrate specificity, they show distinct mRNA expression patterns in tissue and developmental stage. Different studies showed that ST8SiaIV gene is constantly expressed in both normal and tumour tissues. In contrast, the ST8SiaII gene is not expressed in normal tissues, and its expression in tumour tissue is closely correlated with tumour progression. Crucially, in both cases gene expression in normal tissue does not correlate with polySia expression, since polySia expression is limited to the brain [99].

It is thought that it is ST8SiaII enzyme which is most involved in tumour progression, and so the design of a selective inhibitor of ST8SiaII will help not only to inhibit NCAM polysialylation process but also to confirm and

explain which enzyme is more implicated in the tumour progress. Very few polysialyltransferase enzyme inhibitors are known. The only two groups of known polysialyltransferase enzyme inhibitors will be briefly discussed [100].

1.7.1. N-acyl D-mannosamines

Glycosylation requires several enzyme-catalysed steps to synthesise an activated form of a monosaccharide. For sialic acid synthesis, N-acetyl glucosamine is first converted to N-acetyl mannosamine by N-acetyl glucosamine 2-epimerase. N-Acetyl mannosamine is then phosphorylated to N-acetyl mannosamine 6-phosphate by N-acetyl mannosamine kinase. The resulting N-acetylmannosamine 6-phosphate is conjugated to phosphoenolpyruvate by N-acetylneuraminic 9-phosphate synthase, through aldol condensation, forming N-acetylneuraminic 9-phosphate. The product in turn yields N-acetylneuraminic acid (NeuAc) by N-acetylneuraminic acid 9-phosphatase. N-Acetylneuraminic acid is then activated by conjugation to CTP by N-acetylneuraminyl cytidyltransferase, forming cytidyl N-acetylneuraminic acid 5-phosphate, cytidylmonophosphate (CMP)-NeuAc. This reaction occurs in the nucleus. In animal and plant cells, the transfer of sialic acid, as CMP-NeuAc, to acceptor carbohydrates takes place in the Golgi apparatus; thus, CMP-NeuAc needs to be transported to the lumen of the Golgi by the CMP-NeuAc transporter. Once there, CMP-NeuAc is transferred to acceptor glycans by various sialyltransferases (Figure1.13) [101,102].

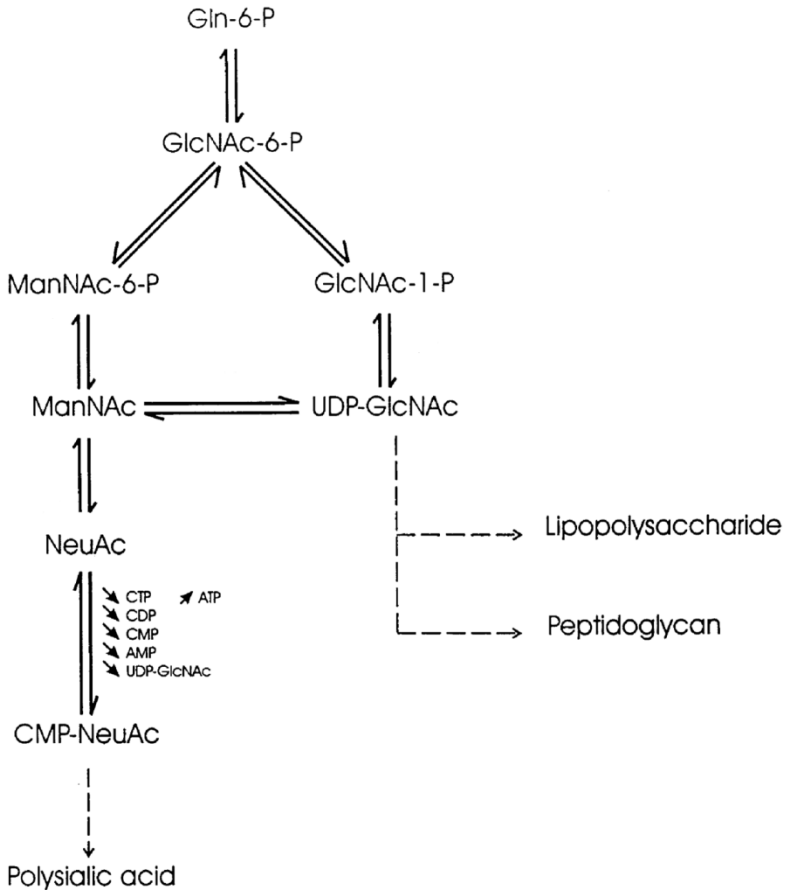

Figure 1.13 PolySia biosynthesis and activation pathways [102,103]

The promiscuity of the polySia biosynthesis pathways has been exploited by several studies to remodel the cell surface landscape of tumours both *in vitro* and *in vivo*. Unnatural N-acyl D-mannosamines are an example of agents designed for the inhibition of NCAM polysialylation. These compounds were modified N-acetylmannosamines (ManAc) (Figure 1.14) (the physiological precursor of sialic acid) ultimately resulting in the introduction of unnatural sialosides into surface glycoconjugates [103], where the quaternary complex, transiently formed between the polysialyltransferases and NCAM in the Golgi apparatus, becomes destabilised by non-natural sialic acids, leading to a premature dissociation of NCAM and thus to a premature cessation of the polymer chain synthesis [104]. In addition, these modifications serve to increase the immunogenicity of these antigens or, alternatively, to

metabolically label the tumour cells with non-natural sialic acids, followed by their specific targeting with therapeutic antibodies [103].

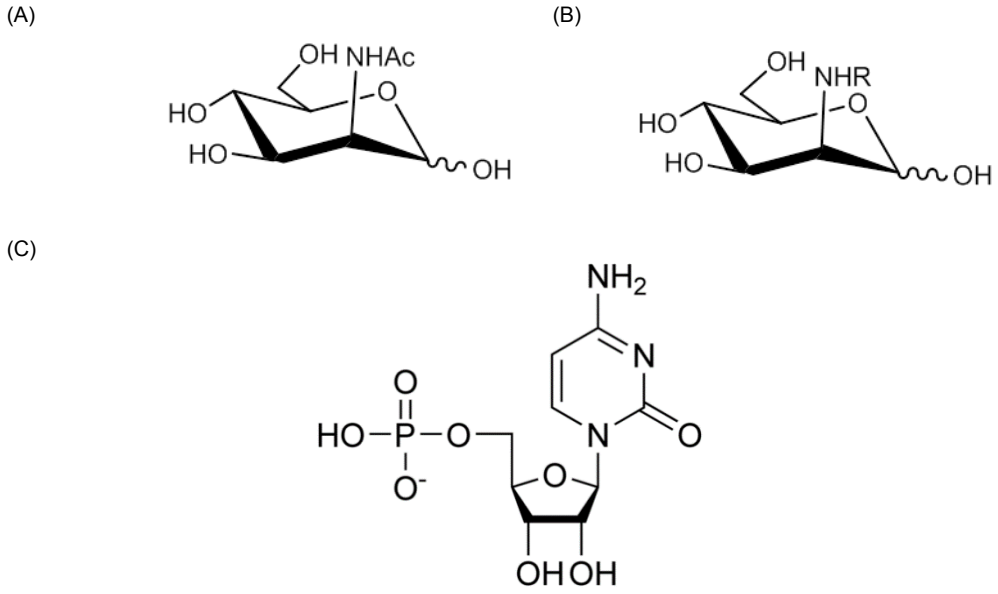

Figure 1.14 Chemical structure of N-Acetyl mannosamine (A), general structure of N-acyl modified derivative (B) and chemical structure of cytidine monophosphate (C) [105].

Different mannosamines have been studied for their ability to inhibit polySia biosynthesis. Flow cytometry and specific antibodies to different cell surface polySia have demonstrated that the unnatural sialic acid precursors ManProp and, significantly, ManBut are incorporated into growing polySia chains. ManBut was additionally found to inhibit the polySia biosynthesis process [106]. A study performed by Horstkorte R. *et al* showed that using mutant Chinese hamster ovary (CHO) cells, which express polySia-free NCAM, stably transfected with ST8SiaII and IV, respectively and treating both cells with ManProp resulted in a reduction of polySia synthesis in cells expressing ST8SiaII but not ST8SiaVI which can be used to study the differences between ST8SiaIV and ST8SiaII activity.

Small-molecule inhibitors such as N-butanoyl mannosamine (ManBut) and N-propanoyl mannosamine (ManProp) have the advantages of temporal control and reversibility. Transient disruption of polySia expression by N-acylmannosamines might be used to study the roles of polySia in modulating

cell adhesion and tumour metastasis. However, this evidence is the subject of debate since some studies argue against the ability of these unnatural sialic acid precursors to inhibit the NCAM polysialylation process, claiming that although N-acylmannosamine treatment results in lower expression of polySia, neither of the small molecule sialic acid precursors behave as metabolic inhibitors nor abrogated polySia expression [103,106]. These contradictory reports in the literature are a focus of some of the work presented in this thesis: some of the experimental data generated in this thesis addresses these issues.

1.7.2. Cytidine monophosphate (CMP)

Several studies have shown that feeding cells N-acylmannosamines can inhibit polyST activity [106]. In these studies, it was essential that all of the enzymes required for CMP-NeuAc synthesis noted above (Section 1.7.1.) tolerate the increase in size of the N-acyl group from an acetyl to a butyl group. In contrast, polysialyltransferases, in particular ST8SiaII (STX), utilise higher N-acylmannosamines (such as CMP-N-butylmannosamine) much less efficiently than CMP-N-acetylneuraminic acid. This inhibition leads to decreased synthesis of polySia by ST8SiaII. These observations suggest that glycosylation efficiency may decrease substantially when the structure of a precursor carbohydrate residue is modified [101].

A variety of nucleotides and nucleosides have been evaluated for their effect on inhibition of polySia formation. Of the nucleotides studied, CMP was the most active, inhibiting sialoprotein assembly by 74.5% at a concentration of 1 mM in an *in vitro* study as measured by Lary J. et al. Cytidine diphosphate and triphosphate were less effective, inhibiting by 51 and 37%, respectively, at a concentration of 2 mM. The monophosphate derivatives of adenosine, uridine, and guanosine inhibited this process by 42, 46, and 40%, respectively, but were less active than CMP. Similar results existed for the diphosphate nucleotides [107]. Most of these studies were performed on cell lysates so direct enzyme inhibition by the nucleotides was not determined.

The cytidine compound has been more recently shown to inhibit polysialyltransferase in a competitive fashion [108,109]. It appears that the nucleotide portion of the nucleotide-sugar binds directly to the active or regulatory site of the enzyme. Indeed, it is for this reason that analogues of CMP rather than of sialic acid have been tested for their inhibitory activity toward polysialyltransferase. However, it was found that CMP or its derivatives 2-O-methyl CMP and 5-O-methyl CMP, although being able to be transported to the Golgi apparatus and to compete with CMP-NeuAc, only decrease the expression of cell surface polySia by 30–40% [101]. Since CMP may be converted and used for many natural synthetic reactions, the use of CMP may have unwanted side effects. Besides, CMP lacks drug-like properties since it is very polar and charged (Figure 1.14C). For these reasons CMP is likely to have limited therapeutic potential. However it can be used as a useful tool for studying polysialyltransferase enzyme activity. Until now, polySia could be efficiently modulated only by genetic manipulations or by enzymatic digestion [59,101,106].

1.8. Aims of the study

The ultimate aim of the wider project for which the work presented in this thesis is a part, is to develop a potent polysialyltransferase inhibitor anti-metastatic drug that helps improve the prognosis of neuroblastoma patients.

The major aim of the work presented is this thesis was to design a quantitative, rapid and reliable cell-free assay to enable the analysis of potential polysialyltransferase inhibitors. A further aim was the development of quantitative cell-based methodology for analysis of tumour cell-surface polySia expression.

Having successfully established both cell-free and cell-based assays, the goal was to evaluate potential polyST inhibitors, and to identify promising hits for more detailed study. Effects of polyST inhibition on a key facet of the metastatic process was explored, namely migration. Furthermore, effects of inhibition on key intracellular signalling pathways were explored, and the potential involvement of polySia on cellular behaviour under hypoxic conditions was investigated.

These aims were achieved through the following objectives:

- The development and optimisation of a cell-free chromatographic assay that can provide an accurate and robust quantitative analysis of polyST small molecule inhibitors.
- The development of a cell-based chromatographic target assay in order to quantify the effect of the polyST inhibitors on polySia expression.
- Evaluation of polyST inhibitors and selection of promising molecules for further investigations, using both cell-free and cell-based chromatographic assays.
- Analysis of the ability of the promising inhibitors to inhibit neuroblastoma cell migration and to assess selectivity utilising isogenic cells.
- Investigation of the possible additive anti-migratory effects of using these pathway inhibitors in combination with an ST8SiaII inhibitor.

- Evaluation of the potential role of polySia expression on cancer cell behaviour under hypoxic conditions.

Chapter 2. Development of cell-based and cell-free chromatographic assays for evaluation of polysialyltransferase (ST8SiaII) inhibitors

2.1. Introduction

Despite their abundance and crucial rule, analysing glycosyltransferases is still challenging. The lack of efficient techniques for high throughput, sensitive and quantitative assessment of enzyme inhibition is one of the major factors that hinder the progress of drug discovery in the polysialyltransferase (polyST) area of glycoscience [110].

Human sialyltransferases (STs) are a functional family of at least 18 different intracellular, Golgi membrane-bound glycosyltransferases [111]. These enzymes have a slightly different enzymatic specificity when compared to each other [43]. Studying polySTs presents particular challenges since they are less catalytically active than the majority of the ST family [112] and the catalytic mechanisms underpinning their function are still poorly understood. PolySTs could be considered as one of the few STs which are specific for a particular protein type, and in this case recognition seems to be dependent on the final folded form of the protein acceptor [45]. All of these factors dictate a pressing need for a new strategy to assay polyST inhibition.

The methods already described as ST assays in the literature can be broadly divided into four groups: radioactive assays, non-radioactive assays, phosphatase-coupled assays and chemical conjugation methods. These have been summarised in Table 2.5. The use of methods which involve chromatography for data analysis have been found to have many advantages over other techniques; they allow not only sensitive and quantitative analysis of glycosyltransferase activity, but can also reveal product profile characteristics for each enzyme. In this study we are interested in improving a chromatographic technique to make it utilisable for high throughput analysis of human polysialyltransferase activity and polyST inhibition.

In order to develop an efficient method for polysialyltransferase analysis, the available techniques have been reviewed in order to understand the advantages and disadvantages of each technique to optimise an assay that evades the disadvantages and preserves the required qualities.

2.1.1. Radioactive assays

Radioactive assays for analysis of polyST activity typically involve monitoring the transfer of radiolabelled sugars, most frequently radiolabelled CMP-[^{14}C]-NeuAc is used as a donor substrate [113], from the donors to acceptors where the detection of radioactive transfer requires the separation of products from substrates, which is typically achieved using methods such as filtration plate, column or thin-layer chromatography. Both identification and quantification of the reaction product are usually carried out using SDS-PAGE (sodium dodecyl sulphate polyacrylamide gel electrophoresis) and autoradiography [114-116].

The use of this assay for analysis of polySTs (ST8SiaII and ST8SiaIV) was described in different studies. For example, in a study carried out by Monika Marks et al., using a radioactive assay system, a clear difference in the ability of ST8SiaII and ST8SiaIV to polysialylate NCAM was demonstrated. In this study, Ig-purified recombinant zebrafish polySTs (ST8SiaIV and ST8SiaII) and NCAM proteins were incubated overnight in media containing the radioactive-labelled donor substrate CMP-[^{14}C]Neu5Ac. The ability of both enzymes to polysialylate NCAM with the radioactive CMP-[^{14}C]Neu5Ac was examined. The results were analysed using SDS-PAGE and autoradiography [116].

The use of radioactive assays for analysis of polyST enzyme activity has been optimised in various studies. For example, in a study by Fukuda et al., an assay was optimised for the analysis of human ST8SiaIV. The enzyme activity was measured by incubating α-2,3-linked sialic acid in sodium cacodylate buffer and CMP-[^{14}C]NeuNAc. To this substrate solution, the human ST8SiaIV enzyme solution was added. The product was directly subjected to SDS-PAGE and the incorporated radioactive sialic acids were visualised by fluorography [117]. Another study involved the optimisation of different aspects of this assay; study by Liepkans *et al*., investigated the optimisation of the aforementioned assay conditions by using colorectal carcinoma cells (SW1116) membrane fractions instead of recombinant

enzyme as a source of ST8SiaIV [118]. Optimising the assay through characterisation of the acceptor preference, by testing the ability of the ST8SiaIV enzyme to use different polysaccharides as acceptors was also performed [119].

To sum up, radioactive analysis has been a useful approach for polyST analysis for over thirty years. The assay has been optimised in several studies, which has resulted in a highly sensitive and reliable method for polyST activity analysis. However, there are some major drawbacks to this technique. The technique does not show the characteristics of the reaction product in terms of polySia chain length (or molecular weight), which results in a failure to characterise any differences between the ST8SiaII and ST8SiaIV enzymes. Another disadvantage of the assay is that, to-date, the assay is not optimised for high throughput analysis, which is a significant requirement in the drug discovery field; the screening attrition rate in current drug discovery protocols suggests that one marketable drug emerges from approximately one million screened compounds. This leads to pressure to screen larger libraries in order to continue the pipeline [120,121].

2.1.2. Non-radioactive assays

Non-radioactive analysis of polySTs relies on reagents that can specifically bind to and thus detect substrates or products, such as fluorescent chemosensors, e.g. trisialyl lactoside (GT3), and enzyme-linked assays [122].

The use of this technique has been described in a number of studies [100,123,124]. Most of the enzyme-linked assays depend on detection of polySia chains using anti-polySia antibodies (12E3, 12F8 or m735) such as enzyme-linked immunosorbent assay (ELISA), which can efficiently detect both bacterial and human polySia [125].

Unlike radioactive assays, optimisation for this technique for high throughput analysis has been achieved. In a study by Ching-ching Yu et al., a trisialyl lactoside (GT3) (Figure 2.15) serving as the acceptor substrate (in place of NCAM) was immobilised on a 384-well plate by click chemistry. Incubation with bacterial ST8SiaIV and CMP-sialic acid for 30 min resulted in

polysialylation. The immobilised polySia was then directly detected using a green fluorescent protein (GFP)-fused polySia-binding protein consisting of the catalytically inactive double mutant of an endosialidase (GFP-EndoNF DM) [126]. This assay showed robust and reliable high throughput analysis of polySTs inhibitors.

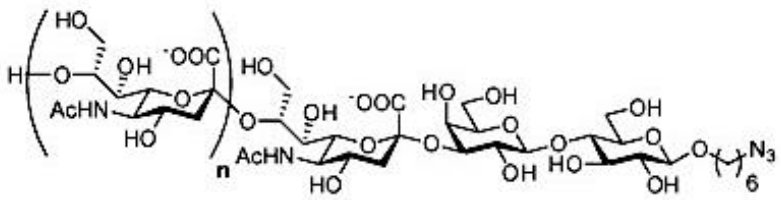

Figure 2.15 Chemical structure of trisialyl lactoside (GT3)(n=2) [126].

Although high throughput analysis of polySTs inhibitors was achieved with this protocol, only bacterial polySTs enzymes were successfully analysed. Human PolySTs belong to CAZy family GT-29 while bacterial polySTs are grouped into their own CAZy family, GT-38 [60]. Mammalian and bacterial PolySTs share no significant sequence similarity. Although they both catalyse the same reaction, different cellular environments and different acceptor substrates are involved [126]. Subsequently, high throughput analysis techniques specific for the human enzymes must be optimised.

In summary, non-radioactive assays have yet to provide high throughput analysis of the human polySTs enzymes. They also have the disadvantage of the sensitivity of the results to the reaction conditions, such as non-specific antibody binding with enzyme-linked assays and background fluorescence associated with the use of GFP for the detection of enzyme inhibition [127,128].

2.1.3. Phosphatase coupled assay

The phosphatase coupled assay depends on the release of inorganic phosphate quantitatively from the leaving nucleoside phosphates (CMP-sialic acid) produced during polyST reactions. The released phosphate is then detected using malachite green phosphate detection reagent [122].

Phosphatase coupled assays have previously been used for the analysis of several enzymes, such as sulfotransferases. Sulfotransferases are a group of enzymes that transfer sulfate from the donor substrate 3'-phosphoadenosine-5'-phosphosulfate (PAPS) to various acceptor substrates, generating 3'-phosphoadenosine-5'-phosphate (PAP) as a by-product. Golgi-resident PAP-specific 3'-phosphatase is used to release the 3'-phosphate from PAP, generating 5'-adenosine monophosphate (5'-AMP) [129]. The assay was also successfully applied to a number of different enzymes such as human glucokinase [111], and flaviviral RNA-dependent RNA polymerase (RdRp) enzymes [122].

Using this assay allowed the analysis of a wide range of sialyltransferase enzymes. It was optimised for the analysis of human ST8SiaII enzyme, because the assay detects the leaving nucleotides common to most glycosyltransferases, the method may be universally applied to all enzymes of this nature (Figure 2.16) [122,130].

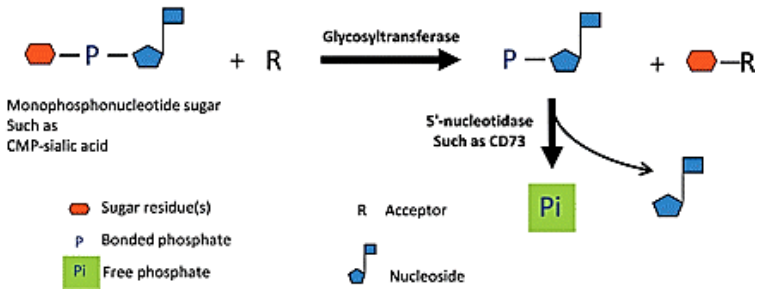

Figure 2.16 Schematic representation of phosphatase-coupled glycosyltransferase assay. This strategy can be applied to any glycosyltransferase reaction where the leaving group contains a removable phosphate. Glycosyltransferase reaction with a monophosphonucleotide leaving group can be coupled to a 5′-nucleotidase. The inorganic phosphate released by the coupling phosphatase may be detected using various phosphate detection reagents [131].

Key advantages of this approach are that it eliminates the need for both radioisotope labelling and substrate-product separation, and is high-throughput compatible. This method can be used to obtain accurate kinetic parameters of the glycosyltransferase such as Michaelis–Menten kinetics (K_m and V_{max} values) and can be performed in multi-well plates and quantitated by a plate reader, thus making it amenable to high-throughput screening.

However, the assay shares a major drawback with the other aforementioned assays, which is the inability to provide sufficient resolution to characterise individual product lengths; i.e. it cannot be used to study the way the enzyme affects polySia chain length. Therefore this assay cannot provide detailed analysis of ST8SiaIV/ST8SiaII inhibition. Furthermore, the assay lacks sensitivity, with large concentrations of enzyme and substrate (NCAM) required.

2.1.4. Chemical conjugation assay

Relatively little is known about the precise molecular mechanisms underlying the polysialylation process. Such mechanistic investigations require sensitive and accurate methods that provide quantitative information and single product resolution.

A range of fluorescently-labelled ganglioside analogues such as GT3–FCHASE [6-(fluorescein-5-carboxamido) hexanoicacid N-hydroxysuccimidylester], trisialyllactosyl–BODIPY (boron dipyromethene) and GD3–FCHASE have been used as a fluorescent acceptor molecule for the polysialylation reaction, combined with HPLC–FD. This technique has been used for bacterial polysialyltransferase characterisation and represented a major advance in this field, since it allowed HPLC-mass spectrometric analysis of the reaction product. In this assay, the tri-sialylated oligosaccharide GT3-FCHASE is incubated with the polyST enzyme and the soluble product contained in the supernatant is analysed by HPLC.

These acceptors have been shown to prime the polysialyltransferases from *Escherichia coli* K1, *E. coli* K92, *Neisseria meningitidis* serogroup B (*Nm*B), and *N. meningitidis* serogroup C (*Nm*C). Although these fluorescent acceptors provided mechanistic understanding into bacterial polysialyltransferase activity through providing molecular weight data of the product, the structures are fairly challenging owing to multistep chemo-enzymatic syntheses. Most of the available fluorescent-tagged acceptor substrates require significant work to produce a milligram of pure compound.

Besides, these fluorescent acceptors have not been shown to prime mammalian polySTs [132].

To sum up the findings obtained by reviewing the available methods for polySTs assessment, the ideal assay for ST8SiaII analysis should have the following features: ability to show the characteristics of the reaction product(s) in terms of polySia chain length (or molecular weight) in order to enable characterising the enzyme inhibition; allows for high throughput analysis of enzyme inhibitors and rapid analysis of results; the acceptor should ideally be a reagent that is readily available (or can be easily synthesised) and efficiently prime the human ST8SiaII enzyme and finally, the results should be reproducible and reliable.

A study by Keys G. *et al*., used a new non-ganglioside fluorescent acceptor consisting of a trimer of α2,8-linked Sia (DP3) directly conjugated to a 1,2-diamino-4,5-methylenedioxybenzene (DMB) label, which is synthesised in a single step from commercially accessible reagents (Figure 2.17) [132]. This acceptor was found to offer a quantitative and high-resolution analysis of bacterial polySTs and was also shown to be useful for a mammalian (murine) enzyme. A comparative analysis carried out with a panel of six polySTs emphasised different mechanisms of chain elongation and subsequently dramatic differences in the length distribution of products. Altogether, the DMB–DP3 acceptor and HPLC–FD analysis provides a way to a complete mechanistic characterisation of the human polySTs [109]. However the assay conditions were not optimised to be used for high throughput analysis.

Here the use of DMB-DP3 as an acceptor for ST8SiaII was adapted in order to design a simple, reliable and high throughput assay. The principal of the developed assay is to optimize the conditions of the polysialylation reaction of DMB-DP3 with human ST8SiaII enzyme in order to yield a single product DMB-DP4 with one extra sialic acid added to the acceptor molecule. The product DMB-DP4 is the then quantified in the presence/absence of different ST8SiaII inhibitors and the percentage inhibition of product formation caused by each inhibitor is quantified (Figure 2.17).

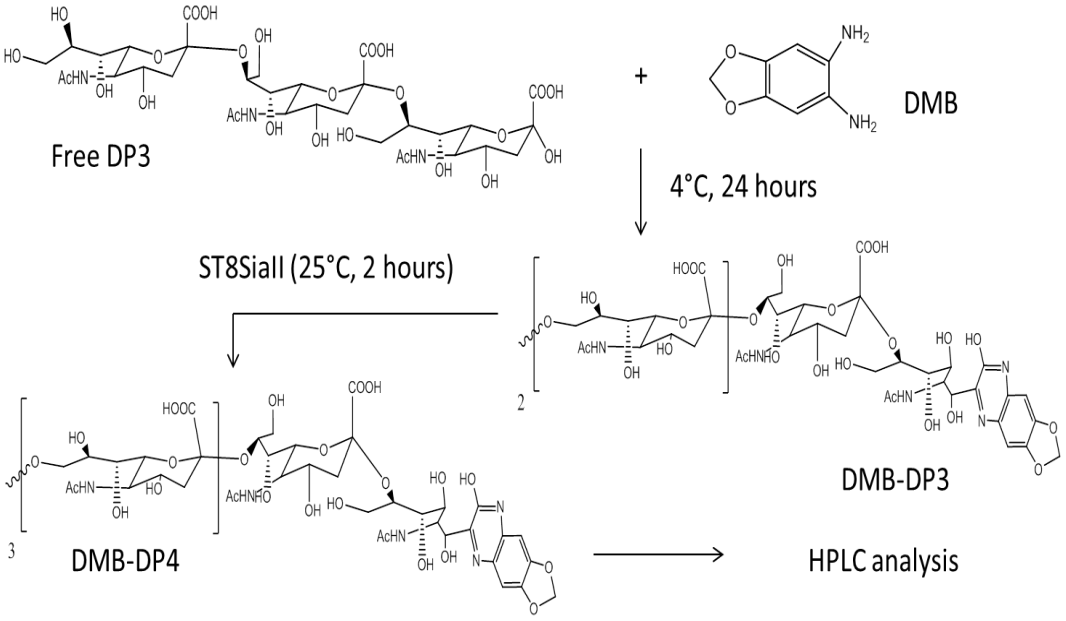

Figure 2.17 Chemical reaction of DMB-DP3 synthesis [133].

2.1.5. Aims and objectives

In this chapter, optimisation of the conditions for a cell-free HPLC chromatography assay for use in simple, quantitative and high throughput analysis of small molecule polyST inhibitors is described. Furthermore, the development of a cell-based-HPLC technique for quantitative analysis of polySia expression is also reported. Cell-based assays can be distinguished from cell-free assays by the fact that cell-based assays offer the advantage of examining inhibitors within the full cellular context and functionality, in terms of the cell-signalling pathways, as it relates to the function of the ST8SiaII enzyme.

A cell-based polyST inhibition assay that examines the recovery of polySia expression after biological removal (using the Endo-N enzyme), in the presence or absence of different polyST inhibitors has been previously reported [109]. However, whilst this assay is effective, it has the disadvantage that it does not mimic the likely scenario *in vivo,* since in practice a polyST inhibitor will be administered to cells that already express polySia on the cell surface [109].

In the cell-based assay described in this chapter, polySia chains from the cancer cell membrane were carefully cleaved using mild acidic hydrolysis or Endo-N enzyme after the incubation of the cell with different polyST inhibitors. The released polySia is then hydrolysed into sialic acid monomers, which are quantified with multiple reaction monitoring using ultra high-pressure liquid chromatography (UPLC/MS/MS) and compared with the released sialic acid from untreated cells.

Multiple Reaction Monitoring (MRM) is a type of highly selective (targeted) mass spectrometric analysis that allows fine-tuning of mass spectrometer to specifically detect molecular weights of interest. This approach allows for greater specificity, sensitivity, speed and quantitation of polyST inhibition [134].

The released sialic acid monomers were also examined using mass spectrometry in order to analyse any modification to the polySia structure caused by administration of *N*-acylmannosamine compounds.

The results obtained from the cell-free assay were linked to the results obtained using SH-SY5Y neuroblastoma cells (which express ST8SiaII) in the developed cell-based assay. This enabled correlation of the results obtained from the cell-free assay to the effect of the inhibitor in the complex conditions of the cellular environment and also allowed for study of mechanistic aspects of different polyST inhibitors *in vitro*.

Table 2.5 Comparison of the commonly used methods for the assessment of sialyltransferase enzyme activity.

Method	Principle	Advantages	Disadvantages
Radioactive methods	Monitoring the transfer of radiolabelled sugars from the donors to acceptors where the detection of radioactive transfer requires the separation of products from substrates, which is typically achieved using methods such as column or thin layer chromatography [135]	Highly sensitive Reproducible Can be used for quantitative and qualitative analysis Amenable to high throughput analysis	Time-consuming Special precautions are needed for the handling of radioactive materials
Non-radioactive methods	Relies on reagents that can specifically bind to and thus detect substrates or products, such as fluorescent chemosensors that bind to nucleotide leaving groups and enzyme-linked antibodies that bind to glycan products [114,132]	High specificity Safe to perform	Time consuming The results are very sensitive to the reaction conditions
Chemical conjugation methods	Involves chemical conjugation on either donor or acceptor substrates, such as fluorescent-tagged acceptor substrates [132]	Quantitative High resolution analysis	The use of HPLC needs special training Most of the available fluorescent-tagged acceptor substrates require significant work to produce a milligram of pure compounds To date, there is no such high resolution/high throughput assay system has been reported for the human polysialyltransferases analysis It is more difficult to attach labeled polySia than one labeled sialic acid monomer due to steric hindrance that is why it is more complicated to use this technique to assay polysialyltransferase than sialyltransferases.
Phosphata-se coupled assay	Depends on the release of inorganic phosphate quantitatively from the leaving nucleoside phosphates produced during glycosyltransferase reactions [131]	Can be used to obtain kinetic parameters of the glycosyltransferase High throughput screening Have been applied successfully to a wide range of glycosyltransferases including sialyltransferases	Using this assay for testing glycosyltransferase enzymes couldn't show a product profiles characteristic for each enzyme Insufficient resolution to characterise individual product lengths (can't be used to study the way the enzyme is affecting the chain length)

2.2. Material and methods

All general chemicals, media and media supplements were obtained from Sigma-Aldrich (Poole, UK) unless otherwise specified. Endo-N was obtained from Abcys (Paris, France). Human recombinant ST8SiaII was obtained from R&D Systems, United Kingdom.

A) Cell-free chromatographic assay

2.2.1. Gel electrophoresis and western blot analysis

2.2.1.1. Sample preparation

Samples were prepared by incubating NCAM (2.5 ng/µL) with human ST8SiaII enzyme (12.5 ng/µl) suspended in manganese chloride (10 mM) and sodium cacodylate buffer (10 mM, pH 6.7) for five minutes at 37°C, the reaction then was started by adding CMP-N-acetylneuraminic acid (CMP-Neu5Ac, 10 mM) and incubated at 37°C for 30 minutes. A negative control was prepared without the ST8SiaII enzyme to compare the results. Samples for analysis were incubated in one-quarter the final volume of loading buffer composed of Tris HCl (180 mM, pH 6.8), 40% glycerol, 4% SDS, 0.04% bromophenol blue and β-mercaptoethanol (200 mM).

Samples were denatured by heating at 75°C for 10 minutes, cooled to room temperature and then loaded onto SDS-polyacrylamide gels consisting of 5% stacking gel and 6% resolving gel. The resolving gel was made up of tris base (0.37 M, pH 8.8), 6% acrylamide mix, 0.1% SDS, 0.1% ammonium persulfate and 0.08% TEMED, while the stacking gel was made of tris base (0.12 M, pH 6.8), 5% acrylamide mix, 0.1% SDS, 0.1% ammonium persulfate and 0.1% TEMED, both gels were prepared in distilled water. SDS-polyacrylamide gels were stacked in an electrophoresis tank (BioRad, UK) filled with running buffer which consists of tris base (19 mM), glycine (192 mM) and 0.2% SDS at pH 8.3. Besides the samples, one lane of the stacking gel was loaded with PageRuler plus pre-stained protein ladder (Fermantas, UK), electrophoresis was run at 20 mA for an hour and half.

2.2.1.2. Protein transfer from gels to PVDF membrane

Blots were generated by transferring proteins from the gels to ethanol pre-soaked polyvinylidene difluoride (PVDF) membranes using a transfer kit immersed in transfer buffer consisting of tris-base (19 mM), glycine (192 mM), 0.04% SDS and 20% ethanol. The transfer was carried out at 40 mA for approximately 1.5 hours.

2.2.1.3. Incubation of membranes with antibodies

Blotted membranes were blocked by incubation with skimmed milk (0.05 g/ml) prepared in 0.05% PBSB for an hour at room temperature. Membranes were then incubated in 1:3500 mouse anti-polySia-NCAM mAb overnight at 4°C. Afterwards, membranes were washed three times with 0.05% PBSB each for 15 minutes and were incubated with 1:3500 HRP-labelled rabbit anti-mouse mAb for an hour at room temperature, then membranes were washed 3 times again with 0.05% PBSB buffer (each 15 minutes).

2.2.1.4. Protein detection in membranes.

Membranes were exposed to ECL chemiluminescent agent as described by the manufacturer, drained from excess agent and then exposed to X-ray film processor for 10 minutes. Films were then developed using Ilford film processor (Harman, Germany).

2.2.1.5. ST8SiaII inhibition by CMP

PolyST enzyme (ST8SiaII) and neural cell adhesion molecule (NCAM) were treated with various concentrations (0.1-10 mM) of cytidine monophosphate (CMP) and cytidine (5 mM), the reaction was initiated by the addition of the sugar-nucleotide donor, CMP-Neu-5Ac, and incubated for 30 minutes at 37°C and then analysed on 6% SDS-polyacrylamide gel electrophoresis as described before. The reaction mixture of the samples is summarised and described below (Table 2.6)

Table 2.6 The reaction mixture for western blot analysis of the polysialylation of NCAM with ST8SiaII enzyme in the presence/absence of enzyme inhibitors at different concentrations (the concentrations in this table are the final concentrations of the reaction mixture).

Reaction	CMP/Cytidine	DMSO	Na. cacodylate (pH 6.7)	NCAM	$MnCl_2$	ST8SiaII
Negative control	–	0.5 µM	10 mM	2.5 ng/µl	10 mM	–
Positive control	–	0.5 µM	10 mM	2.5 ng/µl	10 mM	12.5 ng/µl
CMP (0.1 mM)	0.1 mM	–	10 mM	2.5 ng/µl	10 mM	12.5 ng/µl
CMP (0.25 mM)	0.25 mM	–	10 mM	2.5 ng/µl	10 mM	12.5 ng/µl
CMP (1 mM)	1 mM	–	10 mM	2.5 ng/µl	10 mM	12.5 ng/µl
CMP (5 mM)	5 mM	–	10 mM	2.5 ng/µl	10 mM	12.5 ng/µl
CMP (10 mM)	10 mM	–	10 mM	2.5 ng/µl	10 mM	12.5 ng/µl
Cytidine (5 mM)	5 mM	–	10 mM	2.5 ng/µl	10 mM	12.5 ng/µl

2.2.2. High performance column chromatography analysis

2.2.2.1. Analysis of sialic acid

For labelling of sialic acid with the fluorescent dye 1,2-diamino-4,5-methylenedioxybenzene (DMB), sialic acid (32.3 mg/ml) was dissolved in DMB (20 mM) with sodium hydrosulfite (40 mM) and β-mercaptoethanol (1 M). The polySia solution was then mixed with an equal volume of ice-cold trifluoroacetic acid (40 mM, TFA). The reaction mixture was incubated for 24 hours at 4°C. After the incubation was completed, the derivatisation reaction was stopped by the addition of one-fifth reaction volume of sodium hydroxide (200 µM). Aliquot of 1 µL of the reaction mixture was separated, diluted with 99 µL of tris (100mM, pH 8.0)/ EDTA (5 mM) buffer and analysed by HPLC.

2.2.2.2. Analysis of polySia chains

2.2.2.2.1. Conditions of polySia labelling reaction

For polySia labelling, the same conditions used for sialic acid labelling were used however, the concentration of polySia used was (10 mg/ml) instead of (32.3 mg/ml).

2.2.2.2.2. HPLC analysis

A Waters 2695 Alliance HPLC system operated by Masslynx software was connected with fluorescence (RF-10A) (Shimadzu, Japan) and photodiode array detectors (Waters 2996) (Waters, UK) and used to analyse samples. Separation was achieved using DNAPac© PA-100 analytical anion exchange column with diameters of 4 x 250 mm packed with 0.1 µM microbeads (Dionex, UK). DMB fluorescence (excitation 373 nm/emission 456 nm) was monitored with a fluorescence detector. The mobile phases used were: 100% water (mobile phase A) and ammonium acetate buffer (5 M, pH 7.4, mobile phase B) with the following gradient (Table 2.7). The total run time was adjusted to 182.5 minutes followed by washing the column for up to 240 minutes with 5.0 M ammonium acetate buffer.

Table 2.7 HPLC gradient for analysis of DMB-labelled polySia(Flow rate 1 ml/min)

Time (minutes)	% Mobile phase A	% Mobile phase B
0	100	0
5	100	0
15	92	8
20	90	10
35	87	13
55	84	16
145	75	25
182.5	60	40
190	0	100
210	100	0
240	100	0

2.2.2.3. Optimisation of the DMB-labelling conditions

In order to determine the optimum conditions for the polySia-DMB labelling reaction, different conditions of the reaction were explored, including different incubation times (30 minutes, 24, 48 hours), temperature (4, 50 °C) and different concentrations of the substrate. The efficiency of the assay was then determined by HPLC analysis.

2.2.2.4. Analysis of polysialyltransferase (ST8SiaII) enzyme activity using DMB-DP3

2.2.2.4.1. DMB-DP3 Labelling reaction and purification

For the DMB labelling of DP3, the same conditions as polySia labelling were used. After the incubation was completed, the derivatisation reaction was stopped by the addition of sodium hydroxide (40 mM). The sample was diluted in distilled water (1:1) and then separation of the sample was accomplished by using two different systems: anion exchange chromatography or reversed phase chromatography.

DMB-DP3 purification by reversed phase chromatography

Separation was achieved by reversed phase chromatography on a Hichrom RPB C18 column (25 cm x 4.6 mm, 250 A) (Hichrom, UK). Chromatography was performed at 1.2 ml/min with ammonium formate (5 mM, pH 6) (mobile phase A) and 55% methanol (mobile phase B). The elution of DMB-DP3 was performed with a linear isocratic method of 90 %: 10 %, mobile phase A: mobile phase B over 70 minutes. The separation was monitored by mass spectrometer (Waters ZMD) (Micromass, United Kingdom), photo diode array detector (373, 303 and 250 nm) and fluorescence detector (RF-10A), (excitation 373, emission 484 nm). A single fraction containing the DMB-DP3 was collected (confirmed by detecting the molecular weight and comparing the retention time with standard DMB-DP3). Fractions from several runs were pooled and freeze dried. The dried material was weighed and dissolved in water to form 200 µM DMB-DP3 solution and stored at -20°C.

DMB-DP3 purification by anion exchange chromatography

A Waters 2695 Alliance HPLC system operated by Masslynx software was connected with fluorescence and photodiode array detectors and used to analyse samples. Separation was achieved using DNAPac PA-100 analytical anion exchange column (Dionex, UK) with diameters of 4 x 250 mm packed with 0.1 µM microbeads, DMB fluorescence (excitation 373 nm/emission 456 nm) monitored with a fluorescence detector RF-10 AXL. The mobile phases used were: 100% water (mobile phase A) and ammonium acetate buffer (5 M, pH 7.4, mobile phase B) for 30 minutes and 1 ml/min flow rate, with the following gradient (Table 2.8).

Table 2.8 HPLC gradient for DMB-DP3 purification using anion exchange chromatography (Flow rate 1 ml/min).

Time (min)	% Mobile phase A	% Mobile phase B	Flow rate (ml/min)
0	100	0	1
5	100	0	1
25	98	2	1
30	100	0	1

The peaks representing DMB-DP3 were collected from several purification runs at retention time between 9-11 minutes and freeze dried. The dried material was weighed and dissolved in water to form a 200 μM solution and stored at -20°C.

2.2.2.4.2. General procedure for mass spectrometric analysis of DMB-DP1, 3 and 4

Liquid chromatography-mass spectrometry analysis was carried out using a Waters ZMD (Micromass, Manchester, United Kingdom) single quadrupole mass spectrometer connected in series to a Water Alliance 2695 system. The mass spectrometer was operated in negative ion electrospray mode. A solvent flow of 1.2 ml/min (split 1:10) with a nitrogen gas flow of 55.6 litres/h and a source temperature of 120°C was used to produce stable spray conditions. The cone voltage was set at 30 V, and this gave clear mass -/spectra from these samples. The mass spectra were continuously scanned from *m/z* 100 to *m/z* 1500 throughout the entire high-performance liquid chromatography separation. Masslynx software was used to process the mass spectral data and produce both total ion chromatograms and single ion recording chromatograms for the key masses of interest.

2.2.2.4.3 Measurement of polysialyltransferase (ST8SiaII) enzyme inhibition

Human ST8SiaII enzyme analysis

Recombinant human ST8SiaII enzyme (250 ng/μl) was incubated at 25°C overnight in solution of DMB-DP3 (10 to 100 μM), $MgCl_2$ (5 mM), CMP-Neu5Ac (0.5 mM) and sodium cacodylate buffer (0.1 M, pH 6.7). Aliquots were taken after different time points and the reaction was stopped using 10-fold dilution of tris-HCl (100 mM, pH 8.0)/ EDTA (5 mM). The results were compared with a negative control (without the addition of the ST8SiaII enzyme). Samples were then analysed by either anion exchange or reversed phase HPLC.

Analysis of ST8SiaII enzyme inhibition using anion exchange HPLC system

A Waters 2695 Alliance HPLC system operated by Masslynx software was connected with fluorescence and photodiode array detectors and used to analyse samples. Separation was achieved using DNAPac PA-100 analytical anion exchange column with diameters of 4 x 250 mm packed with 0.1 µm microbeads, DMB fluorescence (excitation 373 nm/emission 456 nm) monitored with a fluorescence detector RF-10 AXL. The mobile phases used were: distilled water (mobile phase A) and ammonium acetate (0.5 M, PH 7.4, mobile phase B) with flow rate of 1.2 (ml/min) and the following gradient (Table 2.9):

Table 2.9 HPLC gradient for Analysis of ST8SiaII enzyme activity using anion exchange HPLC system

Time	Flow rate (ml/min)	% Mobile phase A	% Mobile phase B
0	1.2	100	0
2	1.2	100	0
9	1.2	63	37
11	1.2	100	0
12	1.2	100	0

Analysis of ST8SiaII enzyme inhibition using a reversed phase HPLC system

Reversed phase chromatography on a Hichrom RPB C18 column (25 x 4.6 mm, 250 Å) (Hichrom, UK). Chromatography was performed at 1 ml/min with 5 mM ammonium formate (pH 6, mobile phase A) and 100% methanol (mobile phase B). The elution of DMB-DP3 was performed with a linear isocratic method of 80 %: 20 %, mobile phase A: mobile phase B over 6 minutes. The separation was monitored by photodiode array detector (373,

303 and 250 nm) and fluorescence detector (RF-10A), (excitation 373, emission 484 nm).

Multiple reaction monitoring (MRM) Analysis

DMB-DP3 and DMB-DP4 were subjected to analysis by electrospray UPLC-MS using an Acquity UPLC Waters system and a Quattro Premier XE (Waters corporation, USA) mass spectrometer and an Acquity UPLC BEH C18 column (2.1 x 100 mm), the mobile phases used were: ammonium formate (5 mM, mobile phase A) and methanol (mobile phase B), with a flow rate of 0.3 ml/min and isocratic method of 80% mobile phase A: 20% mobile phase B. The peaks and masses were integrated using Masslynx software. The source temperature was set at 120 °C. MRM transitions acquired at unit resolution in both the Q1 and Q3 quadrupoles to maximise specificity. Cone voltage was adjusted to 25 V while collision energy was adjusted to 20 V for DMB-DP4 and 30 V for DMB-DP3 using positive ionisation mode.

2.2.2.5. Analysis of the DMB-DP3 polysialylation reaction kinetics (Michaelis-Menten kinetics).

To determine the kinetics of the DMB-DP3 polysialylation reaction by human ST8SiaII, activity was determined under the following conditions: ST8SiaII (250 ng/µl), $MgCl_2$ (5 mM), CMP-Neu5Ac (0.5 mM) and sodium cacodylate buffer (pH 6.7, 0.1 M) and varying amounts of DMB-DP3, total volume was adjusted to 20 µl. The reaction mixture was incubated at 25° C for the indicated times. The reactions were terminated by adding Tris–HCl (100 mM, pH 8.0) / EDTA (5 mM). Samples were analysed using DNAPac PA-100 analytical anion exchange column as mentioned before (Section 2.2.2.4.3).

2.2.2.6. Analysis of the assay sensitivity and linearity

In order to determine whether a direct relationship could be established between the concentration of the ST8SiaII inhibitor and DMB-DP3 polysialylation product (DMB-DP4) peak area, known concentrations of CMP inhibitor were incubated with the reaction as described above (Section

2.2.2.4.3). The product DMB-DP4 peak area was recorded for each point and plotted against the corresponding CMP concentration.

B) Cell-based chromatographic assay of polyST inhibition

2.2.3. Cell Lines

Human SH-SY5Y neuroblastoma cells, OSC-19 human oral squamous cell carcinoma, C6-STX glioma cells were obtained from the cell culture facility at the Institute of Cancer Therapeutics, University of Bradford. The methodology for the transfection of C6 cells with pcDNA3-STX plasmid inserted with cDNA encoded full length human STX, has been reported previously [66]. This was carried out by collaborator (Dr. Minoru Fukuda) at the Sanford-Burnham Institute, La Jolla, CA., USA.

SH-SY5Y cells were maintained in minimum essential medium (MEM) and nutrient mixture F-12 Ham (1:1), supplemented with 10% foetal bovine serum, 1% sodium pyruvate and 1% glutamine. OSC-19 cell lines were maintained in RPMI medium supplemented with 10% foetal bovine serum, 1% sodium pyruvate and 1% glutamine while C6-STX glioma cells were maintained in MEM Alpha eagle with ultra-glutamine-I, deoxyribonucleoside and ribonucleosides supplemented with 10% foetal bovine serum. All cell lines were maintained in a humid atmosphere of 5% CO2 and 95% air at 37 °C.

2.2.3.1. Cell maintenance

Cell lines were routinely maintained as monolayer cultures in T75 flasks, where the medium was changed every 4-5 days. As cells reached 60-85% confluency, they were washed with PBS and 5 ml of trypsin was added. Cells were then incubated for 5-10 minutes at 37ºC for detachment. After detachment, 5 ml of fresh medium was added and the cell suspension was centrifuged at 1000 g for 5 minutes. The supernatant was discarded and the cell pellet was re-suspended in fresh medium. Cells were stocked at early passages and discarded every 8 passages thereafter.

2.2.3.2. Cell counting

As cells were detached and re-suspended in a fresh medium, 10 µl of the cell suspension was placed on a hematocytometer chamber, according to the procedure suggested by Sigma (Cook Book Sept 2010 Volume 12). Cells were counted under an inverted microscope at x20 magnification in ten areas of the chamber. Cell counts were expressed as (mean of 10 counts) x 10^4 cells/ml.

2.2.4. Growth curve of SH-SY5Y cells

After cells were counted, the cell suspension was diluted in order to have an appropriate amount of medium and seeding density (1.5 x 10^5 cell/ flask). Five flasks of each cell line were seeded with the same density. The flasks were incubated in a humid atmosphere of 5% CO_2 and 95% air at 37 °C. The duplicate plates were counted every 24 hours. The results were plotted on a log-linear scale. The population doubling time was determined by identifying a cell number along the exponential phase of the curve, tracing the curve until that number has doubled, and calculating the time between the two.

2.2.5. Seeding of cell culture dishes

Cells were seeded at the density of 2 x 10^5 cell/well in a six-well plate and incubated for 48 hours at 37°C in a 5% CO_2 humidified atmosphere.

2.2.6. Cell treatment

After 48 hours incubation, different concentrations of ST8SiaII inhibitors (250, 125 and 25 µM) were added in FBS-free medium (Endo-N protocol) or FBS-containing medium (mild acidic hydrolysis protocol) and incubated for 24 hours at 37° C in a 5% CO_2 humidified atmosphere.

2.2.7. Cleavage of polySia from the cell surface

Two different protocols were used to remove polySia from the cell surface, namely using Endo-N and mild acidic hydrolysis:

2.2.7.1. Endo-N treatment

SH-SY5Y, OSC-19 and C6-STX cells were treated with Endo-N (Abcys, France) (0.5, 1 and 3 µg/ml) for (24 hours), one well was used as negative control where no Endo-N was added. After 24 hours media were collected for analysis.

2.2.7.2. Mild acidic hydrolysis

SH-SY5Y, OSC-19 and C6-STX cells were collected by trypsinisation followed by centrifugation for 5 minutes at 1000 g. Cell pellets were treated with 100 µL of 0.5% Igepal CA-630 followed by incubation at 37 °C for 1 hour and vortexing for 5 minutes in order to solubilise polySia from the cell surface. The insoluble material was removed by centrifugation and the supernatant was used for analysis.

2.2.8. Sialic acid labelling

For determination of total Neu5Ac, samples were hydrolysed in TFA (0.1 M) for 2 h at 80 °C. TFA was removed under vacuum and the residue was incubated with the DMB reagent for 24 h at 4 °C as described previously (Section 2.2.2.1).

2.2.9. HPLC analysis

2.2.9.1. Mixed phase column-HPLC-fluorescence detector (FD) analysis of total sialic acids released from SH-SY5Y cell surface

A Waters 2695 Alliance HPLC system operated by Masslynx software was connected with fluorescence (RF-10A) (Shimadzu, Japan) and photodiode array detectors (Waters 2996) (Waters, UK) and used to analyse samples. An Obelisc™ HPLC column (Sielc technologies, USA) column (with multiple separation mode; normal phase HPLC and ion exchange HPLC) was used for the separation of DMB labelled sialic acid separated from the cell surface and other DMB-labelled components of the cell. DMB fluorescence (excitation 373 nm/emission 456 nm) was monitored with a fluorescence

detector. The mobile phases used were: A (5 mM Ammonium formate) and B (100% acetonitrile) with the following gradient (Table 2.10).

Table 2.10 Gradient used for the HPLC analysis of total sialic acids released from SH-SY5Y cell surface(Flow rate 0.8 ml/min).

Time (minutes)	% Mobile phase A	% Mobile phase B
0	0	100
13	13	87
14	0	100
27	0	100

2.2.9.2. Multiple reaction monitoring (MRM) analysis

DMB-DP1 was subjected to analysis by electrospray UPLC-MS using Acquity UPLC Waters system and Quatro premier XE (Waters corporation, USA) mass spectrometer as described above. Cone voltage was adjusted to 25 V while collision energy was adjusted to 20 V using positive ionisation mode.

In the MRM assay, on the basis of the channels established in the present experiments, 5 µl of labelled samples (using the aforementioned conditions) proved to be sufficient for quantitative analysis of the inhibition of polySia synthesis caused by ST8SiaII inhibition.

2.2.10. Immunofluorescence analysis of polySia-NCAM

2.2.10.1. Coating of cell culture dishes and cell fixation

SH-SY5Y, OSC-19 and C6-STX cells were seeded on cover slips onto six-well plates (2 x 10^4 cell/well). Dishes were incubated for approximately 24 h at 37 °C, allowing cells to adhere and spread. For the detection of polySia inhibition with ICT-3128, cells were treated with different concentrations of inhibitor and incubated for 24 hours. Cells were washed twice with PBS and then fixed by incubating in 100% methanol (chilled at -20°C) at room temperature for 10 min. The cells then were allowed to air-dry for 10 minutes at room temperature. Cells were rehydrated with PBS for 15 minutes (three washes of 5 minutes each).

2.2.10.2. Blocking and incubation

Cells were incubated with 1.5% normal mouse serum prepared in PBS (NRS-PBS) for 10 min to block unspecific binding of the antibodies. After removal of serum, cells were immunolabelled with mouse anti-polySia antibody (clone: mAb 735, 15 µg/ml) prepared in 1.5% NRS-PBS for 30 minutes at room temperature for the detection of polySia expression. Cover slips were then washed three times in PBS for 5 minutes followed by incubation with TRITC-conjugated rabbit anti-mouse (dilution 1:50) secondary antibody prepared in PBS for 30 minutes in darkness. A control sample was carried out by adding the secondary antibody only, to establish background fluorescence and non-specific staining of the primary antibody.

2.2.10.3. Counter staining and mounting

Cover slips were washed three times in PBS for 5 minutes and then mounted with Vectashield hardset fluorescent mounting medium containing DAPI. The resulting slides were stored at 4ºC until analysis. Samples were examined by fluorescence microscopy.

2.2.11. Statistics

All experiments were repeated three times independently unless otherwise specified. Statistical analyses were performed using Excel and GraphPad Prism software. Differences between two groups were evaluated with Student's t test (Two tailed) where the P value significance is: P value (P) >0.05 was deemed not significant, $P < 0.05$ * was statistically significant, $P < 0.01$ ** and $P < 0.001$*** were statistically highly significant.

2.3. Results and discussion

Section A) Cell-free chromatographic assay for analysis of ST8SiaII activity

2.3.1. Synthesis of DMB-DP3 and validation of labelling protocol

2.3.1.1. Gel electrophoresis and western blot analysis

Western blot analysis is an established technique for the analysis of NCAM polysialylation that has been used in several previous studies [132,136]. Western blot assay for polysialylation analysis utilises anti-polySia antibody (m735). NCAM is used as sialic acid acceptor and CMP-Sia is used as sialic acid donor.

Here, western blot analysis has been used as a pilot experiment in order to determine the ability of recombinant human ST8SiaII enzyme to polysialylate NCAM *in vitro* and as a basis for comparison with the newly developed cell-free HPLC assay (see section 2.3.9).

NCAM polysialylation by human ST8SiaII

Western blot analysis of NCAM polysialylation by human ST8SiaII illustrated the ability of the enzyme to add polySia to the NCAM molecule. PolySia-expressing NCAM migrated as a large molecular mass band (above 250 kDa, indicating a range of different polySia chain lengths). A second polySia-NCAM band was also detected just below the original band, which could possibly be explained by the polysialylation of the ST8SiaII enzyme itself, since there is precedent in the literature for both ST8SiaIV and ST8SiaII enzymes themselves being modified by polySia chains, a process known as auto-polysialylation (Figure 2.18) [112,137].

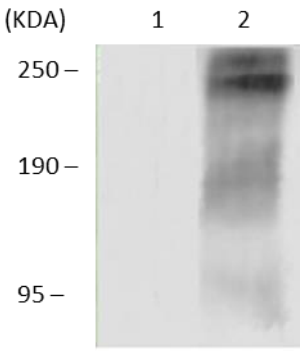

Figure 2.18 Polysialylation of NCAM by human ST8SiaII enzyme.Lane 1 represents the negative control (without the ST8SiaII enzyme), lane 2 represents the polysialylation reaction. Blot is representative of three independent experiments.

2.3.1.2. Validation of DMB labelling protocol using HPLC analysis

The results obtained from western blot analysis confirmed that recombinant human ST8SiaII can polysialylate NCAM *in vitro*. However, this method cannot easily be used to screen large numbers of polyST inhibitor compounds since it is time consuming and non-quantitative. HPLC separation in conjugation with fluorescence detection (HPLC-FD) in contrast, potentially enables high throughput, sensitive and quantitative detection of polyST activity. As described earlier, DMB-DP3 is a potential acceptor in place of NCAM. HPLC was used for two purposes: first to purify labelled DMB-DP3 and provide pure material that is efficiently polysialylated by the human ST8SiaII enzyme, and secondly to detect polyST activity (and therefore polyST inhibitor activity) by determining the percentage of DMB-DP3 converted to DMB-DP4.

PolySia chains (in the form of commercially-available colominic acid) and sialic acid were first labelled and analysed in order to validate the labelling and HPLC analysis techniques. HPLC was then used to determine qualitatively and quantitatively the conversion of DMB-DP3 into DMB-DP4.

2.3.1.2.1. Labelling and analysis of sialic acid

Sialic acid was first labelled in a small scale and analysed by anion exchange–HPLC system in order to validate the labelling conditions and to choose the appropriate conditions for HPLC analysis before going any

further with the polySia and DP3 labelling and analysis. This would additionally minimise the cost of the study since sialic acid is much cheaper than polySia and DP3-Sia.

It was found that the procedure used for sialic acid labelling, which was performed according to a previously published study [132], were appropriate and that the labelled DMB-sialic acid can be effectively detected and separated from the other impurities using a DNAPac PA100 anion exchange column in conjugation with fluorescence detector RF-10 AXL (excitation 373 nm/emission 456 nm), as described in the materials and methods section, which provided a highly sensitive detection. It was found that the peaks could also be detected using photodiode array detector at 303, 250 and 373 nm (Figure 2.19).

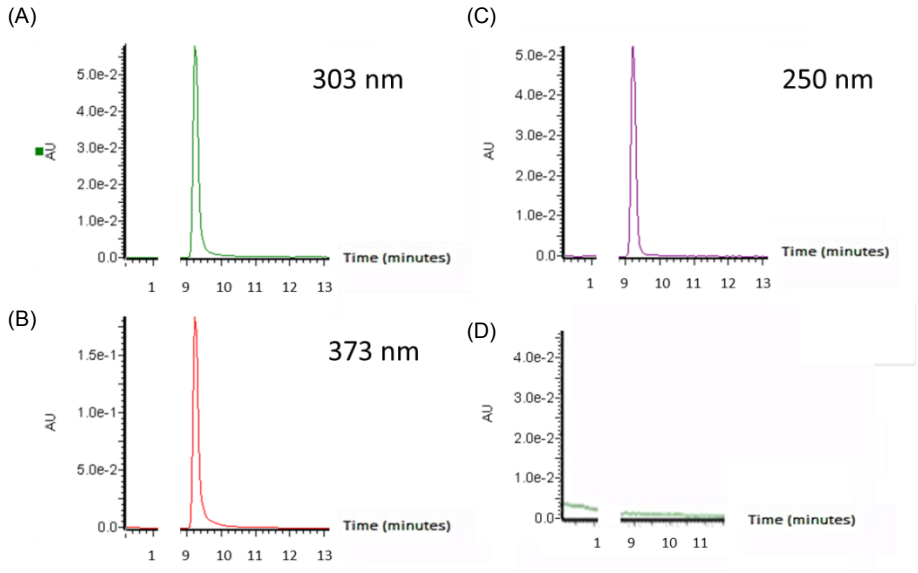

Figure 2.19 Sialic acid labelling reaction detected by photodiode array detector at 303 nm (A), 373 (B), 250 (C) and blank (D).

2.3.1.2.2. Labelling and analysis of polySia chains

2.3.1.2.2.1. Analysis of polySia chains

In order to determine the separation efficiency of the anion exchange-HPLC system and the detectability of the DMB-polySia labelled chains by fluorescence, a polySia standard (colominic acid, partially hydrolysed and purified capsular polysaccharide from *E. coli* K1) was labelled with DMB at

4°C for 48 hours (Figure 2.20A). Separation of polySia according to the chains length was obtained using anion exchange column chromatography and fluorescence detection as described in the material and methods section. The separation of the polySia chains via this system depends on the difference in the charge: the DNAPac PA-100 analytical anion exchange column was used where the stationary phase is positively charged (microbead alkyl quaternary ammonium functionalised latex). The longer the polySia chain, with the higher negative charge, the higher the interaction with the stationary phase, and thus the later the elution from the column. It was found that by using a gradient of 5 M ammonium acetate as mobile phase, this analytical system was able to separate different chain lengths of polySia with excellent resolution (Figure 2.20B). However, it was not possible to obtain the mass associated with each peak, since the high ammonium acetate concentration of the mobile phase is incompatible with a mass spectrometer, a hurdle that has not been solved in any of the previously published studies. So far, detection of molecular weight has only been achieved by western blot or estimated by counting the number of peaks; the first eluted peak is DMB-DP1 then the second is DMB-DP2 and so on [132,138,139].

(A)

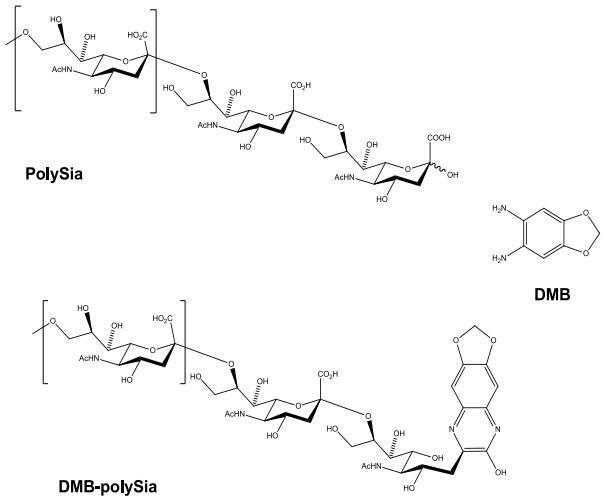

(B)

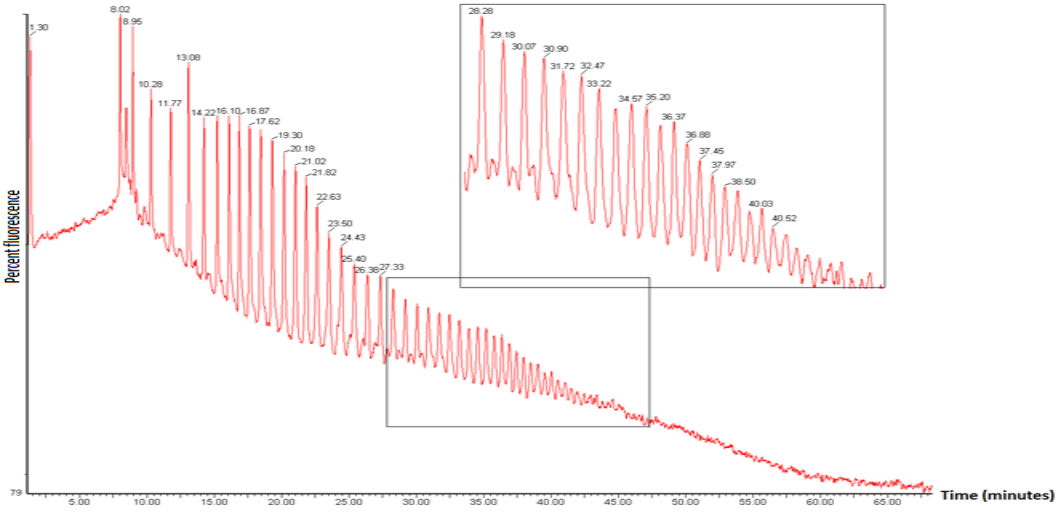

Figure 2.20 Labelling reaction of polySia with DMB chemical reactions (A). PolySia (colominic acid) labelling with DMB as analysed by using HPLC-FD, DNAPac© PA-100 analytical anion exchange column (B).

2.3.1.2.2.2. Optimisation of polySia derivatisation reaction conditions

In order to determine the optimum conditions for the polySia-DMB labelling reaction, different temperatures and incubation times (Table 2.11) were explored. The efficiency of labelling was then determined after HPLC-FD analysis (the efficiency of labelling was determined by calculating the

percentage of the total peak area of each incubation condition compared to the total peak area produced by incubating the reaction for 30 minutes at 50°C). It was found that incubating the reaction at 50°C for 30 minutes resulted in the highest total peak area when compared to incubation at 4°C, for either 24 or 48 hours. However, short polySia chains were found only when the incubation was performed at 4°C, as recorded by the absence of any peaks after short elution time (between 1.3 and 10.5 minutes) when the reaction was incubated at higher temperature (Figure 2.21A, B and C). This suggests that the optimum conditions for polySia derivatisation reaction that does not result in the breakdown of short chains, is by incubating at 4°C for 48 hours.

Table 2.11 Different conditions for the polySia derivatisation reaction. Relative peak areas normalised to the peak area obtained for the 30 min/50°C reaction conditions. These results represents mean of two duplicate independent repeats.

Incubation conditions	Relative peak area	Absolute peak area
30 minutes 50°C	% 100	737537
48 hours 4°C	% 54.61 ± 7.2	402770
24 hours 4°C	% 13.7 ± 5.4	101058

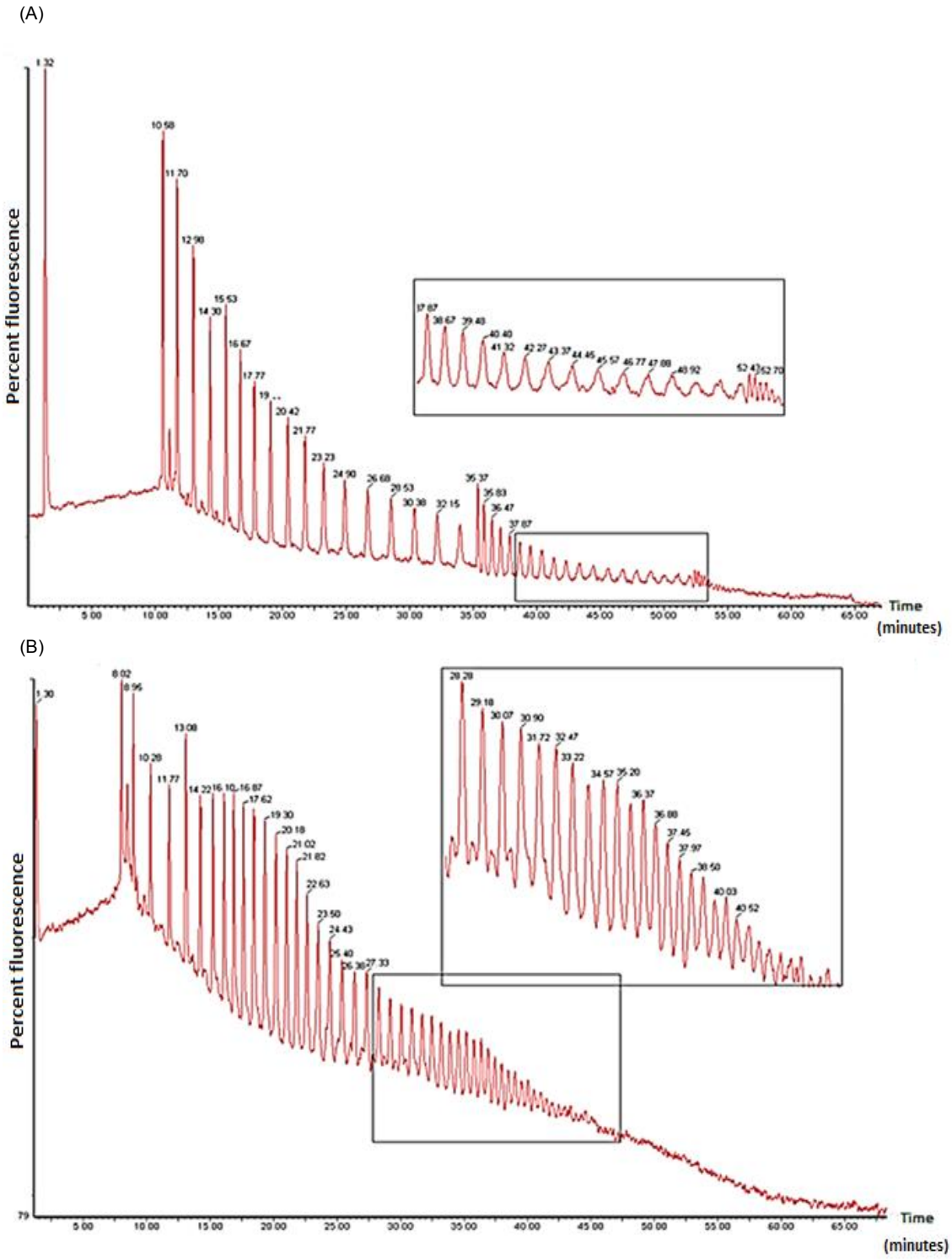

Figure 2.21 HPLC chromatograms showing PolySia (colominic acid) labelling with DMB, analysed using anion exchange-HPLC after 30 minutes at 50°C (A) and 48 hour at 4°C (B).

(C)

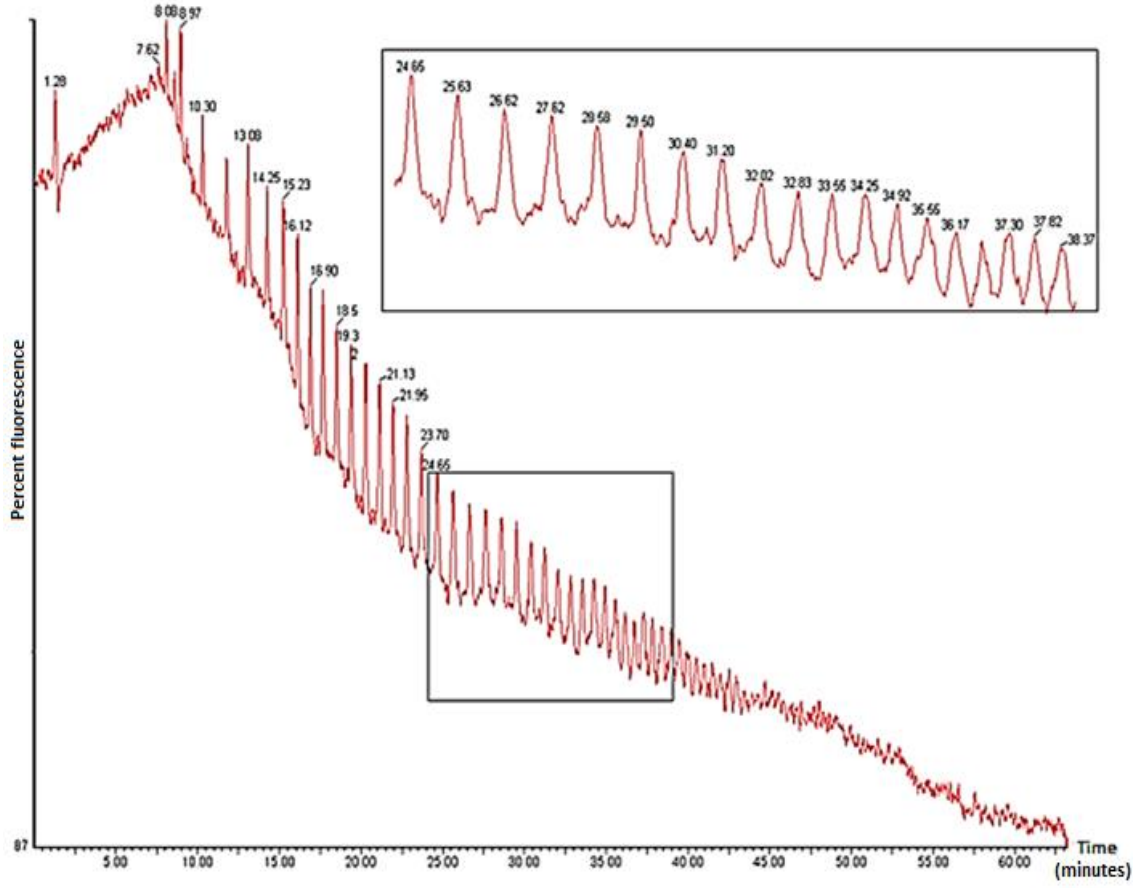

Figure 2.21 C. PolySia (colominic acid) labelling with DMB using Anion exchange-HPLC 24 hours at 4°C. . PolySia chains peaks start at 8.08 minute when the incubation is performed at 24°C in (B-C) while at (A) smaller chain length are not detected.

2.3.1.2.2.3. Optimisation of polySia HPLC analysis conditions

An attempt to optimise the HPLC conditions (running time and gradient) for analysis of polySia chains was performed. A simpler gradient with a shorter running time (60 minutes instead of 240 minutes) was used and the limit of resolution of anion exchange-HPLC-FD method was examined; shortening the analysis time would be useful to analyse the effect of different inhibitors on the distribution of the chain length of polySia. Although studying this effect of polyST inhibitors was not the focus of this particular aspect of the study, it is useful to optimise the assay for different possible applications.

Although the new method was able to separate short chains, it did not show the full separation achieved by using the previous longer gradient, which means that the short gradient would not be ideal for the analysis of the effect of polyST inhibitors on polySia chain length distribution (Figure 2.22). No further work was carried out on this optimisation since it was not expected that the DMB-DP3 would produce a wide range of different polySia acid chain lengths as suggested by previous study [109], which was approved during the analysis of the DMB-DP3 polysialylation product.

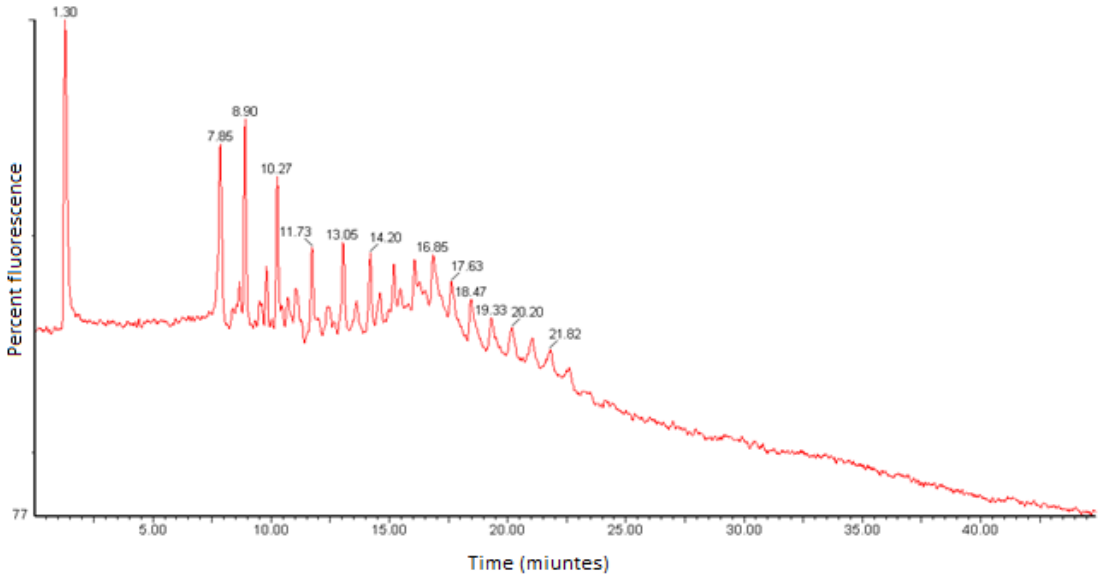

Figure 2.22 Optimisation of polySia anion exchange-HPLC analysis conditions aiming to reduce the running time showing less efficient separation from the previously used longer gradient.

2.3.1.2.3. Labelling of DMB-DP3

The same conditions used for polySia (colominic acid) chain labelling were successfully used for labelling DP3. However, for the labelled DMB-DP3 to be used for the analysis of different polysialyltransferase inhibitors, we had the additional requirement of high purity. Therefore the labelling step had to be followed with a highly efficient purification step.

2.3.2. Purification of DMB-DP3

2.3.2.1. Characterisation of impurities using mass spectrometry

Two different HPLC separation methodologies were used to obtain highly pure DMB-DP3: RP-HPLC and anion exchange-HPLC. These systems were chosen for the purification of the compound after detailed analysis of the impurities to be removed was performed using RP-HPLC-MS. The mobile phases used were: mobile phase A (1% methanol, 0.01% formic acid (pH 3.5) and mobile phase B (55% methanol, 0.01% formic acid, pH 5.8). It was found that the DMB-DP3 impurities were mainly: sialic acid monomer (DP1, molecular weight 309.2), DMB-DP1 (molecular weight 424.3) and [DMB-DP3 - H_2O] (molecular weight 988.3). [DMB-DP3 - H_2O] is thought to be the lactonised form of DMB-DP3, which has been reported previously [140]) (Figure 2.23). These impurities have different charges and different polarity, caused by carboxylic acids in the different chemical structures, which allows both RP- and anion exchange-HPLC system to separate them effectively.

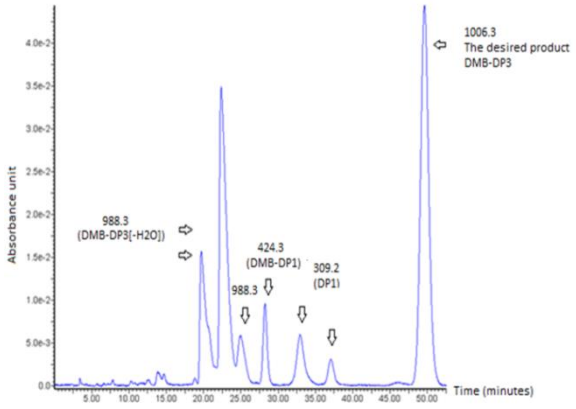

Figure 2.23 Crude DMB-DP3 as detected by LC/MS at 373 nm.The numbers over the peaks represent the detected mass/charge (*m/z*) ratio.

2.3.2.2. Optimisation of DMB-DP3 purification conditions

Reversed phase system

Three systems were used in order to determine the optimum conditions for DMB-DP3 purification using RP-HPLC (Table 2.12). The purification of DMB-DP3 dissolved in distilled water (1 µl DMB-DP3: 1000 µl water) was achieved first by RP-HPLC system where the mobile phases used were: 1% methanol, 0.01% formic acid (pH 3.5) (mobile phase A) and 55% methanol, 0.01% formic acid (mobile phase B), the peaks were analysed by mass spectrometry. It was found that both lactonised and unlactonised forms of DMB-DP3 were detected (Figure 2.25A).

Table 2.12 Conditions explored for DMB-DP3 purification by RP-HPLC.

System	% Mobile phase A	% Mobile phase B	Method
1	1% methanol, 0.01% formic acid (pH 3.5)	55% methanol, 0.01% formic acid (pH 5.8)	Isocratic separation of 85% mobile phase A and 15% mobile phase B for 50 minutes
2	5 mM Ammonium formate buffer (pH 6)	55% methanol, 0.01% formic acid (pH 5.8)	Isocratic separation of 85% mobile phase A and 15% mobile phase B for 50 minutes
3	5 mM Ammonium formate buffer (pH 6)	55% methanol (pH 7.2)	Isocratic separation of 90% mobile phase A and 10% mobile phase B for 50 minutes

The formation of the lactonised form of DMB-DP3 during the purification process was previously reported in more than one study [132,140,141] and was attributed to the acidic conditions (Figure 2.24). In order to prevent the lactonisation of DMB-DP3 by reducing the mobile phase pH: Mobile phase A was changed from 1% methanol, 0.01% formic acid (pH 3.5) to ammonium formate buffer (pH 6). However, it was found that the lactonisation of DMB-DP3 was not improved using this system (Figure 2.25B).

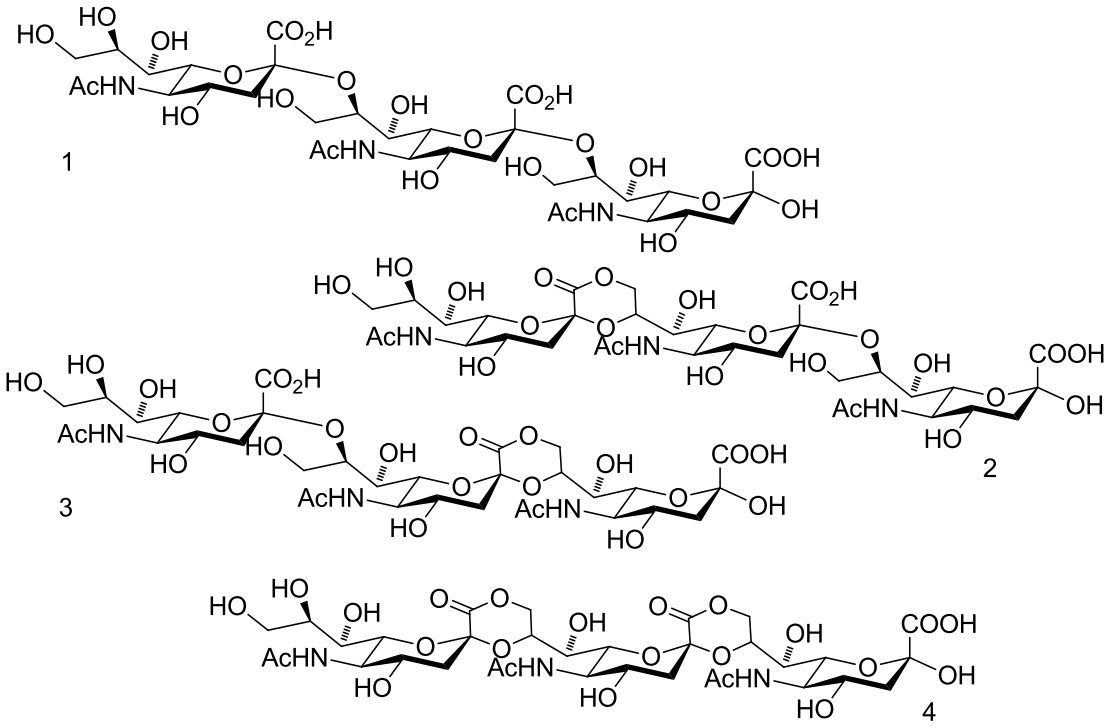

Figure 2.24 DP3 lactonised forms. Structures of unlactonised alpha-2,8-linked sialic acid trimer (1), 1-monolactone trimer (2), 2-monolactone trimer (3), and dilactone trimer (4) [142]

A third attempt aimed at inhibiting the DMB-DP3 hydrolysis and lactonisation was performed by changing mobile phase B from 55% methanol, 0.01% formic acid (pH 5.8), to 55% methanol only (pH 7.2) and changing the gradient from 85% A, 15% B to 90% A, 10% B so better separation could be obtained. This system was found to successfully minimise the lactonisation of the DMB-DP3 (calculated by % peak area of lactonised form compared to the total peak area). Although, lactonisation was not completely abolished, it was found that changing the gradient also resulted in a more efficient separation (Figure 2.26). A single fraction containing the DMB-DP3 was collected between 11 and 15 minutes. Fractions from several runs were pooled and freeze dried. The dried DMB-DP3 was dissolved in water to form 200 µM solution and stored at -20°C.

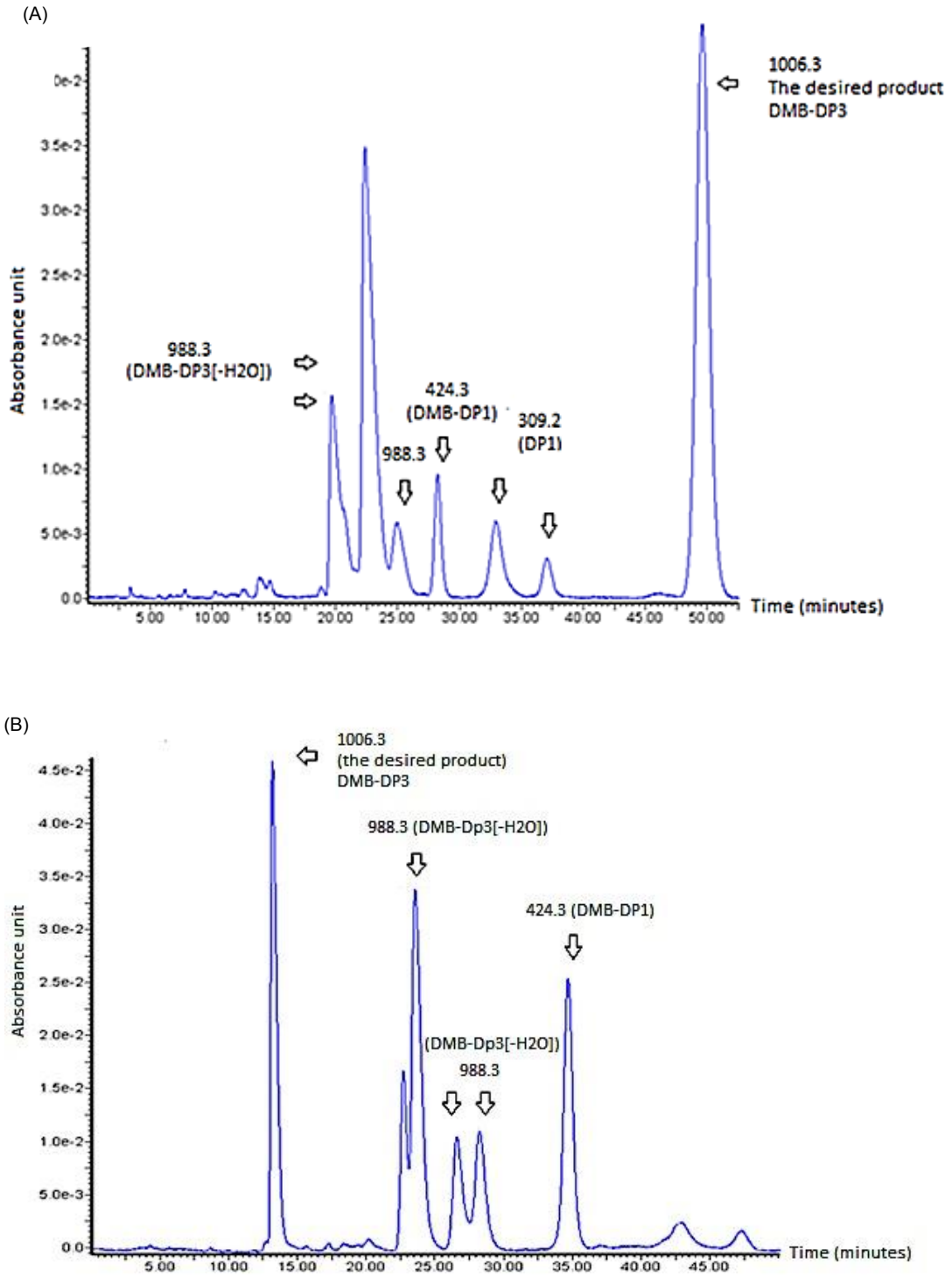

Figure 2.25 Different systems used for the purification of DMB-DP3. In the first system the used mobile phases were: 1% methanol, 0.01% formic acid (pH 3.5, mobile phase A) and 55% methanol, 0.01 formic acid (pH 5.8, mobile phase B) (A), in the second system the used mobile phases were: Ammonium formate buffer (pH 6, mobile phase A) and 55% methanol, 0.01 formic acid (pH 5.8, mobile phase B) (B).

(C)

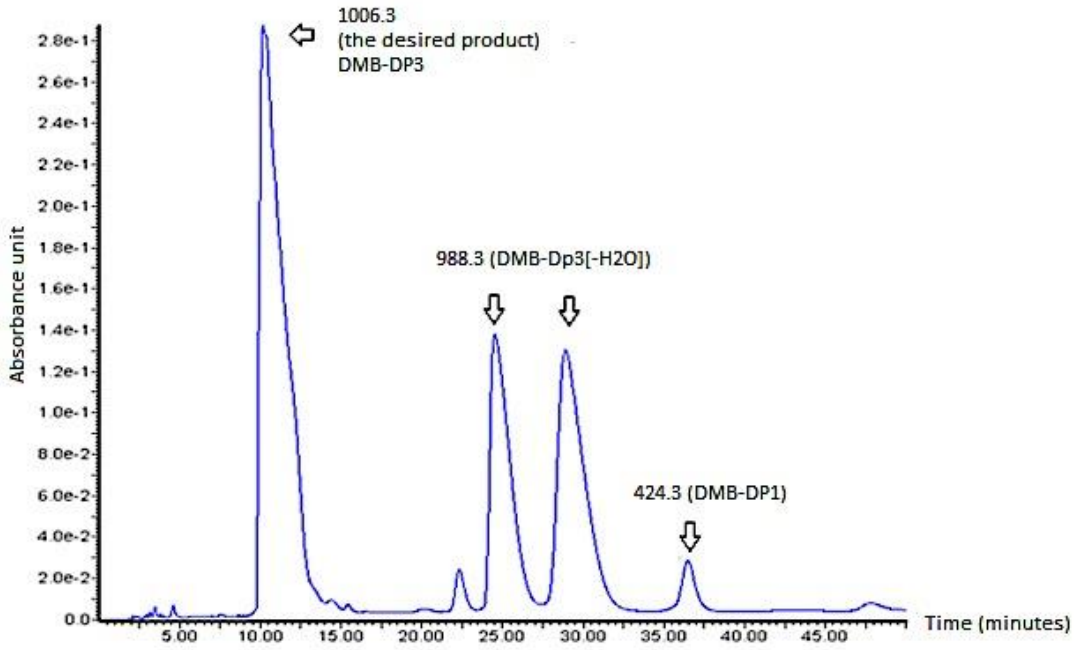

Figure 2.26 Third RP-HPLC system used for the purification of DMB-DP3, the used mobile phases were: ammonium formate buffer (pH 6, mobile phase A) and 55%methanol (pH 7.2, mobile phase B) (C).

Anion exchange HPLC system

DMB-DP3 purification using anion exchange-HPLC was achieved using a DNAPac PA-100 analytical anion exchange column, 100% water (mobile phase A) and 5 M ammonium acetate buffer (pH 7.4, mobile phase B). Three peaks were detected using fluorescence detector. DMP-DP3 was determined to be the peak with the retention time of 9.42 min (Figure 2.27A), as confirmed by comparing its absorbance spectrum and retention time with DMB-DP3 standard (separated by RP-HPLC and its molecular weight confirmed using MS) since the mobile phase used in the anion exchange HPLC system is not compatible with the MS (5 M ammonium acetate) and therefore the DMB-DP3 peak cannot be detected directly by mass spectrometry.

Although the peaks appeared well resolved when using fluorescence detection, when examined by the photodiode array detector at 303 nm and 373 nm, it was found that there are in fact two peaks that are merged under the peak representing the DMB-DP3 (Figure 2.27A). In order to separate these peaks the gradient was changed (Table 2.13), which resulted in complete separation of the two peaks (Figure 2.27B, 2.27C). The peak representing DMB-DP3 was collected then from several runs and freeze dried, the solid was weighed and dissolved in distilled water to form a 200 µM solution and stored at -20 °C (Figure 2.27D).

Table 2.13 Mobile phases gradient and flow rate for DMB-DP3 purification using anion exchange–HPLC system.

Time (min)	% Mobile phase A	% Mobile phase B	HPLC Flow rate (ml/min)
0	100	0	1
5	100	0	1
25	98	2	1
30	100	0	1

(A)

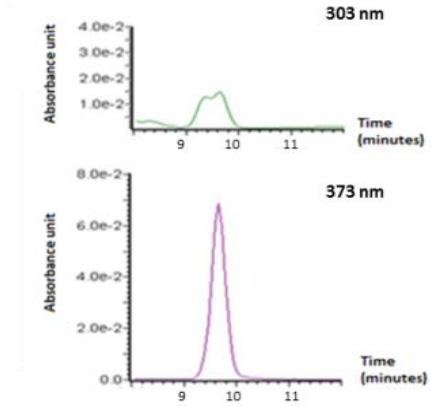

(B)

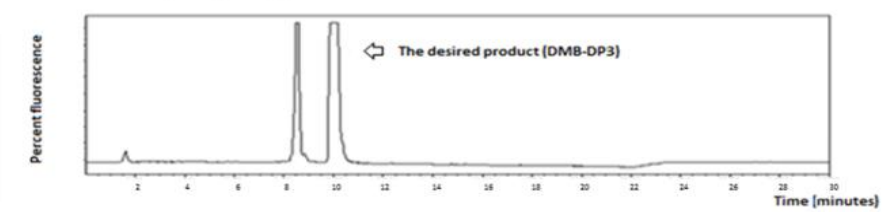

(C)

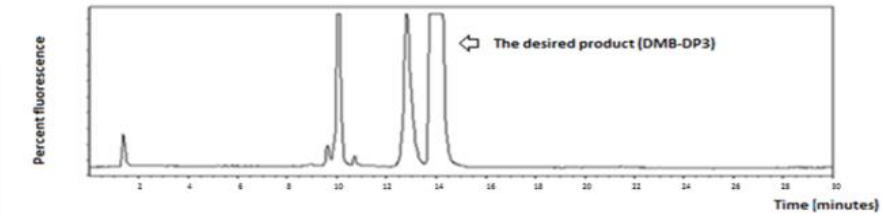

(D)

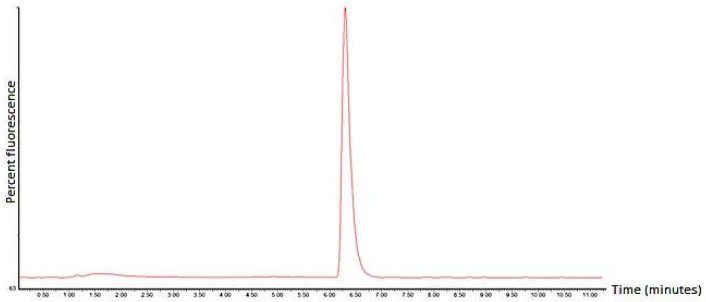

Figure 2.27 DMB-DP3 purification by anion exchange-HPLC. The peak representing DMB-DP3 at 9.42 minutes retention time using fluorescence detector was found to be two merged peaks when detected by photodiode array at 303nm (A). Changing the gradient that resulted in merged peaks (B) to the gradient described in table 2.13, enabled complete separation of the two merged peaks (C). (D) Purified DMB-DP3 by anion exchange-HPLC as observed by HPLC-FD.

2.3.3. Evaluation of polysialyltransferase (ST8SiaII) enzyme activity

After purification of DMB-DP3 was successfully achieved, the percentage of purity was determined. It was found that using the optimized methods the synthesised DMB-DP3 had a purity of ≥ 99%. The purity of the synthesised compound was calculated by dividing the peak area of the DMB-DP3 by the total peak area of all the detected peaks multiplied by 100. Both DMB-DP3 purified by RP- and anion exchange HPLC was evaluated for their potential to act as acceptor for polysialylation reactions catalysed by human ST8SiaII. The incubation reaction was first performed according to the method used for the bacterial enzyme in a previously published paper [132].

Human ST8SiaII incubation with the DMB-DP3 purified by RP-HPLC

To determine the activity of human ST8SiaII, the recombinant enzyme was incubated at 25°C for 24 hours in 20 µl volume containing, Tris HCl (50 mM, pH 8), potassium chloride (25 mM), magnesium chloride (20 mM), 5% glycerol, DMB-DP3 (50 µM), sodium cacodylate (10 mM, pH 6.7), CMP-Neu5Ac (1 mM) and manganese chloride (10 mM). The reaction was quenched using a 10-fold dilution of Tris-HCl (pH 8.0, 100 mM)/ EDTA (5 mM). The results were compared with a negative control (without the addition of the ST8SiaII enzyme). It was found that using these conditions, which are the same conditions used with the bacterial enzyme in previously published paper [109], a very small yield of DMB-DP4 product was observed (Figure 2.28A). As previously discussed in the introduction, although mammalian and bacterial PolySTs catalyse the same reaction, different cellular environments and different acceptor substrates are involved and this is likely to be the cause of the difference in the yield DMB-DP4. In an attempt to improve the efficiency of the reaction, the DMB-DP3 concentration was increased from 50 µM to 100 µM and the reaction was again incubated at 25°C for 24 hours and then analysed by anion exchange HPLC.

Although the DMB-DP4 yield was clearly improved (35% conversion) (Figure 2.28B), the efficiency of the reaction was still sub-optimal. These conditions

utilise high concentrations of DMB-DP3 and involve a long incubation time. Ideally, a rapid screen is required, utilising minimal DMB-DP3 and other reagents (e.g. ST8SiaII) to keep costs to a minimum and to enable larger numbers of compounds to be screened as efficiently as possible. To sum up, these conditions were not ideal for high throughput analysis of ST8SiaII inhibitors. Therefore optimisation of the reaction buffers, DMB-DP3 concentration and incubation time was performed in order to determine the most efficient conditions for the enzyme activity.

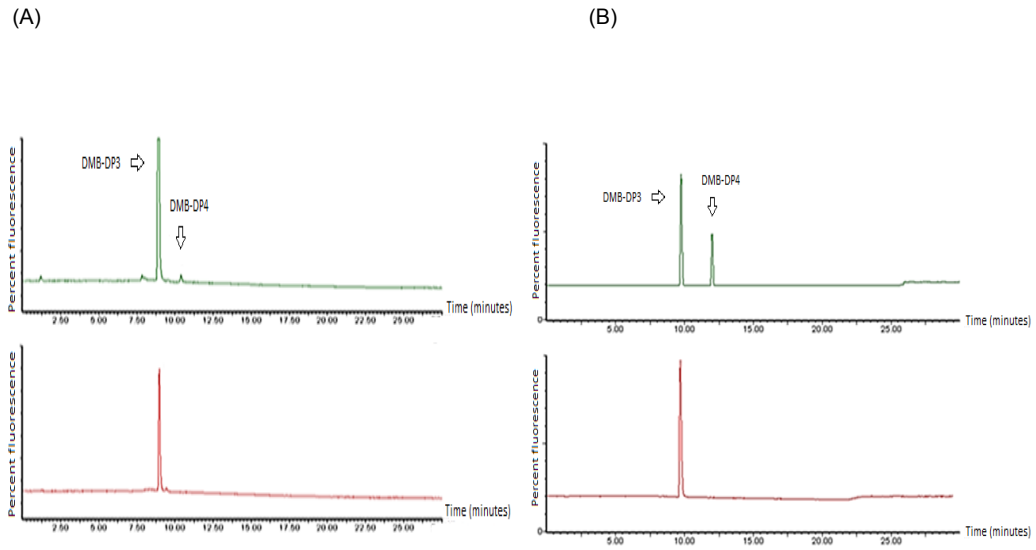

Figure 2.28 Incubation reaction of RP-HPLC-purified DMB-DP3 with human ST8SiaII. (A) Incubation reaction of 50 µM RP-HPLC-purified DMB-DP3 with human ST8SiaII after 24 hours incubation (upper chromatogram), negative control of the reaction (lower chroatogram). (B) Incubation reaction of 100 µM RP-HPLC-purified DMB-DP3 with human ST8SiaII after 24 hours incubation (upper chromatogram), negative control of the reaction (lower chromatogram).

2.3.3.1. Optimisation of the ST8SiaII incubation reaction buffers

A second protocol of the incubation reaction was performed by using human ST8SiaII (250 ng/µl), DMB-DP3 (100 µM), $MgCl_2$ (5 mM), CMP-Neu5Ac (0.5 mM) and sodium cacodylate buffer (pH 6.7, 0.1 M) only, with the same incubation conditions previously described in protocol 1 (section 2.3.3). It was found that the reaction still proceeds after the removal of the remaining components (Tris HCl, KCl, $MnCl_2$ and glycerol), which suggests they are not essential for enzyme activity in the absence of NCAM (Figure 2.29).

Comparing the results of both protocols using the same DMB-DP3 concentration and the same incubation time revealed that there is no major difference in the peak area obtained (and thus product produced) between the two protocols.

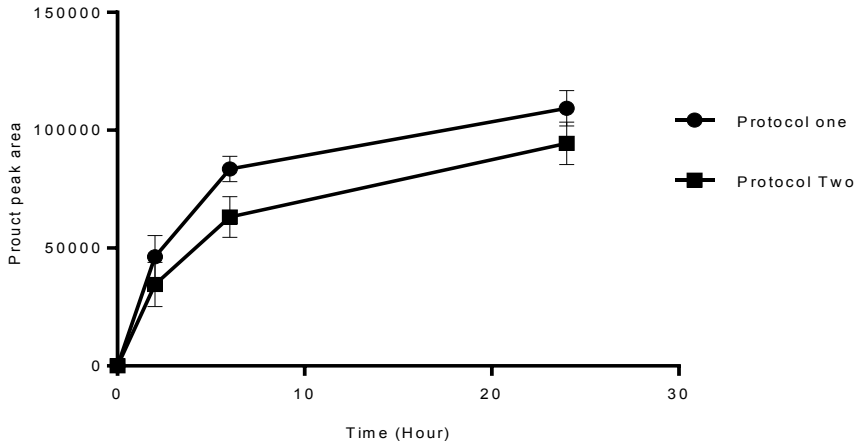

Figure 2.29 Optimisation of the DMB-DP3/ST8SiaII incubation reaction buffers. The upper curve shows the peak area of DMB-DP4 produced using protocol 1; the lower curve shows the peak area of DMB-DP4 produced using protocol 2. These are duplicate results representative of two independent experiments.

2.3.3.2. Determination of the optimum concentration of DMB-DP3

Protocol 2 (with the optimum buffer composition) was repeated using a concentration range of DMB-DP3 from 10-100 μM and the same conditions as outlined previously, with incubation times of 2 and 24 hours. Both 20 μM and 100 μM DMB-DP3 concentrations showed no considerable difference in the DMB-DP4 product peak area after either 2 or 24 hours incubation (Figure 2.30).

Despite the optimisation of the RP-HPLC purified DMB-DP3 incubation reaction, still the efficiency was lower than the required; the product DMB-DP4 at early incubation time (2 hours) was deemed insufficient to enable use for high throughput assessment of potential small molecule polyST inhibitors. The DMB-DP3 to DMB-DP4 conversion rate of less than 5% results in a very small peak area for DMB-DP4 and thus of limited utility in screening compounds.

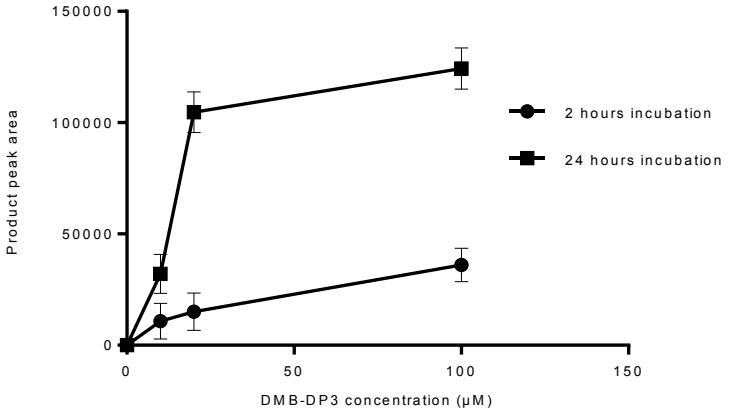

Figure 2.30 Determination of the optimum concentration of DMB-DP3. The upper curve shows the peak area of DMB-DP4 after 24 hours incubation using 10, 20 and 100 µl of DMB-DP3, while the lower one shows the peak area of the product after 2 hours incubation. These are duplicate results representative of two independent experiments.

2.3.3.3. Optimisation of the assay incubation temperature

In order to optimise the incubation temperature of the assay, the ST8SiaII /DMB-DP3 reaction was repeated using different incubation temperatures; specifically, 15, 25, 37 and 50 ºC.

It was found that incubating the reaction for 2 hours at 25ºC resulted in higher production of DMB-DP4 (Figure 2.31). This was surprising given that it was expected that incubation at 37ºC would result in the optimum production of DMB-DP4, since 37ºC is the normal body temperature. Nevertheless, significantly greater product formation was observed at 25ºC. This might be explained by the fact that the conditions and buffers used to perform the reaction *in vitro* are completely different from the conditions inside the body. The same observation was recorded by a previous study performed by Keys *et al*., where 25ºC was identified as the optimum temperature for both bacterial and murine polyST activity [132].

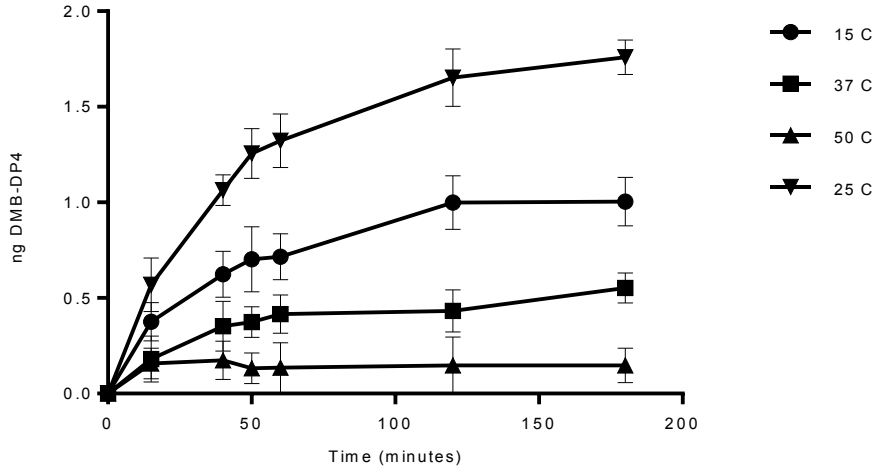

Figure 2.31 Different incubation temperature of DMB-DP3/ST8SiaII reaction.These are duplicate results representative of two independent experiments.

2.3.3.4. Evaluation of the optimum purification strategy of DMB-DP3

To determine whether the optimum purification strategy of DMB-DP3 is via anion exchange-HPLC or RP-HPLC, recombinant ST8SiaII (250 ng/µl) was incubated with anion exchange-purified DMB-DP3 (10-100 µM), $MgCl_2$ (5 mM), 0.5 mM CMP-Neu5Ac and sodium cacodylate buffer (pH 6.7, 0.1 M), with the same conditions as used previously. The results were compared with the DMB-DP3 purified using the RP-HPLC methodology.

It was found that although the polysialylation efficiency was improved using the anion exchange-purified DMB-DP3, the % product peak area of DMB-DP4 compared to the total peak area was still quite low at early incubation times (Figure 2.32).

For the purification of DMB-DP3 using anion exchange column the mobile phases used were: 100% water (mobile phase A) and 5 M ammonium acetate buffer (pH 7.4, mobile phase B) while for the purification using RP-HPLC system the mobile phases used were: ammonium formate buffer (pH 6, mobile phase A) and 55% methanol (pH 7.2, mobile phase B). The final acidic pH of the mobile phases used with the RP-HPLC might have caused the reduction in the efficiency of labelling of the DMB-DP3 purified by this

method, due to the formation of lactonised form, compared to the DMB-DP3 purified by the anion exchange system.

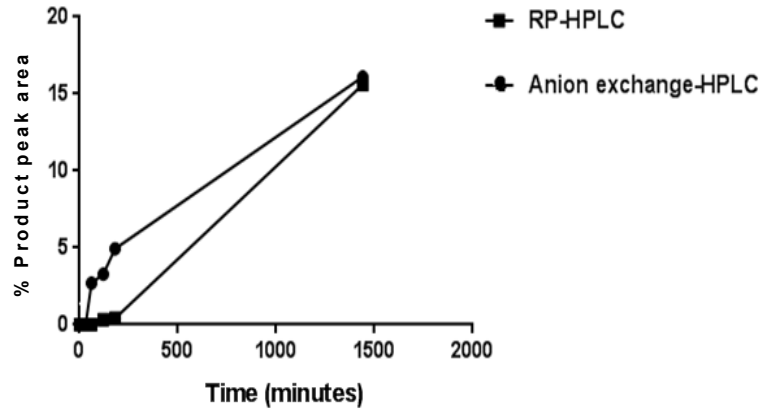

Figure 2.32 Incubation of ST8SiaII with DMB-DP3 purified with RP-HPLC (lower curve) and anion exchange-HPLC (upper curve). These are duplicate results representative of two independent experiments.

However, it was observed that both samples gave an equally high yield of the product DMB-DP4 after 24 hours of incubation with ST8SiaII. This could be explained by completion of the reversible lactonisation reaction of DMB-DP3. In an attempt to decrease the lactonisation of DMB-DP3, solid material purified by anion exchange HPLC was dissolved in sodium cacodylate buffer (pH 8.2), incubated with human ST8SiaII enzyme and analysed by anion exchange-HPLC as described before. It was found that although the analysis of the DMB-DP3 dissolved in sodium cacodylate buffer (pH 8.2) showed only one peak on both RP- and anion exchange-HPLC with no sign of presence of the lactonised form, the high pH used was incompatible with the reaction (abolished enzyme activity). In order to improve the efficiency of the DMB-DP3 polysialylation reaction by human ST8SiaII, the purification of DMB-DP3 was re-visited after it was observed that anion exchange-purified DMB-DP3 showed higher DMB-DP4 product than the RP-HPLC- purified DMB-DP3.

2.3.3.5. Determination of the conditions required to minimise the lactonisation of DMB-DP3

A combination of both RP-HPLC and anion exchange–HPLC was used with the optimised conditions for each technique as mentioned before, (the purified material with RP-HPLC was re-purified by anion exchange HPLC). It

was observed from the previous analysis that the polysialylation efficiency was improved when DMB-DP3 was purified by anion exchange HPLC, which could be explained by the difference of the pH of the mobile phase system used in each purification method. It was assumed that combining both anion exchange and reversed phase HPLC purification methodologies might enhance the efficiency of DMB-DP3 polysialylation to the target DMB-DP4. Peaks representing DMB-DP3 were pooled from several runs and freeze dried. The dried material was dissolved in cacodylate buffer (pH 6.7) and incubated at 37°C for 2 hours.

An incubation of the sample at 37°C for 2 hours at pH 6.7 was performed, after the observation that both previously prepared samples gave a high yield of the product DMB-DP4 after 24 hours of incubation with ST8SiaII, in an attempt to allow the completion of the reversible lactonisation reaction of DMB-DP3. It was previously reported in different studies that the lactonisation reaction is reversible and controlled by pH of the medium. In accordance with that, incubating DMB-DP3 at 37°C for 2 hours at pH of 6.7 may result to shift the reversible reaction towards the formation of the unlactonised form of the DMB-DP3, which is the form of the DMB-DP3 able to react with the enzyme (Table 2.14) [142].

Table 2.14 DP3 lactonisation reaction.Structures of a-2,8-linked sialic acid trimer (1), 1-monolactone trimer (2), 2-monolactone trimer (3), and dilactone trimer (4) as well as the reaction pathway of lactonisation (bottom left) and hydrolysis (bottom right), table reproduced from [142]

Reactable form of DP3 with human ST8SIAII enzyme	Unreactable form of DP3 with human ST8SIAII enzyme
Unlctonised DP3 (the desired product) 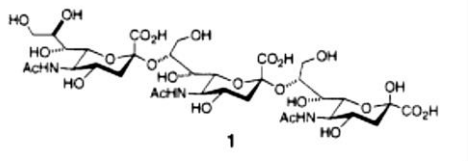 1	monolactone trimer 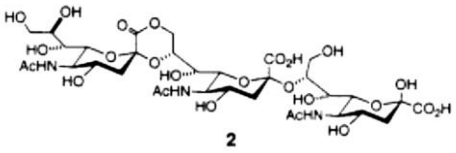 2
	monolactone trimer 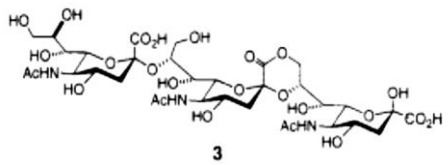 3
	Dilactone trimer 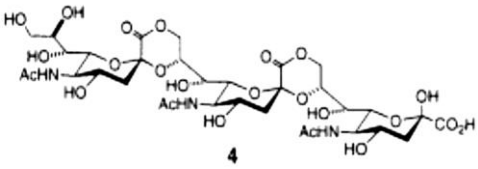 4
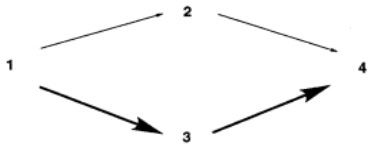	

The results showed that the efficiency of the polysialylation reaction was greatly improved using this protocol. It was found that compared to the product produced (product DMB-DP4 peak area/total peak area x100) with either RP-HPLC or anion exchange-HPLC without pre-incubation, this protocol showed considerably higher efficiency (Figure 2.33), which could be explained by either the combination of the purification techniques or the incubation of the sample for enough time to reverse the lactonisation process.

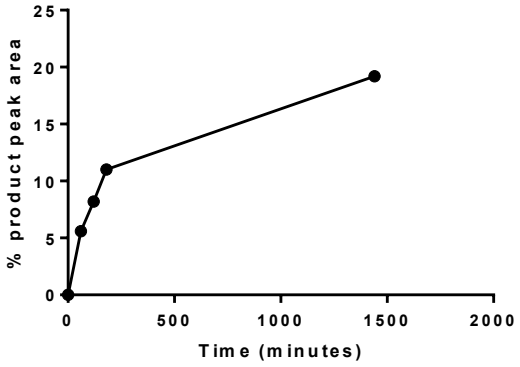

Figure 2.33 Incubation reaction of ST8SiaII enzyme with DMB-DP3 purified with both RP-HPLC and anion exchange chromatography and equilibrated for 2 hours before incubation with the enzyme. These are duplicate results representative of two independent experiments.

To determine whether the improvement in polysialylation efficiency was caused by the combination of the purification techniques or the pre-incubation, the polysialylation of the DMB-DP3 prepared in this way was compared with DMB-DP3 previously prepared by either RP-HPLC or anion exchange HPLC but after incubation of both for 2 hours at 25°C (Figure 2.35).

It was found that the efficiency of DMB-DP3 polysialylation reaction was not extensively affected by the method of the purification, but that reversal of the lactonisation of the DMB-DP3 before the incubation with ST8SiaII is crucial. The equilibration of the DMB-DP3 allows any lactonised DMB-DP3 form to be converted to the unlactonised form, which increases the polysialylation efficiency. To further confirm this hypothesis, the polysialylation reaction of DMB-DP3 purified by RP-HPLC with and without equilibration was performed. The results clearly demonstrate that without equilibration the

reaction efficiency is very low especially at early time points compared to the equilibrated sample (Figure 2.34).

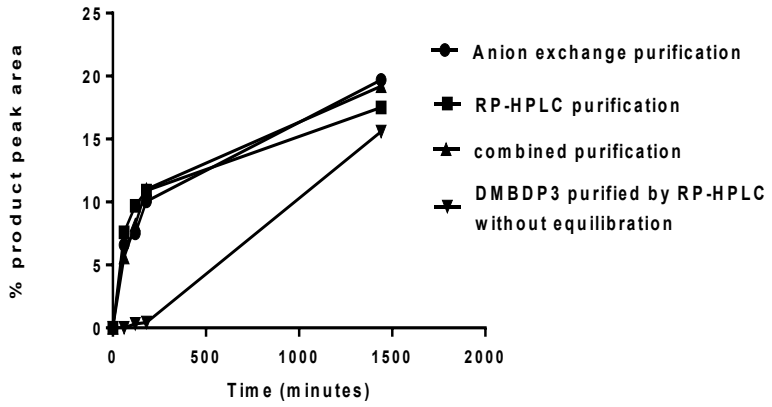

Figure 2.34 Incubation of human ST8SiaII enzyme with DMB-DP3 purified by RP-HPLC, anion exchange HPLC or both techniques combined with/without incubation of the purified DMB-DP3 for 2 hours at 37°C at pH 6.7. The results show that the efficiency of the polysialylation of DMB-DP3 depends on the unlactonisation of DMB-DP3 before the reaction more than its method of purification. These are duplicate results representative of two independent experiments.

The reduction in polysialylation reaction efficiency associated with the DMB-DP3 lactonisation could be explained by the relative inhibition of the ST8SiaII enzyme ability to incorporate new sialic acid monomers within the lactonised structure and strongly suggests that the negatively carboxyl groups are key to activity. The human ST8SiaII enzyme catalyses the reaction of the incoming sialic acid and DMB-DP3 residue at the 2,8 positions. In the lactonised form of the DMB-DP3, the structure and charge of the molecule is different which could result in the molecule not being recognised by enzyme or doesn't fit efficiently into active sites.

To sum up, it was found that lactonisation of oligosialic acid (OSA) is catalysed by acid in aqueous solution and that lactonisation of OSA has an influence on its ability to interact with the human ST8SiaII enzyme, which might be explained by steric hindrance caused by the formation of the lactonised form. It was found also that, consistent with previous studies, lactonisation of DMB-DP3 is a reversible process. Conjugating RP-HPLC or anion exchange-HPLC purification of DMB-DP3 with its incubation at 37°C for 2 hours at pH 6.7 allows the reversal of the lactonisation process. Converting the lactonised forms to the unlactonised form consequently

allows for efficient interactions between DMB-DP3 and the human ST8SiaII enzyme, as demonstrated by the higher DMB-DP4 yield.

2.3.4. Optimisation of the assay quantification technique

In order to determine the mass of DMB-DP4 produced by the reaction of DMB-DP3 and ST8SiaII and to consequently quantify polyST inhibition with small molecule inhibitors, DMB-DP4 was synthesised and purified in the same way as described previously for DMB-DP3. Different concentrations and volumes of the standard DMB-DP4 were injected and a calibration graph for DMB-DP4 weight against peak area was plotted (Figure 2.35). The equation of the line produced from the calibration graph was then used for calculation of the mass of DMB-DP4 produced (in ng) in each analysis, which was then used to calculate the percent DMB-DP4 formation relative to control (no inhibitor was added).

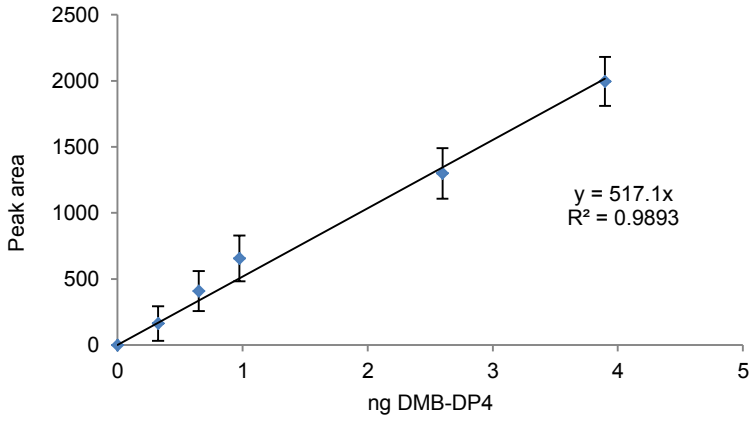

Figure 2.35 Calibration curve of the amount of nanograms of DMB-DP4 standard against peak area. These are duplicate results representative of two independent experiments.

2.3.5. Optimisation of the assay running time

In order to optimise the assay for a medium throughput screen, the gradient of the anion exchange-HPLC analysis used to detect the polysialylation of DMB-DP3 by ST8SiaII was modified from the original gradient (Table 2.13), which requires 30 minutes for analysis of each small molecule inhibitor, to the following gradient that requires only 11 minutes to analyse one inhibitor (Table 2.15).

Table 2.15 Optimised HPLC gradient for medium throughput analysis of polysialyltransferase inhibitors. Mobile phases used were distilled water (Mobile phase A) and 5M ammonium acetate (mobile phase B).

Time	Flow (ml/min)	% Mobile phase A	% Mobile phase B
0	1.2	100	0
2	1.2	100	0
9	1.2	96.3	3.7
11	1.2	100	0

The reproducibility of the new gradient was tested by running different samples of DMB-DP3 polysialylated with human ST8SiaII and examining the retention time of both DMB-DP3 and the product DMB-DP4 for each sample. It was found that this gradient yielded reproducible results at which DMB-DP3 elutes at 5.8 minutes while DMB-DP4 elutes at 7.5 minutes, confirmed by running standard DMB-DP3 and DMB-DP4 using the same gradient (the experiment was repeated three times) (Figure 2.36).

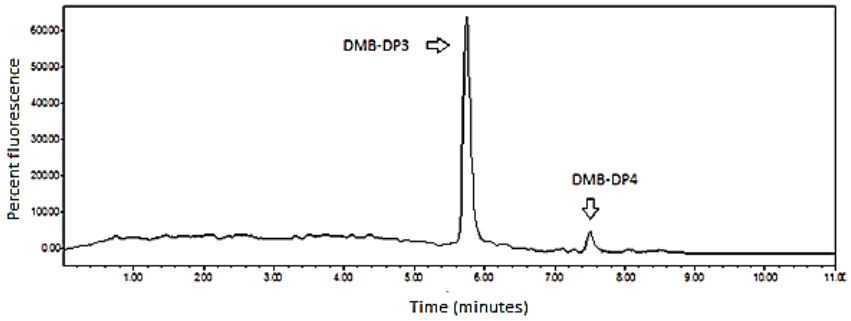

Figure 2.36 Optimisation of the assay running time.A shorter gradient with a higher percentage of mobile phase B was used to decrease the time required for analysis of anti-polyST small molecule inhibitors from 30 minutes to 11 minutes.

Although using this gradient resulted in a short running time and reproducible results, the solvent composition was further modified since the high molarity of mobile phase B (5M ammonium acetate) risked damaging the HPLC equipment (high concentration of ammonium acetate is corrosive to the HPLC material) [143]. In the new gradient, the mobile phases used were: 0.5 M ammonium acetate (pH 7.4) (mobile phase B) and distilled water (mobile phase A) with the following gradient (Table 2.16):

Table 2.16 Optimised HPLC gradient for medium throughput analysis of polysialyltransferase inhibitors that utilise 0.5 M ammonium acetate instead of 5M ammonium acetate as mobile phase B.

Time	Flow (ml/min)	%Mobile phase A	% Mobile phase B
0	1.2	100	0
2	1.2	100	0
9	1.2	63	37
11	1.2	100	0
12	1.2	100	0

2.3.6. Analysis of the polyST assay reproducibility

In order to assess the assay reproducibility and reliability, seven independent control samples using the same concentration of DMB-DP3, ST8SiaII enzyme and CMP-Sia were analysed. The percentage of the product DMB-DP4 was calculated (relative to the total peak area) and the standard deviation and coefficient of variation were calculated.

It was found that the results were reproducible with an average of 7.8 % product and standard deviation of 0.58 and coefficient of variation of 0.07, meaning the results were reproducible (Figure 2.37).

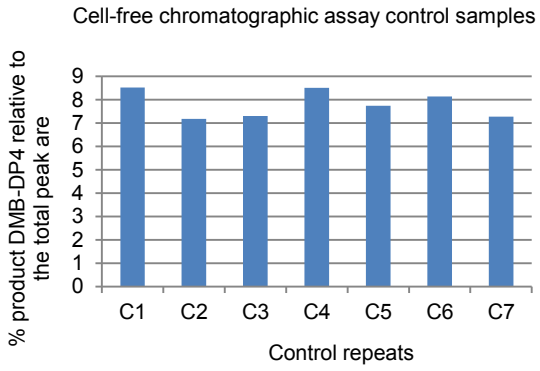

Figure 2.37 Analysis of the reproducibility of the results obtained by running seven independent control samples shows a standard deviation of 0.58 and coefficient of variation of 0.07

2.3.7. Determination of the limit of detection of the product DMB-DP4

In order to determine the limit of detection of the product DMB-DP4 (smallest peak area that is distinguishable from baseline) produced in the DMB-DP3 polysialylation reaction, different concentrations of standard DMB-DP4 were injected (1 – 50 nM). The peak area corresponding to each concentration was recorded and plotted against the DMB-DP4 concentration. It was found that using the previously mentioned optimised conditions of the assay chromatography, 1 nM (0.001 µM) concentration of DMB-DP4 could be detected (which is 1/10000 of the added concentration of DMB-DP3) (Figure 2.38).

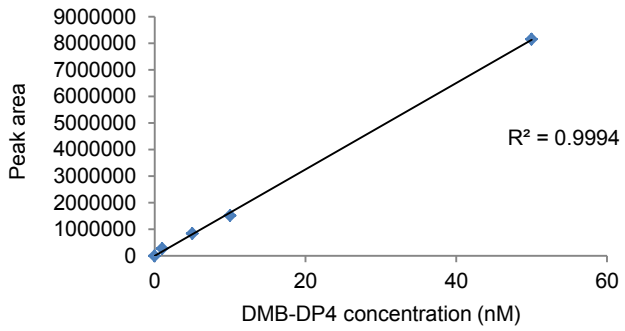

Figure 2.38 Detectability of the product DMB-DP4 using anion exchange HPLC chromatography and fluorescence (RF-10A) (Shimadzu, Japan) detector (sensitivity set, 1 and gain set 3). These are duplicate results representative of two independent experiments.

2.3.8. Analysis of the DMB-DP4 stability

Since this assay is designed to be used for high throughput analysis, it is expected that a large number of ST8SiaII inhibitors would be analysed in the same day. These inhibitors would thus potentially remain in the HPLC machine overnight. If different time points and/or concentrations for a large number of inhibitors were assessed in the same 24 h period, the stability of the DMB-DP3 acceptor and DMB-DP4 product over this lengthy period are crucially important. So, in order to confirm the stability for the product DMB-DP4 and DMB-DP3 present in each assay, a control assay (with no inhibitor) was tested for its content of DMB-DP3 and DMB-DP4 at different time points over 48 hours at room temperature. It was found that the DMB-DP3 and

DMB-DP4 content in the assay is stable over 48 hours at room temperature (Figure 2.39).

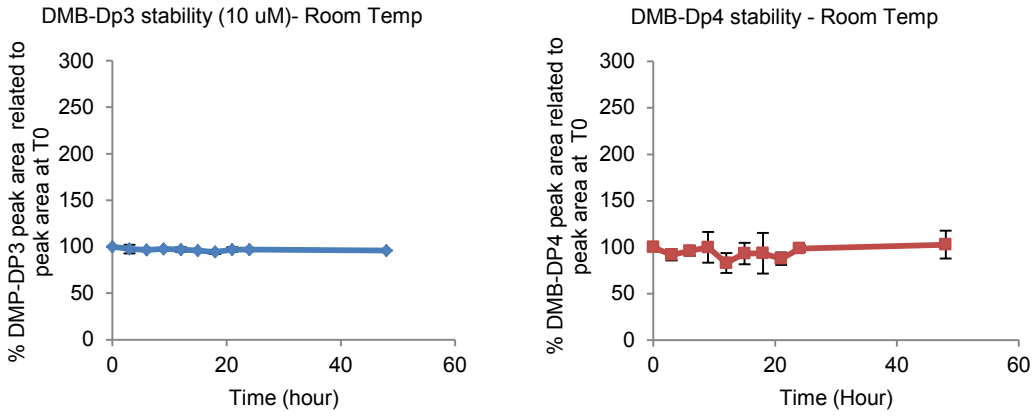

Figure 2.39 Stability of DMB-DP3 and DMB-DP4 over 48 hours. The experiment is carried out by incubating DMB-DP3 and DMB-DP4 at room temperature for 48 hours, 10 µl of the sample at T0 was analysed using HPLC then the same volume of the sample was analysed after a series of time points, peak area was detected and the percent of the peak area compared to T0 was calculated and blotted against the corresponding time point. The experiment was repeated three times and the standard deviation was calculated.

2.3.9. Characterisation of Cytidine Monophosphate (CMP) as an ST8SiaII inhibitor

Gel electrophoresis and western blot analysis

CMP was used as a standard inhibitor to validate the developed cell-free HPLC high throughput assay. In order to have a reference from which to compare polyST inhibition achieved in the new assay, CMP was first analysed using western blot (a method employed in the lab previously).

Using NCAM, in the presence of recombinant human ST8SiaII and CMP-Neu5Ac (the substrate for polysialylation reactions), CMP was shown to abolish polysialylation consistent with previous studies [107,109]. To identify the optimum concentration of CMP required for complete ST8SiaII enzyme inhibition, NCAM was used in the presence of recombinant human ST8SiaII and CMP-Neu5Ac (the substrate for polysialylation reaction) and different concentrations of CMP (0.1 - 10 mM). The results were compared with positive control (without CMP) and negative control (without ST8SiaII). It was

found that CMP significantly inhibited NCAM polysialylation at a concentration of 1 mM (no polySia was detected on western blot). The reaction was repeated using a narrower concentration range of CMP (0.1, 0.25, 0.4, 0.8 and 1 mM) in order to determine the minimum concentration of CMP required for the inhibition of ST8SiaII enzyme, 0.4 mM CMP was found to completely inhibit the enzyme (Figure 2.40). The concentration-dependent inhibition of polysialylation of NCAM was indicated as a fainter bands rather than a change of the range of molecular weights. This suggests that CMP (and thus polyST inhibition) affects the number of polySia chains synthesised rather than modulating the length of individual chains. This is interesting and warrants further investigation.

Previous studies by Yousef M. J. et al. showed that at 0.5 mM CMP produced no significant polyST inhibition when administered to cells, specifically the IMR-32 neuroblastoma cell line [109]. This might be explained by the difference in the inhibition capacity of an inhibitor within cell-free and cell-based systems. This confirms that both cell-free and cell-based assays are required for a complete understanding of inhibitor activity.

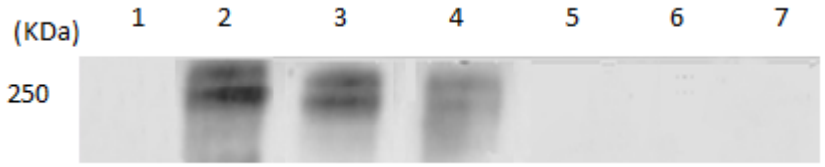

Figure 2.40 The effect of various concentrations of CMP on the polysialylation of NCAM. Lane 1 represents the negative control (without the ST8SiaII enzyme), lane 2 represents the positive control (without CMP), lanes 3 - 7 represent reactions with 0.1, 0.25, 0.4, 0.8 and 1 mM CMP respectively. Blot is representative of three independent experiments.

ST8SiaII inhibition by Cytidine

Cytidine was evaluated as a possible negative control. This would also determine the significance of the phosphate group as present in CMP, for inhibition of ST8SiaII. Cytidine did not significantly inhibit the polysialylation process (Figure 2.41), even at high concentrations (5 mM), which is consistent with previous studies [101] and confirms that the phosphate group is

necessary for ST8SiaII inhibition. Cytidine thus served as a useful negative control to aid validation of the assay.

To sum up, the results obtained by western blot validated the developed cell-free HPLC high throughput assay and confirmed the concentration required for complete inhibition of polySia synthesis. CMP and cytidine were consequently utilised as tool compounds for validation of a cell-free chromatographic assay.

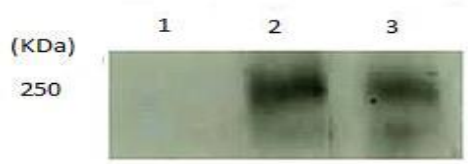

Figure 2.41 The effect of cytidine on the polysialylation of NCAM by ST8SiaII enzyme. Lane 1 represents the negative control (without the ST8SiaII enzyme), lane 2 represents the positive control (without cytidine) and lane 3 represents the reaction with 5 mM Cytidine. Blot is representative of three independent experiments.

2.3.10. Analysis of polysialylation reaction kinetics, assay sensitivity

The study of enzyme kinetics is important as it helps explain how enzymes function. Michaelis–Menten kinetics is one of the best-known models of enzyme kinetics that describes two values, K_m and V_{max}. V_{max} (maximum velocity) represents the maximum reaction rate achieved by the system, at maximum (saturating) substrate concentrations. The Michaelis constant K_m is the substrate concentration at which the reaction rate is half of V_{max}. K_m thus provides a measure of affinity of the substrate for the enzyme [144].

ST8SiaII activity was determined by incubating the enzyme with CMP-Neu5Ac and varying amounts of DMB-DP3 acceptor. The assay kinetic parameters (K_m, V_{max}) were then calculated (Figure 2.42A, B). The K_m value of the DMB-DP3 was calculated using a Lineweaver-Burk plot (Figure 2.42B). The experiment was repeated and the average K_m value was calculated (K_m = 29.5 µM, consistent with previous study [109]). The V_{max} value of the reaction was also calculated using the same plot (V_{max}= 14.8 µmol/min/mg).

The V_{max} value of polyST/ CMP-Neu5Ac reaction was previously reported in different studies (V_{max}= 58.8 ± 2.1). However, these studies reported the reaction using the bacterial ST8SiaII rather than the human enzyme, which suggests that the human enzyme does not convert as much substrate to product per unit of time, when the enzyme is saturated with substrate compared with the bacterial enzyme.

In order to determine the assay sensitivity towards a small concentration of inhibitor and the ability to establish a direct relationship between the concentration of the ST8SiaII inhibitor (CMP) and DMB-DP3 polysialylation product (DMB-DP4) peak area, the activity of ST8SiaII, as measured by DMB-DP4 product formation, was assessed in the presence of varying concentrations of CMP. The concentration of DMB-DP3 acceptor was maintained at a constant level. It was found that a direct relationship between CMP inhibitor concentration and the degree of DMB-DP3 polysialylation could be established and that even small changes in the concentration of the inhibitor could be observed in the product formation (Figure 2.42C). In order to determine the inhibition constant (K_i) value of CMP, the concentration required to produce half maximum inhibition of polyST activity, which was used as standard inhibitor for the assay, three concentrations of CMP were used (20, 50 and 150 µM). Each concentration was assessed in the presence of different concentrations (250, 425 and 500 µM) of CMP-Sia (sialic acid donor). The K_i value, the concentration of inhibitor which is required to decrease the maximal rate of the reaction to half of the uninhibited value, was determined using Dixon plot. The experiment was repeated and the average K_i value was found to be 12 µM (Figure 2.42C) which is consistent with previously published studies [109].

Here we have determined the K_i value of the inhibitor rather than an IC_{50} value since K_i value is an intrinsic quantity that is independent of the substrate (ligand) but depends on the enzyme (target) and inhibitor. In contrast the IC_{50} value depends on the concentrations of the enzyme (or target molecule), the inhibitor, and the substrate (or ligand) along with other

experimental conditions [145]. In short, an IC_{50} can vary between experiments, whereas the K_i is an absolute value.

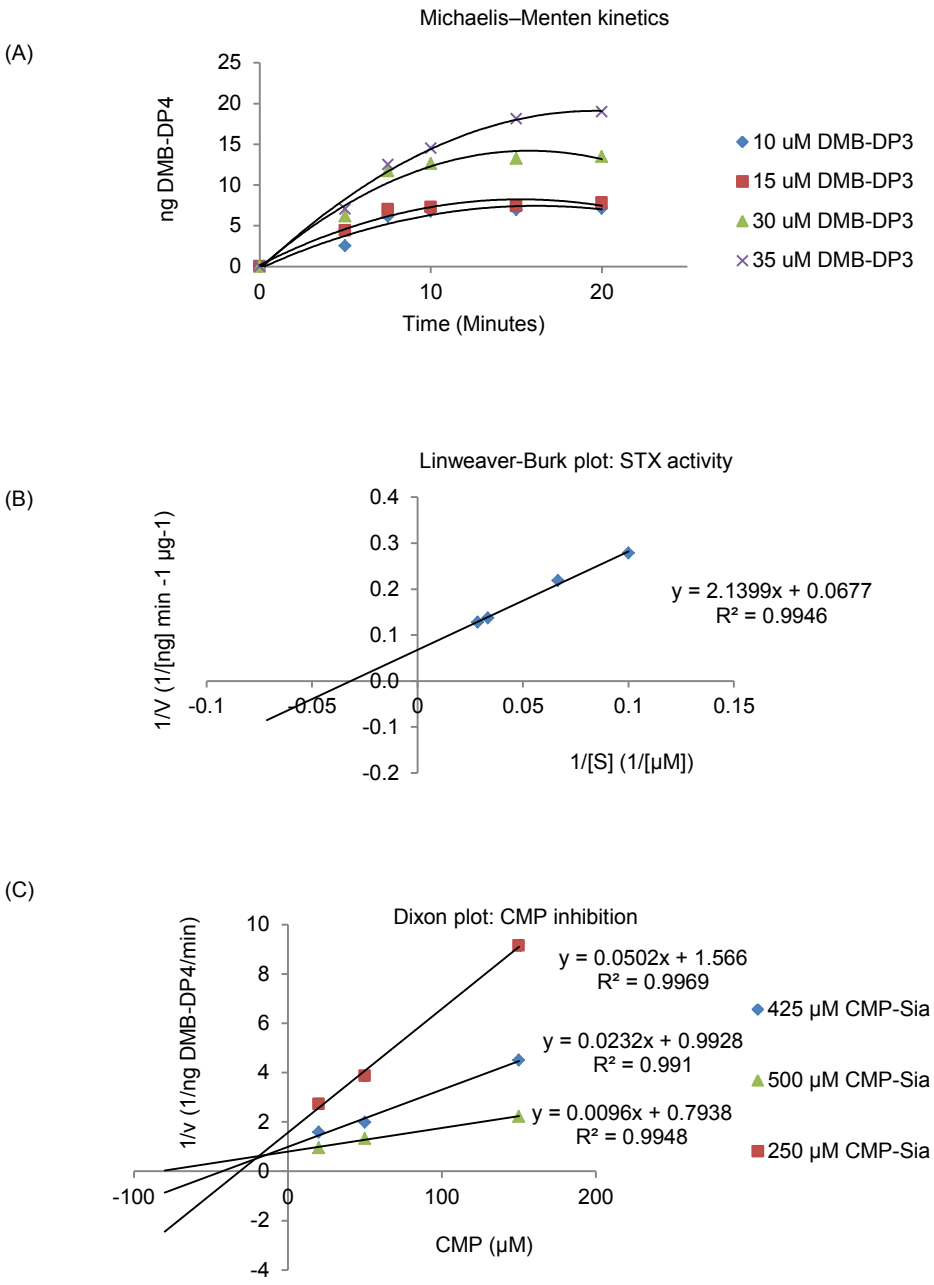

Figure 2.42 Michaelis-Menten data (A), Lineweaver-Burk plot (B) and Dixon plot (C). K_m of DMB-DP3 for ST8SiaII (derived from x axis intercept, Lineweaver-Burk plot) was calculated as 29.5 µM and V_{max} value (calculated from y axis intercept) was calculated as 14.8 µmol/min/mg. The K_i value of CMP was calculated from the Dixon plot. Graph lines converge above the x axis; where they intersect is -K_i. Data points are from a single determination representative of two independent experiments.

2.3.11. Optimisation of chromatography to allow high throughput analysis of polyST inhibition

2.3.11.1. Reversed phase-HPLC

Previously we have optimised the assay chromatography for medium throughput analysis of polyST inhibition using anion exchange-HPLC (Section 2.3.5). In order to optimise the HPLC assay for high throughput analysis of small molecule ST8SiaII inhibitors, further optimisation was carried out by analysing the assay using RP-HPLC instead of anion exchange-HPLC.

RP-HPLC allows for rapid, sensitive and reproducible analysis due to the fact that the column needs no time for re-equilibration between analyses since the method is isocratic rather than the gradient elution used with anion exchange chromatography. Another advantage of using RP-HPLC is the ability to conjugate it with mass spectrometry, which allows for very specific product characterisation and provides molecular weight information.

The mobile phases used were: ammonium formate (5 mM, mobile phase A) and methanol (mobile phase B), with a flow rate of 1 ml/min and an isocratic gradient of 80% mobile phase A: 20% mobile phase B. Using this method, DMB-DP4 eluted at 3.9 minutes while DMB-DP3 eluted at 4.9 minutes (Figure 2.43A). Six samples were run using this method to assess the reproducibility of the analysis (Figure 2.43B). It was found that the retention time of both DMB-DP3 and DMB-DP4 were reproducible throughout the six repeats, which confirmed the reliability of the developed chromatography.

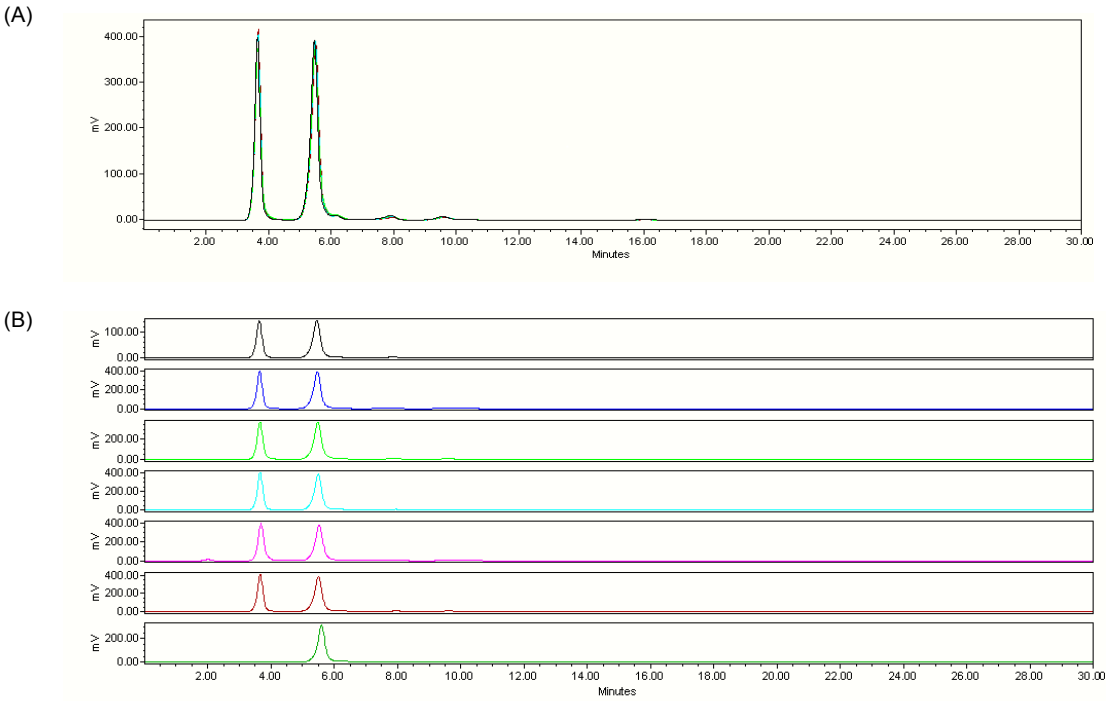

Figure 2.43 Optimisation of the chromatography to allow high throughput-HPLC analysis. Using isocratic method reduced the run time and allowed direct re-injection of new samples without the need to re-equilibrate the column between analyses. A) The first peak at 3.9 minutes represents DMB-DP4 while the second peak at 5.9 minutes represents DMB-DP3, B) the reproducibility of the results when running 6 samples of standard DMB-DP3 and DMB-DP4 consecutively. The last chromatogram shows DMB-DP3 only.

2.3.11.2. MRM analysis

In order to set an MRM channel for specific DMB-DP3 and DMB-DP4 detection, the mobile phases used were: ammonium formate (5 mM, mobile phase A) and methanol (mobile phase B), with a flow rate of 0.3 ml/min and isocratic method of 80% mobile phase A: 20% mobile phase B. The mass spectra were continuously scanned from *m/z* 300 to *m/z* 1200 for DMB-DP3 and *m/z* 1500 for DMB-DP4 throughout the entire HPLC separation and the mass spectrometer was operated in positive ion electrospray mode. The optimal cone voltage and collision energy associated with each transition were established, the run time was optimised to 6 minutes where the DMB-DP3 and DMB-DP4 eluted at 2.5 and 1.8 minutes respectively (Figure 2.44).

(A)

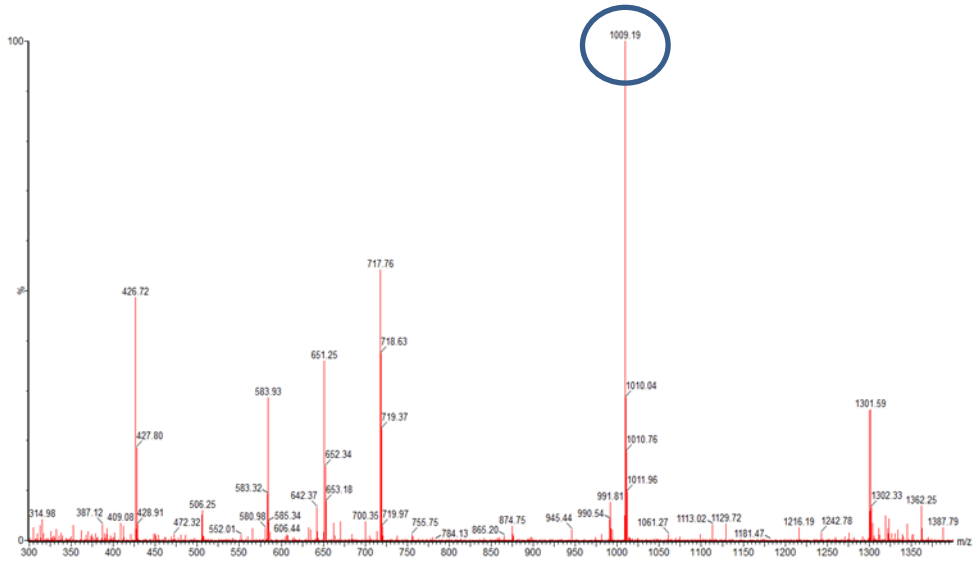
1009.19
717.76
426.72
718.63
651.25
583.93
1010.04
719.37
1301.59
427.80
1010.76
652.34
1011.96
583.32
642.37
653.18
991.81
1302.33
1362.25
314.98
387.12
409.08
428.91
506.25
472.32
580.98
585.34
700.35
719.97
755.75
874.75
945.44
990.54
1061.27
1113.02
1129.72
1216.19
1242.78
1387.79
m/z

(B)

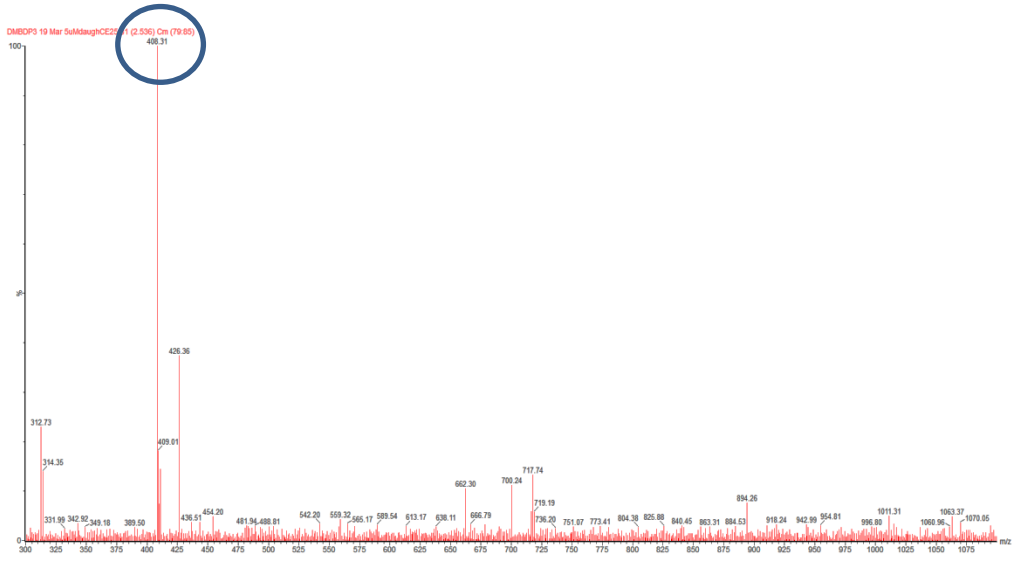
408.31
426.36
312.73
409.01
314.35
717.74
700.24
662.30
719.19
894.26
736.20
1011.31
1063.37
1079.86
m/z

(C)

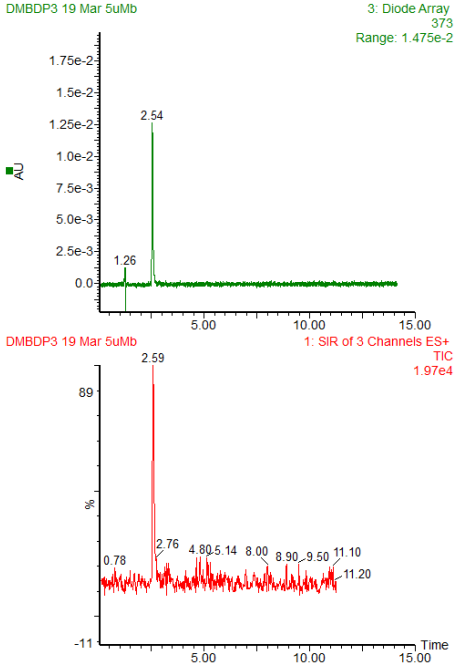

(D)

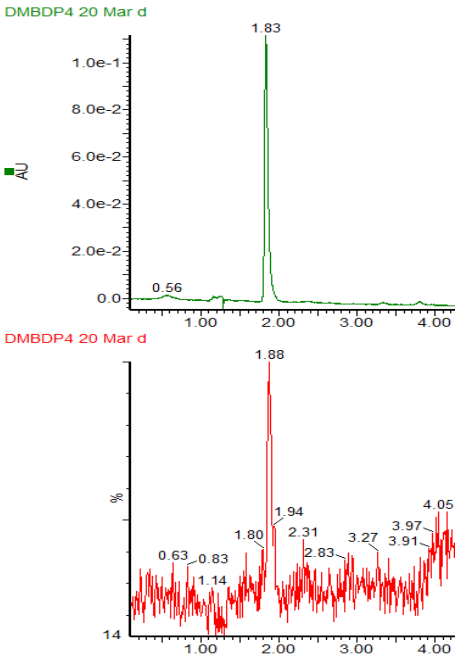

(E)

Transitions	Molecular weight (mwt)	Z	Parent ion (m/z)	Daughter ion (m/z)	CV (V)	CE (eV)	Dwell time (s)
DMB-DP3	1007.9	+1	1009	407.9	25	20	0.2
DMB-DP4	1299.15	+2	651.25	408	25	30	0.2

Figure 2.44 MRM analysis of DMB-DMB3/4. Example of mass spectrum used for MRM channel setting of DMB-DP3/4 showing parent ion selection for DMB-DP3 analysis (A) and daughter ion selction (B). (C) Detection of DMB-DP3 (C) and DMB-DP4 using the optimised MRM technique, with either photodiode array detector (upper chromatogram) or mass spectrometry (lower chromatogram). (D) Table showing MRM transitions, cone voltage (CV) and collision energy (CE) determined for DMB-DP3 and DMB-DP4.

In the MRM assay, on the basis of the channels established in the present experiments, 5 µl of labelled samples (10 mM DMB-DP3, 250 ng ST8SiaII) proved to be sufficient for quantitative analysis of the inhibition of polySia synthesis caused by ST8SiaII inhibition.

2.3.12. Evaluation of novel small molecule potential ST8SiaII inhibitors

Using the developed high throughput cell-free chromatographic assay, a panel of small molecule ST8SiaII inhibitors that were designed at the Institute of Cancer Therapeutics (University of Bradford) were evaluated. These compounds are listed in Table 2.17.

The compounds synthesised were designed as polyST inhibitors based on the results of molecular modelling studies carried out at the ICT. The compound structures are variations to ICT-3125. Small changes to functional groups were made in order to find out the effects on biological activity. CMP was included as a known, previously studied inhibitor.

The average product (DMB-DP4) formation relative to control sample was calculated in order to identify the most promising compounds, and to determine hits to be further analysed in more complex assays (Table 2.17, Figure 2.45). Each experiment was repeated three times and the standard deviation and standard error mean was calculated.

According to the results obtained from this assay, it was found that the most active polyST inhibitors were ICT-3234 (78.6 ± 2.8% inhibition at 5 μM), ICT-3233 (61.6 ± 2.6% inhibition at 12.5 μM), ICT-3276 (78.7 ± 7.22% inhibition at 25 μM), and ICT-3143 (37.5 ± 9.1% inhibition at 12.5 μM). The polyST inhibition, as measured by reduction of polySia expression was found to be concentration-dependent (Figure 2.46).

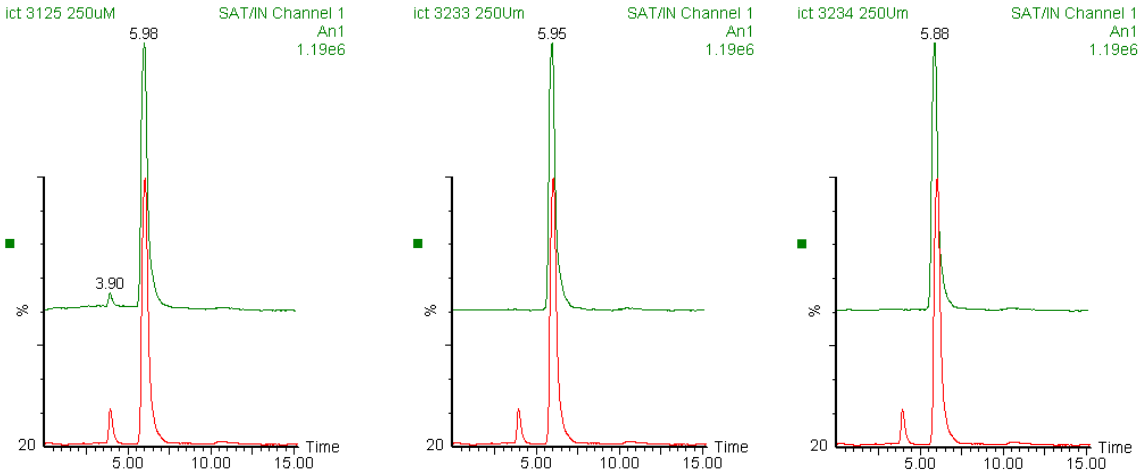

Figure 2.45 Representative examples of the chromatograms produced using the developed HPLC technique (RP) for the analysis of the inhibition of ST8SiaII enzyme using different inhibitors.The lower line represents the control reaction (no inhibitor), with the production of DMB-DP4 (left peak in each chromatogram), while the upper line represents the DMB-DP4 production after incubation of ST8SiaII with polyST inhibitors (DMB-DP4 production is reduced or inhibited completely).

Table 2.17 Evaluation of a series of novel small molecule polyST inhibitors using the cell-free HPLC assay developed in this study. Each experiment was repeated three times and the standard deviation and standard error mean was calculated.

Inhibitor	% Average DMB-DP4 formation	Standard deviation	Standard error mean
ICT-3276, 250 µM	8.1	2.1	1.2
ICT-3276, 125 µM	14.8	1.3	0.7
ICT-3276, 25 µM	21.3	7.2	4.1
CMP, 250 µM	30.6	1.0	0.6
CMP, 125 µM	38.3	3.2	1.8
CMP, 25 µM	86.7	2.3	1.3
ICT-3233, 50 µM	19.7	2.7	1.5
ICT-3233, 25 µM	37.6	2.8	1.6
ICT-3233, 12.5 µM	38.4	2.6	1.5
ICT-3125,250 µM	8.8	1.9	1.1
ICT-3125,125 µM	11.3	1.0	0.5
ICT-3125,12.5 µM	87.0	10.0	5.8
ICT-3274, 25 µM	3.5	0.6	0.3
ICT-3274, 5 µM	69.8	18.0	10.4
ICT-3143, 50 µM	35.6	3.4	1.9
ICT-3143, 25 µM	51.5	7.9	4.5
ICT-3143, 12.5 µM	62.4	9.1	5.3
ICT-3234, 12.5 µM	20.7	2.2	1.2
ICT-3234, 5 µM	21.1	2.8	1.6
ICT-3126, 250 µM	88.9	7.7	4.4
ICT-3130, 250 µM	77.8	9.0	5.2
ICT-3142, 250 µM	36.6	2.9	1.6
Cytidine, 250 µM	84.7	15.3	8.8
L-fucose, 250 µM	88.9	5.4	3.1
ICT-3242, 250 µM	57.4	10.2	5.8
ICT-3245, 250 µM	92.5	22.4	12.9
ICT-3246, 250 µM	114.9	9.9	5.7
ICT-3247, 250 µM	65.7	9.0	5.2

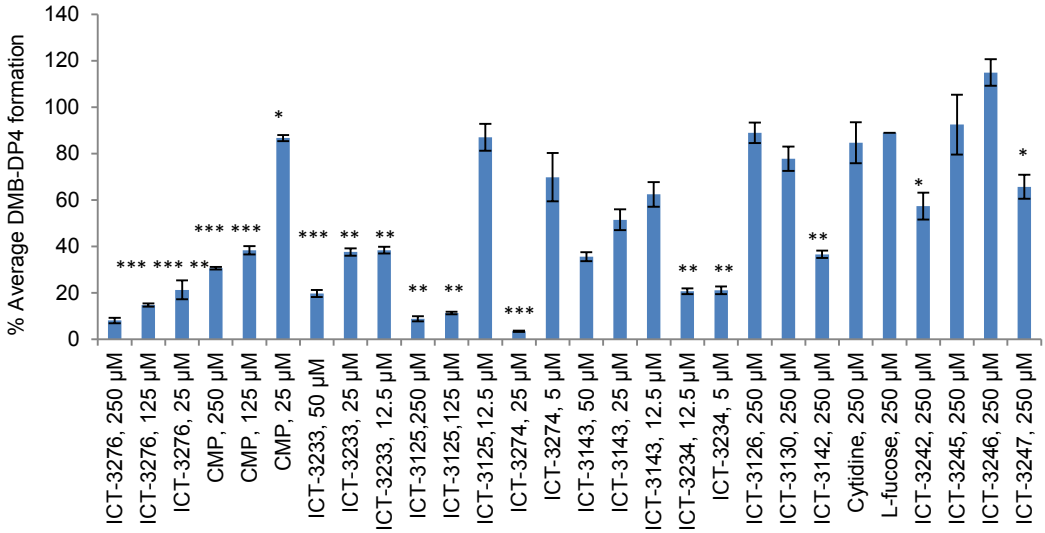

Figure 2.46 Evaluation of the inhibition of polySia synthesis by a series of novel small molecule ST8SiaII inhibitors using the cell-free HPLC assay developed in this study.Each experiment was repeated three times. * P< 0.05, ** P<0.01 and *** P < 0.001.

Section B) Cell-based chromatographic assay for analysis of ST8SiaII activity

Following successful demonstration of polyST inhibition and identification of promising compounds, the next step was to evaluate these compounds in cells. The second major part of this study was therefore the development of a cell-based chromatographic assay for the analysis of polyST inhibition, as represented by reduction of cell-surface polySia expression. Although cell-free assays play a very important role in the early stages of the drug discovery process, cell-based assays are the next logical step since they have additional complexity and functionality, for example in terms of intracellular cell signalling pathways. They additionally allow assessment of the ability of individual compounds to penetrate cell membranes.

2.3.13. SH-SY5Y cell growth curve

In order to develop a cell-based chromatographic assay, the doubling time of the cell line to be used had to be calculated in order to determine the suitable seeding density of the six-well plates used in this assay. A growth curve of SH-SY5Y cells was plotted as described in the materials and methods section. Plotting the number of cells/ml of the duplicate flasks for five consecutive days showed that SH-SY5Y cells have a doubling time of 48 hours (Figure 2.47). According to these results, 2 x 10^5 cell/ml was seeded in a 6 well plate (2 ml/well) and the cells were incubated for 48 hours to double and form 70-80% confluent wells before treatment with ST8SiaII inhibitors.

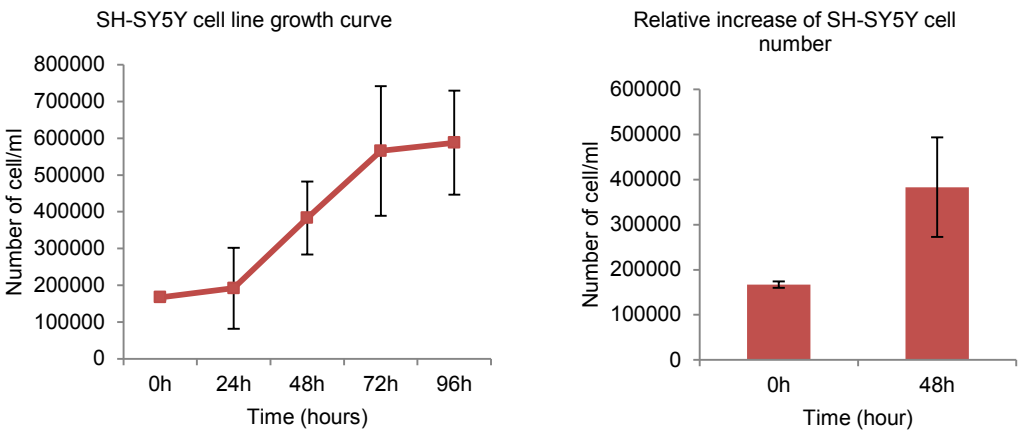

Figure 2.47 Growth curve of SH-SY5Y cells showing that the cell line requires 48 hours for duplication.These results represents mean of three independent experiments.

2.3.14. Use of Endo-N for the removal of polySia from the cell surface

2.3.14.1. Optimisation of Endo-N concentration

Endoneuraminidase-N (Endo-N) is an endosialidase which degrades rapidly and specifically linear polymers of polySia with a minimum length of 7-9 residues[146]. Cells were treated with Endo-N (0.5, 1 and 3 µg/ml) for 24 hours, while one well was used as negative control where no Endo-N was added. After 24 hours, media was collected for analysis using mixed phase column - HPLC-FD as described in the material and methods section (Section 2.2.9.1).

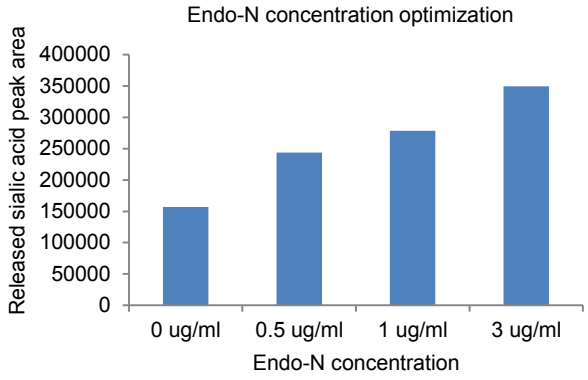

Figure 2.48 Optimisation of the concentration of Endo-N required for the removal of polySia from SH-SY5Y cell surface suggests a linear relationship between the concentration of Endo-N and the released polySia up to the concentration of 3 µg/ml. These are duplicate results representative of two independent experiments.

A linear relationship between the concentration of Endo-N and the released polySia up to the concentration of 3 µg/ml was detected (Figure 2.48). Two drawbacks were recorded with this technique, however: the presence of sialic acid in the control sample where no Endo-N was added, which might be due to the presence of sialic acid in fetal bovine serum (FBS) added to the medium, and the need to use high concentration of expensive Endo-N in order to remove polySia from the cell surface.

2.3.14.2. Optimisation of incubation media to eliminate sialic acid in control sample

In order to overcome the issue of the presence of sialic acid in the control samples, media was removed from the cells, after cells were attached to the six-well plate, and the cells were washed twice with PBS before adding Endo-N in FBS-free medium. It was found that using this technique resulted in the disappearance of sialic acid from the control samples. In order to further confirm that FBS was the source of the sialic acid in the control, FBS-containing medium was analysed by HPLC. It was found that the amount of sialic acid in the control sample was equivalent to the amount of sialic acid when injecting the same volume of media only.

The incubation of cells with Endo-N in FBS-free medium was not a perfect solution, however, since FBS contains growth factors required for the cell to survive, grow and divide. Maintenance of the cells for 24 hours in FBS-free medium might affect the cells, causing them to rupture and release the sialic acid present within and therefore give unreliable results. Therefore, a control sample where no Endo-N was added has to be examined with every analysis to confirm that no such rupture and release of sialic acid occurred as a result of the use of FBS-free medium.

2.3.14.3. Optimisation of SH-SY5Y cell number

In order to minimise the quantity of Endo-N used in the experiment and consequently reduce the associated costs, a 24-well plate was used instead of using 6 well plate, thereby reducing the amount of media required to cover the cells from 2 ml to 0.5 ml. However, this approach proved unsuccessful

since the amount of sialic acid produced from the associated lower number of cells (10^5 total cell number was used instead of 4 x 10^5 used previously in the 6 well plate) produced an undetectable amount of sialic acid.

2.3.15. Use of mild acidic hydrolysis for the removal of polySia from the cell surface

Instead of using Endo-N to remove polySia from the cell surface, solubilisation of cell-bound polySia was achieved by using a mild non-ionic non-denaturing detergent; IGEPAL CA-630, according to previously published methodology [147]. Cells were collected by trypsinisation followed by centrifugation for 5 minutes at 1000 g. Cell pellets were treated with IGEPAL followed by incubation at 37 °C for 1 h and vortex mixing for 5 minutes in order to solubilise polySia from the cell surface. After removal of the insoluble material by centrifugation, the supernatant was then incubated with triflouroacetic acid (TFA) for 2 hours at 80°C in order to hydrolyse polySia into sialic acid monomers which were then derivatised with DMB (as described previously).

Although using this approach did not result in complete removal of polySia from the cell surface, the amount of detected sialic acid was equivalent to that detected using 1 µg/ml of Endo-N. This approach solved the problem of having free sialic acid in the control sample since the medium was discarded and only the cells were used (Figure 2.49). It significantly reduced the cost of the assay. In order to confirm that using acidic hydrolysis resulted in the removal of the same amount of polySia from the cell surface and consequently give reproducible results, three independent experiments with the same cell seeding number and incubation time were analysed, it was found that the standard deviation didn't exceed ±10%.

To sum up, using mild acidic hydrolysis for the removal of polySia from the cell surface instead of using Endo-N allowed for a reliable, cost-effective assay and eliminated the need to use FBS-free medium which was problematic as previously discussed.

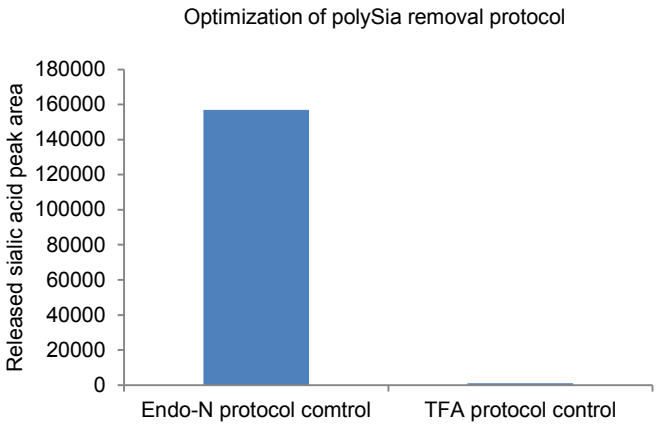

Figure 2.49 Comparison between the amounts of sialic acid present in control samples using Endo-N or mild acidic hydrolysis for the removal of polySia from SH-SY5Y cell surfaces. These are duplicate results representative of two independent experiments.

In order to confirm that using mild acidic hydrolysis to remove polySia from SH-SY5Y cell surface results in the removal of polySia chains and not the sialic acid monomers also normally present on the cell surface [148], a control sample was performed in which cells were treated in the same way as described before but without adding TFA for 2 hours at 80°C. In this case polySia is not hydrolysed to sialic acid monomers and therefore any detected DMB-DP1 will be the result of the solubilisation of sialic acid monomers from the cell surface by IGEPAL CA-630 (Figure 2.50). No sialic acid was detected in this control sample, which confirmed the release of only polySia from the cell surface using this mild acid hydrolysis protocol which is consistent with previously published studies [147].

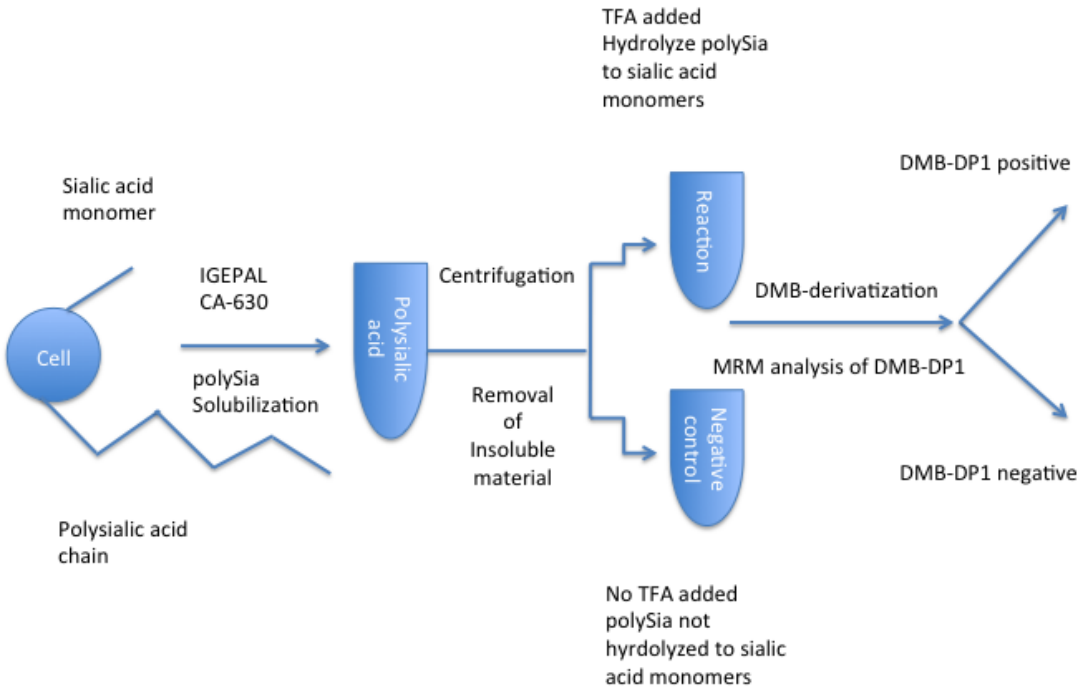

Figure 2.50 Schematic representation of the design of the control for polySia removal using mild acidic hydrolysis

2.3.15.1. Optimisation of polySia solubilisation technique

In order to improve the efficiency of solubilisation of polySia from cell surface using IGEPAL, two different techniques were used. The first involved incubation of the cell pellet with 100 µl of 0.5% IGEPAL at 37 °C for 1 h and vortex mixing for 5 minutes while the second involved vortex mixing the cell pellet with IGEPAL for the entire 1 h. Neither of these two techniques was found to increase the efficiency of polySia solubilisation: there was no difference in the efficiency using any of the techniques and they all resulted in solubilisation of polySia equal to 1 µg/ml of Endo-N.

2.3.16. Labelling and detection of standard DMB-DP1

A DMB-DP1 standard was prepared using the same technique previously described for DMB-DP3 and DMB-DP4. Standard DMB-DP1 was analysed using an Obelisc™ mixed-phase HPLC column, 5 mM ammonium formate (mobile phase A), Acetonitrile (mobile phase B) and 0.8 ml/min flow rate as described in the methods and materials section.

The Oblesic column is a mixed phase column that operates with multiple separation modes (normal phase, ion exchange and hydrophilic interaction

chromatography). This column has the advantage of efficient separation of polar and charged analytes, which makes it a good choice for separation of DMB-DP1 from the other components within the cell. The total run time was adjusted to 13 minutes, since DMB-DP1 was eluted at 10.87 minutes (Figure 2.51), followed by washing the column for up to 27 minutes with 100% acetonitrile to allow re-equilibration of the column after the end of the gradient.

The same method was used for the analysis of sialic acid released from cells with/without adding ST8SiaII inhibitors. The DMB-DP1 standard was re-injected with each analysis to ensure the reproducibility of the results (the same elution time was observed as previously recorded).

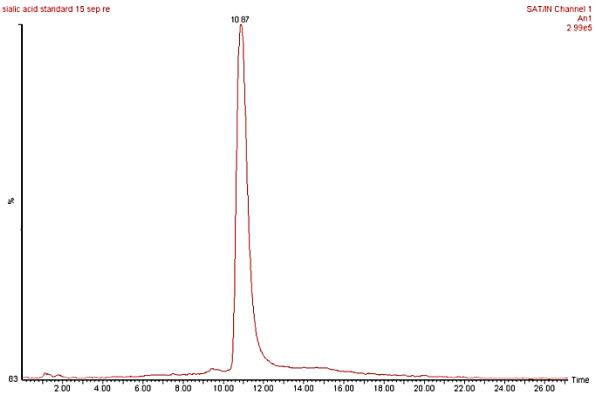

Figure 2.51 Analysis of standard DMB-DP1 using the Oblesic mixed phase column.

2.3.17. Cell-based analysis of ST8SiaII inhibitors

2.3.17.1. Mixed phase-HPLC analysis

Analysis of inhibition of polySia expression using CMP in a cell-based assay has previously been reported [109]. In the in-house study by Al-Saraireh et al., 5 mM CMP was found to cause approximately 40% inhibition in polySia synthesis as examined using flow cytometry and IMR-32 cells (NCAM +; ST8SiaII +; polySia +).

CMP was therefore used to validate the developed assay. CMP (5 mM) was added to the cells for 24 hours, and the polySia released from the cell

surface was analysed using HPLC. It was found that 5 mM CMP resulted in 32.1 ± 0.6 % inhibition of polySia expression, which is consistent with the results reported previously [109].

After validation of the assay, selected promising compounds identified from the cell-free HPLC assay for polyST inhibition were then evaluated. However, it was found that using the previously described HPLC methodology was not ideal for this particular assay. Two peaks were found to overlap at the same retention time of DMB-DP1. When the molecular weight of these peaks was analysed by MS it was found that they represent compounds with molecular weights of 424.2 and 383.1 (Figure 2.52). These suggest the presence of DMB-labelled sialic acid and N-deacetylsialic acid respectively.

The formation of de-acetylated sialic acid has been previously reported in a number of studies. Study by Chikako M. et al., reported the modification of sialic acid in several cultured lymphocytic leukemia cell lines, through first de-N-acetylation of sialic acid moiety through ubiquitous de-N-acetylationyre-N-acetylation cycle, followed by the dehydrative cyclisation of de-N-acetyl sialic acid to form ‘‘cyclic sialic acid’’. This study suggested a possible physiological significance of this reaction to be a rapid inactivation of selectin binding activity at the cell surface [149].

The presence of the second peak representing de-acetylated sialic acid reduced the quantification efficiency of the technique since it resulted in broadening of the peak and overlapping with adjacent peaks. A second drawback of the technique was that DMB doesn’t only label sialic acid; it was found that DMB also labelled other components of the cell extract, which resulted in multiple unidentified peaks, also reducing the efficacy of the detection of the sialic acid peak through overlapping with it (Figure 2.53). In order to overcome these problems, an MRM technique using UPLC/MS/MS was developed for the detection of DMB-DP1.

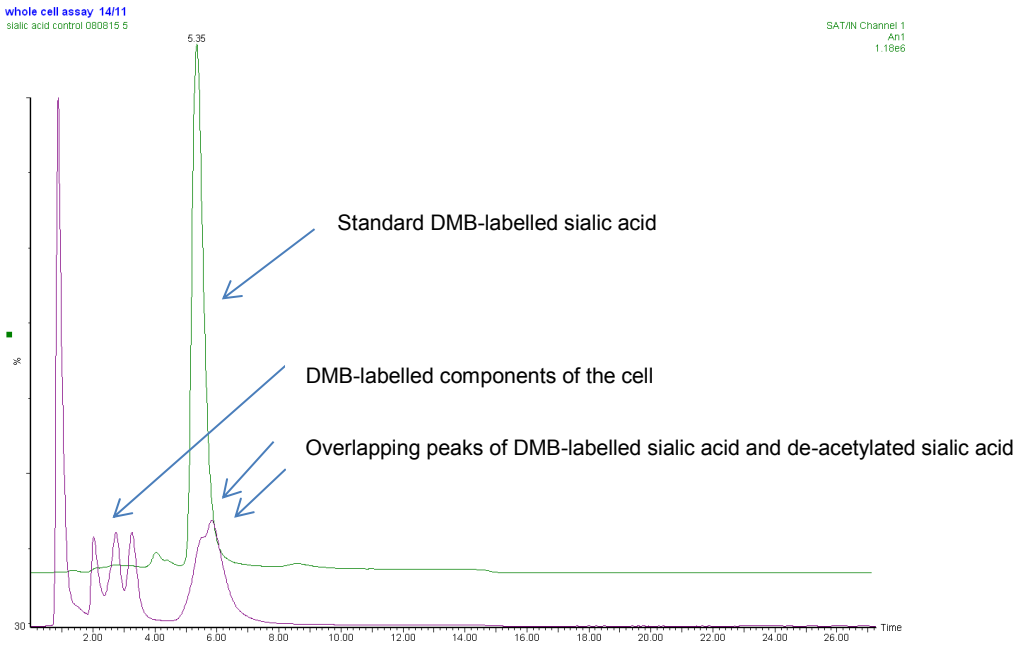

Figure 2.52 Analysis of released sialic acid using mild acidic hydrolysis and mixed phase-HPLC technique showing two peaks of labelled sialic and de-acetylsialic acid at the same retention time. Labelling of other components of the cells with DMB which are adjacent to the DMB-sialic acid peak is also shown.

2.3.17.2. MRM analysis of DMB-DP1

In order to set an MRM channel for specific DMB-DP1 detection, the mobile phases used were: ammonium formate (5 mM, mobile phase A) and methanol (mobile phase B), with isocratic method of 80% mobile phase A: 20% mobile phase B. The optimal cone voltage and collision energy associated with each transition were established and the run time was optimised to 6 minutes where the DMB-DP1 eluted at 4.9 minutes (Figure 2.53A).

(A)

Transitions	Molecular weight (mwt)	Z	Parent ion (m/z)	Daughter ion (m/z)	CV (V)	CE (eV)	Dwell time (sec)
1	425.4	+1	426	229.23	25	20	0.2
2	425.4	+1	426	313.02	25	20	0.2

(B)

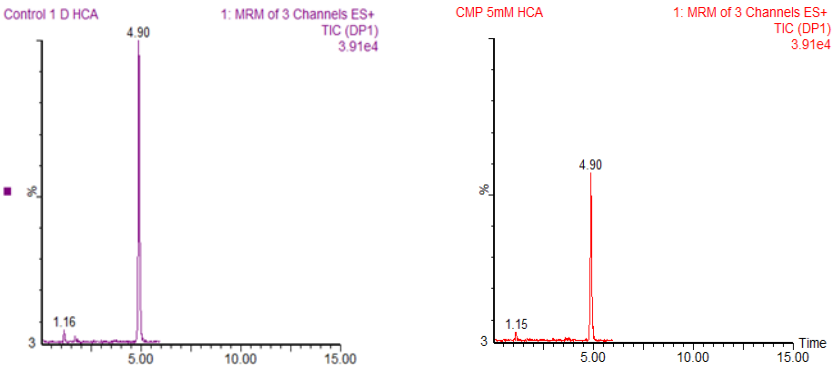
Control 1 D HCA
1: MRM of 3 Channels ES+
TIC (DP1)
3.91e4
4.90
1.16
5.00
10.00
15.00
CMP 5mM HCA
1: MRM of 3 Channels ES+
TIC (DP1)
3.91e4
4.90
1.15
Time
5.00
10.00
15.00

(C)

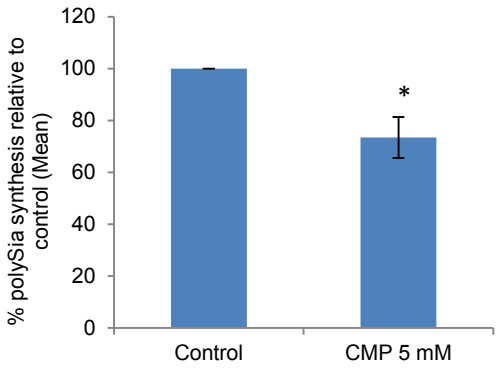
% polySia synthesis relative to control (Mean)
120
100
80
60
40
20
0
*
Control
CMP 5 mM

(D)

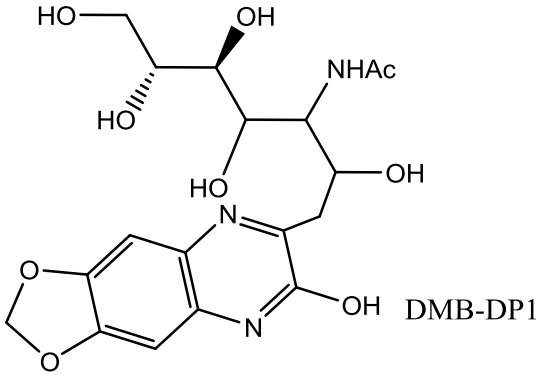
HO
OH
NHAc
HO
HO
OH
N
O
O
N
OH
DMB-DP1

(E)

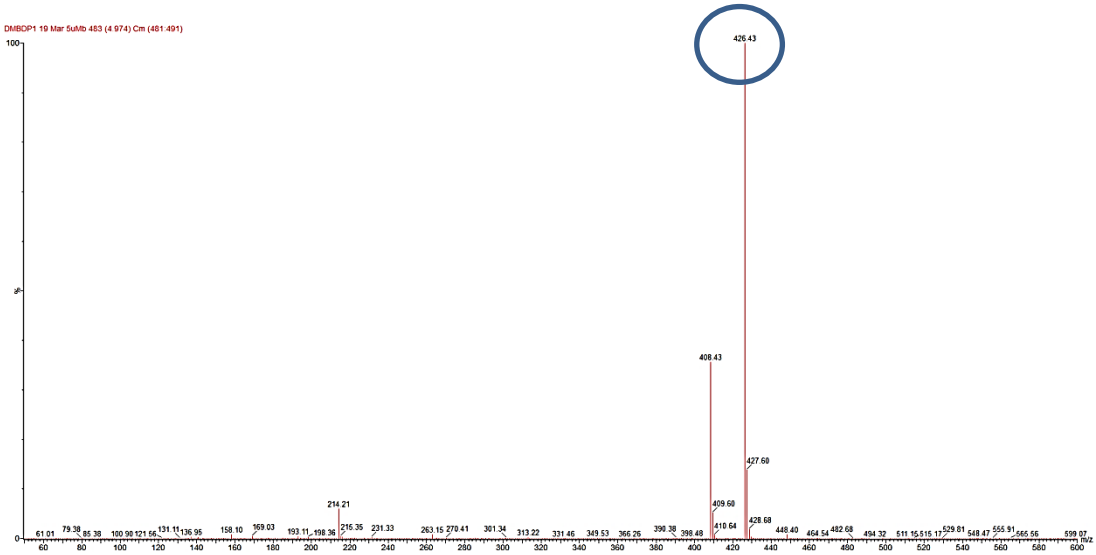
426.43
408.43
427.60
409.60
214.21
410.64
428.68

(F)

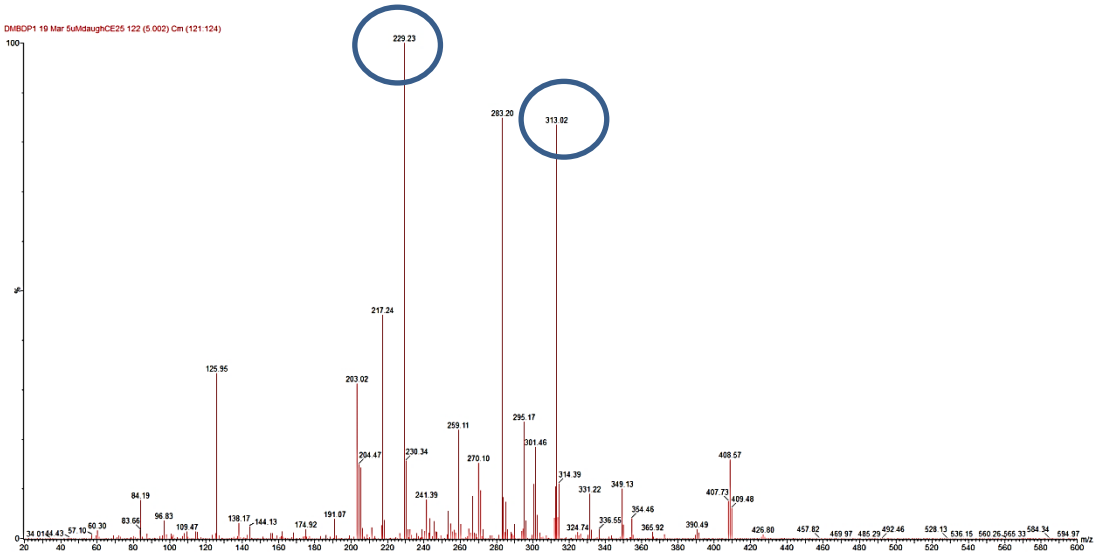

Figure 2.53 MRM transitions, cone voltage (CV) and collision energy (CE) determined for DMB-DP1 (A). Experimental conditions: Waters mass spectrometer; 5 mM ammonium formate used as mobile phase A, methanol was used as mobile phase B, flow rate was set to be 0.3 ml/min with isocratic method of 80% mobile phase A: 20% mobile phase B. B, C) Detection of ST8SiaII inhibition with 5 mM CMP using the optimised technique shows specific detection of one peak representing DMB-DP1 at 4.9 minutes. (D) Chemical structure of the parent ion of DMB-DP1. Results represents mean of three independent experiments. Example of mass spectrum used for MRM channel setting of DMB-DP1 showing parent ion selection for DMB-DP1 analysis (E) and daughter ion selection (F).

5 mM CMP was analysed using the optimised TFA protocol along with the MRM analysis; it was found that using this technique enabled highly efficient quantitative detection with no overlapping peaks of de-acetylated DMB-sialic acid (Figure 2.53B, C).

2.3.18. Applications of the developed cell-based HPLC assay

2.3.18.1. Application of the cell-based HPLC assay to understand the mechanism of action of N-acylmannosamine compounds

The effect of N-acylmannosamine derivatives treatment on polySia expression in NCAM- and ST8SiaII -expressing cell lines has been a matter of debate; some studies suggest that treatment of polySia-expressing cells with N-acylmannosamine compounds significantly reduces their cell surface polysialylation through competitive inhibition of ST8SiaII [150]. On the other hand, other studies have shown that N-propanoylsialic acid (SiaProp), generated from N-propanoylmannosamine (ManNProp), is readily accepted

by polySTs and permits the extension of modified polySia (in the form of polySiaProp) on NCAM. It is suggested that, despite being immunologically distinct, the subtle structural differences in polySia resulting from the incorporation of SiaProp residues do not alter the anti-adhesive properties of polysialylated NCAM [151].

In this experiment, SH-SY5Y cells were treated with ManNProp (ICT-3128, 250 µM) for 24 hours and the ability of ManNProp to either incorporate into the polySia chains (giving modified polySia) or to block the polySia synthesis by competitive inhibition of ST8SiaII enzyme was examined.

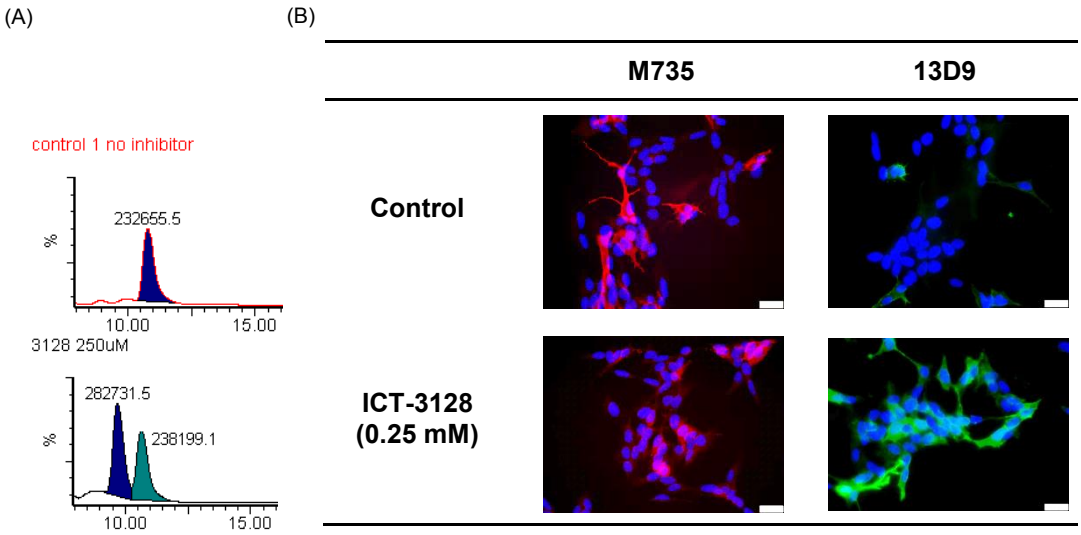

Figure 2.54 Analysis of the effect of ManNProp treatment on SH-SY5Y polySia synthesis showing the incorporation of the compound in the polySia chains giving modified prop-Sia (A), immunofluorescence staining of manNProp treated cells and control untreated cells with m735 mAb (specific for polySia) and 13D9 mAb (specific for modified Prop-Sia) shows that treatment of SH-SY5Y cells with ManNProp results in the formation of modified Prop-Sia chains (B). Scale bar represents 250 µm.

The results were analysed using mixed-phase HPLC technique to determine the synthesis of the modified prop-Sia chains and/or polySia chains. A second peak was detected at an elution time of 9.8 minutes (Figure 2.54A). The molecular weight was found to be equal to the molecular weight of DMB-N-propanoylsialic acid (439.2) when analysed with mass spectrometry. This suggests that ManNProp was ultimately incorporated in the polySia chain resulting in the formation of modified polySia chains but did not inhibit polySia formation. These results were confirmed by staining SH-SY5Y cells that had been treated with ManNProp with M735 mAb (specific for polySia)

and 13D9 mAb (specific for modified Prop-Sia) [152] and comparing them to control untreated cells (Figure 2.54B). It was found that control cells stained negative for Prop-Sia and positive for polySia while ManNProp-treated cells stained positive for both.

To sum up, this work confirmed that administration of ManNProp to SH-SY5Y cells resulted in modified polySia chains (Prop-Sia) and did not significantly cause competitive inhibition of ST8SiaII. This is the first conclusive evidence to resolve the conflicting reports in the literature.

Confirmation of the incorporation of ManNProp into polySia on cancer cell membrane starts a new discussion about the potential significance of polySia chain modification on cancer cell migration, invasion and recognition by the body's natural immunity. Sialylated oligosaccharides on the cell surface of bacteria are thought to provide a protective barrier to evade detection and attack by the host's immune system [153]. Therefore, changes in polySia structures on cancer cell surface might render them recognisable to immune cells, which requires further investigation.

The results obtained in this study have been confirmed with mass spectrometry giving the molecular weight of the released monomers from the sialic acid chains unlike earlier studies, which utilised HPLC-FD or western blot. This will allow the study of not only the inhibitory effects but also the mechanism of action of different polySTs inhibitors in the complex functional system of the cell.

2.3.18.2. Application of cell-based HPLC assay for quantitative detection of polySia expression in different cancers

To-date, ELISA and western blot have been the main techniques used for the quantification of polySia expression in different cancers[154-156]. Although they both provide a robust, specific and clear qualitative measurement of polySia expression, the quantification associated with these assays is always problematic. Besides that, the antibodies required for these assays are highly

costly and need specific measurements to be target specific. Here we have used the developed cell-based HPLC assay to measure polySia expression in different cell lines. PolySia was harvested from the cell surface of SH-SY5Y, C6-STX and OSC-19 cell lines (10^6 cells/cell line) as described previously and quantified using MRM technique.

The results were presented as a percentage of polySia expression relative to that observed with C6-STX cells. It was found that SH-SY5Y expressed 91.6%, while OSC-19 expressed 98.9% of that measured with C6-STX cells. This technique can also be amended to express the results as nanograms of polySia per given number of cells by using a calibration curve of standard DMB-DP1 with known concentrations (the same technique used for the quantification of DMB-DP4 in the aforementioned cell-free HPLC assay). The results were confirmed using immunofluorescence which showed similar expression of polySia in the three cell lines (Figure 2.55).

The results obtained from this assay regarding SH-SY5Y and C6-STX cell lines were consistent with previously published data[109,157]. However, this was the first report of analysis of the expression of polySia in a head and neck cancer cell line (i.e. OSC-19). Sialic acid has previously been reported as a tumour marker in head and neck cancer [158], but here it was proved for the first time that polySia is also over-expressed in head and neck cancer. This may have a significant effect on the prognosis of the disease. Further studies with different head and neck cancer cell lines are required, but this is an exciting initial finding.

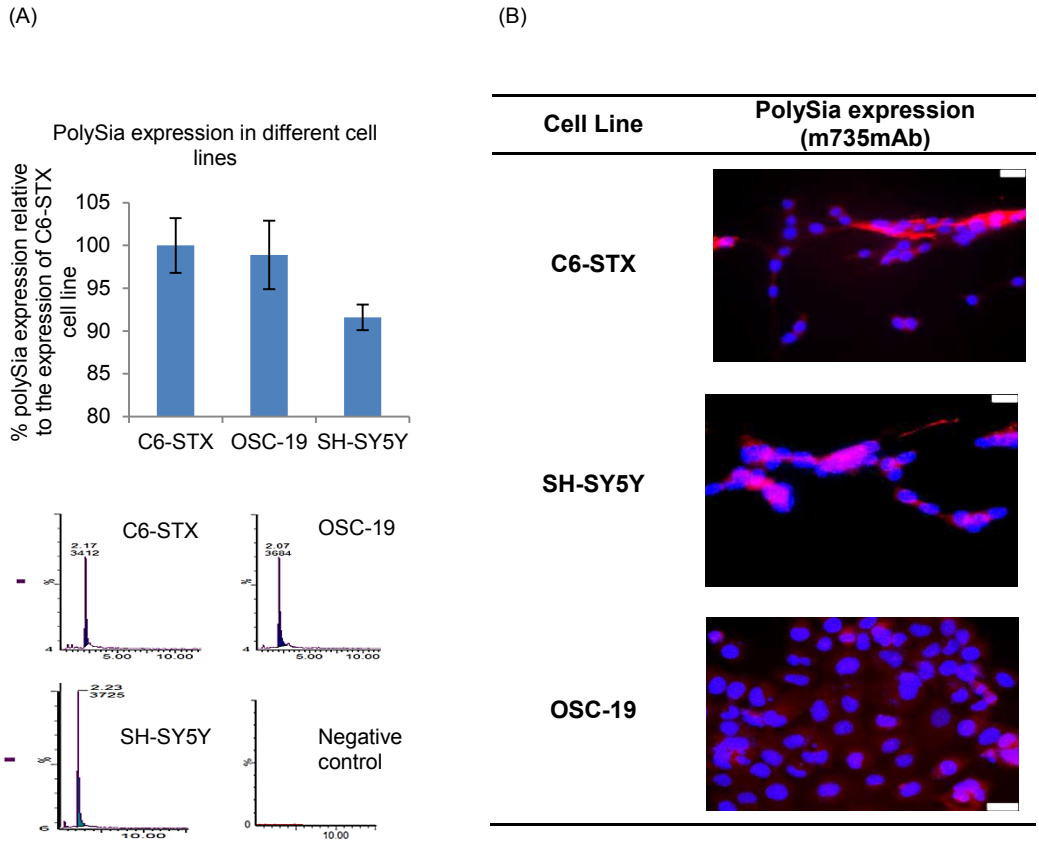

Figure 2.55 Analysis of polySia expression in SH-SY5Y, C6-STX and OSC-19 cell lines using the developed cell-based chromatographic assay, showing that SH-SY5Y express 91.6% while OSC-19 express 98.9% relative to C6-STX cells (A). The results were confirmed using immunofluorescence staining with m735 mAb specific for polySia, where it was found that the three cell lines showed similar expression of polySia (B). Results represents mean of three independent experiments. Scale bar represents 250 µm.

2.3.18.3. Application of cell-based HPLC assay for quantitative analysis of polySia synthesis inhibition by selected polyST inhibitors

Using the developed high throughput cell-based chromatographic assay, a panel of small molecule polyST inhibitors was evaluated. This panel included two sets of compounds; hit compounds identified from the cell-free chromatographic assay, namely: ICT-3143, ICT-3233, ICT-3234, ICT-3276 and other compounds including CMP-sialic acid precursors (N-acylmannosamines) including ICT-3176, ICT-3128 and ICT-3141. The difference in the mechanism of action of both will be discussed in detail in the next chapter. Average polySia expression relative to control was calculated following compound administration in each case (Table 2.18, Figure 2.56).

Table 2.18 Analysis of a panel of polyST inhibitors using the new cell-based HPLC assay. Each experiment was repeated three times and the standard deviation and standard error mean was calculated.

Inhibitor	% Average polySia synthesis relative to control	Standard deviation	Standard error mean
ICT-3176, 250 µM	49.4	9.5	6.7
ICT-3176, 500 µM	22.0	5.7	4.0
ICT-3125, 250 µM	109.3	2.2	1.5
ICT-3141, 250 µM	70.4	6.2	4.4
CMP, 5 mM	73.4	7.8	5.5
ICT-3234, 250 µM	28.5	4.8	3.4
ICT-3233, 250 µM	27.8	4.2	2.9
ICT-3234,125 µM	71.6	7.1	5.0
ICT-3233, 125 µM	73.8	1.6	1.1
ICT-3234, 25 µM	68.8	1.6	1.1
ICT-3233, 25 µM	79.5	12.0	8.5
ICT-3143, 25 µM	83.7	4.6	3.3
ICT-3276, 12.5 µM	83.0	5.2	3.7
ICT-3276, 15 µM	70.5	3.1	2.2
ICT-3276, 20 µM	63.5	4.6	3.3
ICT-3128, 250 µM	100.1	2.5	1.8
ICT-3128, 500 µM	74.1	5.4	3.8

(A)

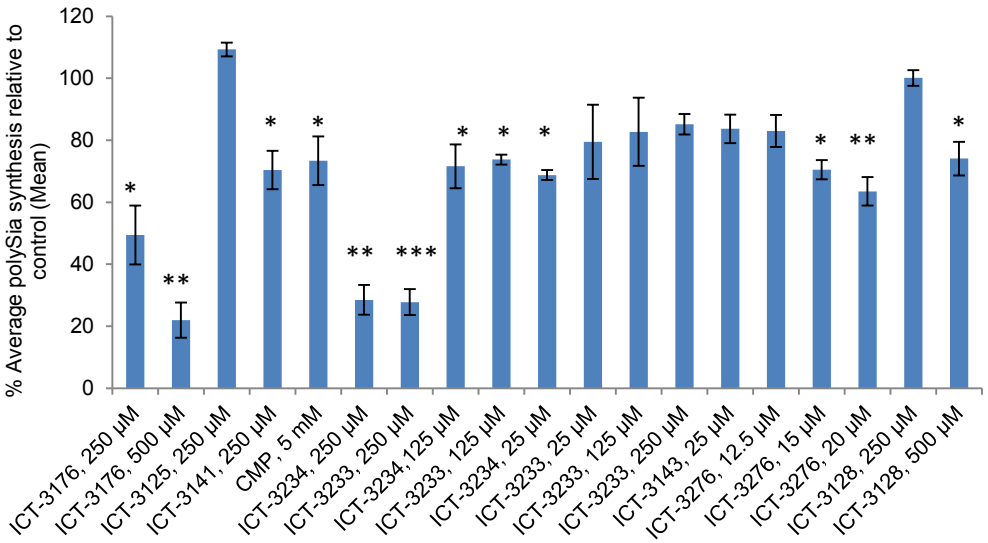
% Average polySia synthesis relative to control (Mean)
120
100
80
60
40
20
0
*
**
*
*
**
***
*
*
*
*
*
*
*
**
*
ICT-3176, 250 µM
ICT-3176, 500 µM
ICT-3125, 250 µM
ICT-3141, 250 µM
CMP, 5 mM
ICT-3234, 250 µM
ICT-3233, 250 µM
ICT-3234,125 µM
ICT-3233, 125 µM
ICT-3234, 25 µM
ICT-3233, 25 µM
ICT-3233, 125 µM
ICT-3233, 250 µM
ICT-3143, 25 µM
ICT-3276, 12.5 µM
ICT-3276, 15 µM
ICT-3276, 20 µM
ICT-3128, 250 µM
ICT-3128, 500 µM

(B)

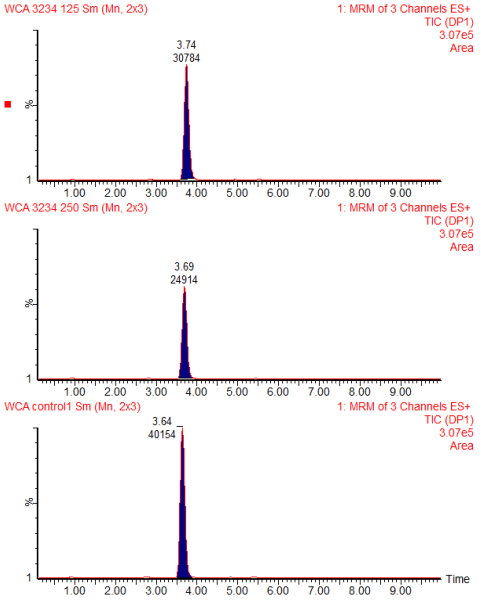
WCA 3234 125 Sm (Mn, 2x3)
1: MRM of 3 Channels ES+
TIC (DP1)
3.07e5
Area
3.74
30784
WCA 3234 250 Sm (Mn, 2x3)
3.69
24914
WCA control1 Sm (Mn, 2x3)
3.64
40154
Time

(C)

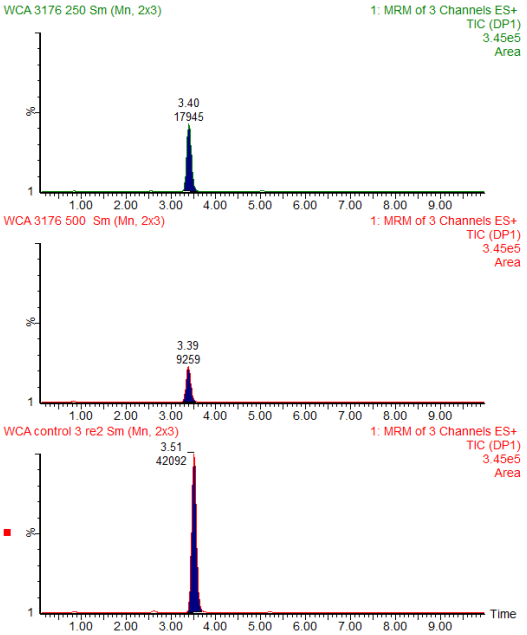
WCA 3176 250 Sm (Mn, 2x3)
1: MRM of 3 Channels ES+
TIC (DP1)
3.45e5
Area
3.40
17945
WCA 3176 500 Sm (Mn, 2x3)
3.39
9259
WCA control 3 re2 Sm (Mn, 2x3)
3.51
42092
Time

(D)

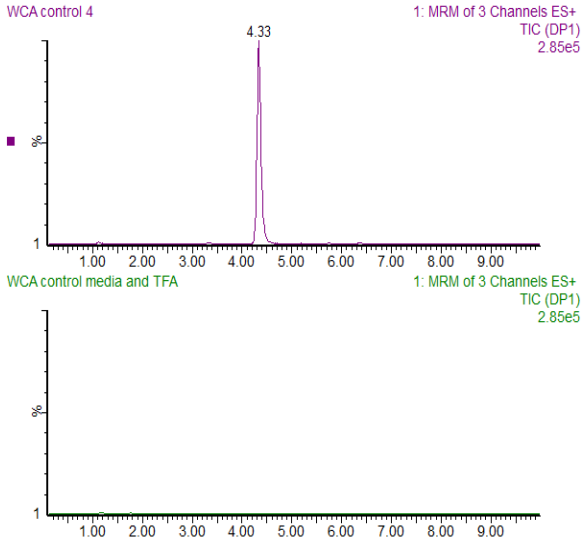

Figure 2.56 The reduction of polySia expression following administration of polyST inhibitors (A). (B) and (C) represent examples of chromatograms produced using the new cell-based assay for analysis of ST8SiaII inhibitors such as ICT-3234 and 3176 respectively, D) represents the analysis of different controls of the assay first control (upper) represents sialic acid released from polySia chains in untreated cells, control two (lower) represents analysis of sample at which all the chemicals and media were added but without adding cells in order to analyse the presence of any sialic acid monomers in the media. * P< 0.05, ** P<0.01 and *** P < 0.001.

According to the results obtained from this assay, it was found that the most active polyST inhibitors were ICT-3276 (36.4 ± 4.6% inhibition at 20 μM), ICT-3234 (71.4 ± 4.8% inhibition at 250 μM), ICT-3233 (72.1 ± 4.2% inhibition at 250 μM) and ICT-3176 (78 ± 5.7% inhibition at 500 μM). The polyST inhibition, as measured by reduction of polySia expression was found to be concentration-dependent.

The results showed that the rationally-designed polyST inhibitors generally exhibited higher potency than N-acylmannosamine compounds. This could be explained by the fact that some N-acylmannosamine compounds such as ManNProp have the ability to be incorporated in the polySia chains, giving modified polySia instead of terminating polySia chain elongation, as has been discussed earlier in this chapter and supported by previous studies (Section 2.3.18.1) [106,148].

Comparing the results of the cell-based and cell-free chromatographic assays shows correlation between the results from the two assays; compounds that showed the highest inhibition of recombinant ST8SiaII in the cell-free assay also showed the highest polyST inhibition in the cell-based

setting. This further validates the novel cell-free chromatographic assay for high throughput analysis of small molecule polyST inhibitors.

However, in cell-free assay it was found that ICT-3234 and ICT-3233 exhibit higher inhibitory effect than compound ICT-3276 while in cell-based assay compound ICT-3276 showed higher inhibitory effect than both ICT-3234 and ICT-3233, this could be explained by the possible difference in the uptake of the inhibitors in the cell-based setting that may be caused by difference in the polarity of the compounds.

2.4. Conclusion

PolySia over-expression is characteristic for several malignant tumours and is highly correlated with tumour growth and metastasis. The role of polySia in cancer progression highlights the need for selective polyST inhibitors (or inhibitors of polySia biosynthesis). The aim of the work discussed in this chapter was to develop reliable, sensitive and high throughput techniques for quantitative analysis of polyST inhibition in cell-free and cell-based protocols.

To obtain a highly pure and easy-to-handle fluorescent acceptor for fast and reliable testing of recombinant human polyST enzyme inhibition in the cell-free assay, a DMB-labelled oligosialic acid acceptor (DMB-DP3) was synthesised. Methods of labelling and purification were optimised to give high yields of a ≥99% pure compound.

In order to optimise the assay to be used for high throughput analysis of polyST inhibitors, a MRM method for the analysis of the assay product was developed using UPLC/MS/MS. This technique allowed the analysis of one inhibitor analytical sample in just six minutes. Besides, use of RP-UPLC allowed for rapid, sensitive and reproducible analysis, with the ability for the method to be conjugated with mass spectrometry to allow very specific product characterisation and generation of molecular weight information.

The second major part of the study involved the development of a cell-based chromatographic assay for the analysis of cell-surface polySia expression. In this assay, Endo-N and mild acidic hydrolysis techniques for harvesting polySia from the cell surface were used and optimised. The advantages and disadvantages of each technique were investigated in order to establish a reproducible, efficient and reliable technique. MRM analysis of the released sialic acid was also achieved, which allowed a very sensitive quantitative analysis of the effect of different polyST inhibitors on polySia biosynthesis and expression.

This new technique has been applied to study different aspects of polyST activity. The analysis of monomers released from polySia chains on the cell

surface and their identification with mass spectrometry allowed the investigation of potential modifications in the structure of these polySia chains caused by different inhibitors.

Another application of the developed cell-based assay was to give a quantitative and/or semi-quantitative measurement of polySia expression on the cell surface of different cancer cells. This technique can replace the multi-step, costly and less specific ELISA and western blot-based methods, which are the major techniques to have been used to date for the measurement of cellular polySia expression. We were able to demonstrate and quantify the expression of polySia in OSC-19 human head and neck cancer cells for the first time, and to compare levels with that observed in neuroblastoma cell line.

Two panels of polyST inhibitors were examined using these assays. The first set of compounds included rationally-designed polyST inhibitors synthesised at the Institute of Cancer Therapeutics. Investigation of these compounds contributed to understanding structure-activity relationships, which enables the determination of the chemical groups responsible for the interaction with ST8SiaII enzyme. This data will allow modifications to the structure of the compounds to be made in future, to optimise the potency of the inhibitors.

The second panel of compounds included CMP-sialic acid precursors (N-acylmannosamines). The effect of these compounds on the synthesis of polySia has always been a matter of debate. Some studies demonstrate that all artificial sialic acid precursors including ManProp, ManNBut and ManNPent strongly inhibit polySia biosynthesis [106,151,159]. Other studies suggest the capacity of human cell lines to incorporate unnatural sialic acids into modified polySia chains [104,150].

We have proved that treating tumour cells with ManNProp results in incorporation of modified sialic acid into the polySia chains. This was confirmed using LC/MS analysis, for the first time, to confirm the molecular weight of the monomers. The modified polySia chains were identified. Findings were further confirmed by immunofluorescence staining of the

treated cells with 13D9 (anti-propSia) and m735 (anti-polySia) monoclonal antibodies.

In conclusion, the developed techniques provide a quantitative and highly sensitive assay format for testing of polyST activity in both cell-free and cell-based settings. Both qualitative and quantitative information gained from these assays will continue to give new mechanistic insights into this important class of enzyme.

Analysis of different polyST inhibitors enabled the assessment of their potency and the identification of the most active compounds for further investigation. In order to determine the effect of polyST inhibition on cancer cell function, study in more complex assays is required. This will be explored in the next chapter.

Chapter 3. Evaluation of selected novel polysialyltransferase inhibitors in cell-based functional assays

3.1. Introduction

In the previous chapter, the development and optimisation of cell-based and cell-free high throughput chromatographic assays that allow for quantitative and sensitive analysis of polySia inhibition was described. Consequent to the development and validations of the assays, a series of rationally designed polyST inhibitors has been evaluated in order to determine the most promising compounds. In the work described in this chapter, selected small molecule inhibitors were analysed using MTT, migration and immunofluorescence assays in order to examine the effect of polyST inhibition on the migration of neuroblastoma SH-SY5Y cells and investigate their selectivity.

Current drug discovery strategies include target-based screening, phenotypic (functional) screening, modification of natural substances and biologic-based approaches; such as identifying monoclonal antibodies [160]. The focus of target-based screening is a gene product, known as a target. Molecular and chemical knowledge is used to investigate specific molecular hypotheses. On the other hand, the focus of phenotypic (functional) screening is to measure a clinically meaningful phenotype in a physiologically relevant system such as an animal or cell; the assays do not require prior understanding of the molecular mechanism of action [161].

There has been an increasing interest in the use of phenotypic screens in drug discovery as an alternative to target-focused approaches [162]. A frequent question is whether target-based approaches or phenotypic approaches provide better starting points for drug discovery.

A study by Swinney and Anthony found that among the 183 small-molecule drugs across all therapeutic areas approved between 1999 and 2008, 58 (32%) were discovered using phenotype-based approaches. Importantly, 28 (56%) of the 50 small-molecule first-in-class new molecular entities identified in their study resulted from phenotypic screening approaches, whereas 17 (34%) resulted from target-based approaches[160,162].

Focusing on target-based drug discovery in the absence of validated molecular mechanisms of action (MMOAs) was suggested to be a major technical factor contributing to the high attrition rates of small-molecule first-in-class medicines observed in the clinic [162].

A key conclusion of that paper, repeated in more recent reviews, was that phenotypic assays have the advantage of identifying drug leads and clinical candidates that are more likely to possess therapeutically relevant MMOAs. From this conclusion, one can infer that target-based drug discovery is not an inferior approach but that it is more likely to fail if target modulation is prioritized at the expense of understanding the most desirable MMOAs. These mechanisms can best be demonstrated by functional and phenotypic assays [162,163].

Here we have expanded our understanding of the molecular mechanism of action of the hit polyST inhibitors, determined previously by the chromatographic assays, using a 2D scratch migration assay and immunofluorescence assay, having confirmed non-cytotoxic compound concentrations using an MTT viability assay.

3.1.1. MTT viability assay

MTT (3-(4, 5-Dimethylthiazol-2-yl)-2, 5-diphenyltetrazolium bromide) is a colorimetric assay that measures specific aspects of cellular metabolism. The mechanism underpinning the assay relies on the up-take of MTT tetrazolium salt (colourless) and its reduction by mitochondrial reductases by actively growing cells, which transform it into a coloured formazan product that can be quantified by measuring absorbance using a spectrophotometer (Figure 3.57) [164,165].

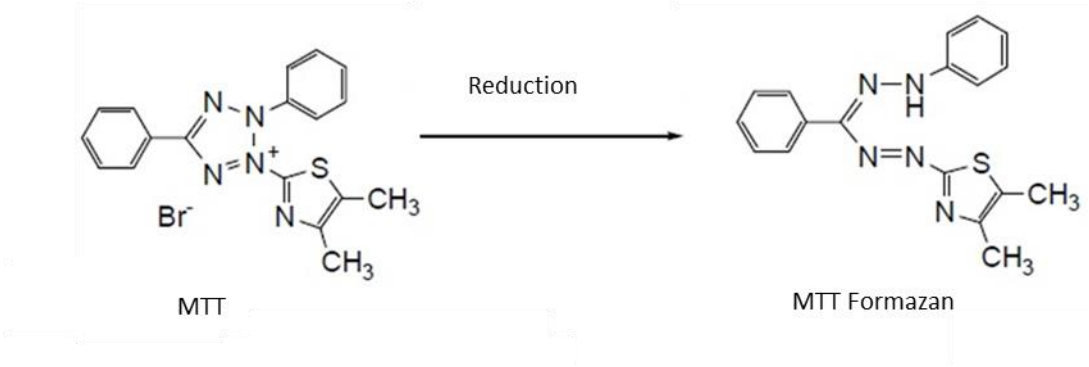

Figure 3.57 Scheme of reduction of MTT to formazan [166].

The MTT assay is thus a very useful tool to obtain information about cell viability in a high throughput manner [165]. Measurement of cell viability and proliferation forms the basis for numerous *in vitro* assays of a cell population's response to external factors. The MTT cell viability assay measures the cell proliferation rate and conversely, when metabolic events lead to apoptosis or necrosis, the reduction in cell viability [167]. Here MTT viability assays have been employed to select non-toxic concentrations of compounds to be evaluated in the 2D migration and immunofluorescence assays.

3.1.2. Scratch 2D migration assay

The *in vitro* scratch assay is an easy, low-cost and well-developed method to measure cell migration *in vitro*. The basic steps involve creating a scratch in a cell monolayer. Upon creation of a new artificial gap in a confluent cell monolayer, the cells on the edge of the newly created gap will move toward the opening to close the scratch until new cell–cell contacts are re-established. Capturing images at the beginning and at regular intervals during cell migration to close the scratch and comparing the images allows the quantification of the migration rate of the cells (Figure 3.58, [168]).

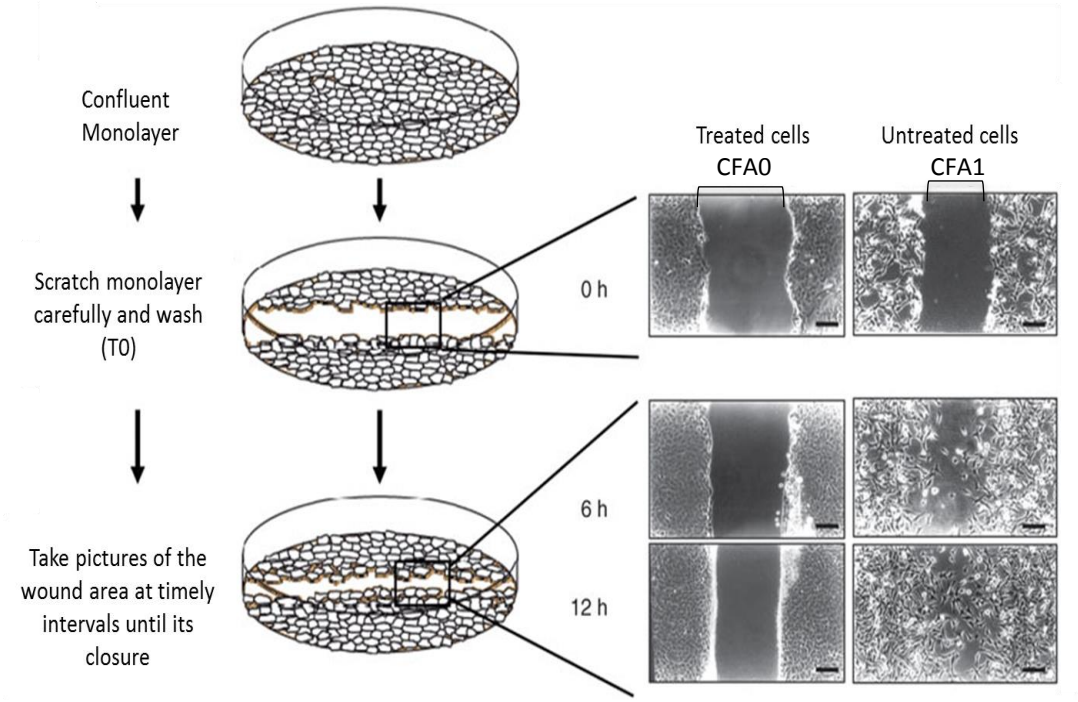

Figure 3.58 Schematic representation of the principal of 2D scratch migration assay [169].

One of the major advantages of this technique is that it mimics to some extent migration of cells *in vivo*. For example, removal of part of the endothelium in the blood vessels will induce migration of endothelial cells into the denuded area to close the wound. Furthermore, the patterns of migration as sheets of cells also mimic the behaviour of these cells during migration *in vivo*. Another advantage of the *in vitro* scratch assay is its particular suitability to study the regulation of cell migration by cell-matrix and cell–cell interactions. In other popular methods such as Boyden chamber assays, preparation of cells in suspension before the assays disrupts cell–cell interactions[169,170].

Here we have used the assay to evaluate the effect of polyST inhibition on the migration of different cell lines. The results contribute to our understanding of the structural requirements for a good inhibitor, by assessing selectivity by comparing effects on the migration of cell lines that express polySia and NCAM, NCAM only or are polySia and NCAM negative.

3.1.3. Assessed polysialyltransferase inhibitors

Two panels of polysialyltransferase inhibitors (polyST) were assessed using the aforementioned assays; polyST competitive inhibitors (hit compounds as determined by the chromatographic assays) and N-acylmannosamine compounds.

3.1.3.1. Rationally-designed competitive polysialyltransferase inhibitors

ICT-3233, 3234, 3143, 3276, 3268 and 3271 are polyST competitive inhibitors that have been derivatized from the parent compound ICT-3125 and designed using computer assisted drug design. ICT-3125 was originally identified from virtual screening of commercially available libraries, using a homology model structure of the ST8SiaII enzyme. In competitive inhibition, a molecule similar to the substrate competes for occupation of the active site, but blocks activity of the enzyme (Figure 3.59) [171].

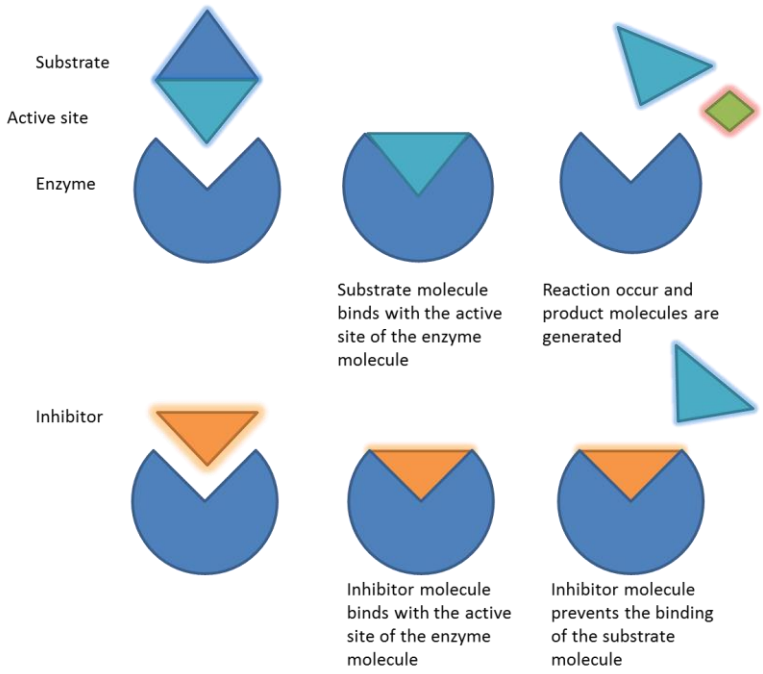

Figure 3.59 Schematic representation of the mechanism of action of competitive inhibition.

3.1.3.2. N-acylmannosamine compounds

Different N-acylmannosamines have been studied for their ability to inhibit polySia biosynthesis. As mentioned earlier (Chapter 1, Section 1.7.1), small-molecule inhibitors such as ManBut and ManProp have the advantages of temporal control and reversibility. In the previous chapter it was shown that, using cell-based chromatographic assay, treating cells with these inhibitors resulted in either modification of polySia structures (ICT-3128) or significant inhibition of polySia expression (ICT-3141).

Here, we have assessed the *in vitro* cytotoxicity of ManPent (ICT-3141), ManProp (ICT-3128) and ICT-3176 and compared this with the cytotoxicity of the rationally designed inhibitors.

Table 3.19 Summary of the compounds to be studied in this chapter.

	Inhibitor molecules
Hit rational-designed ST8SiaII inhibitors (Selected through both cell-based/cell-free chromatographic assays)	ICT-3276
	ICT-3234
	ICT-3233
	ICT-3143
	ICT-3125
N-acyl mannosamine inhibitors	ICT-3128
	ICT-3141
	ICT-3176
	ICT-3149

To sum up, the work presented in this chapter has three main aims. The first aim was the analysis of the *in vitro* cytotoxicity of the rationally designed inhibitors and compare them with the N-acylmannosamine compounds (Table 3.19), and to use these results to select suitable non-toxic concentrations to be further used for the migration assay. The second aim was the analysis of the effect of polyST inhibitors, selected via both cell-free and cell-based chromatographic assays, on the migration of polySia-NCAM

expressing neuroblastoma SH-SY5Y cells. Additionally, the selectivity of these inhibitors was analysed using the C6 glioma isogenic system and polySia negative colorectal carcinoma cell line (DLD-1) as negative control. Finally, the third aim was to characterise cell-surface polySia expression after polyST inhibition with hit inhibitors using immunofluorescence.

3.2. Material and methods

All the materials are purchased from Sigma Aldrich, UK unless otherwise specified.

3.2.1. Cell lines used in this study

Cell lines were maintained as described previously in chapter 2. DLD-1 colorectal adenocarcinoma cells and C6-WT glioma cells were obtained from the cell culture facility at the Institute of Cancer Therapeutics, University of Bradford. The methodology for the transfection of C6 cells with pcDNA3-STX plasmid inserted with cDNA encoded full length human STX, has been reported previously [66]. This was carried out by collaborators (Dr. Minoru Fukuda) at the Sanford-Burnham Institute, La Jolla, CA., USA.

DLD-1 cell line were maintained in RPMI medium supplemented with 10% foetal bovine serum, 1% sodium pyruvate and 1% glutamine while C6 wild type glioma cells was maintained in MEM Alpha eagle with ultra-glutamine-I, deoxyribonucleoside and ribonucleosides supplemented with 10% foetal bovine serum. All cell lines were maintained in a humid atmosphere of 5% CO_2 and 95% air at 37 °C.

3.2.2. Growth curves of cell lines

Cells were maintained and counted as described earlier (Chapter 2). After cells were counted, the cell suspension was diluted in order to have an appropriate amount of medium and that cells achieve a proper seeding density (1.5×10^5 for SH-SY5Y cell line, 2.5×10^4 for C6 cell line and 5×10^5 for DLD-1 cell line). Five flasks of each cell line were seeded with the same cell density. The plates were incubated in a humid atmosphere of 5% CO_2 and 95% air at 37 °C. The duplicate plates were counted every 24 hours. The results were plotted on a log-linear scale. The population doubling time was determined by identifying a cell number along the exponential phase of the curve, tracing the curve until that number has doubled, and calculating the time between the two.

3.2.3. Migration assay

3.2.3.1. Coating of cell culture dishes

Cells were seeded onto six-well plates to create a confluent monolayer (1 x 10^6 for SH-SY5Y cell line, 5 x 10^5 for C6 cell lines and 8 x 10^5 for DLD-1 cell lines). Dishes were incubated for approximately 24 h at 37 °C, allowing cells to adhere and spread completely.

3.2.3.2. Scratch assay

Cell monolayers were scraped in a straight line to create a "scratch" with a p200 pipette tip. The debris were removed and the scratch edge was smoothened by washing the cells once with the growth medium (1 ml) and then replace it with polyST inhibitor-containing medium (2 ml) or fresh medium (containing DMSO in concentration equivalent to the concentration of polyST inhibitor) for the control.

To obtain the same field during the image acquisition, markings were created to be used as reference points close to the scratch. The reference points were made by an ultrafine tip marker on the outer bottom of the dish. After the reference points were made, the dish was placed under a phase-contrast microscope, and the reference marks were left outside the capture image field but within the eye-piece field of view. The first image of the scratch was then acquired using a Lumascope 500 microscope.

Plates were placed in a tissue culture incubator at 37 °C for 16, 24 and 41 h for C6, SH-SY5Y and DLD-1 cell lines respectively. The time-frame for incubation for each cell line was determined according to the results obtained from growth curves. The dishes were taken out of the incubator to be examined periodically and then returned to resume incubation. After the incubation, plates were placed under the Lumascope microscope, reference points were matched, the photographed region acquired at the first image was aligned and a second image was acquired [168].

3.2.3.3. Data analysis

The images acquired for each sample were analysed quantitatively by using ImageJ software. For each image, distances between one side of scratch and the other were measured at certain intervals (µm). By comparing the images from time 0 to the last time point the percentage of wound closure of each compound was measured = (CFA0-CFA1) / CFA0) x 100 and then compared to the control to obtain the % of migration = (wound closure % with compound / wound closure % of control) x 100, where CFA0 is wound size or cell-free area at T0 and CFA1 is wound size or cell-free area at T (16/24 or 41) (Figure 3.59).

3.2.4. MTT assay

3.2.4.1. Reagent Preparation

MTT stock solution (12 mM) was prepared by adding sterile water (20 ml) to MTT (100 mg) and vortex mixing until dissolved. Occasionally there was some particulate material that did not dissolve; this was removed by filtration or centrifugation. Once prepared, the MTT solution was stored up to four weeks at 4°C, protected from light.

3.2.4.2. Coating of cell culture dishes

Cells were seeded onto 96-well plates to create a confluent monolayer (1 x 10^4 cells for the SH-SY5Y cell line, 5 x 10^3 for the C6 cell line and 8 x 10^3 for DLD-1 cells). Dishes were incubated for approximately 24 h at 37 °C, allowing cells to adhere and spread completely. For each plate, three wells were coated with fresh medium, these wells were used later to measure the background absorbance.

3.2.4.3. Cell treatment with potential polyST inhibitors

After 24 hours incubation, media in the 96 well plates was aspirated, and cells were washed once with the growth medium (200 µl). This was then replaced with polyST inhibitor-containing medium (200 µl) at different concentrations (500, 250, 125, 12.5 and 1.25 µM), or fresh medium (containing the same concentration of DMSO as in the polyST inhibitor containing medium. DMSO was limited to a concentration of 0.1%, which was proven to have no effect on cells viability) as a control.

3.2.4.4. MTT treatment

Cell line cultures were removed from the incubator into a laminar flow hood. Re-constituted MTT was added in an amount equal to 10% of the culture medium volume. Cultures were then re-incubated for 4 hours at 37 ºC. After the incubation period, cultures were removed from incubator and the resulting formazan crystals were dissolved by adding an amount of MTT solubilisation solution (DMSO) equal to the original culture medium volume. Solutions were pipetted up and down to completely dissolve the MTT formazan crystals.

3.2.4.5. Data analysis

Absorbance of the samples was measured spectrophotometrically at a wavelength of 540 nm. The background absorbance of multi-well plates was also measured and subtracted from the absorbance observed with the test samples.

The absorbance reading acquired for each sample was analysed quantitatively. For each reading, the absorbance of the multi-well plates was subtracted and the % viability of each compound concentration was calculated (= absorbance with the polyST inhibitor / absorbance of control x 100). The experiments were repeated three times (three independent experiments) and for each experiment 4 technical repeats were carried out.

3.2.5. Immunofluorescence analysis of polySia-NCAM

Immunofluorescence assay was performed as previously described in chapter 2 (Section 2.2.10). For the detection of polyST inhibition, cells were treated with different concentrations of inhibitor and incubated for 16 hours. Cells were immunolabeled with mouse anti-polySia antibody (clone: mAb 735, 15 µg/ml) for the detection of polySia, or mouse anti-NCAM antibody (RNL-1, 10 µg/ml) (abcam, UK) for the detection of NCAM expression or Ki-67 antibody for the detection of cell proliferation (ab15580,1 µg/ml) (abcam, UK).

3.2.6. Inhibitors stock preparation

All inhibitors stock solutions were prepared in DMSO and diluted in fresh medium before use to form a final DMSO concentration ≤ 0.1%.

3.2.7. Statistics

All experiments were repeated three times independently unless otherwise specified. Statistical analyses were performed using Excel software. Differences between two groups were evaluated with Student's t test (Two tailed) where the P value significance is: P value (P) >0.05 was deemed not significant, P < 0.05 * was statistically significant, P < 0.01 ** and P < 0.001*** were statistically highly significant.

3.3. Results and discussion

3.3.1. Confirmation of polySia-NCAM expression in the cell lines used in the study

Four different cell lines were used in order to further investigate the activity of hit polyST inhibitors previously determined by the chromatographic assays; SH-SY5Y, C6-STX, C6-WT and DLD-1. Although the expression of polySia and NCAM of these cell lines were previously investigated and reported in the literature [109], here we carried out two experiments to further confirm these findings; immunofluorescence and western blotting.

3.3.1.1. Immunofluorescence detection of polySia-NCAM in different cell lines

In order to investigate the expression of polySia and NCAM in different cell lines, cells were seeded on a cover slip onto six well plates (2×10^4 cell/well) and immunolabeled with anti polySia antibody (mAb 735) or anti NCAM antibody (RNL-1). The cells were then mounted with Vectashield hardset fluorescent mounting medium containing DAPI for the detection of DNA content and nuclei. Samples were examined by fluorescence microscopy. The results obtained were consistent with the literature: SH-SY5Y and C6-STX were found to be polySia and NCAM positive, C6-WT was polySia negative and NCAM positive and finally, DLD-1 was both polySia and NCAM negative (Table 3.20).

Table 3.20 Expression of polySia and NCAM in SH-SY5Y, DLD-1, C6-STX and C6-WT cell lines. Scale bar represents 250 µm. Results represents three independent experiments.

Cell line	PolySia Expression	NCAM expression
SH-SY5Y	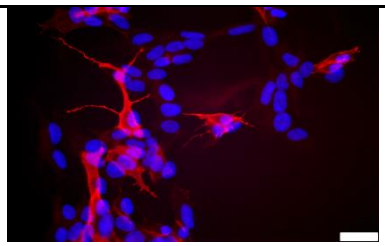	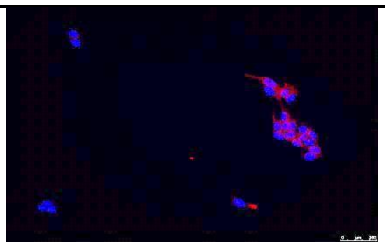
DLD-1	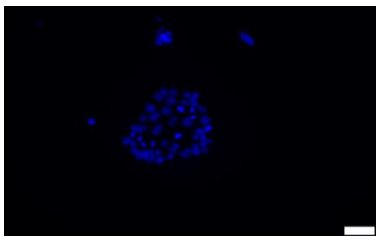	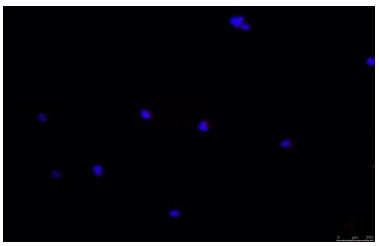
C6-STX	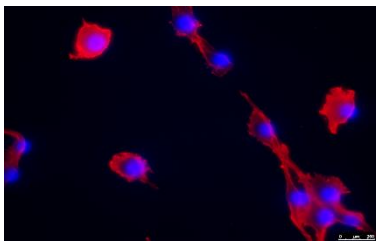	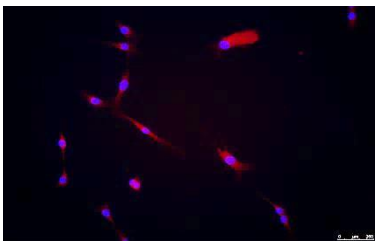
C6-WT	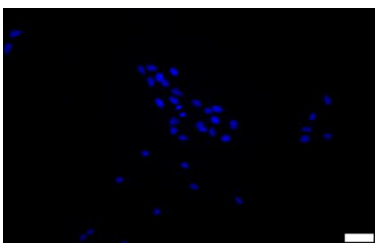	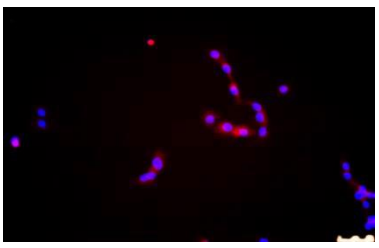

3.3.1.2. Western blot detection of polySia in different cell lines

For further confirmation western blot analysis was performed, as described in chapter 2. The blot was probed with either mAb 735 for the detection of polySia (1:3000) or B-actin antibody (1:5000, sigma). Antibody reactivity was detected by using anti-mouse fluorescent secondary antibody (1:500) (WesternDot 625, life technologies) and infrared digital imaging.

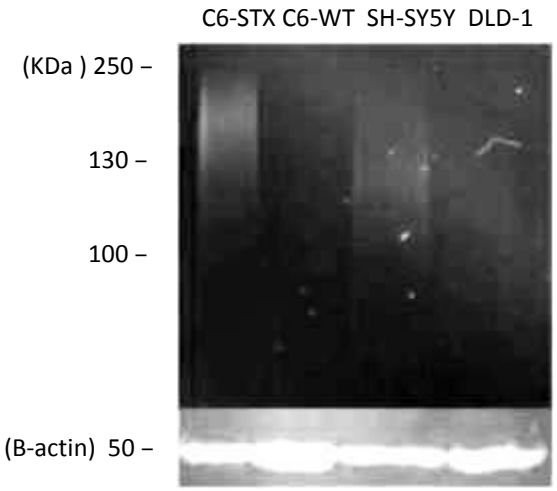

Figure 3.60 Western blot analysis of polySia expression in C6-STX, C6-WT, SH-SY5Y and DLD-1 cell lines using fluorescence detection. Blot represents three independent experiments.

The results obtained by western blot analysis confirmed the expression of polySia in SH-SY5Y and C6-STX cell lines, while no expression was detected with either C6-WT or DLD-1 cell lines (Figure 3.60). The polySia band appeared as continuous smear between 250 and 100 KDa, indicating the expression of different polymer chain lengths (degrees of polymerisation, DP). This method was used only as a confirmative qualitative assay since the previously developed cell-based HPLC assay, described earlier in chapter 2, allowed more accurate method for quantitative detection of polySia expression.

3.3.2. MTT assay: establishment of non-toxic concentrations of polyST inhibitors

The MTT assay (as described above) was used to assess the *in vitro* cytotoxicity of the hit polySTs inhibitors used in this study. Absorbance values were blanked against DMSO and the absorbance of cells exposed to medium only (no polyST inhibitor) were taken as 100 % cell viability (control). The percent cytotoxicity of the treated cells was calculated using the formula: % cytotoxicity = (% cytotoxicity of control/ % cytotoxicity of treated cells) x 100%.

The IC_{50} and IC_{20} values for the STX inhibitors for each cell line was also calculated from the following equation:

$$IC_{50} = [(50-A)/ (B-A)] \times (D-C) + C$$

$$IC_{20} = [(80-A)/ (B-A)] \times (D-C) + C$$

Where:

A = the first point on the curve, expressed as percent inhibition, that is less than 50% (80% for IC_{20})

B = the first point on the curve, expressed as percent inhibition, that is greater than or equal to 50% (80% for IC_{20}).

C = the concentration of inhibitor that gives A% inhibition

D = the concentration of inhibitor that gives B% inhibition.

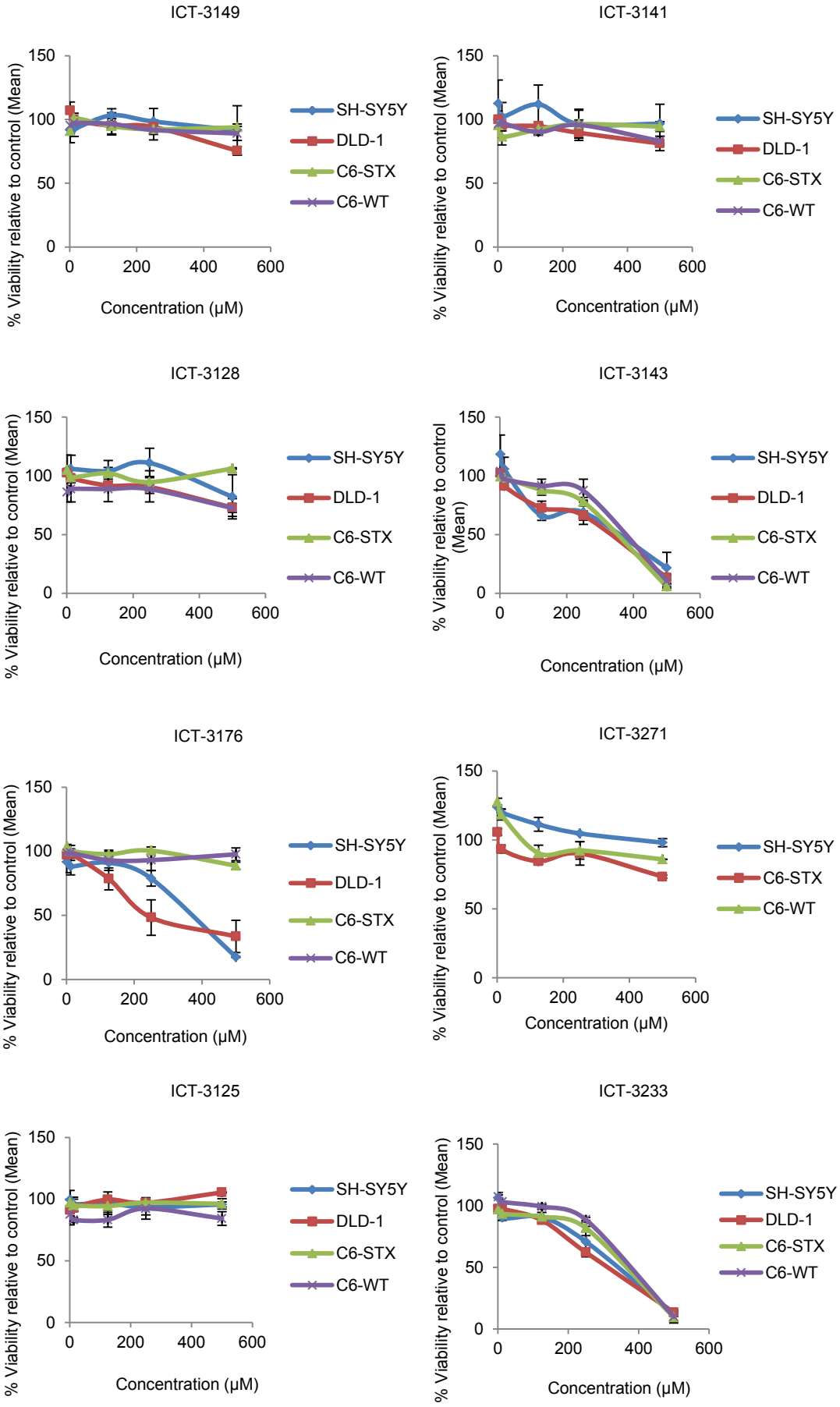
ICT-3149
% Viability relative to control (Mean)
150
100
50
0
0
200
400
600
Concentration (μM)
SH-SY5Y
DLD-1
C6-STX
C6-WT
ICT-3141
% Viability relative to control (Mean)
150
100
50
0
0
200
400
600
Concentration (μM)
SH-SY5Y
DLD-1
C6-STX
C6-WT
ICT-3128
% Viability relative to control (Mean)
150
100
50
0
0
200
400
600
Concentration (μM)
SH-SY5Y
DLD-1
C6-STX
C6-WT
ICT-3143
% Viability relative to control (Mean)
150
100
50
0
0
200
400
600
Concentration (μM)
SH-SY5Y
DLD-1
C6-STX
C6-WT
ICT-3176
% Viability relative to control (Mean)
150
100
50
0
0
200
400
600
Concentration (μM)
SH-SY5Y
DLD-1
C6-STX
C6-WT
ICT-3271
% Viability relative to control (Mean)
150
100
50
0
0
200
400
600
Concentration (μM)
SH-SY5Y
C6-STX
C6-WT
ICT-3125
% Viability relative to control (Mean)
150
100
50
0
0
200
400
600
Concentration (μM)
SH-SY5Y
DLD-1
C6-STX
C6-WT
ICT-3233
% Viability relative to control (Mean)
150
100
50
0
0
200
400
600
Concentration (μM)
SH-SY5Y
DLD-1
C6-STX
C6-WT

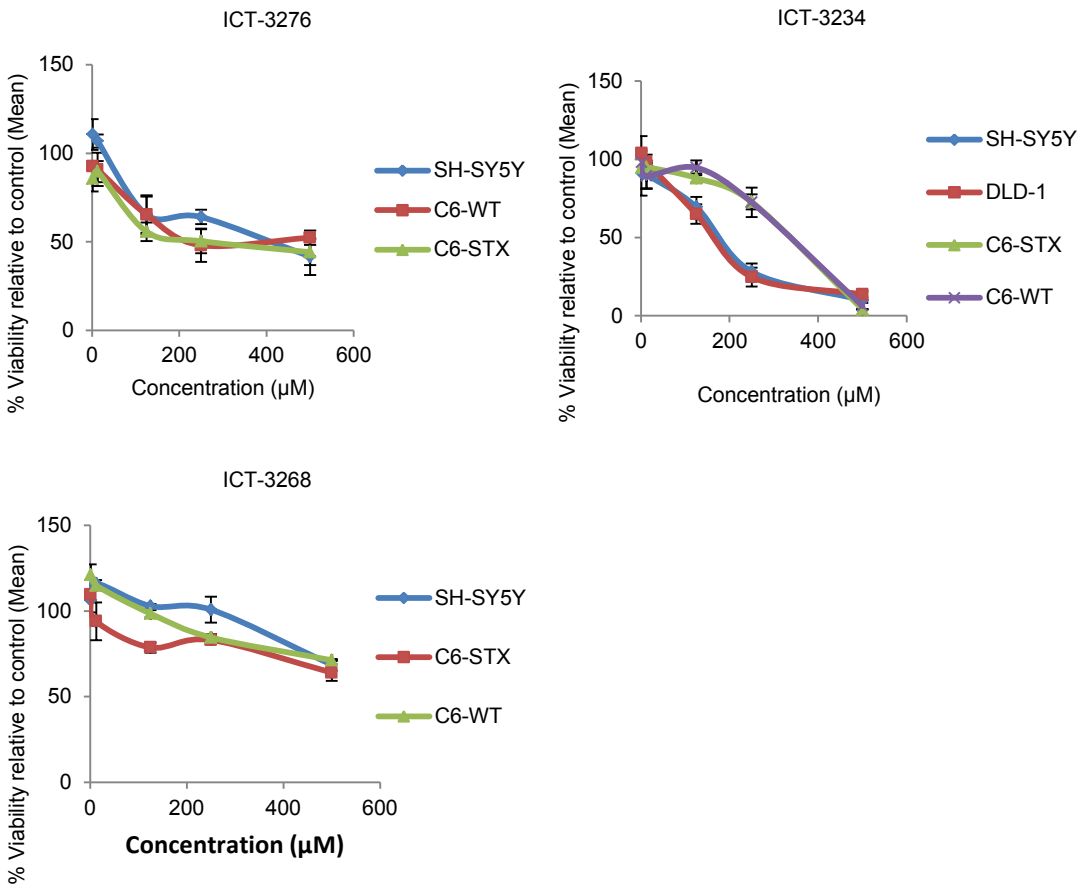

Figure 3.61 Analysis of viability of SH-SY5Y, C6-STX/WT and DLD-1 cell lines after treatment with different polyST inhibitors after 24, 16 and 41 hours respectively. Results represent three independent experiments.

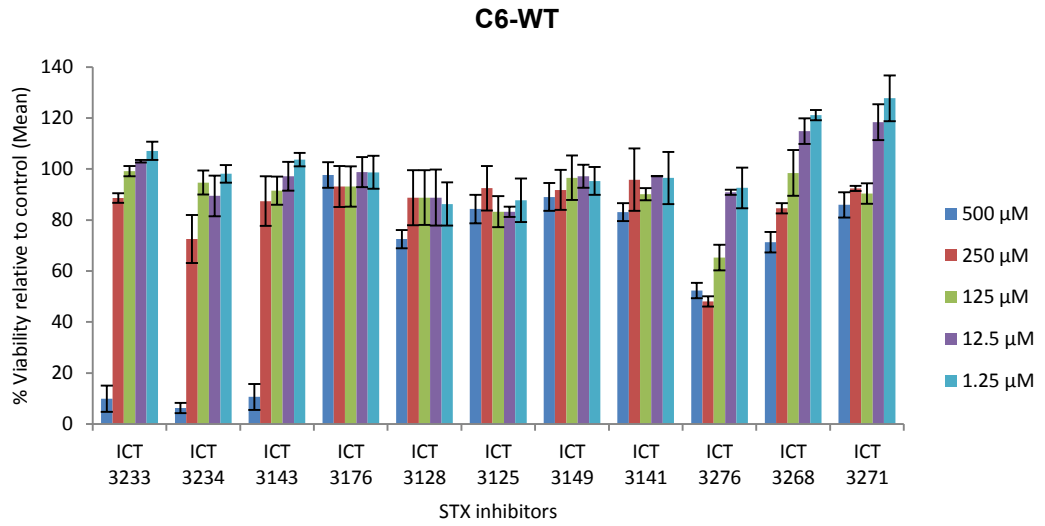
C6-WT
% Viability relative to control (Mean)
140
120
100
80
60
40
20
0
ICT 3233
ICT 3234
ICT 3143
ICT 3176
ICT 3128
ICT 3125
ICT 3149
ICT 3141
ICT 3276
ICT 3268
ICT 3271
STX inhibitors
500 µM
250 µM
125 µM
12.5 µM
1.25 µM

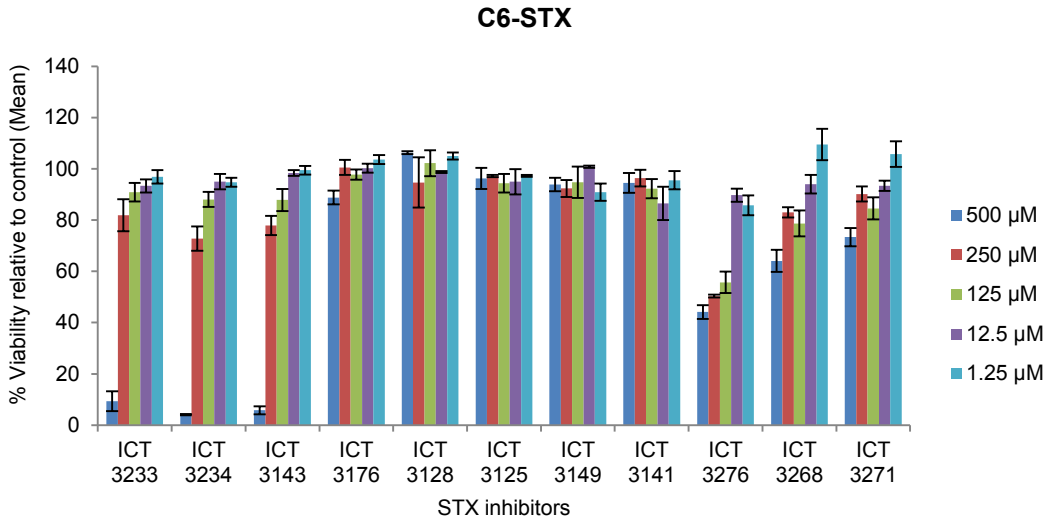
C6-STX
% Viability relative to control (Mean)
140
120
100
80
60
40
20
0
ICT 3233
ICT 3234
ICT 3143
ICT 3176
ICT 3128
ICT 3125
ICT 3149
ICT 3141
ICT 3276
ICT 3268
ICT 3271
STX inhibitors
500 µM
250 µM
125 µM
12.5 µM
1.25 µM

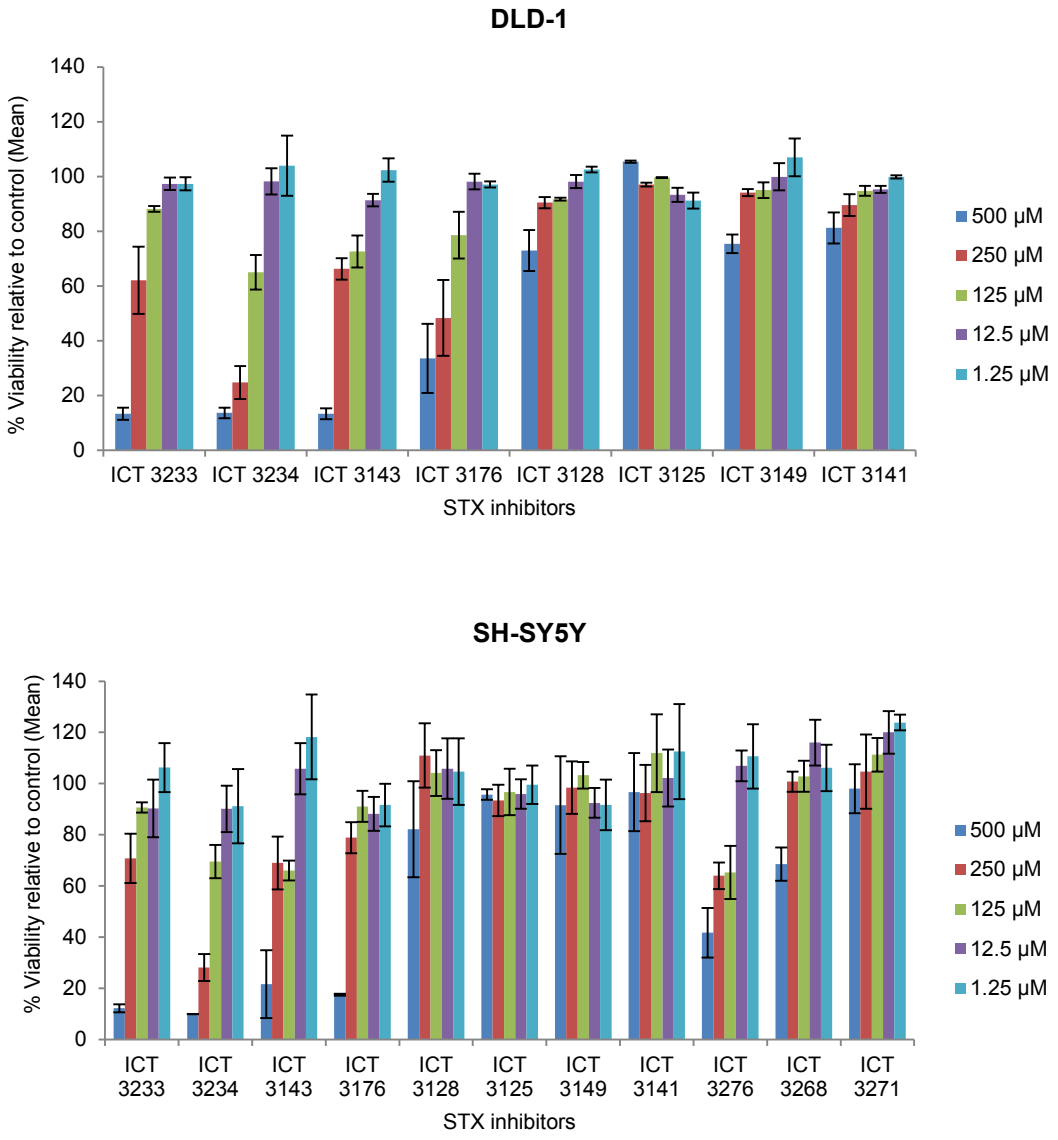

Figure 3.62 Results of MTT assay of different polyST inhibitors on different cell lines. Concentrations of agent that caused loss of viability in more than 20% of the cell population compared to control were considered to be toxic. Each experiment was repeated three times and the standard deviation was calculated.

According to the results obtained from the MTT assay (Figure 3.61, 3.62), the range of concentrations of each inhibitor used to perform migration assays was determined. The concentrations that caused less than 20% reduction in the viability of the cells compared to the control (IC_{20}) were chosen as non-toxic concentrations (Table 3.21).

Table 3.21 IC_{50} and IC_{20} values of different polyST inhibitors as determined by MTT assay on different cell lines. The results represent mean values of three independent experiments.

Cell line	C6-STX		C6-WT		SH-SY5Y		DLD-1	
Viability	IC_{50} (μM)	IC_{20} (μM)	IC_{50} (μM)	IC_{20} (μM)	IC_{50} (μM)	IC_{20} (μM)	IC_{50} (μM)	IC_{20} (μM)
ICT-3233	359±7	256±12	372±10	277±4	338±3	192±13	312±4	164±21
ICT-3234	332±10	190±9	335±4	207±18	183±6	67±8	171 ± 4	74±11
ICT-3143	346±8	223±7	371±10	274±19	350±18	85±14	326 ± 6	80 ± 7
ICT-3176	> 500	377±5	> 500	> 500	367±10	238±9	243 ± 21	116±24
ICT-3128	> 500	494±13	> 500	384±15	> 500	> 500	> 500	399±4
ICT-3125	> 500	> 500	> 500	> 500	> 500	> 500	> 500	> 500
ICT-3149	> 500	> 500	> 500	> 500	> 500	> 500	> 500	438±3
ICT-3141	> 500	> 500	> 500	> 500	> 500	380±15	> 500	> 500
ICT-3271	> 500	401±4	> 500	> 500	> 500	> 500	-	-
ICT-3276	263±7	44±6	235±3	60±2	407±5	85±3	-	-
ICT-3268	> 500	290±6	> 500	290±4	> 500	411±4	-	-

3.3.3. Migration assay

3.3.3.1. Optimisation of incubation time

In order to determine the optimum incubation time required for the migration assay, two factors were considered; the time required for closure of at least 80% of the induced scratch in the cell line monolayer, and time required for cell proliferation i.e. the incubation time had to be less than the cell doubling time to ensure that the measured effect is due to migration only and not proliferation.

Doubling time for C6-WT, C6-STX, DLD-1 and SH-SY5Y cell lines was determined by constructing a growth curve, and using the exponential phase of the curve. It was found that 24 and 48 hours were the doubling times for C6-WT/C6-STX and DLD-1/SH-SY5Y cells respectively, using full growth medium. Two time points, below 24 hours, where thus used to determine the suitable incubation time required to induce 80% closure of the scratch in C6-WT/STX cell lines; 13 and 16 hours and 24, 41 hours, below 48 hours, for DLD-1/SH-SY5Y cell lines.

It was found that 16, 24 and 41 hours are the most suitable incubation times for performing of scratch assay on C6-STX/C6-WT, SH-SY5Y and DLD-1 cell lines respectively (Table 3.22).

Table 3.22 Optimisation of incubation times for migration assay using C6-WT, C6-STX, DLD-1 and SH-SY5Y cell lines. The optimum incubation time was defined as the time required for 70-85% closure of the initial scratch. 16, 41 and 24 hours were used as the optimum incubation time for C6-WT/STX, DLD-1 and SH-SY5Y cell lines respectively. Results represents three independent experiments.

	T = 0 h	T = 13 h	T = 16 h
C6-WT	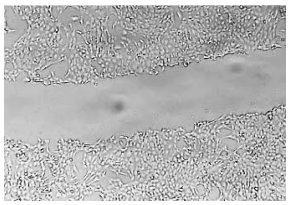	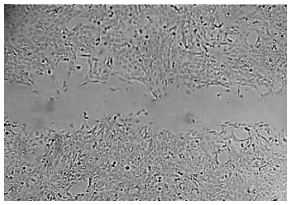	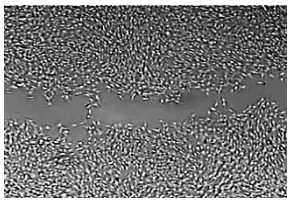
C6-STX	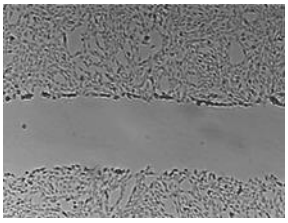		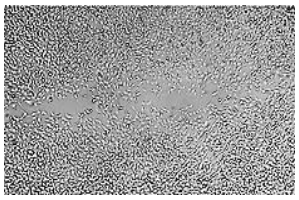
	T = 0 h	**T = 24 h**	**T = 41 h**
DLD-1	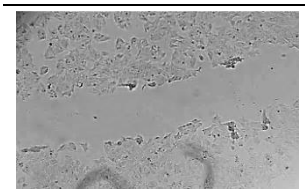	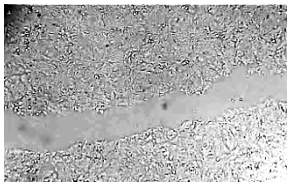	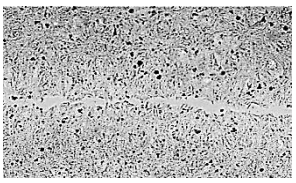
	T = 0 h	**T = 16 h**	**T = 24 h**
SH-SY5Y	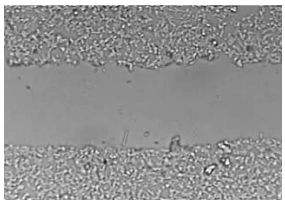	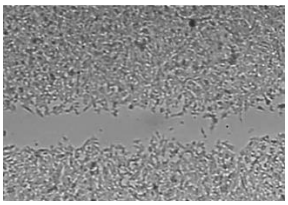	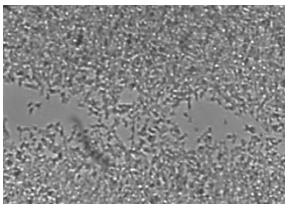

3.3.3.2. Detection of cell proliferation using immunofluorescence assay

The Ki-67 protein is a cellular marker for proliferation [172]; an antibody for Ki-67 was used as an indication of proliferation of the C6-STX and C6-WT cells at the edge of the scratch after 16 hours incubation. The assay was used with C6-STX and C6-WT cell lines specifically because the incubation time

(16 hours) and the doubling time (24 hours) for these cell lines were close to each other.

It was confirmed by this assay that after 16 hours incubation of C6-WT and C6-STX cell lines no evidence of proliferation was detected at the edge of the scratch, as evidence by a lack of immunostaining (Table 3.23).

Table 3.23 Immunofluorescence staining of C6-WT and C6-STX cell lines with Ki-67 proliferation marker suggesting an absence of proliferation at the edge of the scratch in the migration assay after 16 hour incubation. Scale bar represents 250 µm. Results represents three independent experiments.

Ki-67 immunofluor -escence staining	T0	T16
C6-STX	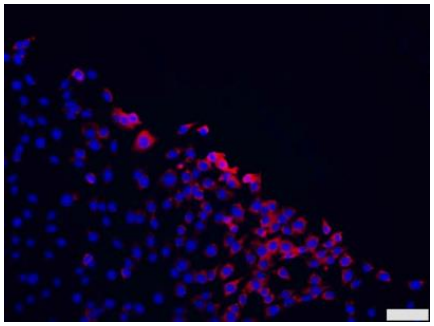	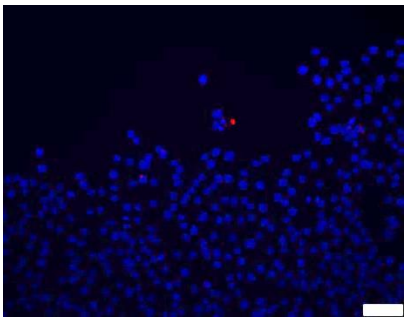
C6-WT	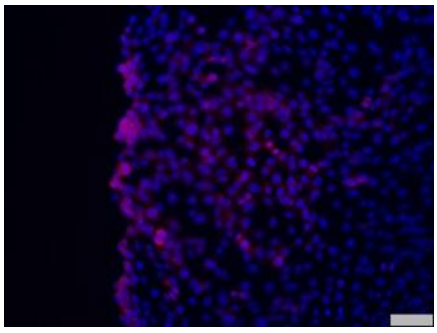	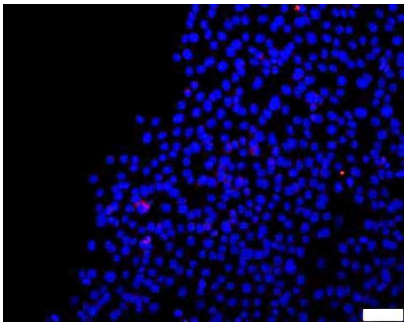

3.3.3.3. Results of scratch assay using different polySia inhibitors on different cell lines

Following the determination of the hit compounds that caused significant inhibition of ST8SiaII using the high throughput HPLC analysis, the impact of ST8SiaII inhibition on tumour cell migration was investigated using the scratch assay.

ICT-3234, ICT-3233, ICT-3143, ICT-3268, ICT-3271 and ICT-3276 were investigated for anti-migratory effects on the four cell lines using different concentrations. ICT-3125, the parent molecule from which the other compounds were derivatised, was additionally included as a baseline control (Table 3.24 A-F). Its anti-migratory effects were also investigated in order to study the outcome of structural changes made to other molecules in the series on polyST inhibitory activity.

Table 3.24A Evaluation of the effects of ICT-3234 on the migration of C6-STX, C6-WT, SH-SY5Y and DLD-1 cells. The compound was evaluated at the concentrations shown. Images in the next four tables are representative of the scratch induced in the cell line monolayer at T0 and T16/24 or 41 after treatment with the inhibitor. NP = not performed since the concentration was determined as toxic by MTT assay. Results represent three independent experiments.

C6-STX	Control	250 µM	125 µM	25 µM
Initial scratch	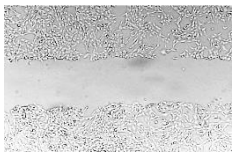	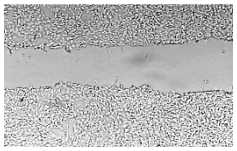	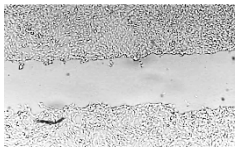	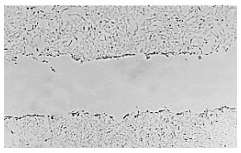
16 hours incubation		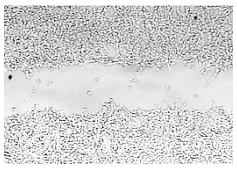	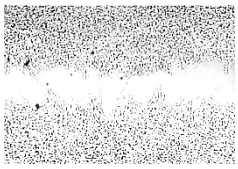	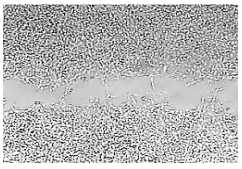
C6-WT	Control	250 µM	125 µM	25 µM
Initial scratch	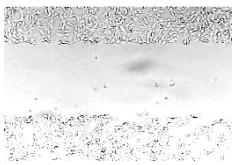	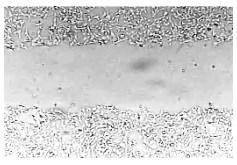	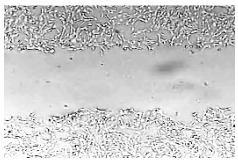	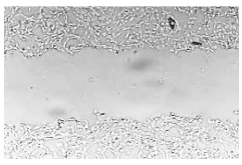
16 hours incubation	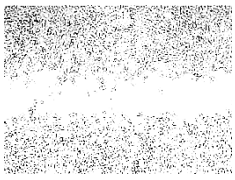	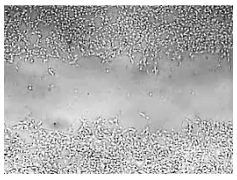	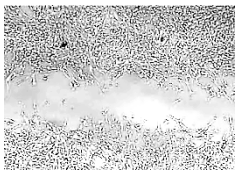	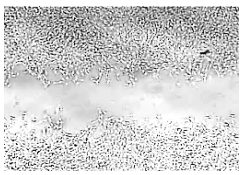
SH-SY5Y	Control	250 µM	125 µM	25 µM
Initial scratch	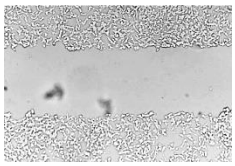	NP	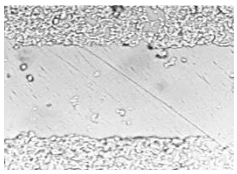	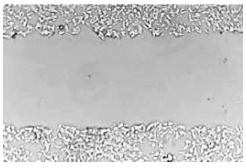
24 hours incubation	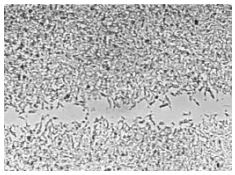	NP	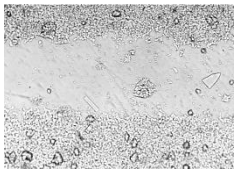	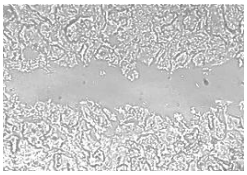
DLD-1	Control	250 µM	125 µM	25 µM
Initial scratch	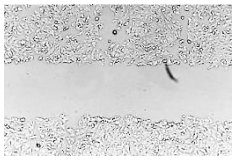	NP	NP	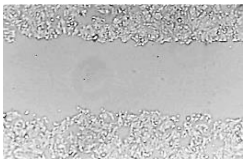
41 hours incubation	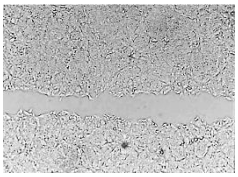	NP	NP	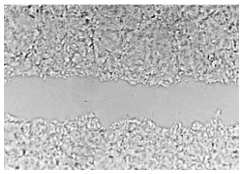

Table 3.24B Migration assay of ICT-3143 using different cell lines and different concentrations.

C6-STX	Control	250 µM	125 µM	25 µM
Initial scratch	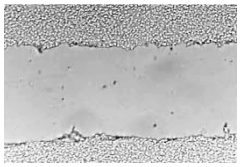	NP	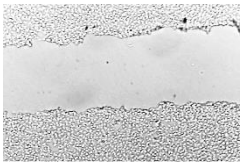	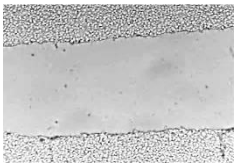
16 hours incubation	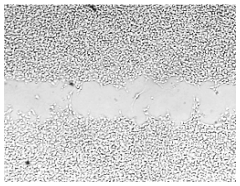	NP	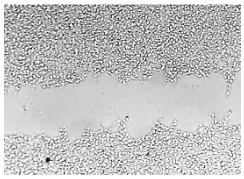	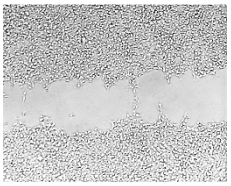
C6-WT	Control	250 µM	125 µM	25 µM
Initial scratch	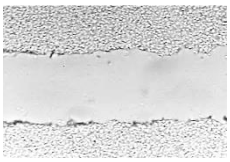	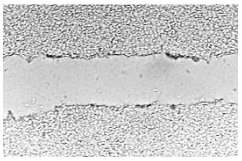	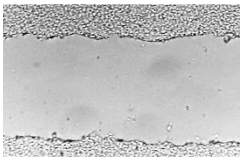	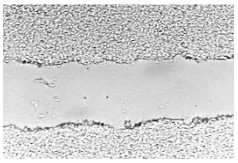
16 hours incubation	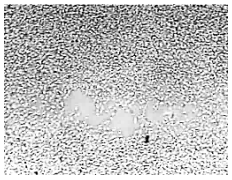	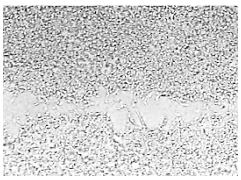		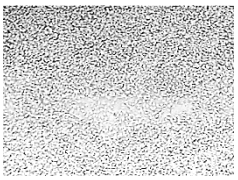
SH-SY5Y	Control	250 µM	125 µM	25 µM
Initial scratch	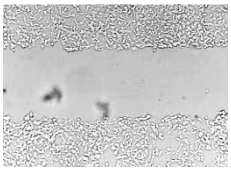	NP	NP	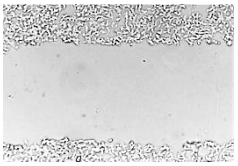
24 hours incubation	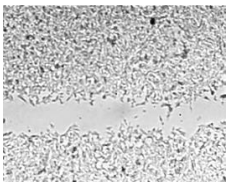	NP	NP	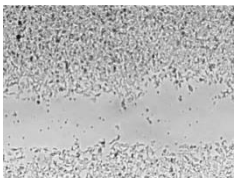
DLD-1	Control	250 µM	125 µM	25 µM
Initial scratch	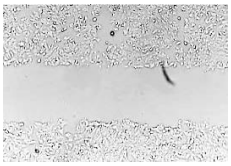	NP	NP	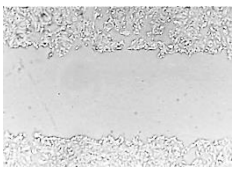
41 hours incubation	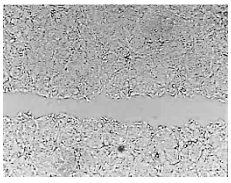	NP	NP	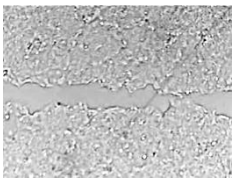

Table 3.24C Migration assay of ICT-3233 using different cell line and different compound concentrations.

C6-STX	Control	250 µM	125 µM	25 µM
Initial scratch	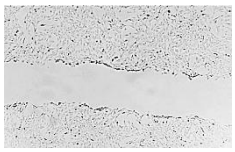	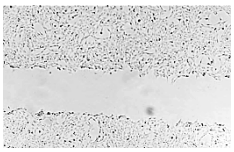	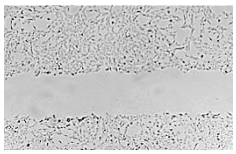	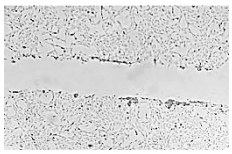
16 hours incubation	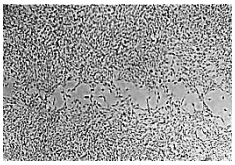	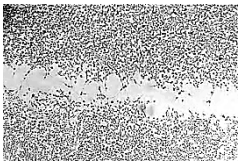	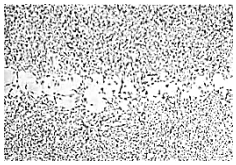	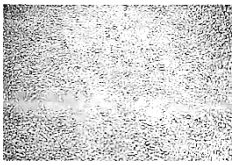
C6-WT	Control	250 µM	125 µM	25 µM
Initial scratch	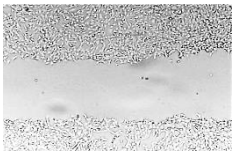	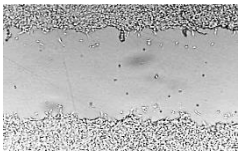	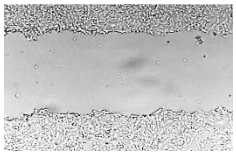	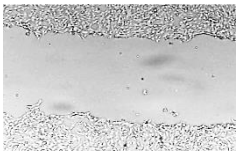
16 hours incubation	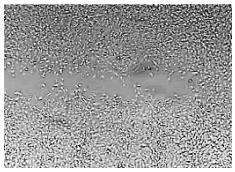	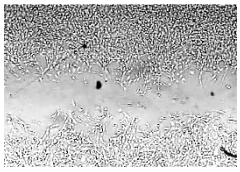	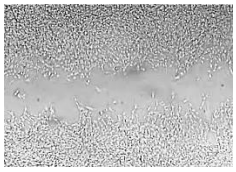	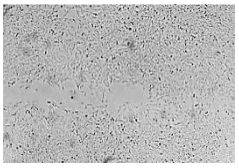
SH-SY5Y	Control	250 µM	125 µM	25 µM
Initial scratch		NP	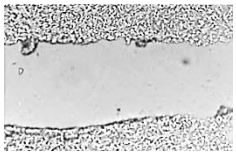	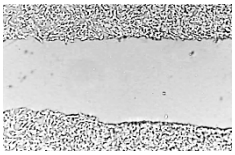
24 hours incubation	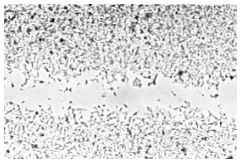	NP	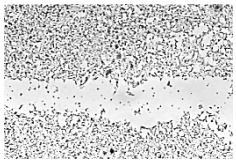	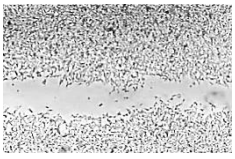
DLD-1	Control	250 µM	125 µM	25 µM
Initial scratch	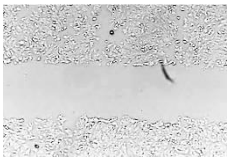	NP	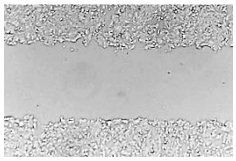	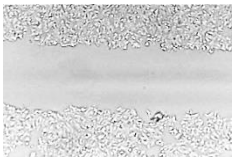
41 hours incubation	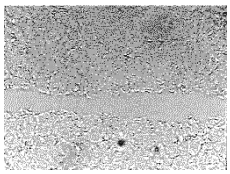	NP	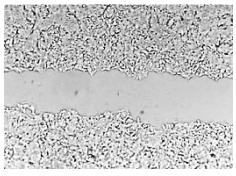	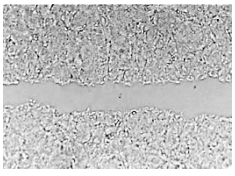

Table 3.24D Migration assay of ICT-3125 and CMP using different cell line and different compound concentrations

	CMP		ICT-3125	
C6-STX	**Control**	**5 mM**	**Control**	**250 µM**
Initial scratch	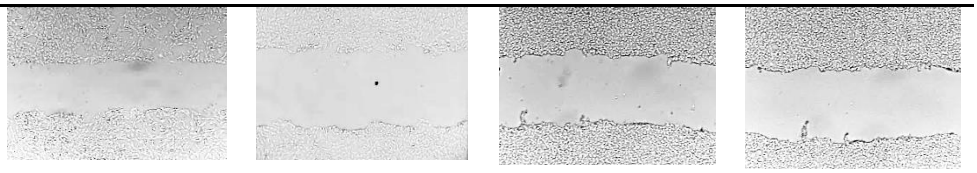			
16 hours incubation	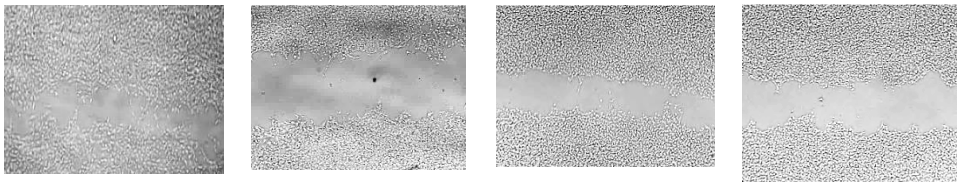			
C6-WT	Control	5 mM	Control	250 µM
Initial scratch	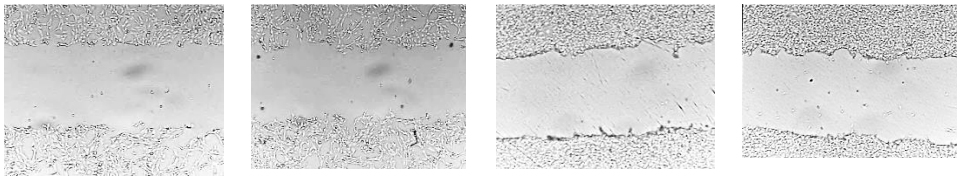			
16 hours incubation	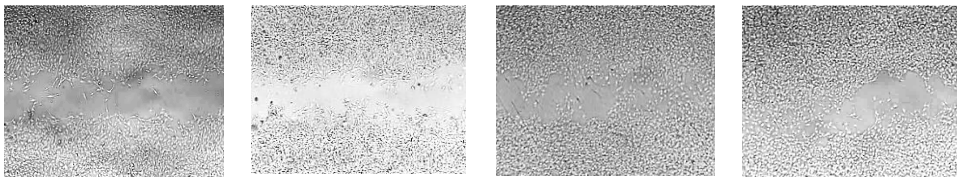			
SH-SY5Y	Control	5 mM	Control	250 µM
Initial scratch	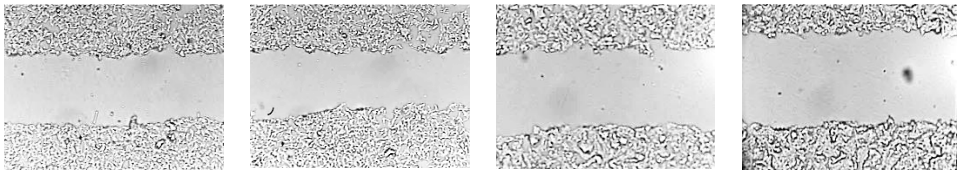			
24 hours incubation	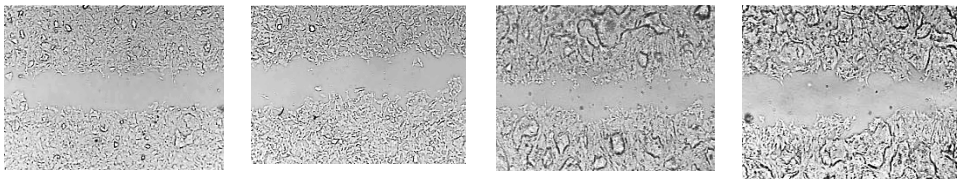			
DLD-1	Control	5 mM	Control	250 µM
Initial scratch	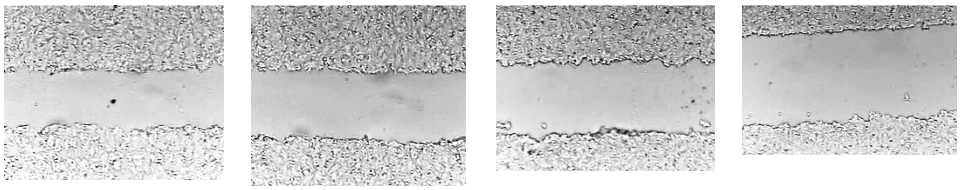			
41 hours incubation	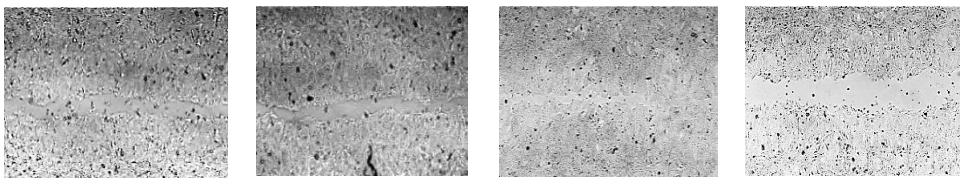			

Table 3.24E Migration assay of ICT-3268 and 3271 using different cell lines

C6-STX	Control	250 µM	125 µM	25 µM
		ICT-3268		
Initial scratch	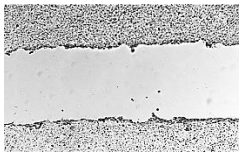	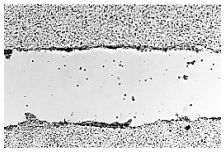	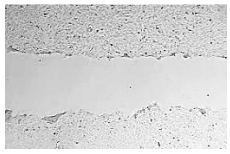	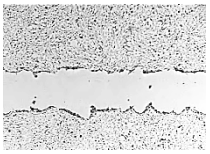
16 hours incubation	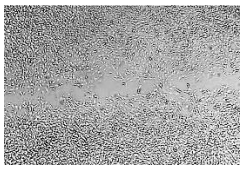	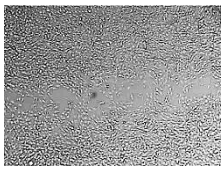	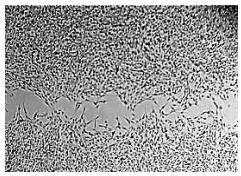	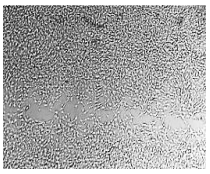
C6-WT	Control	250 µM	125 µM	25 µM
Initial scratch	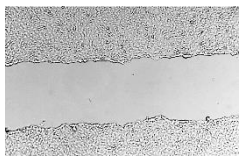	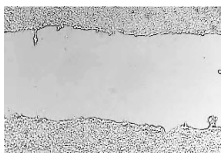	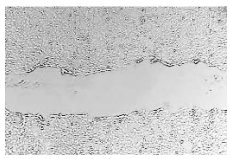	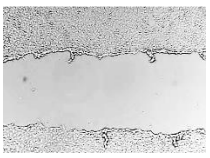
16 hours incubation	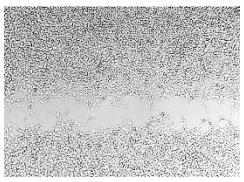	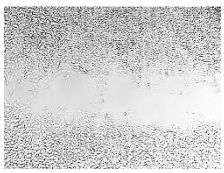	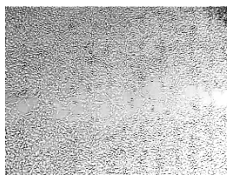	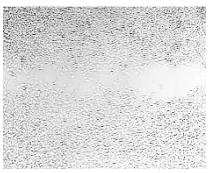
C6-STX	Control	250 µM	125 µM	25 µM
		ICT-3271		
Initial scratch	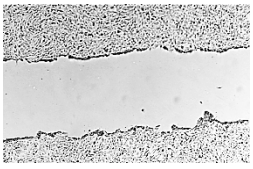	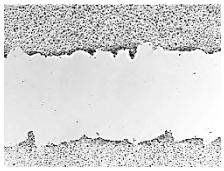	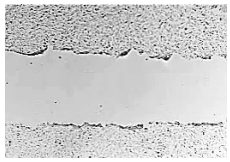	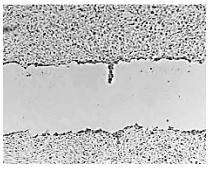
16 hours incubation	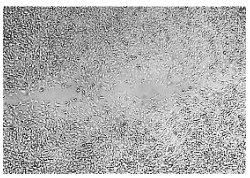	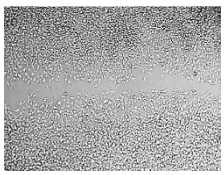	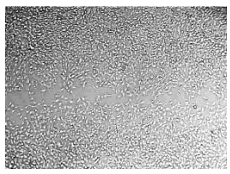	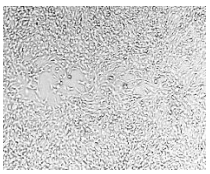
C6-WT	Control	250 µM	125 µM	25 µM
Initial scratch	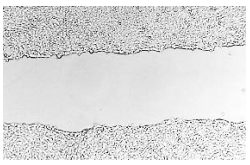	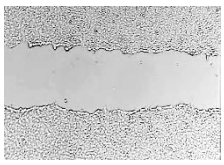		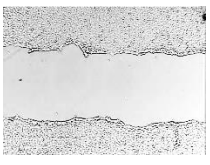
16 hours incubation	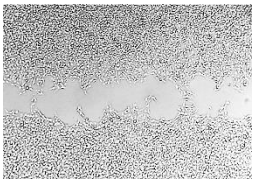	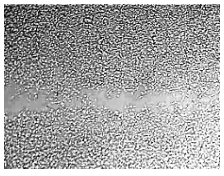	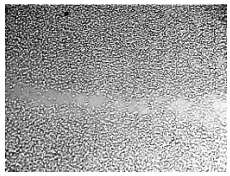	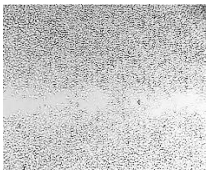

Table 3.24F Migration assay of ICT-3276 using different cell lines and different concentrations

C6-STX	Control	12.5 µM	15 µM	20 µM
Initial scratch	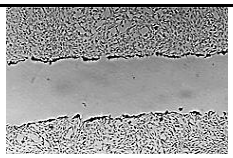	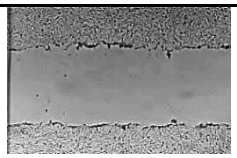	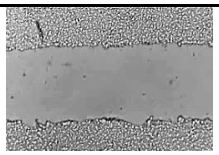	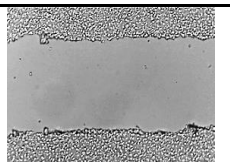
16 hours incubation	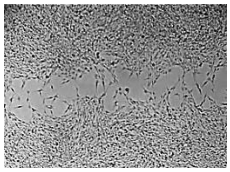	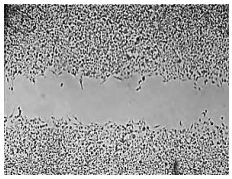	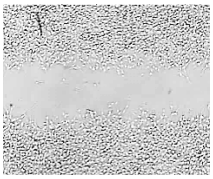	
C6-WT	Control	12.5 µM	15 µM	20 µM
Initial scratch	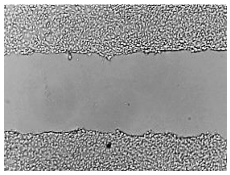	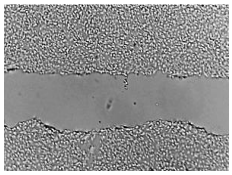	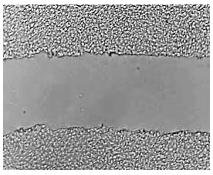	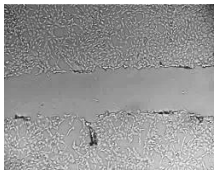
16 hours incubation	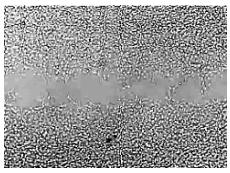	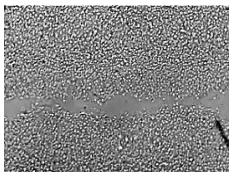	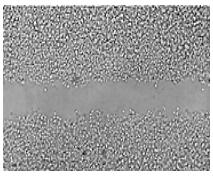	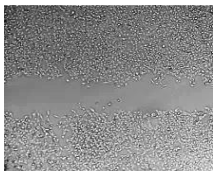

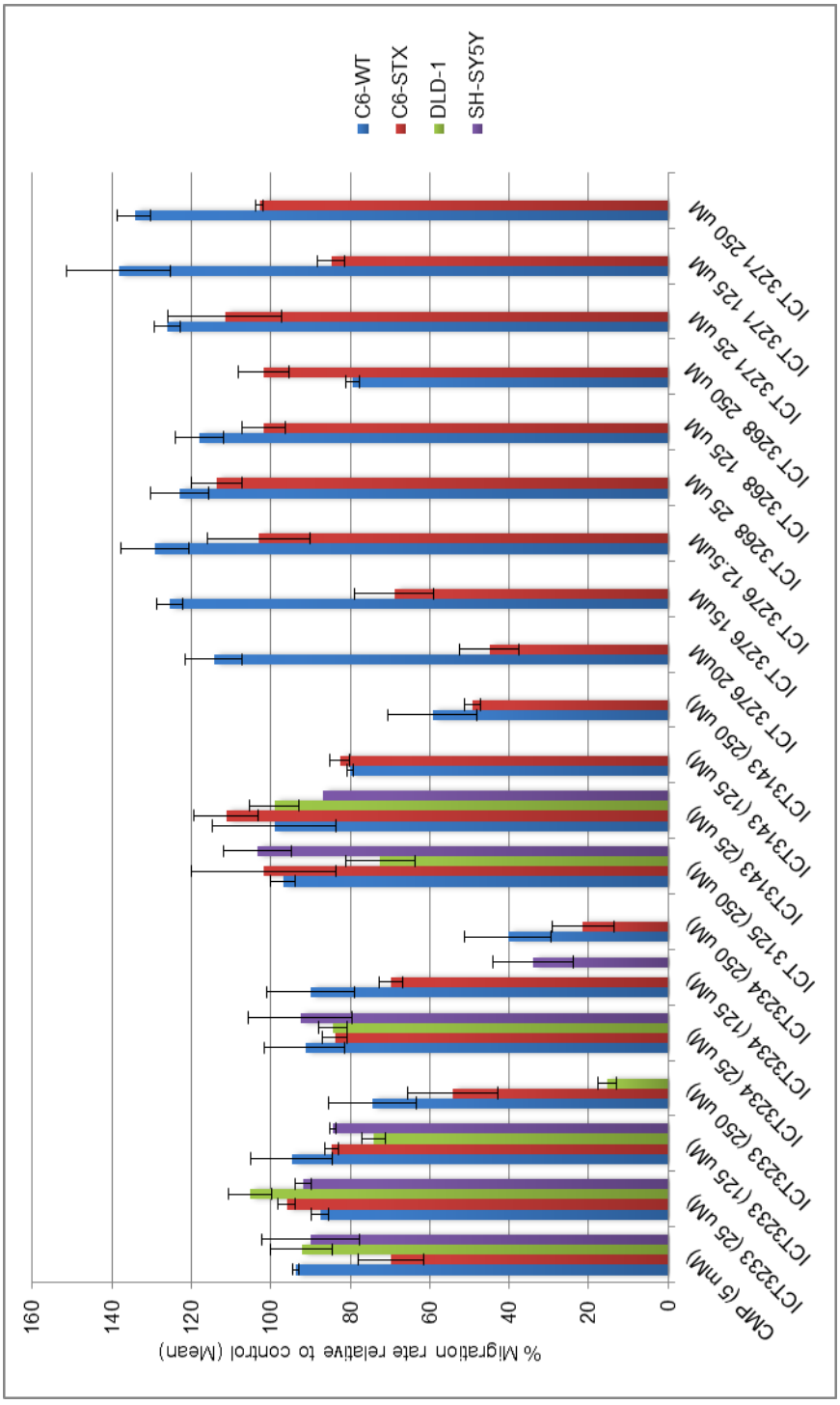

Figure 3.63 Effect of selected polyST inhibitors on the migration of C6-STX, C6-WT, SH-SY5Y and C6-WT cells. The results were observed after 41, 24 and 16 hours for DLD-1, SH-SY5Y and C6-STX/WT cells respectively. The missing concentrations represent the toxic concentrations as determined by MTT assay. The results represent the mean of three independent experiments.

ICT-3234, ICT-3233, ICT-3143 and ICT-3276 were found to exert a significant anti-migratory effect on C6-STX cell line at a concentration of 250 µM; for ICT-3143 (50.73 % inhibition), ICT-3233 (37.1% inhibition) and ICT-3234 (68.1% inhibition), and 15 µM for ICT-3276 (36.81 % inhibition). Besides, ICT-3234 (125 µM) showed also a significant inhibitory effect on SH-SY5Y cell line (66.04% inhibition). However, only ICT-3276 (15 µM), ICT-3233 (250 µM) and ICT-3234 (125 µM) showed a significant inhibition of the migration of C6-STX cell line without simultaneously showing any activity on C6-WT cells, which indicated that the compounds at these concentrations were both active and selective (Figure 3.63, Table 3.25). Both ICT-3268 and ICT-3271 were found to be not completely soluble in media. It was noticed that the both inhibitors re-precipitate after solubilisation in media.

Table 3.25 Percentage of migration of C6-STX and C6-WT cells after treatment with different polyST inhibitors compared to untreated control cells and P significance of different polyST inhibitors effect on the migration of C6-STX and C6-WT cell lines at different concentrations. * P< 0.05, ** P<0.01 and *** P < 0.001. Results represent the mean of three independent experiments.

	C6-STX			C6-WT		
Inhibitor	% migration	P value	Significance	% migration	P value	Significance
CMP, 5 mM	69	0.019	*	93	0.067	Not
ICT-3233, 25 µM	96	0.595	Not	87	0.109	Not
ICT-3233, 125 µM	84	0.141	Not	94	0.702	Not
ICT-3233, 250 µM	54	0.021	*	74	0.260	Not
ICT-3234, 25 µM	83	0.245	Not	91	0.551	Not
ICT-3234,125 µM	69	0.012	*	89	0.528	Not
ICT-3276, 12.5 µM	103	0.567	Not	129	0.074	Not
ICT-3276, 15 µM	68	0.020	*	125	0.066	Not
ICT-3276, 20 µM	44	0.001	***	114	0.183	Not
ICT-3125, 250 µM	101	0.936	Not	96	0.493	Not
ICT-3143, 25 µM	111	0.399	Not	99	0.965	Not
ICT-3143, 125 µM	82	0.042	*	80	0.024	*
ICT-3143, 250 µM	49	0.024	*	59	0.023	*

Although ICT-3276 showed promising results with 56 ± 7.4 % inhibition of C6-STX migration and exerted no effect on the migration of C6-WT cells when administered at a 20 µM concentration, it was noticed that during the incubation of the cells, the

morphology of cells changed. Despite this, it was confirmed using the MTT assay that the compound had no effect on cell viability at this concentration (Table 3.21). To further confirm that the compound did not have a toxic effect on the cells, C6-STX cells were incubated for 16 and 48 hours with 20 μM of ICT-3276 after which the media with the inhibitor was removed and fresh media was added to examine the recovery of the cells. After 16 hours the morphology of the cells treated with the compound had changed slightly (confirming that observed in the migration assay) and after 48 hour of incubation most of the cells changed from the normal nerve-like shape to a circular shape. This effect was reversed after the removal of the compound and addition of fresh media for 24 hours (Figure 3.64). It was thus concluded that the measured effect in the migration assay was not associated with cytotoxicty. These findings are interesting and warrant further investigation.

ICT-3276 was found to be the most potent and selective compound of all the rational-designed inhibitors tested so far, thus close attention must be paid for the aforementioned effect. The change in cell morphology was observed in the C6-STX cells but not C6-WT cells, which suggests that this change may be due to a polySia-associated activity. The next steps would be to assess the effect of the same concentration of agent on both SH-SY5Y and DLD-1 cell lines to examine whether it is exclusive to polySia expressing cells. Examining the cell cycle phase of the C6-STX cells after treatment with the compound and comparing the result with untreated cells using flow cytometry and propidium iodide would also give valuable information about whether the compound is causing change in cell cycle phases.

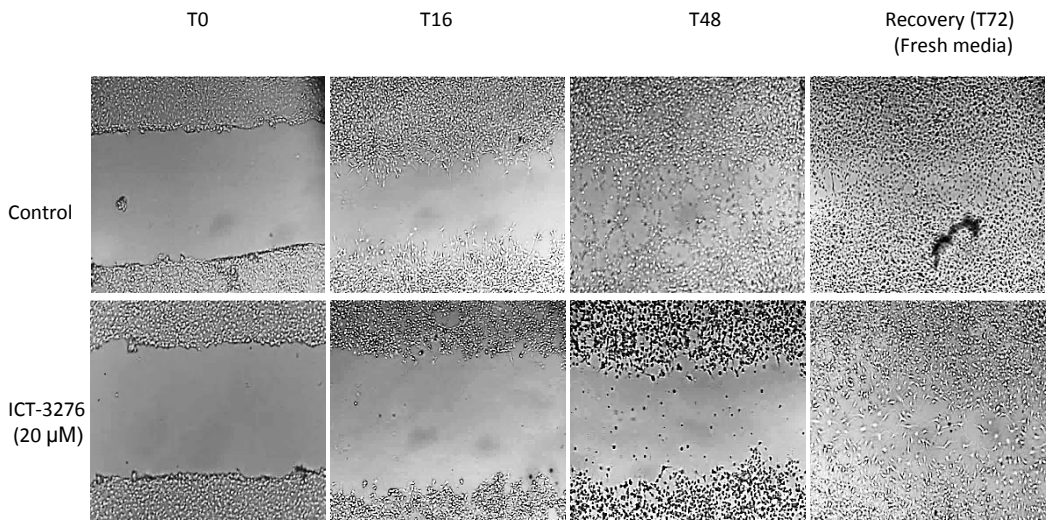

Figure 3.64 Effect of incubation of C6-STX cells with ICT-3276 (20 μM) over 16 and 48 hours and the recovery of the cells after removal of the compound and addition of fresh media for another 24 hours. Control cells are shown in the first panel showing no change in cell morphology over 72 hours while the

addition of ICT-3276 on the lower panel showed changes in morphology, which was reversed by removal of the compound and addition of fresh media. Results represent three independent experiments.

3.3.4. Determination of inhibition of ST8SiaII by measurement of polySia expression using immunofluorescence

Hit compounds which have shown the most potent and selective anti-migratory effect towards cells that express polySia over the control cell lines were chosen for further analysis using immunofluorescence. Examination of polySia chains with immunofluorescence allowed the confirmation of the results obtained earlier.

In this assay ICT-3234, ICT-3276 and ICT-3176 were incubated with C6-STX cells for 16 hours. DAPI (4′,6-diamidino-2-phenylindole); a nuclear and chromosome counterstain, which emits blue fluorescence upon binding to AT regions of DNA, was used to label cell nuclei. PolySia expression was detected in the presence/absence of different concentrations of the inhibitors.

Table 3.26A Expression of polySia after treatment of C6-STX cells with different concentrations of ICT-3234, 3276 and 3176 for 16 hours, detected using mAb 735 polysia antibody. Scale bars represents 250 µm. Results represents three independent experiments.

	DAPI	mAb 735	Overlay
Positive control	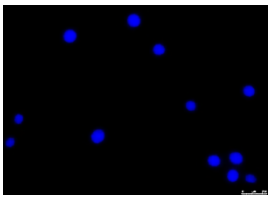	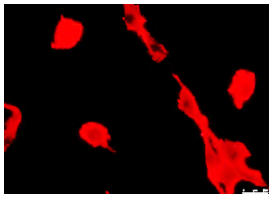	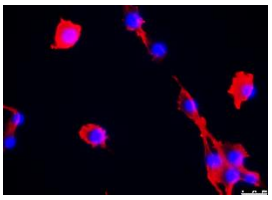
Negative control	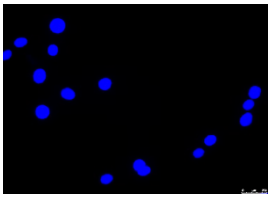	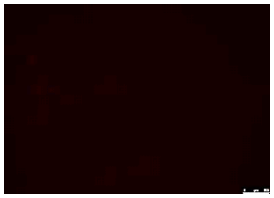	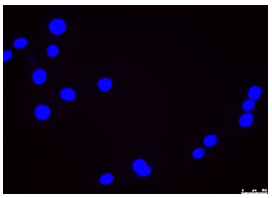
ICT-3234, 250µM	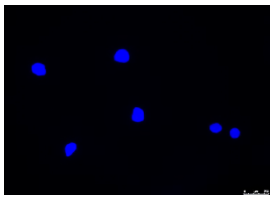		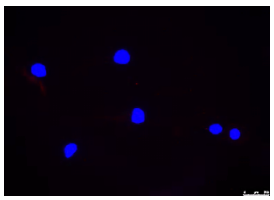
ICT-3234, 125µM	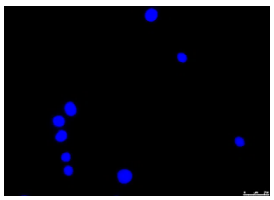		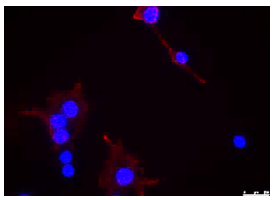
ICT-3234, 25µM	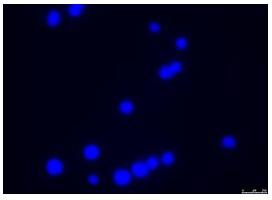	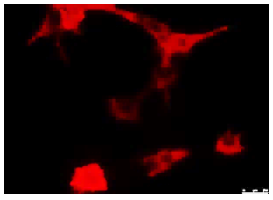	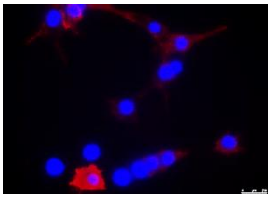

Table 3.26B Expression of polySia after treatment of C6-STX cells with different concentrations of ICT-3276

	DAPI	mAb 735	Overlay
Positive control	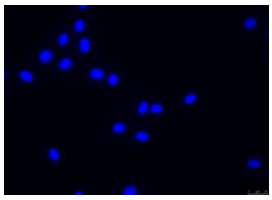		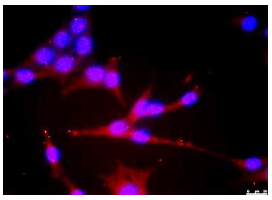
ICT-3276, 50µM	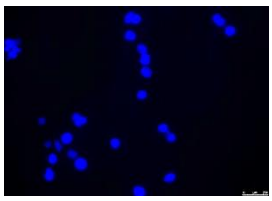	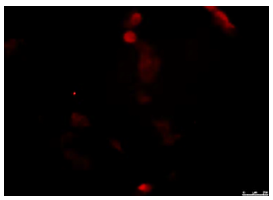	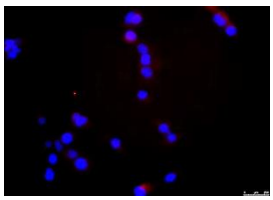
ICT-3276, 20µM	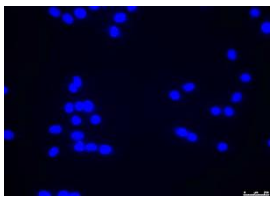	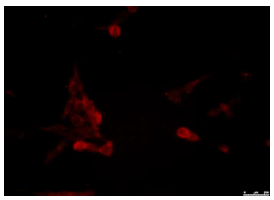	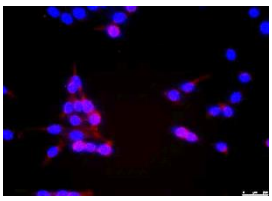
ICT-3276, 15µM	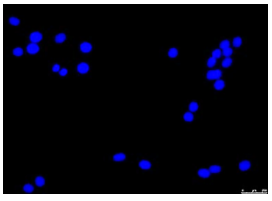	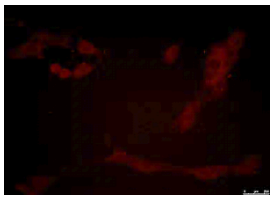	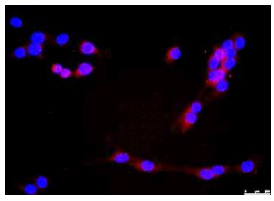
ICT-3276, 12.5µM	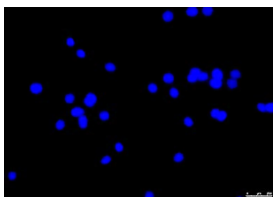	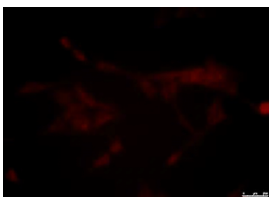	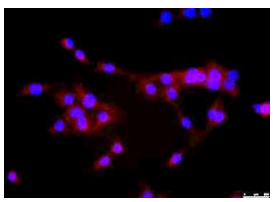

Table 3.26C Expression of polySia after treatment of C6-STX cells with different concentrations of ICT-3176

	DAPI	mAb 735	Overlay
Positive control	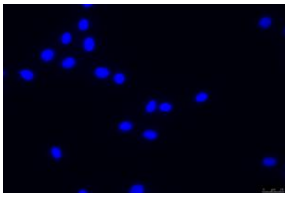	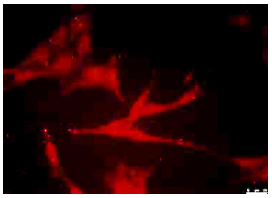	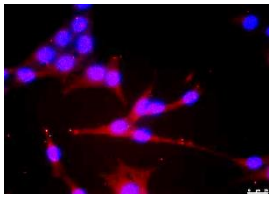
Negative control	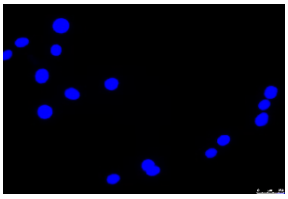	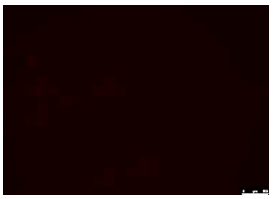	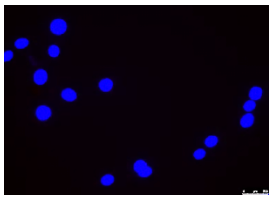
ICT-3176, 500µM	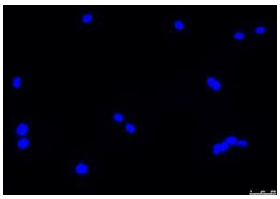	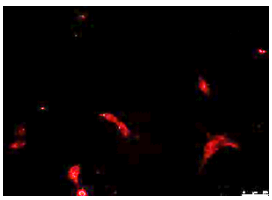	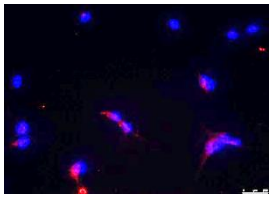
ICT-3176, 250µM	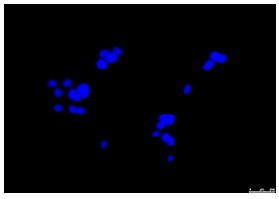		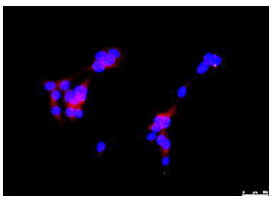
ICT-3176, 25µM	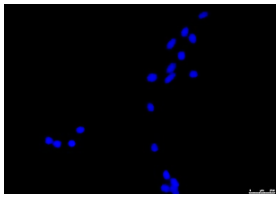	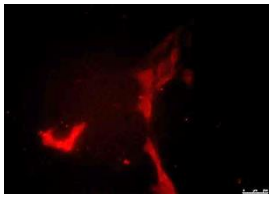	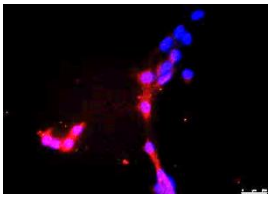

Immunofluorescence confirmed the effects of ICT-3234 and ICT-3276 as inhibitors of polySia synthesis in a concentration-dependent manner, consistent with results obtained from cell-free and cell-based HPLC-chromatographic assays and migration assay. ICT-3176 was also examined by immunofluorescence. It was found that it also leads to a concentration-dependant inhibition of polySia synthesis. However, the inhibitory effect was found to be less than the observed for ICT-3234, which is also consistent with the results obtained by the cell-based chromatographic assay (Figure 3.26A-C).

3.4. Conclusion

In this chapter a number of phenotypic functional assays were exploited in order to investigate the molecular mechanisms of action of selected polyST inhibitors. In order to measure the effect of these inhibitors on the migration of cancer cells, polySia-NCAM expression of the four selected cell lines (namely SH-SY5Y, C6-STX, C6-WT and DLD-1) was first confirmed using immunofluorescence and western blotting. Next, the incubation time required for each cell line to induce 80% wound closure was determined.

Cell migration in the presence of inhibitor was then evaluated in order to provide information to investigate the effect of changes in the chemical structures of rationally designed inhibitors on their selectivity. ICT-3276, 3234 and 3233 were found to be the most active compounds with selective activity towards cell lines that express polySia, with inhibition of the cell migration capacity of 59.06 ± 5.8%, 37.1 ± 9.46% and 30.3 ± 6% for ICT-3276 (20 μM), ICT-3233 (250 μM) and ICT-3234 (125 μM) respectively on C6-STX cells. This is alongside an absence of inhibition on control cell lines. This effect was not caused by reduction of cell viability as confirmed by MTT assy.

To sum up, hit molecules selected using the previously described cell-free and cell-based chromatographic assays were further evaluated using phenotypic functional assays. A significant correlation between the potency of the compounds recorded by the chromatographic assay and their potency as migration inhibitors was established. This provides further evidence for the role of the compounds as polyST inhibitors.

For the first time, data demonstrating rationally designed polyST inhibitors that exhibit selective and significant inhibitory effect (on migration and polySia expression) on polySia expressing cell lines has been presented. ICT-3276 is the first reported rationally designed polyST inhibitor that shows a significant inhibition in the migration of polySia expressing cells with no significant effect on non-expressing cells at a concentration of 15 μM. The information generated from these assays will contribute to generation of a

structure activity relationship (SAR) for STX inhibitors, which will aid the subsequent design of new inhibitors in the future.

Chapter 4. Initial investigation of the potential role of polySia during cancer metastasis under hypoxic and normoxic conditions

4.1. Introduction

As we have explored in earlier chapters, the expression of polySia on NCAM plays a key role in cell migration. Full understanding of its role in NCAM-dependent or NCAM-independent modulation of cell motility and cell–matrix adhesion is yet to be established [57]. Polysialylation of NCAM does not contribute only to specific NCAM-NCAM interactions, but also regulates overall NCAM interactions with other molecules. In this latter mode, the molecule can have both a positive and a negative effect on a wide variety of contact-dependent cellular events [173,174].

Besides increasing inter-membrane repulsion due to the increased negative charge, polySia chains also modulate the NCAM-NCAM interactions, as well as NCAM interactions with other molecules that promote tumour metastasis. Additionally, it was observed that polySia also affects other cell interactions that do not appear to depend directly on NCAM's intrinsic binding function [173]. A study by Ichiro Fujimoto *et al*., has shown that regulation by polySia occurs with adhesion receptors as diverse as an Ig-CAM, a cadherin such as L1, C-cadherin and an integrin such as $\alpha_v\beta_1$ integrin, and does not require NCAM functional domains other than those minimally required for polysialylation. This study suggested that the inhibitory effects of polySia-NCAM on cell adhesion are independent of the nature of the adhesion system and of any intrinsic binding or signalling properties of the NCAM polypeptide itself [175]. However, full understanding of the mechanism by which polySia promotes cancer metastasis is still to be defined.

In this chapter, two areas in which polySia exerts its effects have been explored: (1) the possible additive anti-migratory effects of using certain intracellular signalling pathway inhibitors in combination with a polyST inhibitor, and (2) the effect of polySia expression on cancer cell behaviour under hypoxic conditions. In the next few pages, the background to each of these areas will be considered.

4.1.1. Understanding the interaction of polySia with different cancer signalling pathways

NCAM was initially identified as a cell adhesion molecule exhibiting homophilic and heterophilic binding properties. However it was shown later to exert *trans* binding interactions with molecules of different classes, such as different members of the Ig-CAM superfamily including integrins, cadherins, growth factor receptors and components of the extracellular matrix and possibly others [36]. In accordance with the protein's complexity, it has been involved in several cellular functions, mainly during neural development and plasticity and also in oncogenesis [30].

To date, a number of heterophilic ligands of NCAM have been reported, such as: glial cell line-derived neurotrophic factor (GDNF), fibroblast growth factor receptor 1 (FGFR 1), and GDNF family receptor α, the L1 cell adhesion molecule, TAG-1/axonin-1, neurocan, phosphacan, agrin, various types of collagen, heparin, heparan/chondroitin sulfates, cellular prion protein, the glucocorticoid receptor, receptor tyrosine kinase B, platelet-derived growth factor (PDGF), brain-derived neurotrophic factor (BDNF), rabies virus, ATP, spectrin, focal adhesion kinase, and various cytoskeletal components [35,176].

The interaction of NCAM with different heterophilic ligands is controlled by its polysialylation state [35]. When NCAM is polysialylated to a very low degree or not polysialylated a two-dimensional zipper formation predominates, and consequently there is no room between the NCAM molecules for interactions with other molecules due to the tight packing. On the other hand, *trans* homophilic interactions between polysialylated NCAM molecules results in the formation of one-dimensional zippers, leading to the formation of thread-like clusters of NCAM molecules and allowing association between NCAM and other molecules [35].

In order to examine the potential additive anti-migratory effects of using a polyST inhibitor in combination with certain signalling pathway inhibitors which were previously reported to be modulated with polySia expression, neuroblastoma cells were incubated with non-toxic concentration of a polyST

inhibitor in the presence/absence of the selected pathways inhibitors. The difference in cell migration between the control cells (treated with polyST inhibitor only) and the cells treated with both polyST and signalling pathway inhibitors was recorded to examine the potential additive anti-migratory effect.

Specifically, crizotinib, PF-573228, axitinib, GNF-5837 and SU-5402 were used to study the role of c-MET/ALK, FAK, VEGFR, TRK and FGFR respectively on polySia-mediated tumour cell migration (Table 4.27). These pathways have been chosen to be studied since they have been previously reported to be associated with polySia. In the next few paragraphs, the link between the polysialylation status of NCAM and the activity of the aforementioned signalling pathways will be discussed.

Table 4.27 Mechanism of action of the signalling pathway inhibitors used in this chapter.

Inhibitor	Target signalling pathway	Reference
SU-5402	FGFR	[177,178]
Crizotinib	c-Met/ALK	[179]
PF-573228	FAK	[180]
Axitinib	VEGFR	[181]
GNF-5837	TRK	[182]

4.1.1.1. Hepatocyte growth factor receptor (c-MET)

c-MET is a receptor tyrosine kinase that, after binding with its ligand, hepatocyte growth factor, activates a wide range of different cellular signalling pathways, including those involved in cancer cell proliferation, migration and invasion [183]. Expression of c-MET and its ligand has been observed in tumour biopsies of most solid tumours and c-MET signalling has been documented in a wide range of human malignancies. Studies suggest that c-MET-positive status indicates poor prognosis [184,185].

Tyrosine phosphorylation has been previously implicated in the regulation of cadherin function: receptor tyrosine kinases such as epidermal growth factor receptor (EGFR), hepatocyte growth factor receptor (c-MET) and fibroblast growth-factor receptor (FGFR), phosphorylate E-cadherin, β-catenin, γ-catenin p120-catenin and neuronal (N)-cadherin, resulting in the disassembly

of the cell adhesion complex and disruption of cadherin-mediated cell–cell adhesion [28,96].

Polysialylation of NCAM was also reported previously to represses cadherin-mediated cell-cell adhesion. C-Met activity was found to be regulated by modification of its terminal sialic acid structure [186]. These findings raise the question about a possible role for polySia on c-MET activity.

4.1.1.2. Anaplastic lymphoma kinase (ALK)

Anaplastic lymphoma kinase (ALK), a transmembrane receptor tyrosine kinase (RTK), originally identified in the nucleophosmin (NPM)–ALK chimera of anaplastic large cell lymphoma, has emerged as a novel tumourigenic player in several human cancers. ALK receptor expression, originally documented in a variety of cancer lines, has been documented in many neuronal tumours such as glioblastoma, and mesenchymal neoplasms including melanoma and rhabdomyosarcoma. In this context, ALK over-expression or gain of function mutations have been demonstrated to be tumourigenic [187].

ALK has additionally been identified as a neuroblastoma predisposing gene, and activating mutations have also been identified in a subset of sporadic neuroblastoma tumours. ALK protein expression is significantly up regulated in some metastatic neuroblastoma cases, and overexpression of either mutated or wild type ALK, is a poor prognosis indicator for those patients. Inhibition of ALK activity in neuroblastoma cell lines has already been studied and targeted by using specific small molecules. ALK has 16 highly conserved putative sites of N-linked glycosylation in the extracellular domain. It was demonstrated that inhibition of N-linked glycosylation impairs ALK phosphorylation and disrupts downstream pro-survival signalling, as well as cell viability, in neuroblastoma cell lines harbouring mutated or amplified ALK. This suggests that inhibition of this post-translational modification could be a promising therapeutic approach [32].

4.1.1.3. Focal adhesion kinase (FAK)

Focal adhesion kinase (FAK) is a non-receptor tyrosine kinase that increasingly has been implicated in cancer progression [180]. FAK has been identified as a key mediator of signalling by integrins, a major family of cell surface receptors for extracellular matrix, as well as other receptors in both normal and cancer cells [188]. Activated (phosphorylated) FAK forms a binary complex with Src family kinases, which can phosphorylate other substrates and trigger multiple intracellular signalling pathways to regulate various cellular functions.

Previous studies have shown that polySia removal with Endo-N results in a significant increase in the number of peripheral focal adhesions per cell, characterized as FAK [57]. It was found that homophilic interactions between non-polySia-NCAM accelerate FAK phosphorylation [44,189]. Here we studied the possible role of FAK activity on polySia-mediated cell migration.

4.1.1.4. Vascular endothelial growth factor (VEGF)

VEGF is a potent angiogenic factor which is up-regulated in many tumours and its contribution to tumour angiogenesis is well defined [190]. Anti-VEGF strategies to treat cancers were designed to target the pro-angiogenic function of VEGF and thereby inhibit neovascularisation. Two of the most well-known drugs that have been successful at slowing the progression of disease stimulated by VEGF are monoclonal antibodies bevacizumab and ranibizumab [191]. However, anti-VEGF therapies may have a dual effect since evidence is accumulating to support the existence of both paracrine and autocrine VEGF loops within tumours [192]. It has been suggested that direct stimulation of tumour cells by VEGF may protect the cells from apoptosis and increase their resistance to conventional chemotherapy and radiotherapy [193].

Previous studies have suggested that VEGF has an essential role in guiding directed migration and consequently, it has an important role in cancer invasion and metastasis [194]. A glycosylation-dependent pathway that compensates for the absence of cognate ligand and preserves angiogenesis in response to VEGF blockade has been identified [195]. In-house experiments

showed that treatment with polyST inhibitor down-regulated VEGFR3 phosphorylation (data not shown). Here we investigate the effect of combining polyST and VEGF inhibition on the migration of cancer cells.

4.1.1.5. Tropomyosin receptor kinase (TRK)

Trk receptors are a family of tyrosine kinases that regulates synaptic strength and plasticity in the mammalian nervous system [196]. Tropomyosin-related kinase B (Trk-B), which serves as a receptor for brain-derived neurotrophic factor (BDNF) and for neurotrophic factor 4 (NT4), has been found to be a potentially important mediator of the invasive properties of neuroblastoma [197] and head and neck cancers and a mediator of the epithelial-mesenchymal transition (EMT) [198].

BDNF dimer binds directly to polySia to form a large complex with a molecular weight greater than 2000 kDa under physiological conditions. BDNF, after making a complex with polySia, can bind to the BDNF receptors, TrkB and p75NTR. The complex formation of BDNF with polySia was found to up-regulate growth and survival of neuroblastoma cells. AZD6918, a novel potent and selective inhibitor of the Trk tyrosine kinases was found to increase the sensitivity of neuroblastoma to etoposide [199]. These findings suggest that polySia functions as a reservoir of BDNF and other neurotrophic factors and may serve to regulate their local concentrations on the cell surface [200].

4.1.1.6. Fibroblast growth factor receptor (FGFR)

Abnormalities in FGF and the FGFR pathway have been associated with progression of a wide spectrum of malignancies including myeloma, breast, endometrial, genitourinary, neuroblastoma and gastric cancers [201,202]. Initial efforts in targeting FGFRs with small-molecule tyrosine kinase inhibitors (TKIs) have been tempered by challenges in the drug development process, which illustrates the complexities of developing drugs that target uncommon genomic alterations in tumours, as well as poor tolerability mainly related to non-specificity and off-target effects. Multiple pharmaceutical companies are at different stages of pursuing FGFR blockade, mostly using small-molecule

TKIs, but other approaches using monoclonal anti-FGFR antibodies and FGF trapping molecules are also being investigated. Recently, selective potent FGFR TKIs (eg, JNJ-42756493, BGJ398, AZD4547, LY287445, and TAS120) are being investigated with high *in vitro* kinase activity and specificity against FGFR1, FGFR2, and FGFR3 (enzymatic concentration that causes 50% inhibition [IC_{50}], < 10 nM) in the hope of having a more tolerable safety profile by reducing off-target effects [203].

FGFR is one of the most studied heterophilic partners of NCAM. Binding of FGFR to NCAM has attracted the attention of many researchers due to its functional implications. The FGFR family consists of four members of tyrosine kinase receptors that are typically activated upon binding of cognate growth factors, the FGFs, which results in the recruitment and activation of specific effectors that, in turn, trigger a set of signalling pathways [204,205]. These signalling pathways are implicated in the regulation of key cell behaviour, such as proliferation, differentiation, migration, and survival, and are fundamental to embryonic development, regulation of angiogenesis, and wound healing in adults. Dysregulation of the FGF/FGFR signalling pathway has been associated with many developmental disorders and with cancer where it has been recognized that FGFRs are overexpressed in many cancer cell types [205].

Although the FGFR/NCAM interaction was originally reported in neurons where it was implicated in neurite outgrowth, recent studies showed evidence of physical interaction between the two proteins on non-neural cell types [206]. The ability of polysialylated NCAM to bind to and activate FGFR, results in the induction of a migratory and invasive phenotype to cancer cells through the induction of certain pathways involved in cell migration such as signalling pathways, mediated by PKCβII, AKT family members and SRC family members [206]. Importantly, polySia-NCAM stimulated FGFR undergoes dimerisation to the cell surface resulting in sustained signalling [36].

In some cancer cells, an interaction between NCAM and FGFR1 appears to stabilise receptors on the cell surface and may thereby potentiate signalling

by endogenous FGFs [207]. In other cancer cells an interaction between NCAM and the FGFR4 appears to orchestrate the formation of a higher order-signalling complex that can signal independently of the conventional ligands [30,207]. Likewise, in neurons CAMs appear to be able to act as surrogate ligands for the FGFR and signal via the receptors independently of FGFs [30]. Two molecular switches are thought to regulate the NCAM-FGFR interaction: adenosine triphosphate (ATP) and polySia.

In one study, it was found that removal of polySia results in growth inhibition in neuroblastoma cell lines, a process that is mediated by NCAM-FGFR interactions [37]. Additionally, polySia promotes NCAM-mediated cell migration in an FGFR-dependent manner [189]. This means that modulating FGFR-NCAM binding by inhibiting NCAM polysialylation is a potential mechanism for preventing the dissemination of metastatic tumour cells.

To sum up, several studies have suggested a possible role for polySia in the activity of c-MET/ALK, FAK, VEGFR, TRK and FGFR signalling pathways which opens a debate about whether inhibition of these pathways would result in an additional anti-metastatic activity when used in combination with polyST inhibitors, which is the main focus of the first section of this chapter. In the next few pages the background for the second section of this chapter, which involves initial experiments focused on exploring the effect of polySia expression on cancer cell behaviour under hypoxic conditions, will be discussed.

4.1.2. Exploring the effect of polySia expression on cancer cell behaviour under hypoxic conditions

The tumour microenvironment is intimately connected with the evolution of cancer. In particular, hypoxia, a condition of low oxygen tension occurring in poorly vascularised areas, has a profound effect on tumour cell growth, metastasis, susceptibility to apoptosis, and resistance to radio- and chemotherapy [208]. As a tumour grows, blood supply to the cancer cells often becomes inadequate due to dysfunctional and leaky tumour vasculature, leading to poor or irregular oxygen delivery and tumour hypoxia (Figure

4.65). Normal cells would eventually die under extreme hypoxic conditions, however, cancer cells have genetic alterations that enable them to adapt and thrive in the hypoxic tumour microenvironment. In this way the cancer cells are able to “hijack” the adaptive mechanisms used to cope with hypoxia by activating a number of pathways that favour their survival [209,210].

In solid tumours, oxygen delivery to the respiring neoplastic and stromal cells is frequently reduced or even abolished by a number of factors: deteriorating diffusion geometry since oxygen is only able to diffuse 100–180 μm from the end of the nearest capillary to cells before it is completely metabolised [211], severe structural abnormalities of tumour microvessels and disturbed microcirculation [212], in addition to anaemia and the formation of methaemoglobin or carboxyhaemoglobin which reduce the blood's capacity to transport O_2. As a result, areas with very low (down to zero) oxygen partial pressures exist in solid tumours, occurring either acutely or chronically. These micro-regions of very low or zero O_2 partial pressures are heterogeneously distributed within the tumour mass and may be located adjacent to regions with normal O_2 partial pressures. In contrast to normal tissue, neoplastic tissue can no longer fulfil physiologic functions [213].

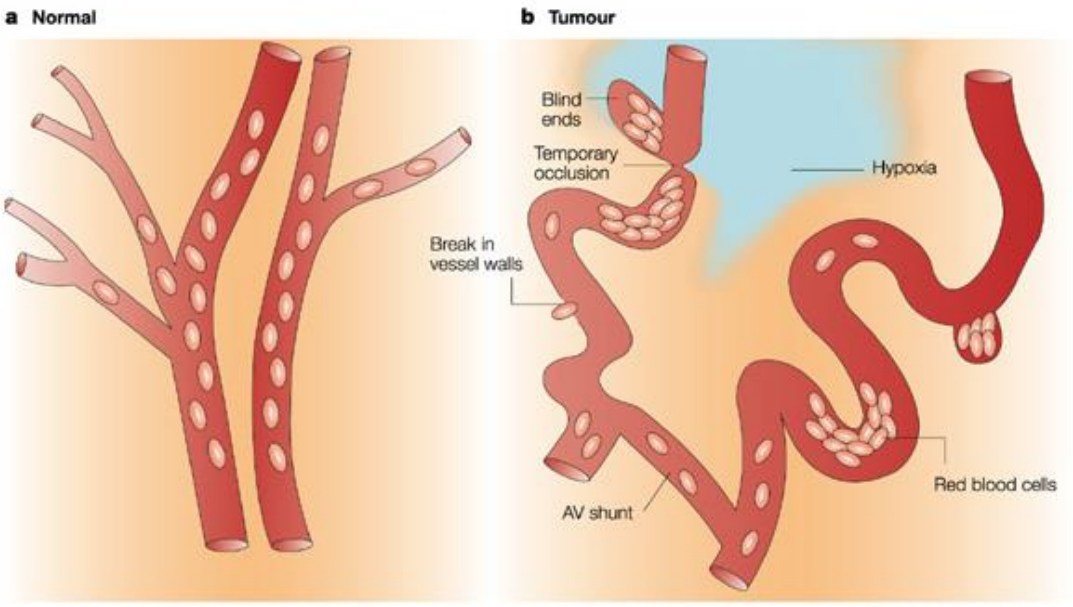

Figure 4.65 The vascular network of normal tissue versus tumour tissue. Normal vasculature (a) is hierarchically organised, with vessels that are sufficiently close to ensure adequate nutrient and oxygen supply to all cells. Tumour blood vessels (b) are chaotic, dilated, tortuous and are often far apart and have sluggish blood flow. As a consequence, areas of hypoxia and necrosis often develop distant from blood vessels [210].

The tumour microenvironment affects behaviour and prognosis of the malignant tumour. Tumour hypoxia has been associated with poor prognosis, enhanced loco-regional spread and metastatic potential [214]. In reality there have been many difficulties to overcome. Established hurdles, such as the difficulties associated with modulating protein-protein interactions, mean that many pharmaceutical companies are reluctant to invest in what is seen to be a high-risk area [209]. However, validating a target that can block the metastasis of both hypoxic and normoxic tumour cells would be an attractive proposition.

Tumour cells in hypoxic regions have a number of hallmarks that make them very difficult to treat. Typically, hypoxic cancer cells are characterised by elevated interstitial pressure [215,216], low extracellular pH, glucose deprivation, high lactate levels, decreased partial oxygen pressure (pO_2 <10 mmHg), accumulation of macrophages [217-219] and recruitment of the stromal cell components of the tumour microenvironment. Furthermore, hypoxic cells include the so-called 'cancer stem cells' that are believed to be the engines driving continuous production of cancer cells [220,221]. They are also highly

invasive and can metastasise away from the primary location to other sites [222] (Figure 4.66).

Figure 4.66 Hallmarks of hypoxic cancer.

The response to hypoxia is associated with changes in gene expression [223]. Hypoxia activates, among others, hypoxia-inducible transcription factors (HIF-1α and HIF-2α), which trans-activate the hypoxia-responsive element (HRE) present in the promoter of many genes encoding angiogenic, metabolic and metastatic factors and contributes to the acquisition of the tumour aggressive phenotype [224,225].

Hypoxia has a negative effect on cancer patient's prognosis, it has been considered as a stressor which selects cells with increased resistance to apoptosis and thus indirectly contributes to treatment resistance. Two different factors have been considered to explain the negative effect of hypoxia on the cancer patient's prognosis. The first factor involves the direct interference of hypoxia with anticancer therapy. The efficacy of ionising

radiation, and also a number of cytotoxic drugs and cytokines, depends directly on adequate oxygen levels. The second factor involves the effects of hypoxia on the biology of tumour and stromal cells since hypoxia is related to malignant progression, increased invasion, angiogenesis and an increased risk of metastasis formation [214]

Recent studies suggest that both hypoxia and the extracellular matrix (ECM) significantly contribute to cancer metastasis. Throughout tumour progression, changes in the composition and content of the ECM changes both its biophysical and biological properties and these significantly affect tumour and stromal cell properties such as proliferation and motility. Recent studies have shown a direct link between hypoxia and the composition of the ECM, which was formerly thought of as independent contributors to metastatic spread. This suggest a new model in which multiple micro environmental signals might unite to synergistically regulate metastatic outcome [222].

Here we have studied the effect of polySia expression, a main regulator of cancer cell-cell adhesion and a pro-migratory molecule on the behaviour of cancer cells under hypoxic conditions.

Hypoxia promotes cancer cell invasion and metastasis through inducing EMT [226]. A study by Justin V. *et al*., has shown that the exposure of non-mesenchymal SNB75 and U87 cells to hypoxia induced a strong change in cell morphology that was accompanied by enhanced invasive capacity and the acquisition of mesenchymal marker expression. It was identified that a HIF1α signalling axis promotes hypoxia induced mesenchymal shift and invasion in glioblastoma cells [227].

There is a positive correlation between HIF-1α and the N-cadherin expression profile [226]. Besides, involvement of HIF in the induction of carbohydrate determinants, such as sialyl Lewis x and sialyl Lewis, was evident in study performed by Tetsufumi Koike *et al* [228]. This suggests that there might be a cross talk between polySia and HIF that results in modulation of cell behaviour under hypoxic conditions.

On the other hand, as mentioned earlier, polySia is suggested to be a modulator of the activity of a number of cancer cell signalling pathways such as c-MET/ALK, FAK, VEGFR, TRK and FGFR. It was found that some of these signalling pathways are also modulated by cancer cell hypoxic/normoxic status such as FGFR and c-MET. In a study by C. Blick, it was found that hypoxia, in part via suppression of miR-100, induces FGFR3 expression in bladder cancer, both of which have an important role in maintaining cell viability under conditions of stress [229]. Another study has shown that in several cancer cell types, hypoxia activates the c-MET promoter, which contains hypoxia inducible factor-1 (HIF-1) binding sites, which can enhance the stimulating effect of SF/HGF on tumour cell migration [230].

This gives strong rationale for studies aimed at the exploring the possible role of polySia on cancer cell behaviour under hypoxic conditions, with the potential to provide a biochemical basis for the development of therapeutic strategies that can specifically block both cancer metastasis and survival within the heterogeneous hypoxic/normoxic characters of tumours.

To sum up, the aim of this chapter is to carry out initial investigations of the possible additional anti-metastatic effects of using certain signalling pathway inhibitors in combination with a polyST inhibitor. Additionally, pilot studies are performed in order to investigate the possible role of polySia on the behaviour of cancer cells under hypoxic conditions.

4.2. Materials and methods

All the materials are purchased from Sigma Aldrich, UK unless otherwise specified.

4.2.1. Cell lines

Cell lines were maintained as previously described in chapter 3. For studies carried out under hypoxic conditions, all the media used were incubated for at least 48 hours under hypoxic conditions (0.1% Oxygen) before being added to the cells.

4.2.2. 3-[4,5- Dimethylthiazol-2-yl]-2,5 diphenyl tetrazolium bromide (MTT) assay

The MTT assay was performed as previously described in chapter 3.

4.2.3. Migration assay

The migration assay was performed as previously described in chapter 3 (Section 3.2.3). Different cell lines were seeded in six well plates in the same density described previously, and cultured for 24 h. For studying the possible additive anti-migratory effect of combining polyST inhibitors with different SPIs: SU-5402, crizotinib, PF-573228, axitinib and GNF-5837 were added at concentrations of 10, 2, 3, 2.5 and 2 μM respectively. Each inhibitor was added to two wells, to one of them ICT-3176 (250 μM) was also added. In one well ICT-3176 (250 μM) only was added to be used as a control and to another well fresh media (containing DMSO in concentration equivalent to the concentration of the added inhibitors in the other wells) was used as negative control, to compare the migration of the cells in the presence and absence of the inhibitors. After 24 hours, images were taken.

For studying the effect of polySia expression on the migration of cancer cells under hypoxic conditions, migration assay was performed under normoxic versus hypoxic conditions (0.1% Oxygen) and images were taken after 16, 24 or 41 hours depending on the cell line, as described in chapter 3.

4.2.4. Growth curve

C6-STX and C6-WT cells were maintained and counted as mentioned earlier (Section 3.2.2). After cells were counted, cell suspensions were diluted in order to have an appropriate amount of the medium and to achieve a proper cell seeding density (2.5 x 10^4). Ten flasks of each cell line were seeded with the same density. Five plates of each cell line were incubated in a humid atmosphere of 5% CO_2 and 95% air at 37 °C while the other five flasks were maintained in a hypoxic chamber (Whitley-H35-hypoxystation) in a humid atmosphere of 5% CO_2, 0.1% O_2 and 95% nitrogen gas at 37°C. The duplicate plates were counted every 24 hours. The results were plotted on a log-linear scale.

4.2.5. Adhesion assay

4.2.5.1. Cell lines preparation

C6-STX and C6-WT cell lines were seeded in a concentration of 2 x 10^5 in two flasks (T75) per each cell line. One flask of each cell line was incubated in a humid atmosphere of 5% CO_2 and 95% air at 37 °C while the other flask was maintained in the hypoxic chamber in a humid atmosphere of 5% CO_2, 0.1% O_2 and 95% nitrogen gas at 37°C, all the media and buffers used with the hypoxic flask were kept in hypoxic conditions at least 48 hours before the experiment.

4.2.5.2. Pre-coating of multi-well plates

Matrigel™ matrix (VWR, USA) was diluted from stock solution to form a final concentration of 40 µg/ml using ice cold PBS (pH 7.4). Matrigel solution (200 µl) was added to the required number of wells in 24-well plates, which were incubated at 37 °C. After two hours, excess Matrigel was removed by inverting the multiwell plate over a plastic reservoir and tapping gently. The wells were then washed twice with cold PBS.

Blocking solution (500 µl) consisting of DMEM media with 10% FBS was added to each well to block non-specific binding. The plates were then

incubated at 37 °C. After 30 minutes the wells were washed once with cold PBS and fresh culture medium was added (200 µl) and the plates were incubated at 37 °C.

4.2.5.3. Cell counting and seeding

Hypoxic and normoxic C6 cell lines were trypsinised and counted. 2 x 10^4 cells in 100 µl medium were added to the pre-coated 24-well plate. For each condition of each cell line, 3 wells were seeded for each technical repeat. Culture medium (300 µl) was added to one well to be used as a blank to calculate the background staining. The plates were incubated at 37 °C for 30 minutes. For the hypoxic conditions all the steps were carried out in a hypoxic chamber.

4.2.5.4. Cell fixation and quantification

After incubation of the cells in the Matrigel-coated plates for 30 minutes, non-adherent cells were removed by inverting the plates on a plastic reservoir. Wells were washed two times with ice-cold PBS (300 µl) containing $CaCl_2$ (1 mM) and $MgCl_2$ (1 mM). Cells were fixed by adding ice-cold 100% methanol (300 µl). After 10 minutes, wells were washed with PBS three times and 0.5% crystal violet solution (100 µl), prepared in 20% ethanol, was added. Plates were placed on a shaker and incubated with crystal violet for 10 minutes at room temperature.

Excess crystal violet was removed by immersing the plates in large beakers filled with distilled water, three immersions of one minute each. Crystal violet was then recovered by adding 100% methanol (200 µl) to each well. The plates were placed on the shaker for 15 minutes at room temperature. 100 µl of the extracted crystal violet was transferred to 96 well-plate.

4.2.5.5. Data analysis

Absorbance of the samples was measured spectrophotometrically at a wavelength of 540 nm. The background absorbance of multi-well plates was also measured and subtracted from the 540 nm measurements.

The absorbance reading acquired for each sample were analysed quantitatively. For each reading, the absorbance of the multi-well plates was subtracted and the % cell adhesion relative to C6-WT cell line was calculated (% adhesion = average absorbance of the C6-WT cells /average absorbance of C6-STX cells in the same condition x 100).

4.2.6. Flow cytometry (Annexin V apoptosis detection assay)

4.2.6.1. Cell line preparation

C6-WT, C6-STX cells were seeded at a cell density of 4 x 10^5 in T75 flasks. Two flasks for each cell line were seeded, one of which was incubated under normoxic conditions (5% CO_2 and 95% air) while the other was incubated under hypoxic conditions (5% CO_2, 0.1% O_2 and 95% nitrogen gas) at 37°C for 96 hours.

4.2.6.2. Annexin V staining

After 96 hours incubation at normoxic/hypoxic conditions, media from each flask was collected and cells were trypsinised. Trypsinised cells along with the collected media, containing floating dead cells, were placed in a 20 ml tube and centrifuged for 5 minutes at 10000 g. After centrifugation, media was discarded and cell pellets were re-suspended in 1 ml of HEPES buffer. Cells were centrifuged again for five minutes at 1500 g.

Cell pellets were re-suspended in propidium iodide / Annexin V mix (1:5) (100 µl). After 15 minutes incubation, the solution was transferred to falcon round bottom tubes (FACS tubes) and Annexin-binding buffer was added (0.5 ml). Samples were analysed by flow cytometry.

4.2.6.3. Data Analysis

Samples were analysed by flow cytometry, (annexin V and propidium iodide fluorescence excitation/emission are 494/518 nm and 535/617 nm respectively). The cell population was separated into three groups: live cells, which show only a low level of fluorescence; apoptotic cells, which show

green fluorescence and dead cells, which show both red and green fluorescence, as summarised in figure 4.67.

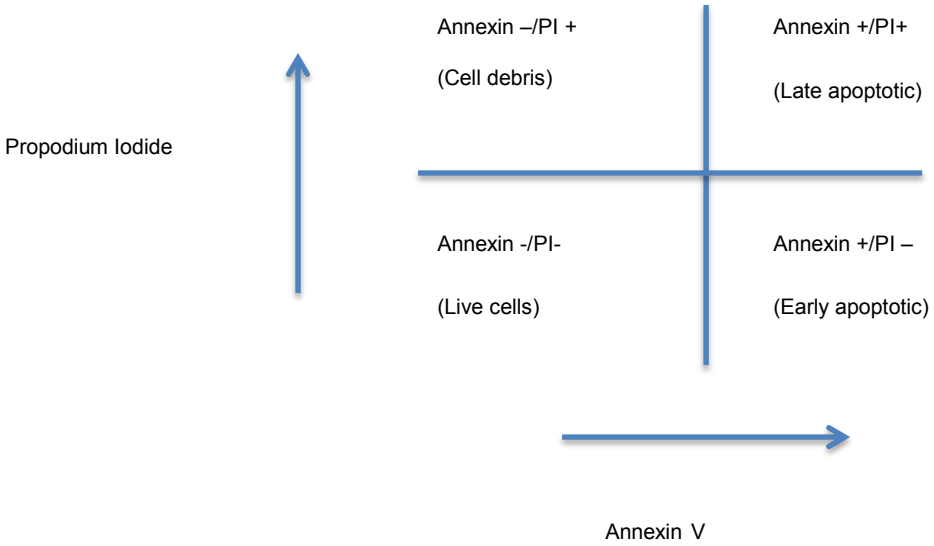

Figure 4.67 Schematic representation of the results obtained by flow cytometry.

4.2.7. Trypan blue exclusion assay for cell viability

Cell lines were prepared as previously described for the Annexin V apoptosis assay (section 4.2.6). Cells were trypsinised and the cell density of each cell line suspension was determined using a haemocytometer. A 0.4% solution of trypan blue was prepared in PBS solution (pH 7.2 to 7.3) and 0.1 mL of trypan blue stock solution was added to 1 mL of cells. Each haemocytometer chamber was loaded with 10 µl of the solution and examined immediately under a microscope at low magnification. The number of blue-stained cells and the number of total cells was counted. Cell viability (%) was calculated as follows:

% Viable cells = [1.00 – (Number of blue cells ÷ Number of total cells)] × 100

4.2.8. Western blot analysis

Western blot assay was performed as previously described in chapter 2. For the experiment carried out in this chapter 12% resolving gel was used. The resolving gel was made up of tris base (0.37 M, pH 8.8), 12% acrylamide mix, 0.1% SDS, 0.1% ammonium persulfate and 0.04% TEMED.

4.2.8.1. Sample preparation

C6-STX and C6-WT cells were seeded at the density of 2 x 10^5 cell/well in a six-well plate and incubated for 24 hours at 37°C in a 5% CO_2 humidified atmosphere to allow cells to adhere. After 24 hours, medium was removed and fresh medium containing different concentrations of $CoCl_2$ was added. Two wells were used as a control where no $CoCl_2$ was added. After 16 hours cells were collected.

4.2.8.2. Protein extraction

After trypsinisation cells were centrifuged and cell pellet was washed with PBS and re-suspended in 200 µl of lysis buffer consists of 10 µl 1X phosphatase inhibitor (P5726, Sigma, UK), 50 µl of 1X protease inhibitors cocktail (S8830, Sigma, UK) and 940 µl of RIPA buffer (NaCl (150 mM), %1 IGEPAL CA-630, 0.5% sodium deoxycholate, 0.1% SDS (GE Healthcare) and Tris (50 mM, pH 8)) in a microcentrifuge tube, maintaining constant agitation for 30 min at 4°C. The lysate was then sonicated three times (3 cycles, 10 seconds each, %10 amplitude) with one minute rest on ice between each ten-second pulse. The lysate was centrifuged at 13,000 x g for 5 minutes at 4°C and the supernatant was collected into new microtubes.

4.2.8.3. Quantification of protein concentration (Bradford assay)

Bradford reagent (GE Healthcare, UK) was diluted with distilled water (4:1). A set of bovine serum albumin (BSA) standards with known concentrations were prepared (0-1mg/ml). Standard and cell lysate samples were added in triplicate into 96 well plate (10 µl per well). Diluted Bradford reagent was added to each well (200 µl), and incubated for 5 minutes. The absorbance of the samples was examined using plate reader (Thermo Scientific multiskan spectrum, Thermo Scientific, UK) (595 nm) and standard curve between the concentration of the standards and its absorbance was created from which the concentration of the samples was calculated.

4.2.9. Statistics

All experiments were repeated three times independently unless otherwise specified. Statistical analyses were performed using Excel software. Differences between two groups were evaluated with Student's t test (Two tailed) where the P value significance is: P value (P) >0.05 was deemed not significant, P < 0.05 * was statistically significant, P < 0.01 ** and P < 0.001*** were statistically highly significant.

4.3. Results and discussion

4.3.1. Investigation of possible additive anti-migratory effect of using selected SPIs in combination with polyST inhibitor

In order to investigate the possible additive anti-migratory effect of using polyST inhibitors in combination with selected SPIs, the effect of a number of signalling pathway inhibitors (SU5402, axitinib, crizotinib, PF-573228, 5-FU and GNF-5837) on polySia-expressing neuroblastoma cell line (SH-SY5Y) migration was investigated in presence/absence of ICT-3176. The expression of these signalling pathways in SH-SY5Y cell line was confirmed by parallel work performed by Dr. Virginie Viprey (Data not shown).

Non-toxic concentrations of the SU5402, axitinib, crizotinib, PF-573228 and GNF-5837, as pre-determined by MTT assay, (10, 2.5, 2, 3 and 2 μM respectively) were used for this analysis; the non-toxic concentrations were chosen to ensure that the reduction in the cell migration is not caused by loss of cell viability. SH-SY5Y cells were treated with SU-5402, crizotinib, PF-573228, axitinib or GNF-5837. Each signalling pathway inhibitor was added to two wells, to one of them 250 μM of ICT-3176 was also added. To one well ICT-3176 only was added. The migration of the cells within all the wells was calculated and compared with control (untreated) wells.

Of the combinations evaluated, only crizotinib in combination with ICT-3176 resulted in an additive inhibitory effect on the migration of SH-SY5Y cells (P value = 0.02) (Figure 4.68). Crizotinib alone produced a non-significant reduction in cell migration. ICT-3176 caused a 35% reduction in cell migration (P value = 0.01). Together, crizotinib and ICT-3176 led to a 60% reduction in SH-SY5Y migration (P value = 0.01).

Axitinib, SU-5402, GNF-5837 and PF-573228 combinations did not show any inhibition compared with ICT-3176 alone at the concentrations tested.

The results obtained from this experiment suggest that there is possibly a cross-talk between polySia-NCAM and c-MET/ALK signalling pathway that is modulating cancer cell migration. These results come in agreement with a number of previous studies which suggested that inhibition of N-linked glycosylation impairs c-MET activity and ALK phosphorylation, resulting in disruption of downstream signalling [32,186].

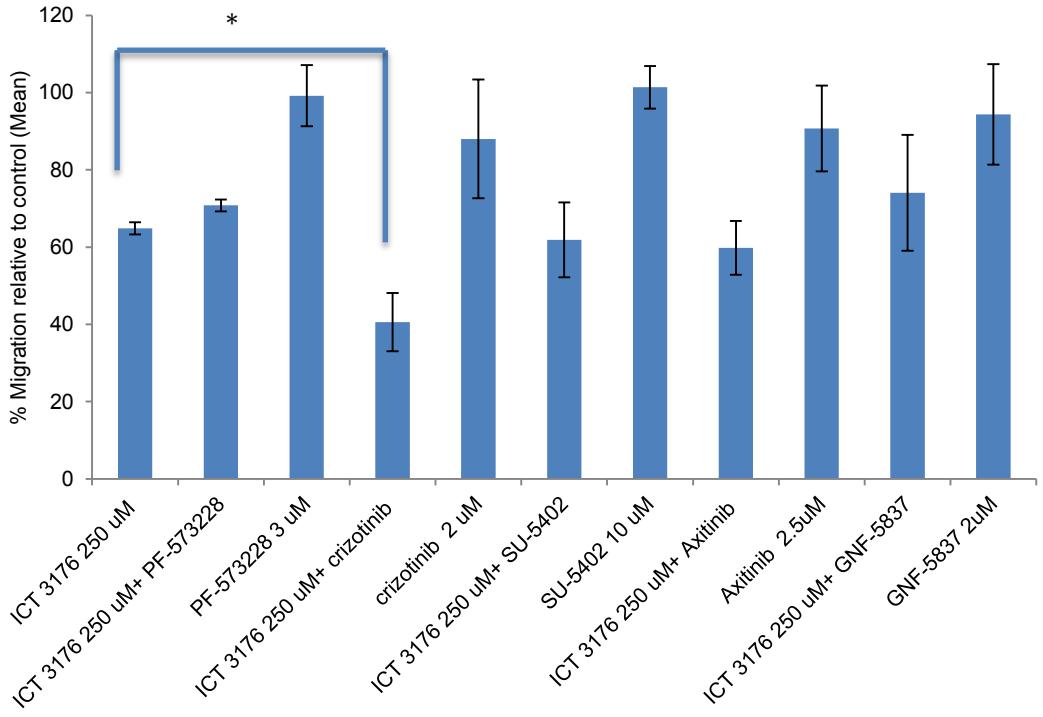

Figure 4.68 Effect of the combination of polyST inhibitor ICT-3176 and different signalling pathway inhibitors on SH-SY5Y cell migration. Concentrations determined previously by MTT assay. , * refers to P < 0.05. Results represent the mean of three independent experiments.

The effect of polySia expression on cancer cell behaviour under hypoxic conditions

4.3.2. Evaluation of the effect of hypoxia on polySia expression

Our first goal was to investigate whether hypoxia has any effect on the level of polySia expression on tumour cells. C6-STX cells (and C6-WT cells, used as a control to eliminate any false-positive results caused by presence of sialic acid in the medium at which the cells are grown) were incubated at 37 °C at either 0.1% oxygen, 5% carbon dioxide and 95% nitrogen (hypoxia) or 5% Carbon dioxide and 95% air (normoxia). After 30 and 48 hours cells were harvested and ST8SiaII expression was confirmed using RT-PCR (Data not shown). polySia expression was quantified using the cell-based chromatographic assay described in chapter 2.

Interestingly, a comparison of the polySia expression of C6-STX cells under hypoxia and normoxia demonstrated a difference. C6-STX cells exhibited a significant reduction (40 ± 6.9 %) in the expression of polySia under hypoxia compared to normoxia. No significant differences in polySia expression were detected between the 30 h and 48 h measurements (Figure 4.69). C6-WT cell were used as negative control where no expression of polySia was detected under both conditions. The cell-based polySia quantification was carried out using both methods, i.e. both Endo-N and mild acidic hydrolysis for the removal of polySia from the cell surface. Similar results were obtained from both experiments (SD ± 15%).

These data strongly indicate that polySia expression in cancer cells is down regulated under hypoxic conditions. To-date, there are no studies that have pointed out the effect of hypoxia on the expression of polySia, however these results are consistent with previous studies that has suggested that acute hypoxia produces a degree of glycocalyx degradation (a 0.2 – 1 μm thick negatively charged anti-adhesive and anti-coagulant carbohydrate-rich layer) [231].

(A) (B)

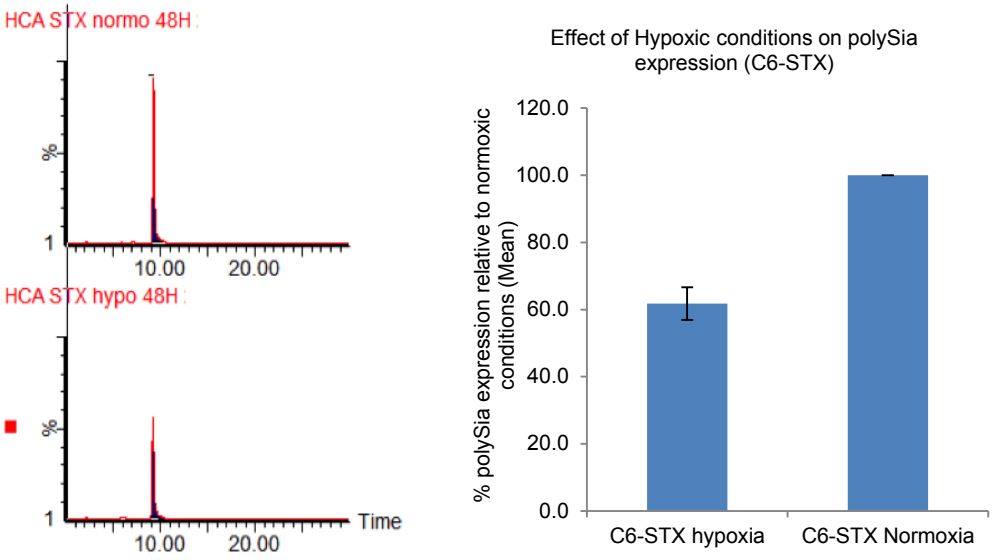

Figure 4.69 Effect of hypoxia (48 hours, 0.1% O_2) on polySia expression in C6-STX cells. Cell-based HPLC analysis was used to detect polySia in C6-STX cells under normoxic (upper curve) and hypoxic conditions (lower curve, after 48 hours of hypoxia) Y-axis represents % abundance while x-axis represents time (A). The graph represents the mean ± SD (n = 3) of the relative integrated signal (B).

4.3.3. Effect of polySia-expression on cancer cell migration under hypoxic conditions

Many reports have revealed that hypoxia promotes cancer cell migration [227,232,233]. Since polySia expression is linked to high migratory potential in cancer cells under normoxic conditions [234], we decided to evaluate whether the reduction in polySia observed under hypoxic conditions translated into a modulation of tumour cell migration.

As previously, the scratch assay was used to study these effects. In addition to the C6-STX and C6-WT cells, the study was expanded to also include SH-SY5Y and DLD-1 cells. Once again, migration under hypoxic and normoxic conditions was compared.

The results demonstrated that for the two polySia-expressing cell lines (C6-STX and SH-SY5Y), no difference in cell migration was observed between the hypoxic and normoxic conditions. This is despite our finding that the level

of polySia expression is reduced in C6-STX cells under hypoxia (Figure 4.70). Interestingly, the control cells (C6-WT and DLD-1), which do not express polySia, showed a significant and marked reduction in cell migration under hypoxia (Figure 4.70).

(A)

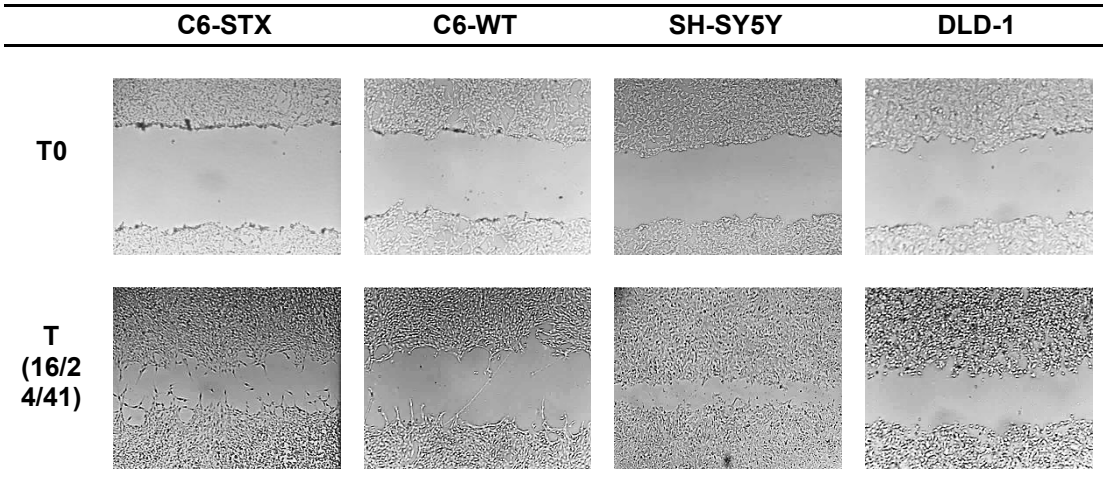

(B)

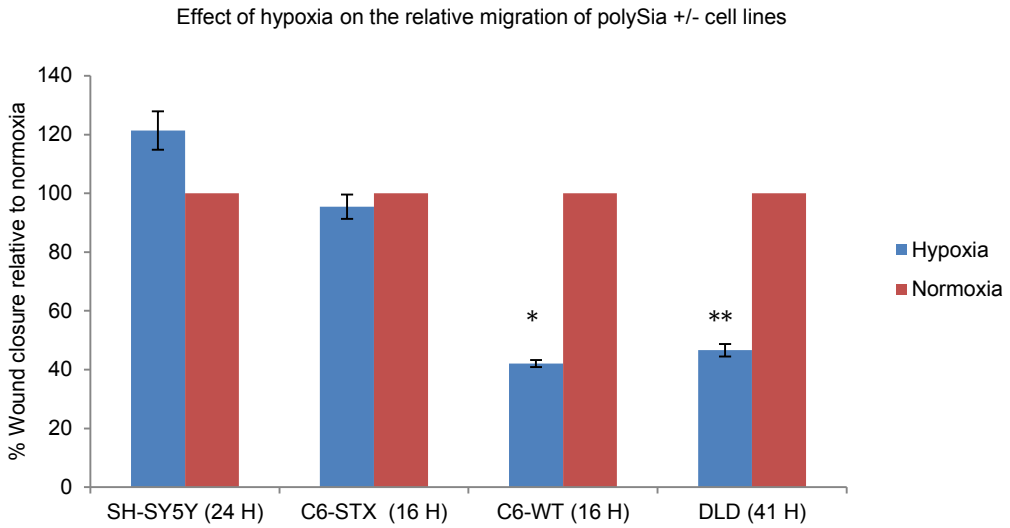

Figure 4.70 Effect of hypoxia on the relative migration of polySia positive/negative cell lines. A) SH-SY5Y, C6-STX cells expressing polySia and negative cell lines C6-WT and DLD-1 were scratch wounded with a micropipette tip and filmed after 16, 24 and 41 hours using time-lapse video-microscopy under hypoxic conditions. Images at t = 0, 16, 24 and 41 hours after scratching illustrate wound closure. B) The graph represents wound closure calculated by measuring the reduction of the wound area over time using Image J software: the percentage of the wound closure under hypoxic conditions is presented relative to that observed under normoxic conditions for each cell line. Results represent the mean of three independent experiments.

We next decided to evaluate the effect of a polyST inhibitor (ICT-3176 at 250 μM) on cell migration under hypoxic conditions. Cell migration was compared with non-treated cells. It was found that treatment of the cells with ICT-3176 resulted in significant inhibition in C6-STX cell migration (22.4 ± 2.5%) (Figure 4.71). This compares to the migration assay of ICT-3176 carried out previously in-house, which showed that ICT-3176 resulted in 30% inhibition of C6-STX cell migration at a concentration of 500 μM under normoxic conditions. Here it was found that at concentration of 250 μM ICT-3176 results in 22.4 ± 2.5% inhibition in C6-STX cell migration under hypoxic conditions. The effect of ICT-3176 is suspected to be greater under hypoxic conditions since less polySia is expressed, as shown earlier (Section 4.3.3). This might be explained by the suggestion that polySia might be affecting cell migration by interacting with different signalling pathways which are over-expressed under hypoxia such as c-MET signalling pathway. Taken together, these results demonstrate that polySia potentially plays an important role in hypoxia-induced cancer cell migration.

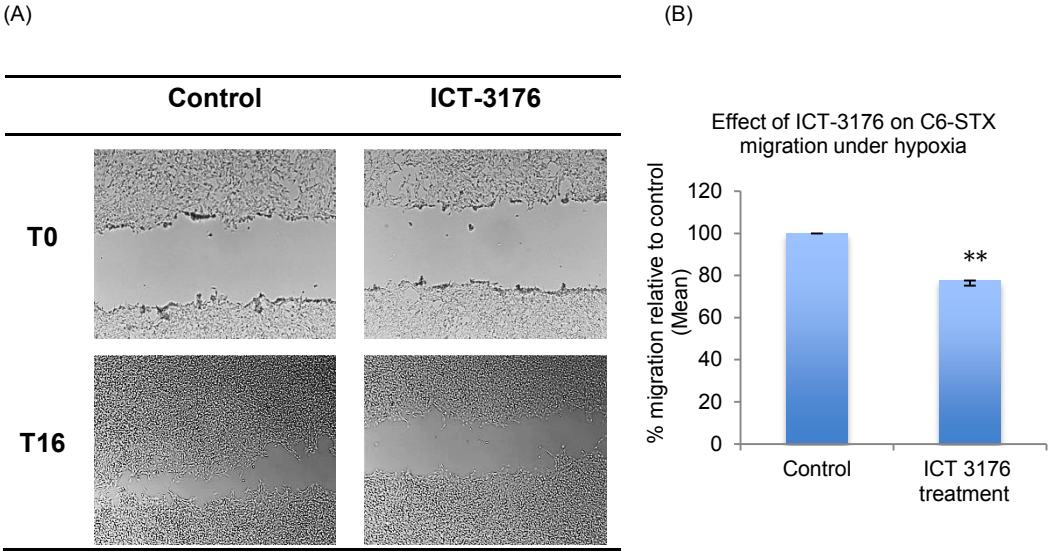

Figure 4.71 Effect of ICT-3176 on the migration of C6-STX cells under hypoxia. A) C6-STX cells were treated with polyST inhibitor ICT-3176 under hypoxic conditions and were scratch wounded with a micropipette tip and filmed after 16 hours using time-lapse video-microscopy under hypoxic conditions. Images at T0 and T16 after scratching illustrate wound closure. B) The graph represents the quantification of the polyST inhibition effect on the wound closure calculated by measuring the reduction of the wound area over time using Image J software; the percentage of the wound closure after treatment with ICT-3176 is presented relative to that observed with the control untreated cells. Results represent the mean of three independent experiments.

4.3.4. Effect of hypoxia on polySia-driven cancer cell-matrix adhesion

As discussed earlier it was previously reported that polySia inhibits cancer cell adhesion through modulation of NCAM-NCAM interactions and NCAM interaction with other molecules in addition to exerting a repulsion force created by the negative charge on the polySia chains (Chapter 1, section 1.4.2). Besides, evidence has been presented suggesting that polySia and hypoxia modulate the c-MET signalling pathway (Section 4.1.2), which have a significant role on cancer cell adhesion [235]. In order to investigate the effect of hypoxia on polySia-mediated adhesiveness of cancer cells, C6-STX and C6-WT were incubated under either normoxic or hypoxic conditions. After 48 hours, cells were harvested and the adhesion assay was performed as described in the materials and methods section.

After 48 hours of incubation under hypoxic conditions, C6-STX cells were less able to adhere to Matrigel©. Adhesion capacity was reduced to 83.7 ± 2.9% of control C6-WT cells adhesiveness (P value= 0.01). This is consistent with previously published studies which suggest that polysialylation of NCAM have an inhibitory effect on cell-adhesion [175]. There was no difference in the reduction of cell adhesiveness between normoxic and hypoxic conditions, however (Figure 4.72). These results suggest that unlike migration, hypoxia does not affect polySia-mediated cell-matrix adhesion. The difference in cell adhesion of C6-STX compared with C6-WT cells was expected to be lower under hypoxic conditions compared with normoxic conditions since less polySia is expressed in C6-STX cells under hypoxic conditions compared to normoxia. One possibility might be that polySia modulates cell adhesion by interacting with different signalling pathways under hypoxic conditions, such as c-MET which is over expressed in hypoxic conditions [183,236]. This warrants further exploration.

Future studies should include other extracellular matrix substrates. It has been previously shown that high levels of polySia have different effects on cell adhesion to different ECM components, such as fibrinocitin, laminin, heparin and Matrigel [98].

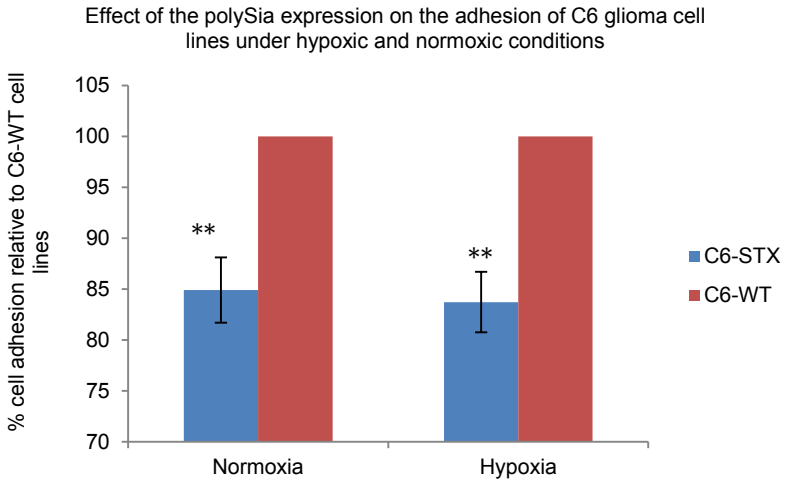

Figure 4.72 Effect of hypoxia on the polySia-mediated adhesiveness of cancer cells, showing a reduction in cell adhesion to Matrigel© in C6-STX compared to C6-WT cells under both normoxic and hypoxic conditions. Results represent the mean of three independent experiments.

4.3.5. Effect of polySia expression on cancer cell survival under hypoxic conditions

In order to determine the effect of polySia expression on the survival of cancer cells under hypoxia, C6-STX and C6-WT cells were subjected to hypoxic conditions for 96 hours while control flasks of the cells were incubated for the same duration under normoxic conditions. After 96 hours, cells were examined under the microscope and then were collected and cell count was determined manually using a haemocytometer. Viable and dead cell count were also calculated using trypan blue staining (Figure 4.73).

Interestingly, it was found that polySia-expressing cells were associated with higher cancer cell survival under hypoxic conditions compared to polySia negative cell lines (Figure 4.73C). C6-WT cells exhibited 56.4 ± 6.2% less survival than C6-STX cells (C6-WT survival was calculated as a percentage of C6-STX survival). These results were further confirmed with trypan blue exclusion assay. C6-WT cells exposed to hypoxia for 96 hours were associated with a significant 85.8 ± 5% reduction in viability compared to polySia-expressing C6-STX cells (C6-STX cell death was calculated as a percentage of C6-WT cell death) (Figure 4.73A, B).

(A)

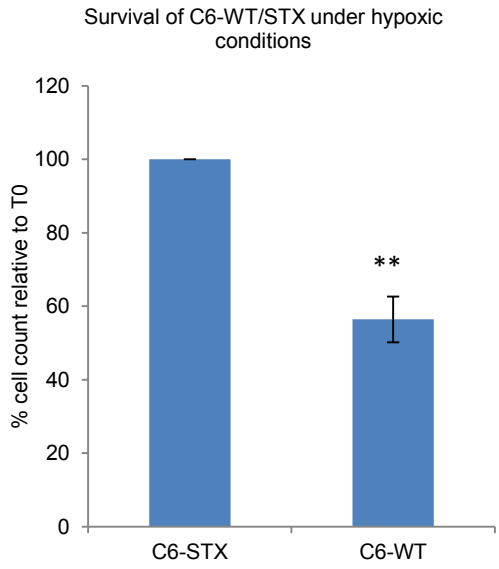

(B)

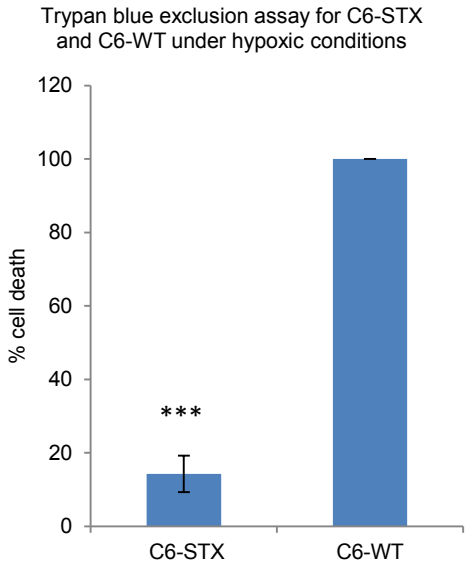

(C)

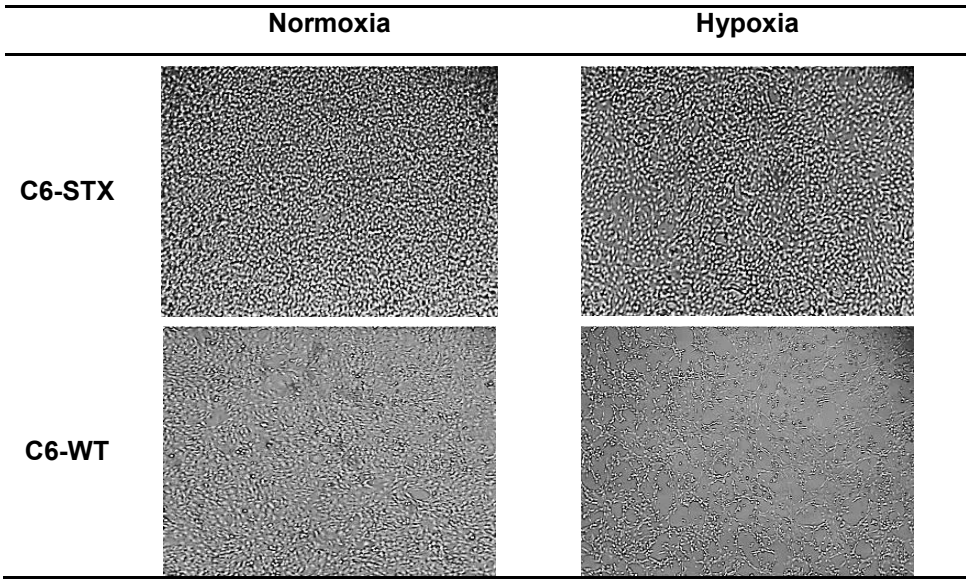

Figure 4.73 Effect of hypoxia on the survival of polySia expressing cells (C6-STX) compared to non-expressing cells (C6-WT). A) Subjecting both C6-STX and C6-WT cells to hypoxia for 96 hours, results in reduction in C6-WT cells survival. Results were confirmed with trypan blue exclusion assay where the induction of cell death caused by hypoxia was 85.8% less in C6-STX compared to C6-WT (B). In graph A the percentage cell count of C6-WT cells is calculated as a percentage of the C6-STX cell count, in graph B, the percentage cell death of C6-STX cells is normalised against the C6-WT cell count. Graph C) shows the morphological change in C6-STX and C6-WT cells after incubation under hypoxic or normoxic conditions for 96 hours. Results represent mean of three independent experiments.

In order to provide further supporting evidence for the results, hypoxia-induced apoptosis was analysed in C6-STX and C6-WT cells using annexin V and propidium iodide (PI) staining. Propidium iodide is widely used in conjunction with Annexin V to determine if cells are viable, apoptotic, or necrotic through differences in plasma membrane integrity and permeability [237].

In this assay, cells were subjected to hypoxia or normoxia and after 96 hours cells were harvested, labelled with annexin V and propidium iodide mixture and analysed using flow cytometry. Cells undergoing apoptosis are Annexin V positive and propidium iodide negative. Propidium iodide staining identifies dead cells while lack of annexin V staining and propidium iodide uptake is observed in live cells (Figure 4.67). The results were compared with control cells incubated under normoxic conditions.

(A)

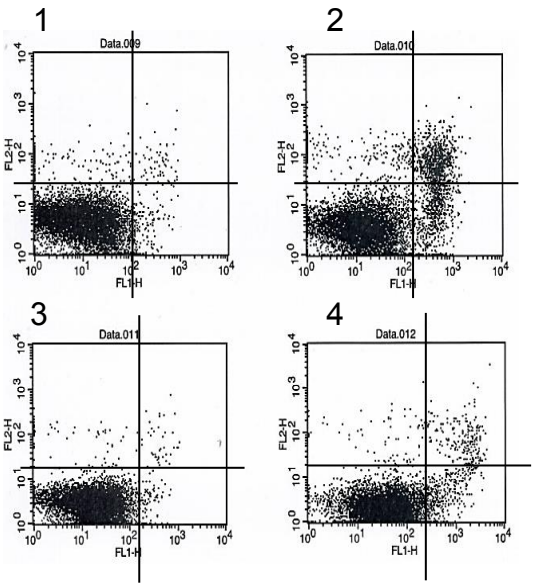

(B)

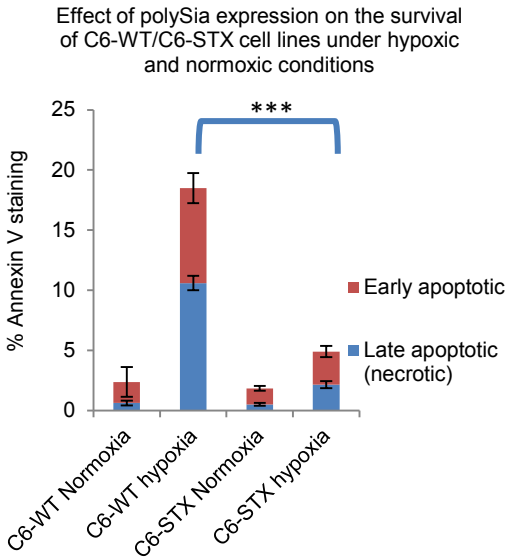

(C)

Average	C6-WT (Normoxia)	C6-WT (hypoxia)	C6-STX (Normoxia)	C6-STX (hypoxia)
Late apoptotic	0.64 ±0.19	10.6±0.60	0.53±0.13	2.16±0.29
Early apoptotic	1.75±1.24	7.89±1.24	1.33±0.19	2.75±0.46
Viable cells	96.22±1.14	79.03± 1.50	97.48±0.37	94.45±0.04

Figure 4.74 Effect of polySia expression on the survival of cancer cells under hypoxic conditions determined by PI/Annexin V apoptosis assay. A) Flow cytometry analysis of C6-STX and C6-WT cells apoptosis under hypoxic and normoxic conditions; (1) represents C6-WT cells under normoxic conditions, (2) represents C6-WT under hypoxia, (3) represents C6-STX under normoxia and (4) represents C6-STX under hypoxia. B) Diagrammatic representations of the result of flow cytometry analysis. C) Percentage of annexin V staining of different cell lines under each condition. Results represent mean of three independent experiments.

The ability of PI to enter a cell is dependent upon the permeability of the membrane; PI does not stain live or early apoptotic cells due to the presence of an intact plasma membrane. In late apoptotic and necrotic cells, the integrity of the plasma and nuclear membranes decreases, allowing PI to pass through the membranes, intercalate into nucleic acids, and display red fluorescence.

Annexins are a family of calcium-dependent phospholipid-binding proteins, which bind to phosphatidylserine (PS) to identify apoptotic cells. In healthy cells, PS is predominantly located along the cytosolic side of the plasma membrane. Upon initiation of apoptosis, PS loses its asymmetric distribution in the phospholipid bilayer and translocate to the extracellular membrane, which is detectable with fluorescently labelled Annexin V. In early stages of

apoptosis, the plasma membrane excludes viability dyes such as propidium iodide (PI), therefore cells which display only Annexin V staining are in early stages of apoptosis. During late-stage apoptosis, loss of cell membrane integrity allows Annexin V binding to cytosolic PS, as well as cell uptake of PI [238].

As shown in figure 4.74, the apoptotic fraction of C6-WT cells was significantly higher than C6-STX cells (73.5% less apoptosis in C6-STX cells) under hypoxic conditions, while no significant difference in the C6-WT and C6-STX cell survival under normoxic conditions was detected. These results suggest that polySia expression might have a role in enhancing cancer cell survival under hypoxic conditions. As discussed earlier both polySia expression and hypoxia have been shown to modulate FGFR expression, which has an important role in maintaining cell viability under conditions of stress (section 4.1.2).

These results support the suggestion by Ajit Varki *et al.*, which indicated that since cancer is a "microevolutionary" process in which only the fittest cells in a genetically heterogeneous population survive, under hypoxic conditions many of the glycan biosynthetic pathways change in order to improve the survival of cancer cells [239].

Under the poorly oxygenated conditions found in locally advanced tumours, hypoxia-resistant cancer cells survive by the principle of natural selection, acquiring hypoxia tolerability through a transcription factor HIF, the nuclear translocation of which is facilitated by inactivation of tumour suppressors such as VHL and p53. Recently, HIF was shown to induce transcription of several genes for glycan synthesis, leading to the significant alteration of glycan profiles in order to promote cell survival under hypoxic conditions [239].

4.3.6. Effect of polySia expression on the proliferation of cells under hypoxic conditions

In order to investigate the effect of polySia expression on the proliferation of cells under hypoxic conditions, growth curves of both C6-STX and C6-WT

cell lines were generated as described in the materials and methods section. It was found that hypoxia significantly reduced cell proliferation regardless of polySia expression status (Figure 4.75A). The results were confirmed by performing the MTT assay on C6-STX and C6-WT cell lines under hypoxic and normoxic conditions (Figure 4.75B).

The reduction in cancer cells proliferation under hypoxic conditions comes in agreement with previous published studies. It was previously reported that cells exposed to hypoxia are generally arrested at the G1/S-phase boundary; O_2 partial pressures of 0.2–1 mmHg disproportionately lengthen the G1 phase or arrest cells in the G1 phase, resulting in the reduction of cancer cells rate of proliferation [213,240].

(A)

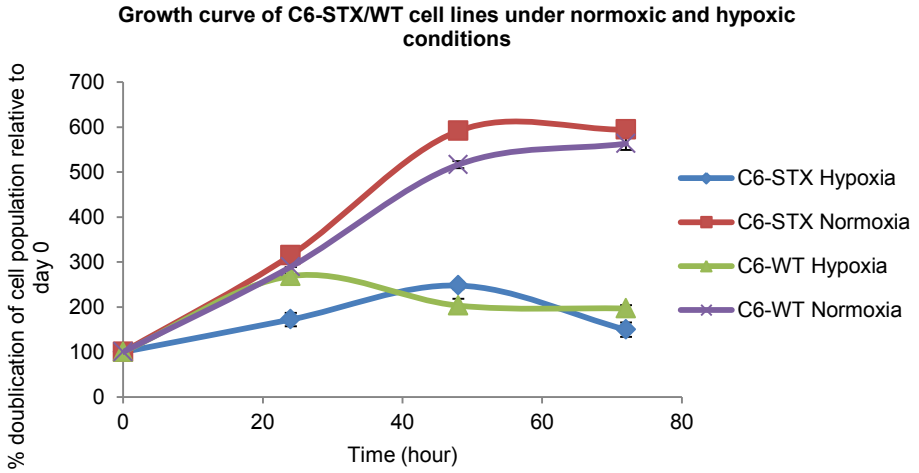

(B)

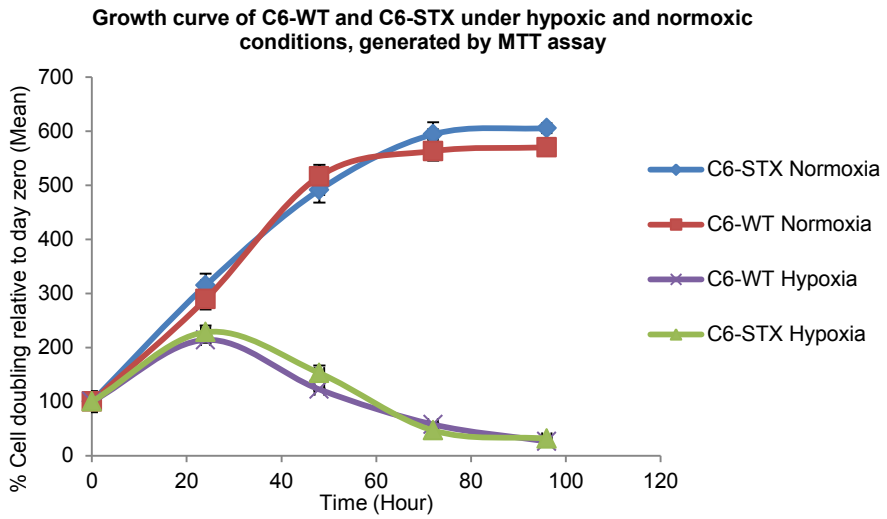

Figure 4.75 Effect of polySia expression on cell proliferation under both hypoxic and normoxic conditions measured by performing growth curve (A) and MTT assay (B). Results represent the mean of three independent experiments.

4.3.7. Initial investigation into the role of hypoxia-inducible factor-1 (HIF-1) in the altered behaviour of polySia-expressing tumour cells under hypoxic conditions

A critical mediator of the hypoxic response is the transcription factor hypoxia-inducible factor 1 (HIF-1) that up regulates expression of proteins that promote angiogenesis, anaerobic metabolism, metastasis and many other survival pathways [241]. HIF-1 is a transcription factor for dozens of target genes, HIF-1α serves as a testimony to the central role of HIF-1; HIF-1 activity in tumours depends on the availability of the HIF-1α subunit, the levels of which increase under hypoxic conditions and through the activation of oncogenes and/or inactivation of tumour suppressor genes [225,242]. In order to investigate whether HIF-1α expression modulates the altered polySia-mediated cancer cell behaviour under hypoxic conditions, cobalt chloride ($CoCl_2$), a known chemical inducer of HIF-1α, which stabilize HIF-1α by blocking HIF-1α posttranslational modification by prolyl hydroxylase was used [243,244].

In the next few experiments, the effect of HIF-1α induction, using cobalt chloride, on the key polySia-induced behavioural changes of cancer cells under hypoxia were examined.

4.3.7.1. Determination of cytotoxicity of cobalt chloride on C6 cells (determination of IC_{50})

In order to determine the suitable concentrations for studying the effect of HIF-1α induction on both migration and survival of C6 cell lines using cobalt chloride, an MTT viability assay was performed. In this experiment, the viability of C6-STX and C6-WT cells was examined after incubation with different concentrations of $CoCl_2$ and the IC_{50} value was calculated. 257.48 ± 9.6 µM and 289.13 ± 11.95 µM were the IC_{50} values of $CoCl_2$ using C6-STX and C6-WT cells respectively. No significant difference in the IC_{50} values of both cell lines was detected (Figure 4.76).

	C6-STX	C6-WT
IC_{50} (µM)	257.48 ± 9.6	289.13 ± 11.95

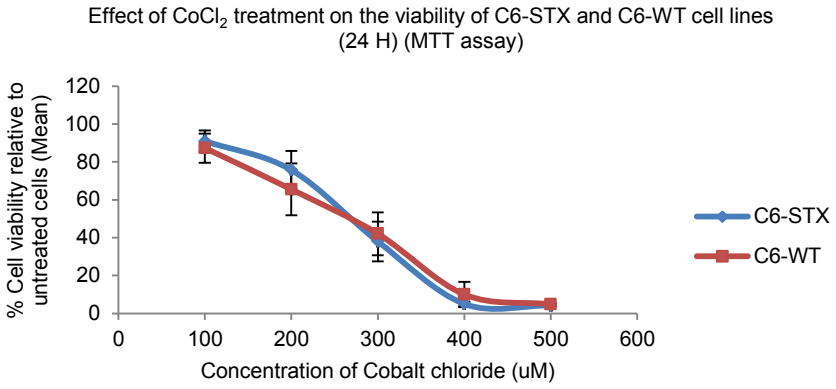

Figure 4.76 Determination of the cytotoxicity (IC_{50} value) of cobalt chloride using C6-STX and C6-WT cell lines after 24 hours of exposure. Results represent mean of three independent experiments.

For the migration assay, concentration of $CoCl_2$ that caused less than 20% loss in the viability of both cell lines were used (100 and 130 µM, as determined from figure 4.77). Non-toxic concentrations were chosen to ensure that the reduction in the migration is not caused by loss of cell viability. On the other hand, a concentration of $CoCl_2$ that induces reduction in cell viability, more than 20%, (200 µM) was used in order to examine cell survival under stress conditions.

In order to confirm the induction of HIF-1α expression using the selected $CoCl_2$ concentrations, a western blot analysis of HIF-1α expression, of both C6-STX and C6-WT cells after treatment with $CoCl_2$ have been performed using monoclonal rat HIF‑1α antibody (R&D systems, UK). It was found that using this antibody no bands were detectable in any of the samples. This could be explained by the low sensitivity of the antibody, in addition to the fact that HIF-1α detection is difficult due to its low abundance and short life time ($t_{½}$: approx. 5 min) [245-247].

Lactate dehydrogenase A (LDHA) is an enzyme that catalyses the conversion of pyruvate and NADH to lactate and NAD+ and is one of several target genes that is induced by HIF-1α [248,249]. Here we have detected the level of LDHA expression as an indicator for the possible expression of HIF-1α in cells treated with $CoCl_2$. The expression of LDHA in both C6-WT and C6-STX $CoCl_2$-treated cells was significantly higher than control untreated cells, which is an indicator of the induction of HIF-1α expression (Figure 4.77).

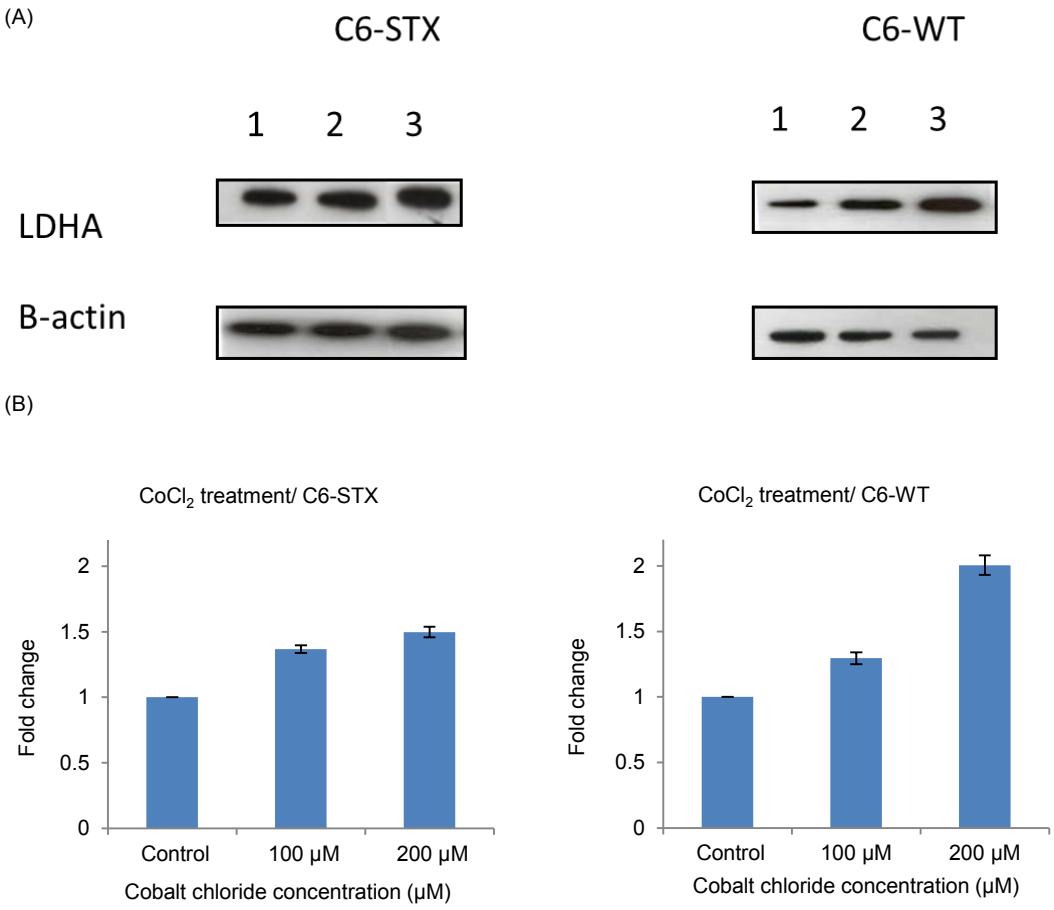

Figure 4.77 Expression of LDHA after treatment of C6-STX and C6-WT cells with different concentrations of $CoCl_2$. (A) Lane 1 represent control untreated cells, lane 2 represents 100 µM $CoCl_2$ and lane 3 represents 200 µM $CoCl_2$. (B) Quantification of LDHA expression after $CoCl_2$ treatment. Results were normalized against actin expression and represent two independent experiments.

4.3.7.2. Effect of HIF-1α induction on polySia-triggered cancer cell migration

In order to investigate whether HIF-1α expression modulates the altered polySia-mediated migration of cancer cells under hypoxic conditions, the migration of C6-STX and C6-WT cells was examined after treatment with 100 and 130 µM cobalt chloride respectively. Two concentrations were used since it was observed that using 130 µM of cobalt chloride, while not causing significant loss of viability of C6 cells as examined by MTT assay, resulted in a change in the morphology of the cells. So, in order to ensure that the effect on cell migration was not caused by any effect on the phenotype of the cells,

a lower concentration (100 μM) was also used that did not cause any change in the cell morphology.

Cells were seeded in 0.5 x 10^6 cell/well density in six-well plates. After 24 hours, the attached cell monolayer was scratch wounded with a micropipette tip and fresh medium containing different concentrations of $CoCl_2$ was added. Plates were incubated for 16 hours at 37°C, filmed after 16 hours using Lumascope microscopy (Table 4.28) and the percentage wound healing was calculated and the results were compared with control untreated cells.

It was found that treatment of the cells with $CoCl_2$ caused significant inhibition in the migration of both C6-STX and C6-WT cell lines compared to the untreated cells. However, the relative percentage of migration inhibition in cobalt chloride treated C6-WT cells was significantly higher compared to C6-STX cells; $CoCl_2$ treatment resulted in significantly higher migration inhibition in C6-WT cells compared to C6-STX cells (difference in the percentage of inhibition is 21.1 ± 9.5% with 100 μM $CoCl_2$, P value= 0.03 and 34.57 ± 15.3% with 130 μM $CoCl_2$, P value= 0.02) (Figure 4.78). Combining these results with the results of the migration assay of different cell lines under hypoxic conditions that showed that cell lines which do not express polySia showed a significant and marked reduction in cell migration under hypoxia (Figure 4.70), these results suggest that the polySia-enhanced migration of cancer cells under hypoxic condition might be modulated by HIF-1α induction.

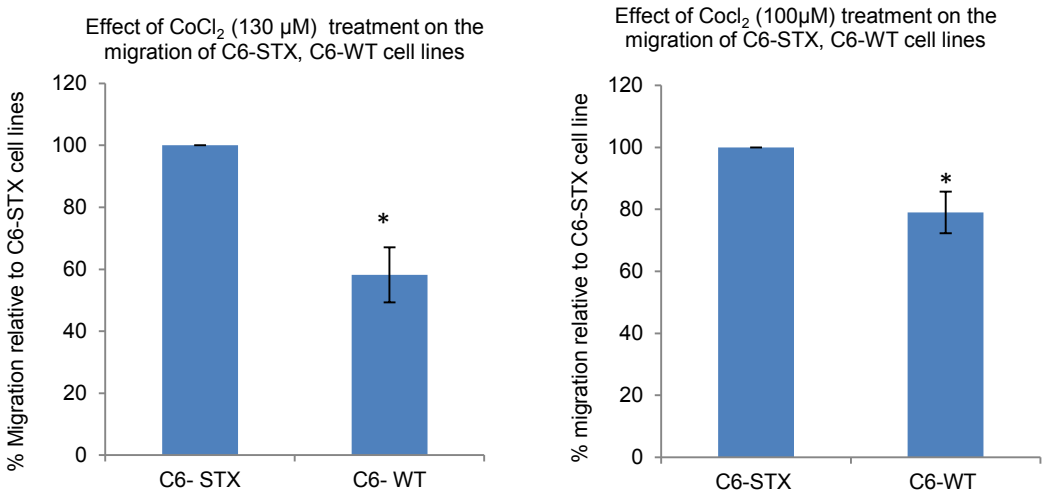

Figure 4.78 Quantification of the effect of $CoCl_2$ on the migration of C6-WT and C6-STX calculated by measuring the reduction of the wound area over time using Image J software. The percentage of C6-WT wound closure after cobalt chloride treatment is calculated as a percentage of the C6-STX wound closure. Results represent the mean of three independent experiments.

Table 4.28 Effect of $CoCl_2$ on the migration of C6-WT and C6-STX. Wound size at t = 0 and 16 hours after scratching C6-STX and C6-WT cells with/without 100 µM cobalt chloride treatment. Results represent three independent experiments.

	T0	T16
C6-STX, Control	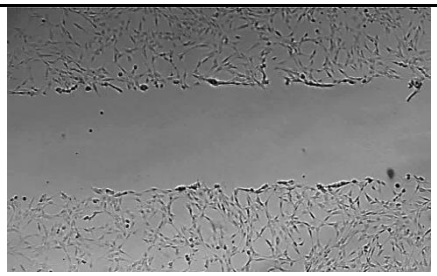	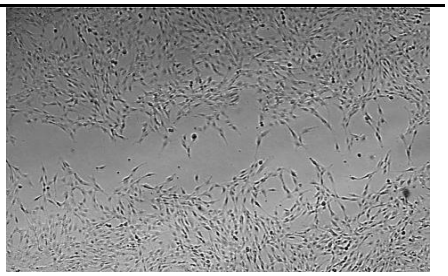
C6-STX, $CoCl_2$, 100 µM	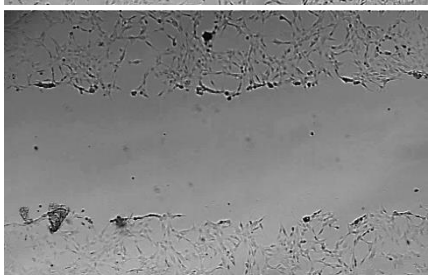	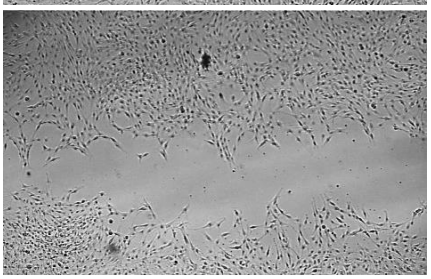
C6-WT, Control	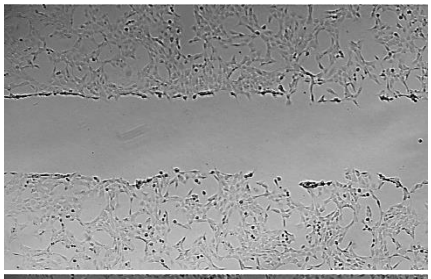	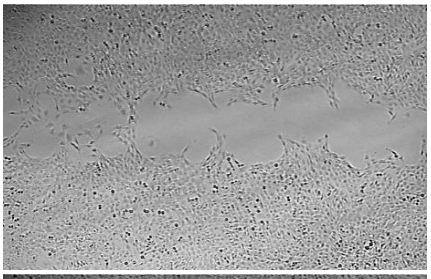
C6-WT, $CoCl_2$, 100 µM	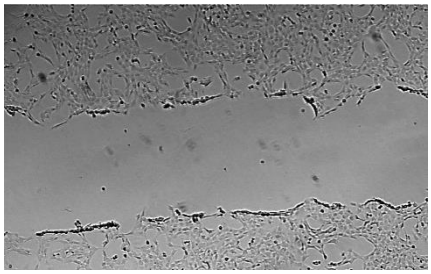	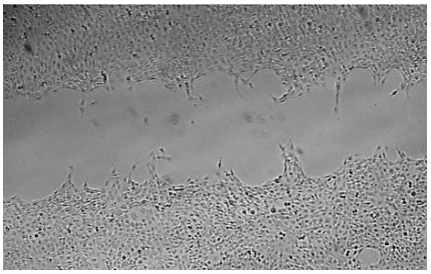

4.3.7.3. Effect of HIF-1α induction by $CoCl_2$ on polySia-expressing cancer cell survival

The effect of HIF-1α induction on the apparently enhanced cell survival observed in polySia-expressing cells was investigated. In this experiment, the percentage cell survival of C6-STX and C6-WT cells was calculated after incubation with 200 μM $CoCl_2$. It was found that there was no significant reduction in the cell survival recorded with C6-WT cells compared to the C6-STX cells (P value = 0.26). Results were confirmed using trypan blue exclusion assay (Figure 4.79).

This suggested that the enhancement of cell survival associated with polySia expression under hypoxic conditions is not linked to HIF-1α up regulation.

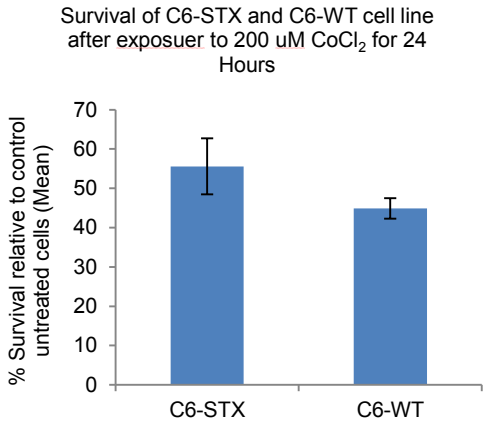

Figure 4.79 Effect of HIF-1α induction on the survival of C6-STX and C6-WT cells. Results represent mean of three independent experiments

4.4. Conclusion

In this chapter, two aspects of the mechanism by which polySia exerts its effects have been explored: the possible additive anti-migratory effect of using selected signalling pathway inhibitors that have been previously suggested to be modulated by polySia expression in combination with a polyST inhibitor and the effect of polySia expression on cancer cell behaviour under hypoxic conditions.

In order to study the possible additive anti-migratory effects of using polyST inhibition in combination with the selected SPIs, the anti-migratory effect of ICT-3176 in combination with the aforementioned SPIs was assessed. It was found that significant reduction in the migration of the SH-SY5Y cells is induced using a combination of ICT-3176 and crizotinib (c-Met/ALK inhibitor) compared to the inhibition in the migration caused by ICT-3176 or crizotinib treatment alone. This suggests that there is possibly a cross-talk between polySia-NCAM and c-MET/ALK signalling pathway that is modulating cancer cell migration.

Crizotinib is an FDA-approved drug used to treat adults with non-small cell lung cancer, a disease that in a subset of patients is caused by translocations of the ALK gene [250]. ALK is also a frequent target of genetic alteration in advanced neuroblastoma [251]. However, certain ALK mutations result in de novo crizotinib resistance, and a phase I trial of crizotinib showed a lack of response in patients harbouring those ALK mutations [252]. Different combinations have been examined in order to enhance the patient's response such as crizotinib combination with topotecan and cyclophosphamide [252]. Here we have shown that combining crizotinib with polyST inhibitor results in enhancing its anti-migratory effect which starts a new potential area of study in order to investigate whether combining polyST inhibitor with crizotinib would result in synergistic effects on proliferation, signalling, and cell death of neuroblastoma cells as well, and whether this would translate into a positive effect on the patient response to the treatment.

The second part of this chapter investigated the effect of polySia expression on cancer cell behaviour under hypoxic conditions. Changes in the composition of the extracellular matrix reflect on its biological properties, these changes result in significant alterations in tumour and stromal cell properties such as migration, proliferation and survival. Recent studies have established a direct link between hypoxia and the composition and organisation of the extracellular matrix. In a study performed by Glikes et al., it was shown that hypoxia promotes extracellular matrix remodelling to facilitate metastasis [222].

Here it was found that expression of polySia reduces cell adhesion and enhances both migration and survival under hypoxic conditions. It is suggested that the polySia-enhanced migration of cancer cells under hypoxic condition might be modulated by HIF-1α induction; it was found that induction of HIF-1α, using cobalt chloride, results in significantly higher migration inhibition C6-WT compared to C6-STX cells. On the other hand, the pro-survival effect of polySia under hypoxic conditions was suggested to be independent of HIF-1α expression.

To sum up, here we have initially investigated certain aspects of the mechanism of polySia activity. It is suggested that polySia-enhanced cell migration might be modulated by c-MET/ALK activity. Besides, polySia expression is suggested to play a role in reducing cancer cell adhesion and enhancing migration and survival under hypoxic conditions. Further studies are needed in order to further confirm the results obtained in this study, which will be discussed in chapter 5.

Chapter 5. General discussion and future perspective

5.1. General discussion

Cancer is among the leading causes of mortality worldwide. In 2012, there were 14 million new cases and 8.2 million cancer-related mortality worldwide [26]. Despite the tremendous work done in this field, today cancer still accounts for about one in every seven deaths worldwide [26]. Metastasis is the most deadly aspect of cancer and results from several interconnected processes including cell proliferation, angiogenesis, cell adhesion, migration, and invasion into the surrounding tissue. Metastasis is still the principal cause of death in cancer patients despite decades of research aimed at restricting tumour growth [26,253].

Although some types of metastatic cancer can be cured with current treatments, most cannot [254]. Metastatic cancer may be treated with systemic therapy (chemotherapy, biological therapy, targeted therapy, hormonal therapy), local therapy (surgery, radiation therapy), or a combination of these treatments. The choice of treatment generally depends on the type of primary cancer; the size, location, and number of metastatic tumours; the patient's age and general health; and the types of treatment the patient has had in the past [255].

Researchers are studying new ways to stop the growth and migration of primary cancer cells and metastatic cancer cells, including new ways to boost the strength of immune responses against tumours. In addition, researchers are trying to find ways to disrupt individual steps in the metastatic process [254]. The primary goal of these studies was to provide an understanding of the nature of cancer cells so they can be more effectively treated and eradicated with the main aim of understanding the basic controls of both normal and cancer cells which allows cancer cells to create an identity. This was achieved by studying the mechanism of action of cancer cell growth, proliferation, metastasis and interaction with local environment and other cells [26].

Although over 90 percent of cancer mortality today are due to metastasis, there is no effective anti-metastatic drug on the market [256,257]. Currently most

FDA licensed or internationally available anti-metastatic drugs have been categorized as anti-vascular (angiogenesis) and matrix metalloproteinase (MMPs) inhibitors with more than 500 related-agents of different chemical formulae having been reported. However, due to indiscriminate molecular inhibitiors and generally low survival benefits for patients, these drugs are far from satisfactory in the clinic [258].

The concept of the work described in this thesis is the development of a novel anti-metastatic drug that depends on inhibiting the migration of cancer cells by inhibiting the synthesis of polySia, a carbohydrate which is re-expressed during progression of a number of malignant human tumours and correlates with increased metastatic potential, tumour progression and poor prognosis [37].

Carbohydrates play a key role in cellular interactions. Until recent years, little attention has been given to these molecules, primarily because they are so diverse and so much more difficult to study than, for example, proteins that are directly encoded by genes. It is only fairly recently that carbohydrates have been given more attention because of overwhelming evidence that they are extensively involved in human health and disease and because of advances that have been made in their synthesis, analysis and manipulation [259,260].

Various carbohydrate-based drugs and diagnostics are currently in use. Zanamivir and Oseltamivir are a monosaccharide-based drug that is used for treating influenza [261]. Heparin, consisting of a mixture of polysaccharides, has been used for decades as an anti-clotting agent [262]. Acarbose is a glycosidase inhibitor that is used to treat type-2-diabetes by regulating carbohydrate digestion, intestinal absorption and carbohydrate metabolism [259,263].

For decades, it has been established by many glycobiologists that the structures of glycans, which decorate all eukaryotic cell surfaces, changes with the progression of cancer, a phenomenon which was first described by Meezan et al. in 1969 [37]. Consequently, glycosylation pattern of a cell can be

considered as a code for cellular physiology. A number of studies have been performed in order to understand this code at both molecular and functional levels. Although glycobiologists are still at the early stages of interpreting this code, their studies have already inspired novel methods to detect glycans characteristic of disease conditions, to prevent disease glycan formation and to destroy cells that display them. However, as mentioned earlier, progress in understanding glycobiology of cancer has been slow relative to studies that target understanding the role of different proteins and nucleic acids in cancer progression.

Many factors contribute to this slow progress, for example, the biosynthesis of glycans, unlike other biopolymers, is not template-driven [264]. Additionally, the link between different carbohydrates expression and malignant function is not fully understood. A range of hypothesis have been suggested ranging from protection of tumour cells from immune surveillance by their glycan coat to promotion of tumour-cell metastasis by glycan-mediated adhesion to distant sites [264,265].

PolySia, as discussed earlier in the introduction, has a significant role in promoting cancer cell migration. It contributes to the metastasis of various types of cancer and therefore, it is a promising drug target in a large population of cancer patients [100]. In this study two general aims were addressed; first, the development and validation of ST8SiaII small molecule inhibitor and second initially investigating the mechanisms by which polySia exerts its effects.

In order to develop and validate a small molecule ST8SiaII inhibitor, a cell-free high throughput chromatographic assay was developed. Using this assay allowed the analysis of an inhibitor every six minutes, giving results that are quantitative, reliable and specific. This is the first high throughput quantitative assay for the analysis of human ST8SiaII enzyme activity that provides sufficient resolution to characterise individual product lengths; i.e. can be used to study the way the enzyme affects polySia chain length to be reported. The development of this assay paves the way for the development

of an effective ST8SiaII inhibitor. Using the results obtained from this assay will allow building a structure activity relationship library for the ST8SiaII enzyme that can be used for the development of more potent inhibitors.

The next step for the development of ST8SiaII inhibitor was to design a cell-based assay that allows the examination of the effect of inhibitors on polySia synthesis in the complex conditions of the tumour environment. The assay was further optimized to allow the analysis of polySia expression in different cell lines for further examination of these compounds on different types of cancer. The expression of polySia in head and neck cancer has been examined here for the first time. This suggests a new field of research about the effect of ST8SiaII inhibition on the progression of the disease.

Although many cell-based assays for the analysis of ST8SiaII activity have been previously reported, the developed cell-based chromatographic assay reported in this study is the first assay that allows understanding of the mechanism of action of the inhibitors by providing molecular weight information about the monomers released from the polySia synthesized in the presence of these inhibitors. Using this assay to analyse the effect of treating neuroblastoma cells with mannosamine compounds has solved the long debate in the literature about the mechanism of action of these compounds. Here we have proven that ManNprop is incorporated in the polySia chains giving modified polySia.

The final step for validation of the design inhibitors was achieved by examining the effect of inhibitors on the migration of cancer cells that express polySia. This not only allowed the investigation of the effect of ST8SiaII inhibition on migration of cancer cells, but also gave some data about the selectivity of the designed inhibitors, helping to further ‘’sieve’’ them to choose the most potent, selective inhibitors.

As discussed earlier in the introduction, so far polySia has been efficiently modulated only by genetic manipulations or by enzymatic digestion. Here, novel, selective and potent ST8SiaII inhibitors that significantly reduce polySia expression and inhibit the migration of the polySia-expressing

neuroblastoma cells have been reported for the first time. Although the inhibitors examined in this thesis are not yet potent enough to start *in vivo* studies, more potent inhibitors are being developed and analysed using the developed assay. Compound SAR is also being established using the novel cell-free assay as will be discussed in the future perspective section.

The second part of this study involved initial investigation of different aspects of polySia activity. This has been achieved by two parallel studies; studying the additive anti-migratory effect of combining a polyST inhibitor with compounds involved in different cancer pathways and studying the impact of polySia expression on the behaviour of cancer cells under hypoxic conditions. From these studies I was able to demonstrate the possible beneficial effects of combining crizotinib (an FDA-approved c-MET/ALK inhibitor drug used for treatment of patients with NSCLC) and ST8SiaII inhibitor (ICT-3176) for inhibiting the migration of neuroblastoma cells.

The other study involved investigating the role of polySia expression on cancer cell behaviour under hypoxic conditions. It was found that polySia expression resulted in more aggressive behaviour of cancer cells presented as increased survival and migration potential and inhibition of adhesion to extracellular matrix.

5.2. Future perspective

A number of open investigations must be solved to allow the development of a potent, selective and druggable ST8SiaII inhibitor. These investigations suggest a variety of research directions that need to be pursued to make such an inhibitor feasible.

Here the future experiments that could be done in the short, medium and long term are described.

5.2.1. Short-term objectives

The developed cell-free chromatographic assay is an efficient tool for building a structure activity relationship library for ST8SiaII inhibitors.

However, more small molecule inhibitors have to be analysed to allow this. Such experiments will allow understanding the chemical groups that are responsible for the inhibitor molecule binding with the ST8SiaII enzyme and blocking its activity. This allows modification of the selectivity and the potency of the inhibitor by changing its chemical structure.

In this study the effect of promising inhibitors was examined by a 2D migration assay. Although it have its advantages, as described earlier in chapter 3, studying the effect of the inhibitor using 3D migration assay and/or tumour spheroid-based migration assay would give more understanding of the effect of the inhibitor in a situation that more closely matches the structure and biochemical environment of native tissue to predict in vivo activity.

Another aspect that should be studied is examining the expression of ST8SiaII enzyme within the layers of neuroblastoma multicellular tumour spheroids to validate the results obtained earlier with the 2D cell-based chromatographic assay. In this thesis, the effect of hypoxia on the expression of polySia was examined in a 2D system at which all the cells were exposed to the same level of oxygen, however *in vivo* different layers of tumour are subjected to different oxygen levels. In order to understand the effect of this oxygen level gradient on polySia expression a 3D model which utilises neuroblastoma spheroids could be used. This will give more detailed understanding of the effect of hypoxia on polySia expression.

This should be followed by studying the effect of inhibiting ST8SiaII, using lead inhibitor and knock down, on the invasion of neuroblastoma multicellular tumour spheroids. Multicellular tumour spheroids (MCTS) mimic the organisation of a tumour and are considered as an invaluable model to study cancer cell biology and to evaluate new drugs [266]. It was shown earlier in this study that ST8SiaII inhibition results in reduction of tumour migration under both hypoxic and normoxic conditions. Using a spheroid model would help to profile the cellular response to ST8SiaII inhibition under the heterogenic

hypoxic/normoxic conditions within the tumour, which closely mimic the in vivo situation.

Detailed assessment of enzyme binding kinetics and druggability of the hit inhibitors have to be investigated. Characterizing the relationship between the pharmacokinetics (PK, concentration vs. time) and pharmacodynamics (PD, effect vs. time) is an important tool in the discovery and development of new drugs [267]. It is recommended that PK/PD strategies be implemented in early research phases of drug discovery projects to enable successful transition to drug development [267]. Druggability is a concept that refers to the properties of the active pharmaceutical ingredient relative to the required properties of the agent to be developed. This includes the physicochemical properties of the agent such as the ability to compress it into a tablet or formulate it for oral administration. As well as its pharmacokinetic properties that reveals dosing requirement and possible drug interaction potential and the possibility of food effect [268].

In the case of an anti-metastatic drug that is aimed for neuroblastoma patients, the ideal pharmaceutical formulation would be an oral liquid formulation to be suitable for the administration to infants and children on a long-term basis.

5.2.2. Medium-term objectives

Designing a model for *in vivo* analysis of anti-metastatic drug would be the next milestone for the design of ST8SiaII inhibitor. This model should be used to study the lead inhibitor selected by using the SAR library and 3D invasion and migration models. Using the *in vivo* model would allow studying the possible side effects of the drug and also the possible beneficial effect of combination therapy. Examining the effect of the selected inhibitor on subcutaneous xenograft in mice would be the first step. This would allow studying the pharmacokinetics of the drug such as its tissue distribution and cellular uptake. This should be followed by the design of metastatic model such as using orthotopic injection transplantation, which more closely

resembles human cancers including tumour histology, vascularity, gene expression, responsiveness to chemotherapy and metastatic biology [269].

Orthotopic metastatic models for studying neuroblastoma have been previously reported. An example of an orthotopic is reported by Khanna C. et al., in this model tumours were established following adrenal injection of different neuroblastoma cell lines in SCID mice where it was found to be more biologically relevant, including angiogenic phenotype, and enhanced spontaneous distant metastasis compared to subcutaneous (heterotopic) injection [270,271].

5.2.3. Long-term objectives

Finally, the long-term objectives would be to start a phase I clinical trial, by first selection of the suitable patients whom might benefit from the treatment (PolySia positive) such as neuroblastoma patients, this can be achieved by examining the tumour biopsy for biomarkers such as ST8SiaII gene expression, and initiate the trial for dosing, safety and early efficacy information, considering that clinical trials of anti-metastatic drug molecules that prevent cancer dissemination are likely to be required for use right after diagnosis, not after failure of standard-of-care therapies.

A parallel phase I/II clinical trial design for combination therapies could be beneficial for studying of the effect of combining ST8SiaII inhibition with different neuroblastoma treatment protocols [272] such as anti-GD2 immunotherapy (Unituxin), which has recently been approved by the FDA and EMA specifically for neuroblastoma (in combination with GM-CSF, Interleukin-2).

5.3. Conclusion

In conclusion, the work presented in this thesis has described the development of two novel assays for the analysis of ST8SiaII inhibition in both cell-free and cell-based settings. In addition, a set of ST8SiaII inhibitors designed and synthesised in house were evaluated for their ability to reduce polySia expression and to modulate cell migration in vitro. Potent ST8SiaII

inhibitors have been reported for the first time. The possible additive anti-migratory effect of combining polyST inhibition with the inhibition of certain signalling pathways has been investigated. Finally, the effect of polySia expression on cancer cell behaviour under hypoxic conditions was examined, where it was found that polySia expression enhanced cell migration and survival and inhibits cell adhesion.

To sum up, greater attention should be paid towards the development of an effective anti-metastatic drug. A successful drug targeting metastasis could therefore make a big impact on patient survival.

Chapter 6. References

1. Registrar General Annual Report - 2010. (Northern Ireland Statistics and Research Agency, Belfast 2011, 2011).
2. UK, C.R. Worldwide cancer statistics. (2012).
3. Deaths Time Series Data, Deaths in Scotland in 2010. (General Register Office for Scotland, Edinburgh 2011, 2011).
4. *Mortality Statistics: Deaths registered in 2010, England and Wales*, (Office for National Statistics, London 2011, 2011).
5. Weinberg, R.A. *The Biology of Cancer*, (Taylor & Francis Group, 2013).
6. Hanahan, D. & Weinberg, Robert A. Hallmarks of Cancer: The Next Generation. *Cell* **144**, 646-674 (2011).
7. Hanahan, D. & Weinberg, R.A. The hallmarks of cancer. *Cell* **100**, 57-70 (2000).
8. Hanahan, D. & Folkman, J. Patterns and emerging mechanisms of the angiogenic switch during tumorigenesis. *Cell* **86**, 353-364 (1996).
9. pecorino, L. *Molecular biology of cancer*, (oxford university press, Oxford, 2012).
10. Talmadge, J.E. & Fidler, I.J. AACR Centennial Series: The Biology of Cancer Metastasis: Historical Perspective. *Cancer Research* **70**, 5649-5669 (2010).
11. Gundem, G.*, et al.* The evolutionary history of lethal metastatic prostate cancer. *Nature* **520**, 353-357 (2015).
12. Hong, M.K.*, et al.* Tracking the origins and drivers of subclonal metastatic expansion in prostate cancer. *Nature communications* **6**, 6605 (2015).
13. Ambrus JL, A.C., Mink IB, Pickren JW. Causes of death in cancer patients. *journal of medicine* **6**, 61-64 (1975).
14. Hadden, J.W. Immunodeficiency and cancer: prospects for correction. *International Immunopharmacology* **3**, 1061-1071 (2003).
15. Fidler, I.J. The pathogenesis of cancer metastasis: the 'seed and soil' hypothesis revisited. *Nature Reviews Cancer* **3**, 453-458 (2003).
16. Hynes, R.O. Metastatic Potential: Generic Predisposition of the Primary Tumor or Rare, Metastatic Variants—Or Both? *Cell* **113**, 821-823 (2003).
17. Begg, C.B., Cramer, L.D., Venkatraman, E.S. & Rosai, J. Comparing tumour staging and grading systems: a case study and a review of the issues, using thymoma as a model. *Statistics in medicine* **19**, 1997-2014 (2000).
18. Yokota, J. Tumor progression and metastasis. *Carcinogenesis* **21**, 497-503 (2000).
19. Takes, R.P.*, et al.* Expression of genetic markers in lymph node metastases compared with their primary tumours in head and neck cancer. *The Journal of Pathology* **194**, 298-302 (2001).
20. Rajeswari Jinka, R.K., Pavana Goury Sistla, T. Avinash Raj, and Gopal Pande. Alterations in Cell-Extracellular Matrix Interactions during Progression of Cancers. *International Journal of Cell Biology* **3**, 1061-1071 (2012).
21. Hunter, K.W., Crawford, N.P. & Alsarraj, J. Mechanisms of metastasis. *Breast Cancer Research* **10** Suppl 1:S2. (2008).
22. Harlozinska, A. Progress in molecular mechanisms of tumor metastasis and angiogenesis. *Anticancer research* **25**, 3327-3333 (2005).
23. Tsai, J.H. & Yang, J. Epithelial–mesenchymal plasticity in carcinoma metastasis. *Genes & development* **27**, 2192-2206 (2013).
24. Kalluri, R. & Weinberg, R.A. The basics of epithelial-mesenchymal transition. *The Journal of Clinical Investigation* **119**, 1420-1428 (2009).
25. Wrighton, K.H. Cell migration: EMT promotes contact inhibition of locomotion. *Nature Reviews Molecular Cell Biology* **16**, 518-518 (2015).
26. Okegawa, T., Pong, R.C., Li, Y. & Hsieh, J.T. The role of cell adhesion molecule in cancer progression and its application in cancer therapy. *Acta biochimica Polonica* **51**, 445-457 (2004).

27. Alberts B, J.A., Lewis J, et al. *Molecular Biology of the Cell*, (Garland Science, New York, 2002).
28. Cavallaro, U. & Christofori, G. Cell adhesion and signalling by cadherins and Ig-CAMs in cancer. *Nature Reviews Cancer* **4**, 118-132 (2004).
29. Shimono, Y., Rikitake, Y., Mandai, K., Mori, M. & Takai, Y. Immunoglobulin superfamily receptors and adherens junctions. *Subcellular Biochemistry* **60**, 137-170 (2012).
30. Kren, A., The role of NCAM signaling and its effector protein, β1-integrin, in tumor progression in Faculty of Science. 2007, University of Basel: Basel. (2007).
31. Soroka, V.*, et al.* Structure and Interactions of NCAM Ig1-2-3 Suggest a Novel Zipper Mechanism for Homophilic Adhesion. *Structure* **11**, 1291-1301 (2003).
32. Berois, N. & Osinaga, E. Glycobiology of Neuroblastoma: Impact on Tumor Behavior, Prognosis, and Therapeutic Strategies. *Frontiers in Oncology* **4**, 114 (2014).
33. Acheson, A., Sunshine, J.L. & Rutishauser, U. NCAM polysialic acid can regulate both cell-cell and cell-substrate interactions. *The Journal of cell biology* **114**, 143-153 (1991).
34. Polo-Parada, L., Bose, C.M., Plattner, F. & Landmesser, L.T. Distinct roles of different neural cell adhesion molecule (NCAM) isoforms in synaptic maturation revealed by analysis of NCAM 180 kDa isoform-deficient mice. *The Journal of neuroscience : the official journal of the Society for Neuroscience* **24**, 1852-1864 (2004).
35. Kiselyov, V.V., Soroka, V., Berezin, V. & Bock, E. Structural biology of NCAM homophilic binding and activation of FGFR. *Journal of Neurochemistry* **94**, 1169-1179 (2005).
36. Dejana, U.C.a.E. Adhesion molecule signalling: not always a sticky business. *Nature Reviews Molecular Cell Biology* **12**, 189-197 (2011).
37. Seidenfaden, R., Krauter, A., Schertzinger, F., Gerardy-Schahn, R. & Hildebrandt, H. Polysialic acid directs tumor cell growth by controlling heterophilic neural cell adhesion molecule interactions. *Molecular Cell Biology* **23**, 5908-5918 (2003).
38. Gerardy-Schahn, R., Delannoy, P. & von Itzstein, M. *SialoGlyco Chemistry and Biology II: Tools and Techniques to Identify and Capture Sialoglycans*, (Springer International Publishing, 2015).
39. Dwek, M.V., Ross, H.A. & Leathem, A.J. Proteome and glycosylation mapping identifies post-translational modifications associated with aggressive breast cancer. *Proteomics* **1**, 756-762 (2001).
40. Aebi, M. N-linked protein glycosylation in the ER. *Biochimica et Biophysica Acta (BBA) - Molecular Cell Research* **1833**, 2430-2437 (2013).
41. Angata, K. & Fukuda, M. Polysialyltransferases: major players in polysialic acid synthesis on the neural cell adhesion molecule. *Biochimie* **85**, 195-206 (2003).
42. Zhou, G.P., Huang, R.B. & Troy, F.A., 2nd. 3D structural conformation and functional domains of polysialyltransferase ST8Sia IV required for polysialylation of neural cell adhesion molecules. *Protein and peptide letters* **22**, 137-148 (2015).
43. Harduin-Lepers, A.*, et al.* The human sialyltransferase family. *Biochimie* **83**, 727-737 (2001).
44. Sato, C. & Kitajima, K. Impact of structural aberrancy of polysialic acid and its synthetic enzyme ST8SIA2 in schizophrenia. *Frontiers in Cellular Neuroscience* **7**(2013).
45. Foley, D.A., Swartzentruber, K.G. & Colley, K.J. Identification of Sequences in the Polysialyltransferases ST8Sia II and ST8Sia IV That Are Required for the

Protein-specific Polysialylation of the Neural Cell Adhesion Molecule, NCAM. *The Journal of Biological Chemistry* **284**, 15505-15516 (2009).
46. Muhlenhoff, M., Rollenhagen, M., Werneburg, S., Gerardy-Schahn, R. & Hildebrandt, H. Polysialic acid: versatile modification of NCAM, SynCAM 1 and neuropilin-2. *Neurochemical research* **38**, 1134-1143 (2013).
47. Nara, K.*, et al.* Expression cloning of a CMP-NeuAc:NeuAc alpha 2-3Gal beta 1-4Glc beta 1-1'Cer alpha 2,8-sialyltransferase (GD3 synthase) from human melanoma cells. *Proceedings of the National Academy of Sciences* **91**, 7952-7956 (1994).
48. Scheidegger, E.P., Sternberg, L.R., Roth, J. & Lowe, J.B. A Human STX cDNA Confers Polysialic Acid Expression in Mammalian Cells. *Journal of Biological Chemistry* **270**, 22685-22688 (1995).
49. KeunLee, Y., SooLee, H. & Gray, R.M. Spectrum quantisation using two-dimensional multiple type frame segmentation. in *Electronics Letters*, Vol. 34 41-42 (Institution of Engineering and Technology, 1998).
50. Nakayama, J., Fukuda, M.N., Fredette, B., Ranscht, B. & Fukuda, M. Expression cloning of a human polysialyltransferase that forms the polysialylated neural cell adhesion molecule present in embryonic brain. *Proceedings of the National Academy of Sciences* **92**, 7031-7035 (1995).
51. Kim, Y.J.*, et al.* Molecular cloning and expression of human α2,8-sialyltransferase (hST8Sia V). *Biochemical and Biophysical Research Communications* **235**, 327-330 (1997).
52. Hamada, Y.*, et al.* Circadian expression and specific localization of a sialyltransferase gene in the suprachiasmatic nucleus. *Neuroscience letters* **535**, 12-17 (2013).
53. Shaw, A.D.*, et al.* Characterisation of genetic variation in ST8SIA2 and its interaction region in NCAM1 in patients with bipolar disorder. *PLoS One* **9**, e92556 (2014).
54. Galuska, S.P., Geyer, R., Gerardy-Schahn, R., Mühlenhoff, M. & Geyer, H. Enzyme-dependent Variations in the Polysialylation of the Neural Cell Adhesion Molecule (NCAM) in Vivo. *Journal of Biological Chemistry* **283**, 17-28 (2008).
55. Sato, C. & Kitajima, K. Impact of structural aberrancy of polysialic acid and its synthetic enzyme ST8SIA2 in schizophrenia. *Frontiers in Cellular Neuroscience* **7**, 61 (2013).
56. Rutishauser, U. Polysialic acid at the cell surface: Biophysics in service of cell interactions and tissue plasticity. *Journal of Cellular Biochemistry* **70**, 304-312 (1998).
57. Eggers, K.*, et al.* Polysialic acid controls NCAM signals at cell–cell contacts to regulate focal adhesion independent from FGF receptor activity. *Journal of cell science* **124**, 3279-3291 (2011).
58. Hildebrandt, H., Mühlenhoff, M., Weinhold, B. & Gerardy-Schahn, R. Dissecting polysialic acid and NCAM functions in brain development. *Journal of Neurochemistry* **103**, 56-64 (2007).
59. Bonfanti, L. & Theodosis, D.T. Polysialic acid and activity-dependent synapse remodeling. *Cell adhesion & migration* **3**, 43-50 (2009).
60. Wang, X.*, et al.* Enhanced expression of polysialic acid correlates with malignant phenotype in breast cancer cell lines and clinical tissue samples. *International journal of molecular medicine* **37**, 197-206 (2016).
61. Korja, M.*, et al.* Absence of polysialylated NCAM is an unfavorable prognostic phenotype for advanced stage neuroblastoma. *BMC Cancer* **9**, 57 (2009).
62. Gluer, S.*, et al.* Serum polysialylated neural cell adhesion molecule in childhood neuroblastoma. *British Journal of Cancer* **78**, 106 - 110 (1998).

63. Gluer, S., Zense, M., Radtke, E. & von Schweinitz, D. [Expression of polysialylated NCAM on neuroblastomas of various histology and clinical stages]. *Langenbecks Archiv fur Chirurgie. Supplement. Kongressband. Deutsche Gesellschaft fur Chirurgie. Kongress* **115**, 289-292 (1998).
64. Falconer, R.A., Errington, R.J., Shnyder, S.D., Smith, P.J. & Patterson, L.H. Polysialyltransferase: a new target in metastatic cancer. *Current cancer drug targets* **12**, 925-939 (2012).
65. Cheung, I.Y., Feng, Y., Gerald, W. & Cheung, N.K.V. Exploiting gene expression profiling to identify novel minimal residual disease markers of neuroblastoma. *Clinical Cancer Research* **14**, 7020-7027 (2008).
66. Suzuki, M.*, et al.* Polysialic acid facilitates tumor invasion by glioma cells. *Glycobiology* **15**, 887 - 894 (2005).
67. Amoureux, M.C.*, et al.* Polysialic acid neural cell adhesion molecule (PSA-NCAM) is an adverse prognosis factor in glioblastoma, and regulates olig2 expression in glioma cell lines. *BMC Cancer* **10**, 91 (2010).
68. Martersteck, C.M., Kedersha, N.L., Drapp, D.A., Tsui, T.G. & Colley, K.J. Unique alpha 2, 8-polysialylated glycoproteins in breast cancer and leukemia cells. *Glycobiology* **6**, 289-301 (1996).
69. Trouillas, J.*, et al.* Polysialylated neural cell adhesion molecules expressed in human pituitary tumors and related to extrasellar invasion. *Journal of Neurosurgery* **98**, 1084-1093 (2003).
70. Wierinckx, A.*, et al.* A diagnostic marker set for invasion, proliferation, and aggressiveness of prolactin pituitary tumors. *Endocrine-related cancer* **14**, 887-900 (2007).
71. Roth, J.*, et al.* Presence of the long chain form of polysialic acid of the neural cell adhesion molecule in Wilms' tumor. Identification of a cell adhesion molecule as an oncodevelopmental antigen and implications for tumor histogenesis. *The American Journal of Pathology* **133**, 227-240 (1988).
72. Gluer, S., Schelp, C., Von Schweinitz, D. & Gerardy-Schahn, R. Polysialylated Neural Cell Adhesion Molecule in Childhood Rhabdomyosarcoma. *Pediatr Res* **43**, 145-147 (1998).
73. Pavelka, M. & Roth, J. *Functional Ultrastructure: Atlas of Tissue Biology and Pathology*, (Springer Wein NewYork, 2010).
74. Krug, L.M.*, et al.* Vaccination of small cell lung cancer patients with polysialic acid or N-propionylated polysialic acid conjugated to keyhole limpet hemocyanin. *Clinical Cancer Research* **10**, 916-923 (2004).
75. Lantuejoul, S., Moro, D., Michalides, R.J., Brambilla, C. & Brambilla, E. Neural cell adhesion molecules (NCAM) and NCAM-PSA expression in neuroendocrine lung tumors. *The American journal of surgical pathology* **22**, 1267-1276 (1998).
76. Miyahara, R.*, et al.* Expression of neural cell adhesion molecules (polysialylated form of neural cell adhesion molecule and L1-cell adhesion molecule) on resected small cell lung cancer specimens: in relation to proliferation state. *Journal of surgical oncology* **77**, 49-54 (2001).
77. Valentiner, U., Muhlenhoff, M., Lehmann, U., Hildebrandt, H. & Schumacher, U. Expression of the neural cell adhesion molecule and polysialic acid in human neuroblastoma cell lines. *International journal of oncology* **39**, 417-424 (2011).
78. Daniel, L.*, et al.* A nude mice model of human rhabdomyosarcoma lung metastases for evaluating the role of polysialic acids in the metastatic process. *Oncogene* **20**, 997 - 1004 (2001).
79. Cheung, I.Y., Vickers, A. & Cheung, N.-K.V. Sialyltransferase STX (ST8SiaII): A novel molecular marker of metastatic neuroblastoma. *International Journal of Cancer* **119**, 152-156 (2006).

80. Reuter-Rice, K. & Bolick, B. *Pediatric Acute Care*, (Jones & Bartlett Learning, LLC, 2011).
81. Esiashvili, N., Goodman, M., Ward, K., Marcus, R.B., Jr. & Johnstone, P.A. Neuroblastoma in adults: Incidence and survival analysis based on SEER data. *Pediatric Blood Cancer* **49**, 41-46 (2007).
82. van der Zwan, J.M.*, et al.* Rare neuroendocrine tumours: results of the surveillance of rare cancers in Europe project. *European Journal of Cancer* **49**, 2565-2578 (2013).
83. Society, A.C. Survival rates for neuroblastoma based on risk groups.
84. Ikeda, H.*, et al.* Experience with International Neuroblastoma Staging System and Pathology Classification. *British Journal of Cancer* **86**, 1110-1116 (2002).
85. Gains, J., Mandeville, H., Cork, N., Brock, P. & Gaze, M. Ten challenges in the management of neuroblastoma. *Future Oncology* **8**, 839-858 (2012).
86. Heck, J.E., Ritz, B., Hung, R.J., Hashibe, M. & Boffetta, P. The epidemiology of neuroblastoma: a review. *Paediatric and perinatal epidemiology* **23**, 125-143 (2009).
87. Cheung, N.-K.V. & Dyer, M.A. Neuroblastoma: developmental biology, cancer genomics and immunotherapy. *Nature reviews. Cancer* **13**, 397-411 (2013).
88. FDA Approval for Unituxin for Pediatric High-risk Neuroblastoma. *Oncology Times* **37**, 4.
89. Yang, R.K. & Sondel, P.M. Anti-GD2 Strategy in the Treatment of Neuroblastoma. *Drugs of the future* **35**, 665- (2010).
90. Weinstein, J.L., Katzenstein, H.M. & Cohn, S.L. Advances in the Diagnosis and Treatment of Neuroblastoma. *The Oncologist* **8**, 278-292 (2003).
91. O'Leary, M., Krailo, M., Anderson, J.R. & Reaman, G.H. Progress in Childhood Cancer: 50 Years of Research Collaboration, A Report from the Children's Oncology Group. *Seminars in oncology* **35**, 484-493 (2008).
92. Small, A.G.*, et al.* Neuroblastoma, Body Mass Index, and Survival: A Retrospective Analysis. *Medicine* **94**, e713 (2015).
93. Ahmed, M. & Cheung, N.-K.V. Engineering anti-GD2 monoclonal antibodies for cancer immunotherapy. *FEBS Letters* **588**, 288-297 (2014).
94. Werneburg, S., Buettner, F.F.R., Mühlenhoff, M. & Hildebrandt, H. Polysialic acid modification of the synaptic cell adhesion molecule SynCAM 1 in human embryonic stem cell-derived oligodendrocyte precursor cells. *Stem Cell Research* **14**, 339-346 (2015).
95. Hildebrandt, H.*, et al.* Polysialic acid on the neural cell adhesion molecule correlates with expression of polysialyltransferases and promotes neuroblastoma cell growth. *Cancer Res* **58**, 779-784 (1998).
96. Schreiber, S.C.*, et al.* Polysialylated NCAM represses E-cadherin-mediated cell-cell adhesion in pancreatic tumor cells. *Gastroenterology* **134**, 1555-1566 (2008).
97. Pinho, S.S. & Reis, C.A. Glycosylation in cancer: mechanisms and clinical implications. *Nature Reviews Cancer* **15**, 540-555 (2015).
98. Guan, F., Wang, X. & He, F. Promotion of cell migration by neural cell adhesion molecule (NCAM) is enhanced by PSA in a polysialyltransferase-specific manner. *PLoS One* **10**, e0124237 (2015).
99. Kudo, M.*, et al.* Cloning and expression of an α-2,8-polysialyltransferase (STX) from Xenopus laevis. *Glycobiology* **8**, 771-777 (1998).
100. Tanaka, F.*, et al.* Expression of Polysialic Acid and STX, a Human Polysialyltransferase, Is Correlated with Tumor Progression in Non-Small Cell Lung Cancer. *Cancer Research* **60**, 3072-3080 (2000).

101. Miyazaki, T., Angata, K., Seeberger, P.H., Hindsgaul, O. & Fukuda, M. CMP substitutions preferentially inhibit polysialic acid synthesis. *Glycobiology* **18**, 187-194 (2008).
102. *Varki A, Schauer R. Sialic Acids. In: Varki A, Cummings RD, Esko JD, et al., editors. Essentials of Glycobiology. 2nd edition. Cold Spring Harbor (NY): Cold Spring Harbor Laboratory Press; 2009. Chapter 14. Available from: http://www.ncbi.nlm.nih.gov/books/NBK1920/*
103. Pon, R.A., Biggs, N.J. & Jennings, H.J. Polysialic acid bioengineering of neuronal cells by N-acyl sialic acid precursor treatment. *Glycobiology* **17**, 249-260 (2007).
104. Horstkorte, R.*, et al.* Selective inhibition of polysialyltransferase ST8SiaII by unnatural sialic acids. *Experimental Cell Research* **298**, 268-274 (2004).
105. Khedri, Z.*, et al.* Probe sialidase substrate specificity using chemoenzymatically synthesized sialosides containing C9-modified sialic acid. *Chemical Communications* **48**, 3357-3359 (2012).
106. Mahal, L.K.*, et al.* A Small-Molecule Modulator of Poly-α2,8-Sialic Acid Expression on Cultured Neurons and Tumor Cells. *Science* **294**, 380-381 (2001).
107. Kilton, L.J. & Maca, R.D. Nucleotide-induced inhibition of surface sialyl transferase activity on cultured Burkitt's lymphoma cells. *Journal of the National Cancer Institute* **58**, 1479-1481 (1977).
108. Klohs, W.D., Bernacki, R.J. & Korytnyk, W. Effects of Nucleotides and Nucleotide:Analogs on Human Serum Sialyltransferase. *Cancer Research* **39**, 1231-1238 (1979).
109. Yousef M. J. Al-Saraireh, M.S., Bradley R. Springett, Friedrich Freiberger, Goreti Ribeiro Morais, Paul M. Loadman, Rachel J. Errington,Paul J. Smith, Minoru Fukuda,Rita Gerardy-Schahn, & Laurence H. Patterson, S.D.S., Robert A. Falconer. Pharmacological Inhibition of polysialyltransferase ST8SiaII Modulates Tumour Cell Migration. *PLoS ONE* **8**(2013).
110. Campbell, M.P., Royle, L., Radcliffe, C.M., Dwek, R.A. & Rudd, P.M. GlycoBase and autoGU: tools for HPLC-based glycan analysis. *Bioinformatics* **24**, 1214-1216 (2008).
111. Wu, Z.L. Phosphatase-coupled universal kinase assay and kinetics for first-order-rate coupling reaction. *PLoS One* **6**, e23172 (2011).
112. Close, B.E.*, et al.* The polysialyltransferase ST8Sia II/STX: posttranslational processing and role of autopolysialylation in the polysialylation of neural cell adhesion molecule. *Glycobiology* **11**, 997-1008 (2001).
113. Nakamura, M., Tsunoda, A. & Saito, M. Radioimmune assay of sialyltransferase and N-acetylgalactosaminyltransferase activities using specific antibodies on a 96-well filtration plate of a multiscreen assay system. *Analytical Biochemistry* **198**, 154-159 (1991).
114. Peterson, D.C., Arakere, G., Vionnet, J., McCarthy, P.C. & Vann, W.F. Characterization and acceptor preference of a soluble meningococcal group C polysialyltransferase. *Journal of bacteriology* **193**, 1576-1582 (2011).
115. Freiberger, F.*, et al.* Biochemical characterization of a Neisseria meningitidis polysialyltransferase reveals novel functional motifs in bacterial sialyltransferases. *Molecular microbiology* **65**, 1258-1275 (2007).
116. Marx, M., Rivera-Milla, E., Stummeyer, K., Gerardy-Schahn, R. & Bastmeyer, M. Divergent evolution of the vertebrate polysialyltransferase Stx and Pst genes revealed by fish-to-mammal comparison. *Developmental Biology* **306**, 560-571 (2007).

117. Nakayama, J. & Fukuda, M. A Human Polysialyltransferase Directs in Vitro Synthesis of Polysialic Acid. *Journal of Biological Chemistry* **271**, 1829-1832 (1996).
118. Liepkans, V., Jolif, A. & Larson, G. Purification and characterization of a CMP-sialic:LcOse4Cer sialyltransferase from human colorectal carcinoma cell membranes. *Biochemistry* **27**, 8683-8688 (1988).
119. Peterson, D.C., Arakere, G., Vionnet, J., McCarthy, P.C. & Vann, W.F. Characterization and Acceptor Preference of a Soluble Meningococcal Group C Polysialyltransferase. *Journal of bacteriology* **193**, 1576-1582 (2011).
120. Macarron, R.*, et al.* Impact of high-throughput screening in biomedical research. *Nature Reviews Drug Discovery* **10**, 188-195 (2011).
121. Carnero, A. High throughput screening in drug discovery. *Clinical and Translational Oncology* **8**, 482-490 (2006).
122. Niyomrattanakit, P.*, et al.* A fluorescence-based alkaline phosphatase-coupled polymerase assay for identification of inhibitors of dengue virus RNA-dependent RNA polymerase. *Journal of biomolecular screening* **16**, 201-210 (2011).
123. Brocco, M., Pollevick, G.D. & Frasch, A.C.C. Differential regulation of polysialyltransferase expression during hippocampus development: Implications for neuronal survival. *Journal of Neuroscience Research* **74**, 744-753 (2003).
124. Angata, K., Lee, W., Mitoma, J., Marth, J.D. & Fukuda, M. Cellular and molecular analysis of neural development of glycosyltransferase gene knockout mice. *Methods in enzymology* **417**, 25-37 (2006).
125. Ding, J.X.*, et al.* Activity of alpha2,6-sialyltransferase and its gene expression in peripheral B lymphocytes in patients with IgA nephropathy. *Scandinavian journal of immunology* **69**, 174-180 (2009).
126. Yu, C.C.*, et al.* A plate-based high-throughput activity assay for polysialyltransferase from Neisseria meningitidis. *Analytical Biochemistry* **444**, 67-74 (2014).
127. Niswender, K.D., Blackman, S.M., Rohde, L., Magnuson, M.A. & Piston, D.W. Quantitative imaging of green fluorescent protein in cultured cells: Comparison of microscopic techniques, use in fusion proteins and detection limits. *Journal of Microscopy* **180**, 109-116 (1995).
128. Odell, I.D. & Cook, D. Immunofluorescence Techniques. *Journal of Investigative Dermatology* **133**, e4 (2013).
129. Prather, B., Ethen, C.M., Machacek, M. & Wu, Z.L. Golgi-resident PAP-specific 3'-phosphatase-coupled sulfotransferase assays. *Analytical Biochemistry* **423**, 86-92 (2012).
130. systems, R.D. Recombinant Human ST8SIA2 Protein, CF..
131. Wu, Z.L., Ethen, C.M., Prather, B., Machacek, M. & Jiang, W. Universal phosphatase-coupled glycosyltransferase assay. *Glycobiology* **21**, 727-733 (2011).
132. Keys, T.G.*, et al.* A universal fluorescent acceptor for high-performance liquid chromatography analysis of pro- and eukaryotic polysialyltransferases. *Analytical Biochemistry* **427**, 107-115 (2012).
133. Ludger. Product Guide for LudgerTag. Sialic Acid Release and Labeling Kit
134. Hammad, L.A., Saleh, M.M., Novotny, M.V. & Mechref, Y. Multiple-Reaction Monitoring Liquid Chromatography Mass Spectrometry for Monosaccharide Compositional Analysis of Glycoproteins. *Journal of the American Society for Mass Spectrometry* **20**, 1224-1234 (2009).

135. Laroy, W., Maras, M., Fiers, W. & Contreras, R. A Radioactive Assay for Sialyltransferase Activity Using 96-Well Multiscreen Filtration Plates. *Analytical Biochemistry* **249**, 108-111 (1997).
136. Franceschini, I.*, et al.* Polysialyltransferase ST8Sia II (STX) polysialylates all of the major isoforms of NCAM and facilitates neurite outgrowth. *Glycobiology* **11**, 231-239 (2001).
137. Close, B.E., Tao, K. & Colley, K.J. Polysialyltransferase-1 autopolysialylation is not requisite for polysialylation of neural cell adhesion molecule. *The Journal of Biological Chemistry* **275**, 4484-4491 (2000).
138. Simon, P.*, et al.* Polysialic acid is present in mammalian semen as a post-translational modification of the neural cell adhesion molecule NCAM and the polysialyltransferase ST8SiaII. *The Journal of Biological Chemistry* **288**, 18825-18833 (2013).
139. Shahraz, A.*, et al.* Anti-inflammatory activity of low molecular weight polysialic acid on human macrophages. *Scientific reports* **5**, 16800 (2015).
140. Zhang, Y. & Lee, Y.C. Acid-catalyzed lactonization of alpha2,8-linked oligo/polysialic acids studied by high performance anion-exchange chromatography. *The Journal of Biological Chemistry* **274**, 6183-6189 (1999).
141. Yu, Y.P., Cheng, M.C., Lin, H.R., Lin, C.H. & Wu, S.H. Acid-catalyzed hydrolysis and lactonization of alpha2,8-linked oligosialic acids. *The Journal of organic chemistry* **66**, 5248-5251 (2001).
142. Cheng, M.-C., Lin, C.-H., Khoo, K.-H. & Wu, S.-H. Regioselective Lactonization of α-(2→8)-Trisialic Acid. *Angewandte Chemie International Edition* **38**, 686-689 (1999).
143. Waters. Solvents and Caveats for LC/MS..
144. Berg JM, T.J., Stryer L. The Michaelis-Menten Model Accounts for the Kinetic Properties of Many Enzymes. . (Biochemistry, New York, 2002).
145. Cer, R.Z., Mudunuri, U., Stephens, R. & Lebeda, F.J. IC(50)-to-K(i): a web-based tool for converting IC(50) to K(i) values for inhibitors of enzyme activity and ligand binding. *Nucleic Acids Research* **37**, W441-W445 (2009).
146. Rutishauser, U., Watanabe, M., Silver, J., Troy, F.A. & Vimr, E.R. Specific alteration of NCAM-mediated cell adhesion by an endoneuraminidase. *The Journal of cell biology* **101**, 1842-1849 (1985).
147. Inoue, S. & Inoue, Y. A challenge to the ultrasensitive chemical method for the analysis of oligo- and polysialic acids at a nanogram level of colominic acid and a milligram level of brain tissues. *Biochimie* **83**, 605-613 (2001).
148. Gnanapragassam, V.S.*, et al.* Sialic acid metabolic engineering: a potential strategy for the neuroblastoma therapy. *PLoS One* **9**, e105403 (2014).
149. Mitsuoka, C.*, et al.* Regulation of selectin binding activity by cyclization of sialic acid moiety of carbohydrate ligands on human leukocytes. *Proceedings of the National Academy of Sciences of the United States of America* **96**, 1597-1602 (1999).
150. Pon, R.A., Biggs, N.J. & Jennings, H.J. Polysialic acid bioengineering of neuronal cells by N-acyl sialic acid precursor treatment. *Glycobiology* **17**, 249-260 (2007).
151. Charter, N.W., Mahal, L.K., Koshland, D.E., Jr. & Bertozzi, C.R. Differential effects of unnatural sialic acids on the polysialylation of the neural cell adhesion molecule and neuronal behavior. *The Journal of Biological Chemistry* **277**, 9255-9261 (2002).
152. Pon, R.A., Zou, W. & Jennings, H.J. Polysialic acid bioengineering of cancer and neuronal cells by N-acyl sialic acid precursor treatment. *Advances in experimental medicine and biology* **705**, 679-688 (2011).

153. Audry, M.*, et al.* Current trends in the structure–activity relationships of sialyltransferases. *Glycobiology* **21**, 716-726 (2011).
154. Yang, Y. & Ma, H. Western Blotting and ELISA Techniques. *Researcher* **1**, 67-86 (2009).
155. Osborne, C. & Brooks, S. SDS-PAGE and Western Blotting to Detect Proteins and Glycoproteins of Interest in Breast Cancer Research. in *Breast Cancer Research Protocols*, Vol. 120 (eds. Brooks, S. & Harris, A.) 217-229 (Humana Press, 2006).
156. Ghaderi, D., Taylor, R.E., Padler-Karavani, V., Diaz, S. & Varki, A. Implications of the presence of N-glycolylneuraminic acid in recombinant therapeutic glycoproteins. *Nature Biotechnology* **28**, 863-867 (2010).
157. Jimbo, T., Nakayama, J., Akahane, K. & Fukuda, M. Effect of polysialic acid on the tumor xenografts implanted into nude mice. *International Journal of Cancer* **94**, 192-199 (2001).
158. Fischer, F. & Egg, G. [N-acetylneuraminic acid (sialic acid) as a tumor marker in head and neck cancers]. *Hno* **38**, 361-363 (1990).
159. Wratil, P.R.*, et al.* A novel approach to decrease sialic acid expression in cells by a C-3 modified N-acetyl-mannosamine. *Journal of Biological Chemistry* (2014).
160. Swinney, D.C. & Anthony, J. How were new medicines discovered? *Nature Reviews Drug Discovery* **10**, 507-519 (2011).
161. Swinney, D.C. & Xia, S. The discovery of medicines for rare diseases. *Future medicinal chemistry* **6**, 987-1002 (2014).
162. Moffat, J.G., Rudolph, J. & Bailey, D. Phenotypic screening in cancer drug discovery [mdash] past, present and future. *Nature Reviews Drug Discovery* **13**, 588-602 (2014).
163. Swinney, D.C. Phenotypic vs. target-based drug discovery for first-in-class medicines. *Clinical Pharmacology & Therapeutics* **93**, 299-301 (2013).
164. Ru Zang, D.L., I-Ching Tang, Jufang Wang, Shang-Tian Yang. Cell-Based Assays in High-Throughput Screening for Drug Discovery. *Lifescience global* **1**(2012).
165. Kepp, O., Galluzzi, L., Lipinski, M., Yuan, J. & Kroemer, G. Cell death assays for drug discovery. *Nature Reviews Drug Discovery* **10**, 221-237 (2011).
166. Kronek, J., Paulovičová, E., Paulovičová, L., Kroneková, Z. & Lustoň, J. *Biocompatibility and Immunocompatibility Assessment of Poly(2-Oxazolines)*, (2013).
167. van de Loosdrecht, A.A., Beelen, R.H., Ossenkoppele, G.J., Broekhoven, M.G. & Langenhuijsen, M.M. A tetrazolium-based colorimetric MTT assay to quantitate human monocyte mediated cytotoxicity against leukemic cells from cell lines and patients with acute myeloid leukemia. *Journal of immunological methods* **174**, 311-320 (1994).
168. Liang, C.-C., Park, A.Y. & Guan, J.-L. In vitro scratch assay: a convenient and inexpensive method for analysis of cell migration in vitro. *Nature Protocols* **2**, 329-333 (2007).
169. Moreno-Bueno, G.*, et al.* The morphological and molecular features of the epithelial-to-mesenchymal transition. *Nature Protocols* **4**, 1591-1613 (2009).
170. Haudenschild, C.C. & Schwartz, S.M. Endothelial regeneration. II. Restitution of endothelial continuity. *Laboratory Investigation* **41**, 407-418 (1979).
171. Rosenthal, M.D. & Glew, R.H. *Medical Biochemistry: Human Metabolism in Health and Disease*, (Wiley, 2011).
172. Scholzen, T. & Gerdes, J. The Ki-67 protein: from the known and the unknown. *Journal of cellular physiology* **182**, 311-322 (2000).
173. Brusés, J.L. & Rutishauser, U. Roles, regulation, and mechanism of polysialic acid function during neural development. *Biochimie* **83**, 635-643 (2001).

174. Rutishauser, U. NCAM and its polysialic acid moiety: a mechanism for pull/push regulation of cell interactions during development? *Development* **116**, 99-104 (1992).
175. Fujimoto, I., Bruses, J.L. & Rutishauser, U. Regulation of Cell Adhesion by Polysialic Acid: Effects on cadherin, immunoglobulin cell adhesion molecule, and integrin function and independance from neural cell adhesion molecule binding or signaling activity. *Journal of Biological Chemistry* **276**, 31745-31751 (2001).
176. Cassens, C.*, et al.* Binding of the Receptor Tyrosine Kinase TrkB to the Neural Cell Adhesion Molecule (NCAM) Regulates Phosphorylation of NCAM and NCAM-dependent Neurite Outgrowth. *The Journal of Biological Chemistry* **285**, 28959-28967 (2010).
177. Lamont, F.R.*, et al.* Small molecule FGF receptor inhibitors block FGFR-dependent urothelial carcinoma growth in vitro and in vivo. *British Journal of Cancer* **104**, 75-82 (2011).
178. Noble, M.E.M., Endicott, J.A. & Johnson, L.N. Protein Kinase Inhibitors: Insights into Drug Design from Structure. *Science* **303**, 1800-1805 (2004).
179. Sahu, A., Prabhash, K., Noronha, V., Joshi, A. & Desai, S. Crizotinib: A comprehensive review. *South Asian Journal of Cancer* **2**, 91-97 (2013).
180. Dunn, K.B., Heffler, M. & Golubovskaya, V. Evolving Therapies and FAK Inhibitors for the Treatment of Cancer. *Anti-Cancer Agents in Medicinal Chemistry* **10**, 722-734 (2010).
181. van Geel, R.M., Beijnen, J.H. & Schellens, J.H. Concise drug review: pazopanib and axitinib. *Oncologist* **17**, 1081-1089 (2012).
182. Albaugh, P.*, et al.* Discovery of GNF-5837, a Selective TRK Inhibitor with Efficacy in Rodent Cancer Tumor Models. *ACS Medicinal Chemistry Letters* **3**, 140-145 (2012).
183. Organ, S.L. & Tsao, M.-S. An overview of the c-MET signaling pathway. *Therapeutic Advances in Medical Oncology* **3**, S7-S19 (2011).
184. Fuse, N.*, et al.* Prognostic impact of HER2, EGFR, and c-MET status on overall survival of advanced gastric cancer patients. *Gastric Cancer*, 1-9 (2015).
185. Liu, Y., Yu, X.-F., Zou, J. & Luo, Z.-H. Prognostic value of c-Met in colorectal cancer: A meta-analysis. *World Journal of Gastroenterology : WJG* **21**, 3706-3710 (2015).
186. Qian, J.*, et al.* α2,6-hyposialylation of c-Met abolishes cell motility of ST6Gal-I-knockdown HCT116 cells. *Acta Pharmacologica Sinica* **30**, 1039-1045 (2009).
187. Barreca, A.*, et al.* Anaplastic lymphoma kinase in human cancer. *Journal of molecular endocrinology* **47**, R11-23 (2011).
188. Zhao, J. & Guan, J.L. Signal transduction by focal adhesion kinase in cancer. *Cancer and Metastasis Reviews* **28**, 35-49 (2009).
189. Li, J., Dai, G., Cheng, Y.B., Qi, X. & Geng, M.Y. Polysialylation promotes neural cell adhesion molecule-mediated cell migration in a fibroblast growth factor receptor-dependent manner, but independent of adhesion capability. *Glycobiology* **21**, 1010-1018 (2011).
190. Duffy AM, B.-H.D., Harmey JH. Vascular Endothelial Growth Factor (VEGF) and Its Role in Non-Endothelial Cells: Autocrine Signalling by VEGF. In: Madame Curie Bioscience Database [Internet]. Austin (TX): Landes Bioscience; 2000-. Available from: http://www.ncbi.nlm.nih.gov/books/NBK6482/.
191. Zou, L., Lai, H., Zhou, Q. & Xiao, F. Lasting Controversy on Ranibizumab and Bevacizumab. *Theranostics* **1**, 395-402 (2011).
192. Harmey, J.H. *Vegf and Cancer*, (Landes Bioscience/Eurekah.com ; New York, N.Y. : Kluwer Academic/Plenum Publishers, 2004).

193. Harmey, J.H. & Bouchier-Hayes, D. Vascular endothelial growth factor (VEGF), a survival factor for tumour cells: implications for anti-angiogenic therapy. *BioEssays : news and reviews in molecular, cellular and developmental biology* **24**, 280-283 (2002).
194. Qi, L., Robinson, W.A., Brady, B.M. & Glode, L.M. Migration and invasion of human prostate cancer cells is related to expression of VEGF and its receptors. *Anticancer research* **23**, 3917-3922 (2003).
195. Croci, D.O.*, et al.* Glycosylation-dependent lectin-receptor interactions preserve angiogenesis in anti-VEGF refractory tumors. *Cell* **156**, 744-758 (2014).
196. Huang, E.J. & Reichardt, L.F. Trk Receptors: Roles in Neuronal Signal Transduction. *Annual Review of Biochemistry* **72**, 609-642 (2003).
197. Bao, W.*, et al.* Upregulation of TrkB promotes epithelial-mesenchymal transition and anoikis resistance in endometrial carcinoma. *PLoS One* **8**, e70616 (2013).
198. Sciavolino, P.J. Tropomyosin-Related Kinases (TRK) Making Headway in Head and Neck Cancer (Targeted oncology, 2015).
199. Li, Z., Zhang, Y., Tong, Y., Tong, J. & Thiele, C.J. Trk inhibitor attenuates the BDNF/TrkB-induced protection of neuroblastoma cells from etoposide in vitro and in vivo. *Cancer biology & therapy* **16**, 477-483 (2015).
200. Kanato, Y., Kitajima, K. & Sato, C. Direct binding of polysialic acid to a brain-derived neurotrophic factor depends on the degree of polymerization. *Glycobiology* **18**, 1044-1053 (2008).
201. Dieci, M.V., Arnedos, M., Andre, F. & Soria, J.C. Fibroblast Growth Factor Receptor Inhibitors as a Cancer Treatment: From a Biologic Rationale to Medical Perspectives. *Cancer Discovery* **3**, 264-279 (2013).
202. Arnz, E.*, et al.* Fibroblast growth factor receptors as therapeutic targets in neuroblastoma. *Klinische Pädiatrie* **226**, A22 (2014).
203. Lewin, J. & Siu, L.L. Development of Fibroblast Growth Factor Receptor Inhibitors: Kissing Frogs to Find a Prince? *Journal of Clinical Oncology* (2015).
204. Zhang, X.*, et al.* Receptor Specificity of the Fibroblast Growth Factor Family: The complete mammilian FGF family. *Journal of Biological Chemistry* **281**, 15694-15700 (2006).
205. Brooks, A.N., Kilgour, E. & Smith, P.D. Molecular Pathways: Fibroblast Growth Factor Signaling: A New Therapeutic Opportunity in Cancer. *Clinical Cancer Research* **18**, 1855-1862 (2012).
206. Zecchini, S.*, et al.* The adhesion molecule NCAM promotes ovarian cancer progression via FGFR signalling. *EMBO Molecular Medicine* **3**, 480-494 (2011).
207. Francavilla, C.*, et al.* The binding of NCAM to FGFR1 induces a specific cellular response mediated by receptor trafficking. *The Journal of cell biology* **187**, 1101-1116 (2009).
208. Fardin, P.*, et al.* A biology-driven approach identifies the hypoxia gene signature as a predictor of the outcome of neuroblastoma patients. *Molecular Cancer* **9**, 185-185 (2010).
209. Applying tumour hypoxia to cancer research. (4 Feb 2014).
210. Brown, J.M. & Wilson, W.R. Exploiting tumour hypoxia in cancer treatment. *Nature Reviews Cancer* **4**, 437-447 (2004).
211. Padhani, A.R., Krohn, K.A., Lewis, J.S. & Alber, M. Imaging oxygenation of human tumours. *European Radiology* **17**, 861-872 (2007).
212. Vaupel, P., Kallinowski, F. & Okunieff, P. Blood Flow, Oxygen and Nutrient Supply, and Metabolic Microenvironment of Human Tumors: A Review. *Cancer Research* **49**, 6449-6465 (1989).

213. Höckel, M. & Vaupel, P. Tumor Hypoxia: Definitions and Current Clinical, Biologic, and Molecular Aspects. *Journal of the National Cancer Institute* **93**, 266-276 (2001).
214. Weinmann, M., Belka, C. & Plasswilm, L. Tumour Hypoxia: Impact on Biology, Prognosis and Treatment of Solid Malignant Tumours. *Oncology Research and Treatment* **27**, 83-90 (2004).
215. Carreau, A., Hafny-Rahbi, B.E., Matejuk, A., Grillon, C. & Kieda, C. Why is the partial oxygen pressure of human tissues a crucial parameter? Small molecules and hypoxia. *Journal of Cellular and Molecular Medicine* **15**, 1239-1253 (2011).
216. Rofstad, E.K., Galappathi, K. & Mathiesen, B.S. Tumor Interstitial Fluid Pressure—A Link between Tumor Hypoxia, Microvascular Density, and Lymph Node Metastasis. *Neoplasia (New York, N.Y.)* **16**, 586-594 (2014).
217. Wels, J., Kaplan, R.N., Rafii, S. & Lyden, D. Migratory neighbors and distant invaders: tumor-associated niche cells. *Genes & development* **22**, 559-574 (2008).
218. Murdoch, C., Giannoudis, A. & Lewis, C.E. Mechanisms regulating the recruitment of macrophages into hypoxic areas of tumors and other ischemic tissues. *Blood* **104**, 2224-2234 (2004).
219. Cramer, T.*, et al.* HIF-1alpha is essential for myeloid cell-mediated inflammation. *Cell* **112**, 645-657 (2003).
220. Semenza, G.L. Cancer-Stromal Cell Interactions Mediated by Hypoxia-Inducible Factors Promote Angiogenesis, Lymphangiogenesis, and Metastasis. *Oncogene* **32**, 4057-4063 (2013).
221. Casazza, A.*, et al.* Tumor stroma: a complexity dictated by the hypoxic tumor microenvironment. *Oncogene* **33**, 1743-1754 (2014).
222. Gilkes, D.M., Semenza, G.L. & Wirtz, D. Hypoxia and the extracellular matrix: drivers of tumour metastasis. *Nature Reviews Cancer* **14**, 430-439 (2014).
223. Chi, J.T.*, et al.* Gene expression programs in response to hypoxia: cell type specificity and prognostic significance in human cancers. *PLoS medicine* **3**, e47 (2006).
224. Kaur, B.*, et al.* Hypoxia and the hypoxia-inducible-factor pathway in glioma growth and angiogenesis. *Neuro-Oncology* **7**, 134-153 (2005).
225. Ziello, J.E., Jovin, I.S. & Huang, Y. Hypoxia-Inducible Factor (HIF)-1 Regulatory Pathway and its Potential for Therapeutic Intervention in Malignancy and Ischemia. *The Yale Journal of Biology and Medicine* **80**, 51-60 (2007).
226. Zhang, L.*, et al.* Hypoxia induces epithelial-mesenchymal transition via activation of SNAI1 by hypoxia-inducible factor -1α in hepatocellular carcinoma. *BMC Cancer* **13**, 108 (2013).
227. Joseph, J.V.*, et al.* Hypoxia enhances migration and invasion in glioblastoma by promoting a mesenchymal shift mediated by the HIF1alpha-ZEB1 axis. *Cancer letters* **359**, 107-116 (2015).
228. Koike, T.*, et al.* Hypoxia induces adhesion molecules on cancer cells: A missing link between Warburg effect and induction of selectin-ligand carbohydrates. *Proceedings of the National Academy of Sciences of the United States of America* **101**, 8132-8137 (2004).
229. Blick, C.*, et al.* Hypoxia regulates FGFR3 expression via HIF-1[alpha] and miR-100 and contributes to cell survival in non-muscle invasive bladder cancer. *British Journal of Cancer* **109**, 50-59 (2013).
230. Eckerich, C.*, et al.* Hypoxia can induce c-Met expression in glioma cells and enhance SF/HGF-induced cell migration. *International journal of cancer* **121**, 276-283 (2007).

231. Johansson Pä, I.*, et al.* Effect of acute hypobaric hypoxia on the endothelial glycocalyx and digital reactive hyperemia in humans. *Frontiers in Physiology* **5**(2014).
232. Nagelkerke, A.*, et al.* Hypoxia stimulates migration of breast cancer cells via the PERK/ATF4/LAMP3-arm of the unfolded protein response. *Breast Cancer Research* **15**, R2 (2013).
233. Onochie, O. & Trinkaus-Randall, V. Hypoxia Affects Cell Migration and Wound Healing by Altering Basal Lamina Proteins and Focal Adhesion Turnover. *The FASEB Journal* **29**(2015).
234. Al-Saraireh, Y.M.*, et al.* Pharmacological inhibition of polysialyltransferase ST8SiaII modulates tumour cell migration. *PLoS One* **8**, e73366 (2013).
235. Tate, A.*, et al.* Met-Independent Hepatocyte Growth Factor-mediated regulation of cell adhesion in human prostate cancer cells. *BMC Cancer* **6**, 197 (2006).
236. Sierra, J.R. & Tsao, M.S. c-MET as a potential therapeutic target and biomarker in cancer. *Therapeutic Advances in Medical Oncology* **3**, S21-35 (2011).
237. Rieger, A.M., Nelson, K.L., Konowalchuk, J.D. & Barreda, D.R. Modified Annexin V/Propidium Iodide Apoptosis Assay For Accurate Assessment of Cell Death. *Journal of Visualized Experiments* (2011).
238. Hammill, A.K., Uhr, J.W. & Scheuermann, R.H. Annexin V staining due to loss of membrane asymmetry can be reversible and precede commitment to apoptotic death. *Experimental cell research* **251**, 16-21 (1999).
239. Varki, A. & Chrispeels, M.J. *Essentials of Glycobiology*, (Cold Spring Harbor Laboratory Press, 1999).
240. Cosse, J.P. & Michiels, C. Tumour hypoxia affects the responsiveness of cancer cells to chemotherapy and promotes cancer progression. *Anti-cancer agents in medicinal chemistry* **8**, 790-797 (2008).
241. Koh, M.Y., Spivak-Kroizman, T.R. & Powis, G. HIF-1alpha and cancer therapy. *Recent results in cancer research* **180**, 15-34 (2010).
242. Powis, G. & Kirkpatrick, L. Hypoxia inducible factor-1α as a cancer drug target. *Molecular Cancer Therapeutics* **3**, 647-654 (2004).
243. An, W.G.*, et al.* Stabilization of wild-type p53 by hypoxia-inducible factor 1alpha. *Nature* **392**, 405-408 (1998).
244. Yeom, C.J.*, et al.* Visualization of Hypoxia-Inducible Factor-1 Transcriptional Activation in C6 Glioma Using Luciferase and Sodium Iodide Symporter Genes. *Journal of Nuclear Medicine* **49**, 1489-1497 (2008).
245. Ke, Q. & Costa, M. Hypoxia-Inducible Factor-1 (HIF-1). *Molecular Pharmacology* **70**, 1469-1480 (2006).
246. Galbán, S. & Gorospe, M. Factors interacting with HIF-1α mRNA: novel therapeutic targets. *Current pharmaceutical design* **15**, 3853-3860 (2009).
247. Semenza, G.L. Targeting HIF-1 for cancer therapy. *Nature Reviews Cancer* **3**, 721-732 (2003).
248. Denko, N.C. Hypoxia, HIF1 and glucose metabolism in the solid tumour. *Nature Reviews Cancer* **8**, 705-713 (2008).
249. Hu, C.J., Wang, L.Y., Chodosh, L.A., Keith, B. & Simon, M.C. Differential Roles of Hypoxia-Inducible Factor 1α (HIF-1α) and HIF-2α in Hypoxic Gene Regulation. *Molecular and cellular biology* **23**, 9361-9374 (2003).
250. Kazandjian, D.*, et al.* FDA approval summary: crizotinib for the treatment of metastatic non-small cell lung cancer with anaplastic lymphoma kinase rearrangements. *Oncologist* **19**, e5-11 (2014).
251. Chen, Y.*, et al.* Oncogenic mutations of ALK kinase in neuroblastoma. *Nature* **455**, 971-974 (2008).
252. Krytska, K.*, et al.* Crizotinib Synergizes with Chemotherapy in Preclinical Models of Neuroblastoma. *Clinical Cancer Research* (2015).

253. Khan, N. & Mukhtar, H. Cancer and metastasis: prevention and treatment by green tea. *Cancer metastasis reviews* **29**, 435-445 (2010).
254. Institute, N.C. Metastatic cancer fact sheet. (2013).
255. Gaertner, J., Wolf, J. & Voltz, R. Early palliative care for patients with metastatic cancer. *Current opinion in oncology* **24**, 357-362 (2012).
256. Stock, A.M., Troost, G., Niggemann, B., Zanker, K.S. & Entschladen, F. Targets for anti-metastatic drug development. *Current pharmaceutical design* **19**, 5127-5134 (2013).
257. Weber, G.F. Why does cancer therapy lack effective anti-metastasis drugs? *Cancer letters* **328**, 207-211 (2013).
258. Stupp, R.*, et al.* Effects of radiotherapy with concomitant and adjuvant temozolomide versus radiotherapy alone on survival in glioblastoma in a randomised phase III study: 5-year analysis of the EORTC-NCIC trial. *The Lancet Oncology* **10**, 459 - 466 (2009).
259. Oppenheimer, S.B., Alvarez, M. & Nnoli, J. Carbohydrate-Based experimental therapeutics for cancer, HIV/AIDS and other diseases. *Acta histochemica* **110**, 6-13 (2008).
260. Dwek, M.V. & Brooks, S.A. Harnessing Changes in Cellular Glycosylation in New Cancer Treatment Strategies. *Current cancer drug targets* **4**, 425-442 (2004).
261. De Clercq, E. Antiviral agents active against influenza A viruses. *Nature Reviews Drug Discovery* **5**, 1015-1025 (2006).
262. Capila, I. & Linhardt, R.J. Heparin-protein interactions. *Angewandte Chemie (International ed. in English)* **41**, 391-412 (2002).
263. Truscheit, E.*, et al.* Chemistry and Biochemistry of Microbial α-Glucosidase Inhibitors. *Angewandte Chemie International Edition in English* **20**, 744-761 (1981).
264. Dube, D.H. & Bertozzi, C.R. Glycans in cancer and inflammation [mdash] potential for therapeutics and diagnostics. *Nature Reviews Drug Discovery* **4**, 477-488 (2005).
265. Gabius, H.J. Biological Information Transfer Beyond the Genetic Code: The Sugar Code. *Naturwissenschaften* **87**, 108-121 (2000).
266. Laurent, J.*, et al.* Multicellular tumor spheroid models to explore cell cycle checkpoints in 3D. *BMC Cancer* **13**, 1-12 (2013).
267. Tuntland, T.*, et al.* Implementation of pharmacokinetic and pharmacodynamic strategies in early research phases of drug discovery and development at Novartis Institute of Biomedical Research. *Frontiers in Pharmacology* **5**, 174 (2014).
268. Barrett, J.S., Gupta, M. & Mondick, J.T. Model-based drug development applied to oncology. *Expert opinion on drug discovery* **2**, 185-209 (2007).
269. Khanna, C. & Hunter, K. Modeling metastasis in vivo. *Carcinogenesis* **26**, 513-523 (2005).
270. Khanna, C., Jaboin, J.J., Drakos, E., Tsokos, M. & Thiele, C.J. Biologically relevant orthotopic neuroblastoma xenograft models: primary adrenal tumor growth and spontaneous distant metastasis. *In vivo (Athens, Greece)* **16**, 77-85 (2002).
271. Daudigeos-Dubus, E.*, et al.* Establishment and characterization of new orthotopic and metastatic neuroblastoma models. *In vivo (Athens, Greece)* **28**, 425-434 (2014).
272. Huang, X., Biswas, S., Oki, Y., Issa, J.P. & Berry, D.A. A parallel phase I/II clinical trial design for combination therapies. *Biometrics* **63**, 429-436 (2007).

Appendix I

Publications associated with this work

Elkashef, S.M, Saeed, R.F., Ribeiro Morais G., Guo X., Sini M., Viprey V., Sutherland M., Loadman P., Laurence H. ‘’Polysialyltransferase ST8SiaII: A novel target for the treatment of neuroblastoma’’ DOI: 10.1158/1538-7445.AM2015-5431. Cancer Research, Volume: 75, Philadelphia, USA

Elkashef, S.M, Loadman P., and Falconer R.A. ‘’Optimised assay for quantitative, high-throughput analysis of polysialyltransferase activity’’, Analyst, manuscript in preparation.

Elkashef, S.M, Loadman P., and Falconer R.A. ‘’Development of cell-based chromatographic assay for the analysis of polysialic acid activity in human cancer, Manuscript in preparation, Target Journal: Carbohydrate polymers.

Elkashef, S.M, Haneen B., Maria S., Klaus P., Loadman P., and Falconer R.A. ‘’Polysialic acid sustains cancer cell survival and migratory capacity in a hypoxic environment’’ Manuscript in preparation, Target journal: Scientific reports.

Elkashef, S.M and Falconer R.A. ‘’Critical review of the available techniques for the analysis of human polysialyltransferase enzyme activity’’, Manuscript in preparation, Target Journal: Cancer and Metastasis Reviews.

Abstract for attended conferences

Elkashef, S.M, Simon Ellison, Paul Loadman, Robert A. Falconer. ‘’Understanding the potential role of polysialic acid on cancer cell behaviour under hypoxic conditions’’ 24th Biennial EACR Congress, 9 July 2016, Manchester, UK. Abstract **368.**

Elkashef, S.M, Saeed, R.F., Ribeiro Morais G., Guo X., Sini M., Viprey V., Sutherland M., Loadman P., Laurence H. Patterson, Shnyder S. and Falconer R.A. “Polysialyltransferase ST8SiaII as a target for neuroblastoma dissemination” AACR Annual Meeting, 16-20 April 2016, New Orleans, USA. Abstract 5051.

Elkashef, S.M.; Springett, B.R.; Viprey, V.; Saeed, R.F.; Ribeiro Morais, G.; Sutherland, M.; Loadman, P.M.; Burchill, S.; Patterson, L.H.; Shnyder, S.D.; Falconer, R.A. “Polysialyltransferase inhibition modulates tumour cell growth, migration and invasion in neuroblastoma.” NCRI Cancer Conference, 1-4 November 2015, Liverpool, UK. Abstract BACR18

Falconer, R.A.; Ribeiro Morais, G.; **Elkashef, S.M**.; Viprey, V.; Saeed, R.F.; Springett, B.R.; Sutherland, M.; Loadman, P.M.; Shnyder, S.D.; Patterson, L.H. “Inhibition of polysialyltransferase modulates neuroblastoma cell migration and invasion.” YCR Annual Scientific Meeting, 2 July 2015, Harrogate, UK. Abstract 7.

Elkashef, S.M.; Viprey, V.; Saeed, R.F.; Springett, B.R.; Sutherland, M.; Loadman, P.M.; Patterson, L.H.; Shnyder, S.D.; Falconer, R.A. “Polysialyltransferase ST8SiaII: a novel target for the treatment of neuroblastoma” AACR Annual Meeting, 18-22 April 2015, Philadelphia PA, USA. Abstract 5431. DOI: 10.1158/1538-7445.AM2015-5431

Elkashef, S.M.; Sutherland, M.; Shnyder, S.D.; Patterson, L.H.; Loadman, P.M.; Falconer, R.A. “Development of an analytical assay to assess polysialyltransferase inhibition.” RSC Organic Division NE Regional Meeting, 1 April 2015, Bradford, UK. Abstract 35.

Viprey, V.; Saeed, R.; Springett, B.R.; **Elkashef, S**.; Sutherland, M.; Loadman, P.M.; Patterson, L.H.; Shnyder, S.D.; Falconer, R.A. “In vitro evaluation of inhibitors of polysialyltransferase ST8SiaII: a new target for neuroblastoma.” BACR Development of Cancer Medicines – From Target to Disease: Modelling Stratified

Approaches in Oncology, 27 November 2014, Royal Society of Medicine, London. Abstract 27.

Elkashef, S.; Sutherland, M.; Shnyder, S.D.; Patterson, L.H.; Loadman, P.M.; Falconer, R.A. “Development of an analytical assay to assess polysialyltransferase inhibition.” YCR Annual Scientific Meeting, 25 June 2014, Harrogate, UK. Abstract 32.

Sara M. Elkashef, SD Shnyder, LH Patterson, M Sutherland, PM Loadman and RA Falconer. ‘’ Development of an analytical assay to assess polysialyltransferase inhibition'' School of life Sciences research and development open day, 15 April 2014, Bradford, UK

Oral presentations

Faculty of life science seminar programme, Bradford, UK **2014**

Faculty of life science, postgraduate’s mini-conference, Bradford, UK. **2014**